The Fuzzy Boundary: The Spatial Definition of Urban Areas

Tao Yang

The Bartlett School of Architecture

UCL

Submitted for the degree of Doctor of Philosophy

December 2018

Copyrights

I, Tao Yang confirm that the work presented in this thesis is my own. Where information has been derived from other sources, I confirm that this has been indicated in the thesis.

Some methods – eg. embeddedness trajectories and mountain scattergrams – developed with Professor Bill Hillier in this thesis have been jointly published in the early papers (Yang and Hillier, 2007, 2012; Hillier, Turner, Yang, Park, 2010; Hillier, Yang, Turner, 2012).

The concept of spatial discontinuity in urban networks, where spatial configurational values change dramatically with depth, has been independently discussed with respect to the unevenly intensified grids in the concluding chapter. This sets the main findings of this thesis within the context of space syntax research today.

Signature ……

I dedicate this thesis to my dearest wife, Fang who passed away recently

for your deepest love, braveness, persistence

Abstract

Can urban areas – such as named areas – as parts of a whole city be defined and described in terms of their relationship to the surroundings? How is the continuous urban grid spatially partitioned into different parts? These questions have been extensively discussed in the theoretical and professional literatures, but there is a relative paucity of references of any precision to the spatial form of areas. The thesis, using a rigorous and empirical methodology developed in the theory of space syntax, seeks to define boundaries between urban areas in terms of the way the areas are spatially embedded into the multi-scale contexts. And then the thesis intends to explore geometric and spatial mechanisms in the formation of the areas. After conducting a pilot study of Canary Wharf and Brindleyplace, the thesis conjectures that area boundaries can be treated as discontinuities in the configuration of space, and such boundaries are shown in some way in the pattern of spatial connection of the urban grid outward from each individual space with an increase of scale, ranging from its immediately neighbouring spaces to the whole grid. Several space syntax techniques are then developed to detect and illustrate the area discontinuities. On this basis, a periodic patchwork pattern, meaning the urban grid, is partitioned into a set of periodic and discrete parts, is brought to light in the empirical studies of the central districts of London and Beijing as well as the London Docklands. It can be argued that the discontinuities between urban areas can be typically considered as the fuzzy boundaries supporting functional differentiation of areas, without spatially self-contained or geometrically limited boundaries. This thesis concludes that it is the syntactic relations of all individual spaces and their multi-scale contexts that account for the spatial definition and aggregation of urban areas.

Impact Statement

The methologies developed in this thesis can be used to detect and analyse the spatial formation of urban areas, and some methods has been jointly published with Professor Bill Hillier. For example, a paper titled *The fuzzy boundary: the spatial definition of urban areas* (Yang and Hillier, 2007) was published in the Proceedings of 6th International Space Syntax Symposium and has been cited 49 times according to the Google Scholar. Another paper titled *Normalising least angle choice in Depthmap and how it opens new perspectives on the global and local analysis of city space* (Hillier, Yang, Turner, 2012) was published in the Journal of Space Syntax and has been cited 122 times also according to the Google Scholar.

The concept of fuzzy boundaries of urban areas, suggested in this thesis, has been discussed and/or cited by Mark David Major (2018), Stephen Law (2017), Jorge Gil (2016), Vítor Oliveira (2016), Mario Boffi (2014), Itzhak Omer and Ran Goldblatt (2012) and Nicholas Dalton (2007, 2010), respectively. And meanwhile, such definition of urban areas, taking account of the multi-scale contexts, had represented in academic events in ETH Zürich, MIT and Tsinghua University of China.

The method of generating periodic patchwork patterns, developed in this thesis, has been applied to the consultant projects – eg. Urban Space Strategy of the city of Changchun – conducted by Space Syntax Limited.

Table of Contents

Acknowledgements

This thesis was developed during many discussions with my principle supervisor, Professor Bill Hillier, and it was his innovative vision that led to the core ideas presented in this thesis. My first and most earnest acknowledgment must go to him for his brilliant theoretical ideas, immense knowledge, generous encouragement, long-lasting patience and kindness. In particular, he has taught me, both consciously and unconsciously, how good scientific research of architecture and cities is conducted. His comments on my research and academic writings are themselves a course in critical thinking that will always inspire me. Professor Bill Hillier has changed my understanding of urban studies and has influenced my way of thinking. He has also always helped me to successfully apply for several scholarships and financial support. I want to thank him for the tremendous support he gave to myself and my wife, when my wife was ill. I could not have imagined having a better principle supervisor.

My deepest gratitude also goes to my second supervisor Professor Laura Vaughan, for being an exceptional teacher and offering me sound advices and friendly encouragement. I would like to express my sincere gratitude to the late Alastair Turner, Shinichi Iida and Eva Friedrich for teaching me to use the space syntax software and providing valuable technical insight.

I am extremely grateful to Professor Alan Penn for offering me an opportunity to participate in an interesting research project and giving me tremendous support, as well as research suggestions. I am thankful for the warm support that David Cobb gave me.

I am deeply indebted to Tim Stonor for funding my study, providing me with a job opportunity in Space Syntax Limited and leading and directing me with a number of exciting projects. I also wish to acknowledge all my SSx colleagues who shared with me their experiences and helped in many ways.

I would like to thank many of my student colleagues for providing a stimulating and fun environment in which I could learn and grow. I am especially grateful to Loon Wai Chau, Wafa Al-Ghatam, Kayla Moore, Hoon-Tae Park, Claudia Ortiz Chao, Lucas Figueiredo, Theodora

Antonakaki, Magda Mavridou, Paula Morais, Gemma Moore, Richard Wang and Yannis Zoiopoulos.

I wish to particularly acknowledge all the attendees for the Thinking Aloud Seminar organised by the Space Syntax Group for inspiring and sharing their latest research ideas with me.

I am very grateful for my years at the Bartlett School of Graduate Studies, that was made possible by the Overseas Research Scholarship, UCL Graduate Research Scholarship, the Chinese Government Award for Outstanding Students Abroad, the EPSRC and HEIF funded Knowledge Transfer Secondment and the sponsorship of Space Syntax Limited.

I wish to thank Ben Sharman for proofreading my text carefully and giving me some useful tips.

Lastly, and most importantly, I wish to thank my wife Fang, both our parents and our son. The completion of this thesis and subsequent Ph.D. has been a long journey. Their full support, emotional encouragement, and good companionship have turned my journey through graduate school into a pleasure. To them I dedicate this thesis.

List of Figures

List of Tables

Chapter One: Introduction

1.1 The definition of research questions

In the final two decades of the twentieth century, cities in many parts of the world have been rapidly transformed through large-scale developments. Sometimes this involves the rapid expansion of an existing city outwards through a patchwork of large-scale separate developments with little co-ordinated planning. Sometimes it occurs within the fabric of the existing city through the re-use of previously industrial land. Either way, the outcome tends to be a patchwork of large-scale urban areas, with little relation to each other apart from being linked by a high speed road network.

Many researchers have investigated this phenomenon from the socio-economic, functional, physical planning, and political points of view (Hall, 1998; Olds, 2001; Fainstein, 2001; Altshuler and Luberoff, 2003), seeing this new type of development broadly as a spatial expression of changing economic and social forces. However, no studies have addressed the spatial dimension of the phenomenon in any depth. Is what we are seeing a new spatial form of urbanism, with recognisable connections to urbanism as it has evolved until now? Or are we seeing a new spatial phenomenon which in the long term is likely to undermine the city as a distinctive kind of spatial form?

Two new urgent spatial questions are therefore raised for such urban phenomena. First, what is the impact of new large-scale developments on their contextual urban structures, and does this in any sense depend on how they are structured and related spatially. Second, what will be the urban future of the typical patchwork developments that so increasingly characterise current growth patterns in cities? Will they eventually develop into a more consolidated network of the kind that is familiar with historic urbanism through the common processes of growth and adaptation that have always been a feature of urbanism? Or are we seeing the birth of a new kind of urbanism, based on the patchwork of spatial self-contained and free standing areas?

This also is of course related to the broader background of *the 'part-whole' problem* at the intra-urban level in cities: that in spite of the fact that most cities have some kind of named area structure, and this often seems important to the perceived character and functioning of the city, it is often very difficult to identify boundaries of named areas in the spatial form of the city. This has historically posed two fundamental questions for the theory and practice of urban spatial planning and design. *What, in terms of space, is an urban area? And how do the areas aggregate to form a spatial whole?*

These questions have been extensively discussed in the theoretical and professional literature of the twentieth century. Most of this work has focused on functional and socio-economic aspects and has tended to distinguish urban parts in terms of land use types, socio-economic variables, physical appearances or historical and cultural characteristics. For instance, borrowing the idea in ecology of how the natural forces shape plant and animal communities, Park (1925) coined the concept of 'natural area', meaning the urban parts within a city formed by competition and differentiated by function and socio-economic status. The competition between individuals sifted and sorted individuals and groups through different functions and cultural identities, and then located and relocated different groups to the areas that were the best fit for them.

However, in this literature there is a relative paucity of references of any precision to the spatial form of areas. In the context of the theoretical and empirical studies of the Chicago School, as well as the Garden City by Howard in the UK, and other community planning practices in the US in the early of last century, Clarence Perry (1923) first spatially defined the idea of Neighbourhood Unit that has had widespread and longstanding influence on urbanism in modern times. With the intention of fostering face-to-face interaction within neighbourhoods, and also addressing the traffic and safety issues that came with increasing automobile traffic, the Neighbourhood Unit, based on a five-minute walking radius, was spatially formulated as an inward-looking physical layout, with an arterial road containing shops running along its perimeter, so that roads within the neighbourhood would be designed to discourage through traffic, and with an elementary school located at the centre (Perry, 1929). The key idea was *the*

clear and well-defined boundary. Towns and cities were thought to be constructed by aggregating various such neighbourhood units with clear boundaries. This was a source for Stein's Radburn project and regional city (1942), Tripp's precinct principle (1942), as well as Forshaw and Abercrombie's London Plan (Forshaw and Abercrombie, 1943, 1944). All of them intended to envisage a well-defined cellular structure.

After the 1950s, many writers started to criticise the concept of clear area boundary and proposed various alterative ideas. For example, Alexander (1977: 88-90) suggested an idea of '*boundary zone*', meaning the wide swathes of public spaces with public facilities and institutes or commercial activities shared by a number of neighbourhoods. Later, he pointed out that the '*boundary zone*' can be expressed as '*thick boundary*', in that if the boundaries are thinner or smaller than the areas they bound, they can not keep the areas separate from the surroundings or unite the areas with the surroundings (2002: 54). Other ideas, such as Krier's urban quarter (1977, 1998), the Urban Village movement (Aldous, 1992; UTF, 1999, 2002; Neal, 2003) and the New Urbanists' models (DPZ, 1994, 1999, 2002; Calthorpe, 1994, 2001), also made the emphasis on the *overlapped or accessible* boundaries in which shared facilities and services are located.

These ideas however still focused attention on how urban areas and/or their boundaries should be, rather than how they were; and meanwhile, they still assumed that a city should be constituted by a group of bounded units, although the boundaries might be overlapping. For example, Duany and Plater-Zyberk's Traditional Neighbourhood Design (DPZ, 1999), as some writers (Neal, 2003; Mehaffy, Porta, Romice, 2015) pointed out, is strikingly similar to Perry's Neighbourhood Unit, regarding their size and spatial layout, except that the former has more shared commercial uses arranged along the main streets encircling the neighbourhoods. The cellular concept seems to have a long life.

In contrast to these ideas, a handful of texts has *explicitly* argued that a city is *a continuous network* and suggested a less determinate and perhaps more original notion of urban areas. Jacobs (1961) called for the abandonment of the conventional idea of neighbourhood unit, and argued that urban areas in cities were '*significantly defined only by their fabric and the life and*

intricate cross-use they generate, rather than by formalistic boundaries' (ibid:193). For her, the neighbourhoods working best have no definitive boundaries setting them apart as distinct units. Lynch (1961) also suggested that the urban area, termed as district in his book, need not to be a unified pattern with a solid boundary. '*District may join to district, by juxtaposition, intervisibility, relation to a line, or by some link such as a mediating node, path or small district…Such links heighten the character of each district, and bring together great urban areas*' (ibid: 104-105). Thus, the pattern of a whole district would be gradually perceived and conceived by sequential experiences, reversed and interrupted, so that all the districts would be connected together to form a sense of wholeness, which Lynch called *sequential continuity* (ibid:115). Like Jacobs, he concluded that a city is not a cluster of well-bounded cells but a continuous fabric (Lynch, 1981: 401). Moreover, Rossi (1984: 63) argued that urban areas, termed as study areas in his book, can be defined by comparison to the complex street system of the overall city in which those study areas are located. In his view, the city in its totality emerges through a historic process of diverse growth and differentiation, and meanwhile, the individual areas of the city, such as centres and sub-centres, gain their own characteristics in terms of their location, their topographic limits, their physical appearance and their density. All these texts will be reviewed in detail in next chapter. And Conzen (1988) developed an idea of the *morphological region*, meaning an area with a unity in respect of its form that distinguishes it from surrounding areas. This sought to unite the the tripartite division of town plan, building fabric, and land and building utilization with a dimension of the process of urban development (Whitehand, 2014; Oliverira, 2016).

Although the ideas of Jacobs, Lynch, Rossi and Conzen are very suggestive of a more complex formation for the urban areas and the whole, compared to the cellular concept, they do not really look at the spatial dimension with any precision or clarity. *Is there then a precise and testable description of this alternative model, so that urban areas might be defined, perceived and described in terms of their relationship to the continuous urban network as a whole?* It was left to the space syntax movement to begin to open up this question. It was Hillier's establishment of a theory of space as configuration (meaning relations taking account of other

relations[1]), and a series of related methodologies, called *space syntax* (Hillier and Hanson, 1984; Hillier, 1996), that cast a new light on the spatial formation of area structure. For Hillier (ibid), the spatial network of a city is a historic record of the spatial ordering and structuring driven by human activities, rather than an inert background of human behaviours; and the continuous network and its parts can be rigorously represented, analysed and interpreted with regard to the configurational relations. He has argued that urban parts are *not* local things, but are created by urban network as a whole (1984, 1988, 1991, 1993, 1996). These will be reviewed in chapter three.

This review in particular addresses methodological questions: *is there a way of rigorously describing the spatial features of a pre-given area (whose boundaries are defined in terms of other socio-economic or physical variables), such as named area, in terms of spatial configuration of the whole network? And, is there a way to use syntax to disaggregate an urban network as a whole into the sort of discrete parts in terms of their configurational relations, and in this way, give a spatial definition of urban areas?* The two questions seek to explore two different syntactic techniques: one for numerically illustrating what a pre-given area is in terms of space, called *the descriptive technique*; the other for detecting and simulating urban areas with regard to the continuous urban network, termed *the generative technique*. They are however related to each other. The descriptive techniques will help us achieve a better understanding of how the *existing* urban areas spatially interact with the whole network. This knowledge will allow us to explore the generative techniques, which perhaps can pave the way for revealing the spatial mechanism involved in the formation of urban areas.

Among the existing descriptive techniques, the widely used method was developed by Hillier (1987a, 1996) to illustrate the extent to which a pre-given area is spatially distinguished from the whole city. Based on a large number of empirical studies, he found a strong and significant correlation between the configuration of the urban grid, measured by integration (meaning how

[1] More accurately, it means a set of relationships among spaces all of which are interdependent in an overall structure. For the detailed definition of configuration, see Hillier (1996) pp.23. Chapter three will review the concept of configuration.

topologically close each space is to all other spaces[2]), and movement rates, and then proposed that the spatial configuration at the more globalised level, rather than at the individual level, is the primary factor that can be used to predict movement (1983, 1984, 1987a, 1988). Urban structure as spatial configuration shaped urban movement, and this then impacted on patterns of land use and building densities, feeding back movement and its relation to urban structure, and creating multiplier effects and created differently scaled centres of the kind normally found in well-functioning cities (Hillier, 1993, 1996). Hillier has also suggested that the part-whole structure of the city was shaped by local and global spatial configurations, correlated with local and global scales of movement (1996). Against this background, Hillier has proposed that the correlation between global integration (expressed by integration Rn[3]) and local integration (measured by integration R3[4]) can be seen as creating synergy between local and global movement, and used to identify urban parts: the steeper the slope of the regression line of a sub-area across the regression line for a whole city perhaps can imply this distinctive sub-area. This suggested the possibility of describing the boundary of a pre-given area by investigating the relationship between its internal layout and the context in which it is embedded. Other existing descriptive techniques will reviewed in chapter three.

Meanwhile, several generative techniques have been proposed in the existing syntactic studies. In a study of towns in Greece, Peponis (1989) proposed that the variable of choice – meaning the degree to which each space lies on topologically shortest routes between any pair of other spaces[5] – would be used to mark out boundaries of sub-areas, in the expectation that the boundaries of the sub-areas should have more through-movement as measured by choice than internal spaces. Later, Read (1999, 2003, 2005) studied Dutch cities and asserted that those cities usually comprise both global supergrid and local grids, self-similar but operating at different scales according to the differentiated movement speeds and the space-time

[2] Integration is a normalised measure of distance from any a space of origin to all others in a system. In general, it calculates how close an origin space is to all other spaces. For detail, see Hillier, B. and Hanson, J. (1984), pp.108-109. Chapter three will review this measure.
[3] Integration Rn reflects how close each space, as a root, is to all other spaces within a system. It is also called global integration. See Hillier (1996) pp. 119.
[4] Integration R3 measures how close each space, as a root, is to all the spaces only two lines away from the root. It is called local integration. See Hillier (1996) pp. 119.
[5] Choice measures the degree of choice each space represents - how likely it is to be passed through - on all shortest routes from all spaces to all other spaces in the system. See Hillier, B. et al (1987) Creating Life: Or, Does Architecture Determine Anything? pp.237. Chapter three will review this.

experiences. He proposed two techniques to explain this biplex urban structure. One was the integration gradient map, picking out streets with high global integration values relative to other streets directly connecting to them, as a way to highlight the supergrid. The other was the area integration map, indicating the concentrations of high local integration through giving a line the average of local integration values of all the lines within a topological distance of two or three – or within a certain metric distance from that line, as a way to highlight areas. However, both studies implied that the identified areas were the self-contained areas enclosed by the streets accommodating the high-speed movement rates (associated with higher choice or integration values).

Some other methods were proposed. Hillier (1987a, 1989) first suggested that sub-areas within a larger continuous fabric would be picked out by using a syntax technique of optimising correlations between spatial configuration measured by integration (calculated in the different scales of the contexts of the sub-areas) and the observed movement rates. Such kinds of sub-areas within urban districts were thought of as '*natural areas*', because their structure could best forecast movement rates. He further argued that those 'natural areas' are not cellular like Neighbourhood Units, but are the parts of a continuous urban network. Hillier did not disaggregate the urban network along the area boundaries defined as the linear spaces of higher choice or integration values, but picked out urban areas in terms of *the change in the correlation between integration and movement rate, as the contexts of these areas vary*. Later, Raford (2004), with Hillier, further developed the technique of the '*correlation contour*' map, meaning the definition of areas through the optimisation of the correlation between local integration and movement, and in this way distinguished sub-areas in the fragmented urban context of downtown Boston. However, those two studies focused on the correlation between syntactic and functional factors, and so that gave more weight to the functional dimension of urban areas, but did not further clarify the spatial mechanism in defining urban areas.

Later, Dalton (2006, 2007, 2011) developed a method he called *point intelligibility/synergy mapping*[6] (meaning that the intelligibility or synergy value of each same sized subsystem

[6] The calculation of the point intelligibility mapping was elaborated as follows: a fixed subsystem connected to a root line, such as the most localised 90 lines to that root, is first defined, and then

selected around a spatial root element is assigned to that root element) to differentiate area boundaries in terms of the relationship between local and global configurations. On this ground he argued that the area boundaries can be created by the configuration of spaces, and this would help us to understand the nature of neighbourhoods. Working with this student, and in parallel to this student's own work, Hillier (Hillier, Turner, Yang and Park, 2007, 2010) developed a technique of identifying urban parts by measuring metric mean depth from each spatial element to all others at a fixed radius (called *radius MMD*). Both these techniques suggested that the urban grid is spatially partitioned into different discrete parts across scales when seen in this way. And Porta suggested that street centrality, measured by variables of spatial configuration with geometric characters of plots, can applied to detect urban places (Porta, et.al, 2006; Porta, Romice, 2014). Recently Gil (2016) also addressed the role of metric variables in the identification of urban areas. Chapter three and four will review them in detail, and use the latter technique, in the development of which this student took part, as part of this thesis.

This leads to the core questions which this thesis eventually addresses: *might urban boundaries between areas in general be best identified in terms of some spatial relation between internal layout and external structures picked out at different scales, with the external perhaps not less important than the internal? Or, is there any way in which we can give more explicit attention to multi-scale contexts from the point of view of defining areas, following the clues that had come out of the earlier syntactic studies?*

In order to explore whether and how boundaries between areas would be identified in terms of spatial configurations at different scales, a diagnostic study of two area-scale developments, Canary Wharf in London and Brindleyplace in Birmingham, was carried out. One development intended to integrate and the other to segregate. This study investigated whether if so and how far the different spatial strategies in the two projects have resulted in different spatial configurations and different relations to, and effects on, the urban contexts. It also further

intelligibility of this subsystem, namely the correlation between connection and integration Rn, is assigned to the root. The point synergy mapping was computed in the similar way. For detail, see Dalton (2006, 2007, 2011). Chapter three will review those two measures in detail.

examined pedestrian movement patterns, both within the sites and in the surroundings, to see how far, if at all, each has impacted on the other. This allows us to further elaborate the existing syntactic ways of studying urban areas, and then explore the nature of the project boundaries.

This study suggested two primary findings. First, the project boundaries of those two cases can be spatially characterised and distinguished according to the way in which their internal layouts spatially interact with the contextual structures. For example, Canary Wharf has a much weaker relationship with its surroundings with increasing radius than Brindleyplace, and so that the former has a relatively harder boundary. And second, the change from the projects to the surroundings can be assessed as *a discontinuity* in the configuration of space, the discontinuity arising from the degree to which the spatial configuration of a project is related to the larger – even much larger- urban context of which it was a part. This seems to cast new light on what an area boundary might mean.

The aim of the thesis is then to try to *develop spatial techniques for identifying the discontinuities between urban areas in terms of spatial configuration, and explicitly exploring geometric and spatial mechanisms in the formation of the urban areas in relation to the discontinuities*. Then the study sets out to explore what becomes the fundamental idea of the thesis: that if there are syntactic discontinuities between areas, then this should show itself in some way in *the pattern of spatial connection of the urban grid outward from an individual space within each area*, where that individual space, as the root space, is at first directly connected to its neighbouring spaces, and then reaches the further spaces via the neighbouring spaces, and so on if necessary until all other spaces within the whole urban grid are counted with regard to the distance to the root.

Pursuing this idea, the thesis seeks to re-examine the basic syntactic entity: the *justified graph*, in which all spaces are represented as the nodes of a graph, one of them is put at the root and then all nodes at depth one from that root are aligned horizontally above it, all nodes at depth two from the root above those at depth one, and so on until all levels of depth from that root are calculated (Hillier and Hanson, 1984:106). The justified graph for any root space can be expected to illustrate the pattern of connection of the graph outward from the root. It represents

the way the root is spatially embedded into its surrounding spaces, according to the distance to them, as radius increases. We call this the *embeddedness trajectory* of a node in chapter four on methodology.

Can we then quantitatively measure the embeddedness trajectory reflecting the shape of the justified graph, and then detect any significant change along it? If so, perhaps this will enable us to find a method of investigating area discontinuities. The simplest and most basic measure for the justified graph is node count at a given radius, meaning the number of the spaces (denoted by nodes) encountered up to that radius, and thus the rate of change in node count approximately captures the variation of the shape of the justified graph in response to an increase of radius. This in fact suggests that the embeddedness trajectory can be numerically illustrated by tracing how node count varies with radius. The conjecture will be that *any discontinuity along the embeddedness trajectory (approximated by the significant change in the pattern of growth in number of nodes), if identified, can perhaps represent a kind of discontinuity in urban grid*.

In order to explore this conjecture, the thesis first investigates the mathematical relationship between node count and radius, based on both axial maps (defined as the least set of the longest straight lines which passes through each convex space and makes all axial links)[7] and segment representations (generated from axial maps, where axial lines are broken at their intersections) [8] of three large urban districts, London, Beijing and London Docklands, by plotting the logarithm of node count on the y-axis against the logarithm of radius on the x-axis, called *the log-log radius plot*, with an aim of getting a better understanding of the embeddedness trajectory. We select these three cases due to their different geometric layouts[9]: London is an organic and irregular structure developed over hundreds of years; Beijing is more like a traditional orthogonal structure, but also has evolved over hundreds of years; but most parts of the London Docklands comprise various large area-scale projects that had been developed and

[7] For detail, see Hillier, B. and Hanson, J. (1984), pp.17, 91; Turner, A., Penn, A., and Hillier, B. (2005) pp.428. Chapter three will review it.
[8] Segment map is a fine-scale representation of urban grid. For detail, see Turner, A. (2004) pp.26-27; Hillier and Iida (2005) pp.481. Chapter three will review it.
[9] Chapter five and six as well as their appendices will further give more introductions of these three regions.

constructed since the 1980s. This enables us to set the experimental analyses in a variety of complex contexts and so aim at a general result.

The thesis then examines the embeddedness trajectory of a group of axial or segment lines representing a pre-given area (illustrated by the log-log radius plot) and meanwhile explore whether discontinuities would be found along this trajectory. This aims to investigate whether we can objectively describe the pre-given area with regard to the shape of its embeddedness trajectory, and in this way we perhaps develop another descriptive technique to explore the nature of area boundary. Now we re-examine the project of Canary Wharf, in that the diagnostic study suggests that Canary Wharf is more spatially segregated from the surroundings and has a hard boundary, as the previous paragraph discussed.

Based on the above analysis, a new technique is proposed for detecting and simulating discontinues in the spatial configuration of urban grid. The thesis first tests the axial maps of London, Beijing and the London Docklands, respectively. Each axial line in the whole map is taken as the root of a graph, and the numbers of axial lines, found with increasing radius from the root is calculated, and expressed as a rate of change in node count (for a more detailed definition, see chapter four). This rate of change value, called *topo-embeddeness* measuring the topological rate at which lines are embedded into the context, is then assigned to the original axial line and expressed through bands of colour. The results show areal effects (See **Fig. 4.9** in chapter four), in that groups of neighbouring lines tend to have similar colouring surrounded by the discontinuities where values and so colours change, and this suggests *a periodic patchwork pattern*, meaning the urban grid is partitioned into a system of periodic patches representing urban parts. Red indicates the patches embedded into the surroundings at a lower pace, and blue denotes those embedded into the contexts at a higher pace. Then, the same experiment is repeated on the segment maps and produces *stronger* periodic patchwork patterns (See **Fig. 4.10** in Chapter Four) by *metric embeddedness* measuring the metric rate at which each segment embedded into the context. The almost same periodic patchwork phenomenon, based on the segment model, is also created by the variable of MMD at different radii (Hillier, 2007, 2010) which was described earlier.

The phenomenon of the periodic patchwork pattern then poses several related questions: *does the multi-scale periodic patchwork phenomenon mean anything in terms of spatially defined urban areas? What is the morphological mechanism accounting for the emergence of the patchwork pattern? And does the generation of the patchwork pattern give a heuristic approach to understand the area structure of city, such as the named area structure?*

The above questions will be investigated by conducing empirical studies of the named areas in the historic central districts of London and Beijing, as well as the newly developed areas in the London Docklands, respectively. The two cities were chosen as both seem to have different geometric layouts (as mentioned earlier). This comparative study provides a first test ground for the two key questions posed in this study: *are there clear spatial senses in which we can identify area structures in historic cities, and how they combine to form the urban whole in terms of the way they are spatially embedded into the contexts?*

We also examine the newly constructed areas in the London Docklands, because those areas were initiated and developed in the 1980s and 1990s, with an aim of transforming the derelict and segregated dock areas into the urban-like district comparable to the West End of London[10]; but most of the development areas with the functional plans were separated by green areas or by water, but connected to the rest of city mainly by motorway, underground 'tube' line and light railway (Brownill, 1990; Edwards, 1992, 1993, 1999). The London Dockland Development Cooperation (LDDC) had clearly specified the boundaries of the development areas that it initiated (LDDC, 1998). Since those development areas are relatively large, we further select smaller areas, such as clearly-defined housing estates, according to the combination of the index of household tenure in 2001 and the field observation (see Chapter Six). This empirical study allows us to examine the nature of those clearly defined boundaries enveloping the newly developed areas like housing estates and office centres in the Docklands, with regard to the interaction between internal and external structures at different scales.

[10] For the detailed objective of the development of the London Docklands, see the Monographs of LDDC (the London Dockland Development Cooperation) published in 1998, which is available at http://www.lddc-history.org.uk/planning/index.html#Foreword.

The above comparison between the historic areas and the newly developed areas not only enables us to test both the descriptive and generative techniques (as elaborated earlier) on the different cases, but also helps us establish the robust empirical ground for developing a conceptual model for explaining the spatial discontinuities in urban grid and how this relates to the nature of the boundaries of urban areas.

1.2 Outline of the thesis

Following this introductory chapter, this thesis takes the following form. **Chapter two** reviews and discusses the history of urban theory and practice and the part-whole problem. This chapter will describe and clarify the various notions of area boundary that have prevailed in previous literature. It focuses on the *spatial* view, rather than the socio-economic or functional interpretations, of defining urban areas. It starts by reviewing the works (e.g. Howard, 1898; Perry, 1925; Stein, 1929; Trip, 1942; Abercrombie, 1945) of those who intended to design new modern cities during the period between the end of the 19th Century and the middle of the 20th Century, and identifies the dominant idea that the *clear boundaries*, such as greenbelt, boulevard and arterial road, were treated as *separators* dividing the whole city into a series of territorially bounded parts, with the intension to support socio-economic, functional or physical differentiations, or even relieve traffic congestion. This is followed by a review of some selected literature, (Alexander, 1965, 1977; Kier, 1977; Aldous, 1992; Calthorpe and Fulton, 2001; Andres Duany et. al. 2001, 2002) written after the 1950s that had addressed the *permeable boundaries* as *connectors* that mediate the functions between urban parts, as well as the possible spatial connections between the centres of urban parts. In particular, a handful of texts (Jacobs, 1961; Lynch, 1960, 1981; Rossi, 1984) explicitly argued that urban areas cannot be defined by boundaries, but are marked out by their locations in the continuous urban fabric. This body of literature however did not suggest methods for precisely revealing spatial structure of a continuous network, nor did they clarify how far the continuous network is spatially related to the emergence of urban areas as well as the notion of area boundaries.

Chapter three moves on to review the relevant theories and methods of space syntax, and then conducts a diagnostic study which aims to explore new dimensions to be investigated and set

the stage for developing new syntactic techniques for this thesis. The first part discusses the syntactic methods which allow us to objectively represent and analyse a continuous spatial network (Hillier, 1983; Hillier and Hanson, 1984; Hillier, 1987a and b, 1996; Turner, 2001, 2004; Dalton, 2001, 2003; Hillier and Iida, 2005), and continues by focusing on the main theories and techniques for investigating urban areas (Hillier, 1987a, 1989; Peponis, 1989; Read, 1999, 2005; Hillier, 1996; Raford, 2004; Dalton, 2006, 2007; Hillier, 2007, 2010). These accumulated studies suggested that the syntactic relationship between the internal layout of an area and its external context is an essential factor in defining the area. In order to further explore the role of the contextual structures in the formation of area boundaries, the second part of this chapter continues by carrying out a diagnostic study of two large-scale developments, Brindleyplace in Birmingham and Canary Wharf in London (Yang, 2005). It mainly investigates whether the two contrasting projects have distinctive and specific interactions between their internal and multi-scale external structures, and if so, we will then examine whether those interactions impact on the spatial formation of the project boundaries. The analysis results suggest that the Canary Wharf project has a hard boundary in the sense that the interaction between the internal and the external changes significantly with increasing radius, which indicates the kind of *discontinuity in spatial configuration* discussed earlier; and in contrast, the Brindleyplace project has a soft boundary in the sense that such interaction remains relatively stable as the radius increases. As discussed in **Section 1.1**, this leads to an argument that the boundaries of urban areas perhaps would be considered of as the discontinuities in the way the areas are spatially embedded into the contexts with increasing scale, rather than the physical barriers locally enclosing them.

Chapter four concentrates on developing a methodology framework for this thesis. It begins by proposing a conjecture of discontinuity, as elaborated in **Section 1.1**, that spatial discontinuities between urban areas perhaps embody themselves in the way each individual space interacts with the contextual spaces within increasing radius. It goes on to discuss the methods for approaching this conjecture. By rethinking the idea of justified graph (introduced in **Section 1.1**), it proposes *the technique of the log-log radius plot* (described in **Section 1.1**) that allows us to *numerically* illustrate the embeddedness trajectory on which each axial line or segment (or even a pre-given area) is embedded into the surroundings with an increase of radius, and then detect the possible *discontinuity along the trajectory*, denoted by the inflexion points in the log-

log radius plot. This helps us to clarify the concept of discontinuity in spatial configuration explained earlier.

It goes on to suggest the variable of *embeddedness*, as discussed in **Section 1.1**, measuring the rate of change in node count. Based on the axial and segment representations of London, Beijing and the London Docklands, it seeks to develop a technique for detecting and visualising the discontinuities, if existed, in the spatial networks by indexing and colouring the values of embeddedness. Periodic patchwork patterns (see **Fig 4.9 and 4.10**) at different radii are created by both topo- and metric embeddedness, though the former produces the stronger patterns. Based on the segment representations, the technique is further compared to Hillier's technique for creating almost the same periodic patchwork pattern by measuring radius MMD (see **Section 1.1**), in order to qualitatively and quantitatively elucidate the relationship between those techniques. In theory, it speculates that radius MMD is a function of metric embeddedness, which will be empirically examined in the latter chapters.

The discovery of the patchwork patterns raises an important question of which spatial mechanism accounts for the creation of the created patches. It continues to discuss the methods that would be deployed to tackle this question, as well as the theoretical ideas that would be associated with these methods, such as *the theory of grid intensification* (meaning the reduction of block size to reduce average metric distance from all points to all others in an urban grid) (Hillier, 1999, 2007). This chapter ends with summarising all the methods that will be applied to the empirical chapters.

Chapter five reports a comparative study of named areas in the historic central districts of London and Beijing. It starts by comparing the spatial structures of the two cities (and their central districts), and this quantitatively shows that they are geometrically and spatially different. In particular, the central district of London, in spite of an irregular grid, is better connected, relatively denser and more integrated, than the central district of Beijing. This suggests that the historic named areas we investigate are embedded in different contexts.

By using the descriptive techniques (discussed in Chapter Four), this chapter then investigates how far the named areas (as pre-given areas) are embedded into the surroundings with increasing radius, with the intention to empirically clarify the role of the multi-scale contexts in defining these named areas. The analysis result demonstrates that all the named areas selected in each case, by and large, can be quantitatively distinguished from each other by plotting their embeddedness trajectories and investigating the discontinuities along the trajectories, although their differences can be more easily detected by examining their metric embeddedness trajectories (in the segment maps), rather than their topo-embeddedness trajectories (in the axial maps).

On this ground, the further analysis undertaken in this chapter seeks to investigate whether and how the boundaries of these named areas visually co-inside with the patches created by metric embeddedness and MMD across radii. The result shows that most of the named areas in the two cases (except for Marylebone and Mayfair of London and Shichahai of Beijing) are associated with the mathematically created patches at different radii, although they are not marked out all at once at a given radius; and the historic developments within those three outliers can be roughly matched by the smaller patches. It can be argued that the created patchwork patterns, representing the discontinuities in the spatial networks, can be used as an objective framework for investigating the historic named areas.

The research moves on to explore the spatial principles that perhaps act as constraints on the formation of the named area structures, seeking to arrive at a better understanding of the part-whole problem raised at the beginning of this thesis. It shows that all the named areas and the created patches (based on the segment representations), in general, can be morphologically classified into two groups, one of which has metric integration values diminishing from centre to edge (called *the centre-to-edge motif*), and the other which has high metric integration values increasing from centre to edge (called *the edge-to-centre motif*). This suggests that the former has a more intensified centre (in terms of the number of the segments encountered within a relatively small radius as a unit, called *the segment density*), but the latter has a more intensified edge. To a large extent, it can be suggested that each historic central district is an *unevenly* intensified grid comprising both higher and lower density parts. This therefore implies

that the boundary of each named area perhaps results from the change in the variation of the segment density from its internal layout to its external structures.

Chapter six studies the newly developed areas including the larger development areas and the smaller areas (see **Section 1.1**) in the London Docklands. The *exact same* family of syntactic methods used in the previous chapter is applied to this case study. The basic analysis demonstrates that the London Docklands, compared to the two historic central districts studied in the previous chapter, is much less integrated and has a much weaker relationship between the local conditions and the global structure, and as a consequence is spatially fragmented. This study allows us to test the syntactic methods in a different situation. First, this study shows that all the newly developed areas can still be quantitatively characterised and distinguished according to the embeddedness trajectories with the inflexion points denoting the discontinuities in urban grid, but their trajectories are more bended, compared with those of the historic areas of London and Beijing. It can be argued that the overall structure of the Dockland areas is inconsistent in the way those areas are spatially added up to the London Docklands. Second, it demonstrates that the majority of the smaller areas have some kind of visual correspondence to the created patches at certain radii, but nearly all the larger development areas cannot be marked out. Many of them, in contrast to the historic areas in London and Beijing, are not represented by a peak or a trough across radii. This suggests that the Dockland areas are not naturally developed to form a well-structured entity, denoted as either the centre-to-edge motif or the edge-to-centre motif. Third, all the created patches (based on the segment map) in the London Docklands, though not extending into the surroundings in all directions (compared with the historic areas), still arise from the change rate of segment density, and this geometric feature also might be deployed to interpret the spatial formation of the newly developed areas.

Chapter seven brings together all the findings of the previous chapters in light of the existing literature reviewed in chapters two and three, and seeks to obtain some generalised results perhaps accounting for the formation of area boundaries. It focuses on the role of contextual structures in describing and characterising urban areas, as well as the spatial mechanism for generating the periodic patchwork patterns. By examining notional cases, it proposes that urban grid might result from a combination of different layers of grid intensification, namely a single

centre-to-edge grid in which the centre of the urban grid as a whole on average is more intensified than the edge, as well as the periodic patchwork patterns in which the centre-to-edge motifs are mixed with the edge-to-centre motifs identified at a series of relatively local radii. Perhaps this process in theory can be called *the multi-scale grid intensification*, aiming to optimise, rather than maximise, metric integrations across radii. It then generates the unevenly intensified grid as a whole. On this ground, it can be argued that the area boundaries might be interpreted as a degree of spatial discontinuity in urban grid, where the relationship between the internal and the external changes significantly. This leads to a theoretical synthesis of the *fuzzy boundary* arising from the spatial interaction between the internal and the multi-scale external, in contrast to clearly defined boundary. This final chapter ends by suggesting social implications of the fuzzy boundary as directions for further research. The degrees of spatial discontinuities, arising from the spatial interactions between the internal and the external, might suggest varying degrees of mixing across social behaviours or groupings. This sets the findings of this thesis within the context of the most recent developments in space syntax research (Boffi, Colleoni, 2014; Law, 2017; Vaughan, 2018; Major, 2018).

Chapter Two: Literature Review

2.1 Introduction

What, in terms of space, are urban areas and how do these areas combine to form a city functioning as a whole? Organised in approximately chronological order, this chapter reviews the existing theories and practices on the *spatial* strategy and mechanism for generating urban parts and the whole. It also aims to identify the extent to which the spatial dimension has been clarified, and which spatial factors have been deployed to differentiate urban areas in those works. The thesis neither seeks to define urban areas in relation to socio-economic or functional factors, nor does it intend to investigate whether spatial layout of urban areas influences human behaviour and social activity, or whether social and economic variables shape physical and spatial environment. Such studies are beyond the scope of this thesis and will not be included in this chapter. This thesis focuses on the spatial ideas that have significant and extensive influence on the spatial design of urban areas in the twentieth century.

It begins by reviewing the works of those who intended to introduce different solutions for spatially organising urban areas and to envisage a new kind of urban layout during the period between the late 19th century and the middle of the 20th century. It brings into focus the part-whole problem by elaborating and comparing the various notions of *area boundary* discussed in those works.

It then goes on to focus and review the ideas proposed after the 1950s, that sought to criticize the new urban layouts developed before the 1950s and suggested alternative approaches for designing and constructing urban areas, a whole city and even an overall region. It aims to investigate how the notions of area boundary were then altered and modified, and specifically to examine whether those notions were conceptualised as spatial tools for separating urban areas from each other, or combining them together, in those works.

Towards the end, this discussion concentrates on a handful of studies that began to investigate whether urban areas, or their boundaries, spatially relate to the whole city as a continuous network of which those areas are the parts. It seeks to clarify whether and if so, how far those works offered an *explicit* and *rigorous* way for spatially describing and interpreting the continuous urban network and its relation to the formation of urban areas.

2.2 Area boundary discussed from the end of the 19th century to the middle of the 20th century

Let us first review how urban parts and their relationship to the whole were envisaged, described and interpreted, in regard to space, in order to tackle the numerous emerging urban problems, such as over-crowding and traffic congestion, during the period from the end of the 19th century to the middle of the 20th century.

2.2.1 Garden City and Social Cities

Among those works, Howard's Garden City, 'a town designed for healthy living and industry' (Howard, 1898/1965: 26), argued by Mumford (1945) and Osborn (1950, 1965), have had a far-reaching influence on the physical structure of the cities built throughout the world. Mumford (1945: 29) even claimed that the Garden City was a great new invention, similar to that of the aeroplane, taking form before our eyes at the beginning of the twentieth century, and becoming the dominant urban form of future. How did Howard spatially define urban parts and then visualise spatial structure in the Garden City?

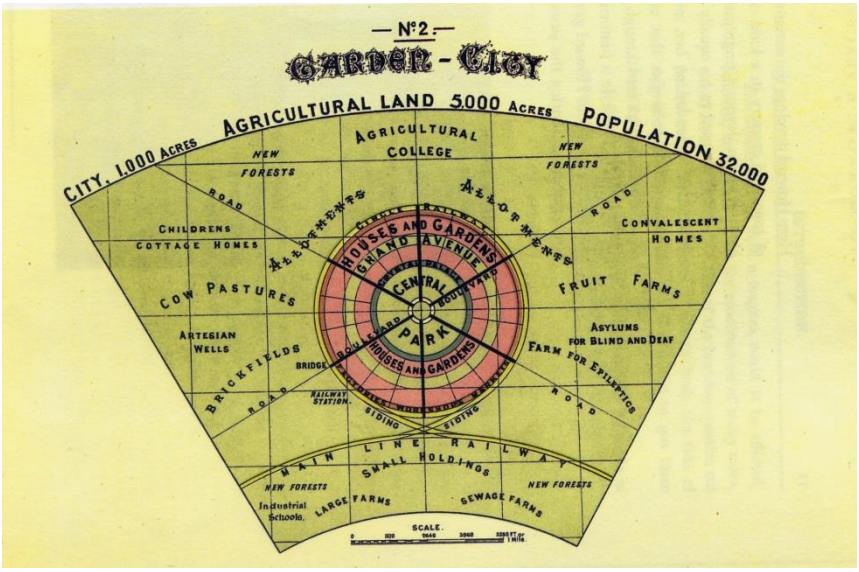

a Each Garden City, divided into six wards, is circled by a permanent greenbelt.

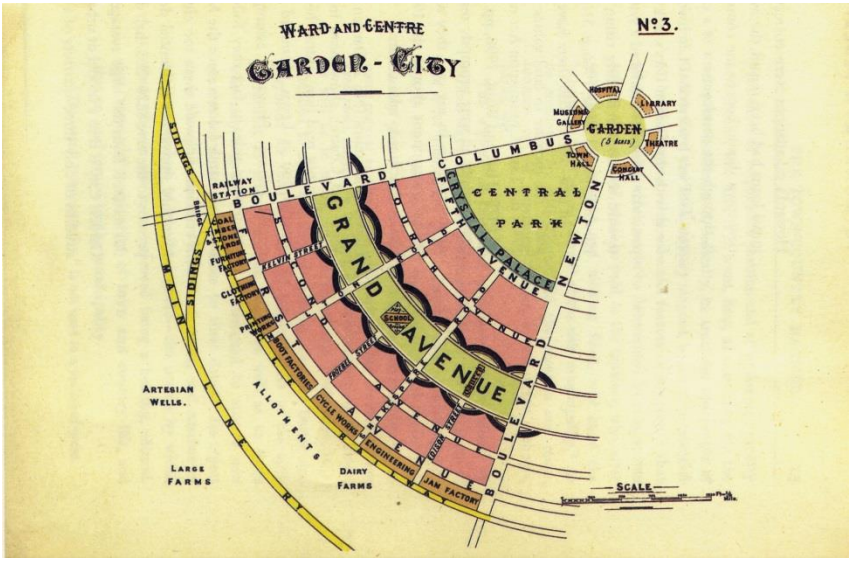

b Each ward is bounded by boulevards and divided into two parts by the Grand Avenue.

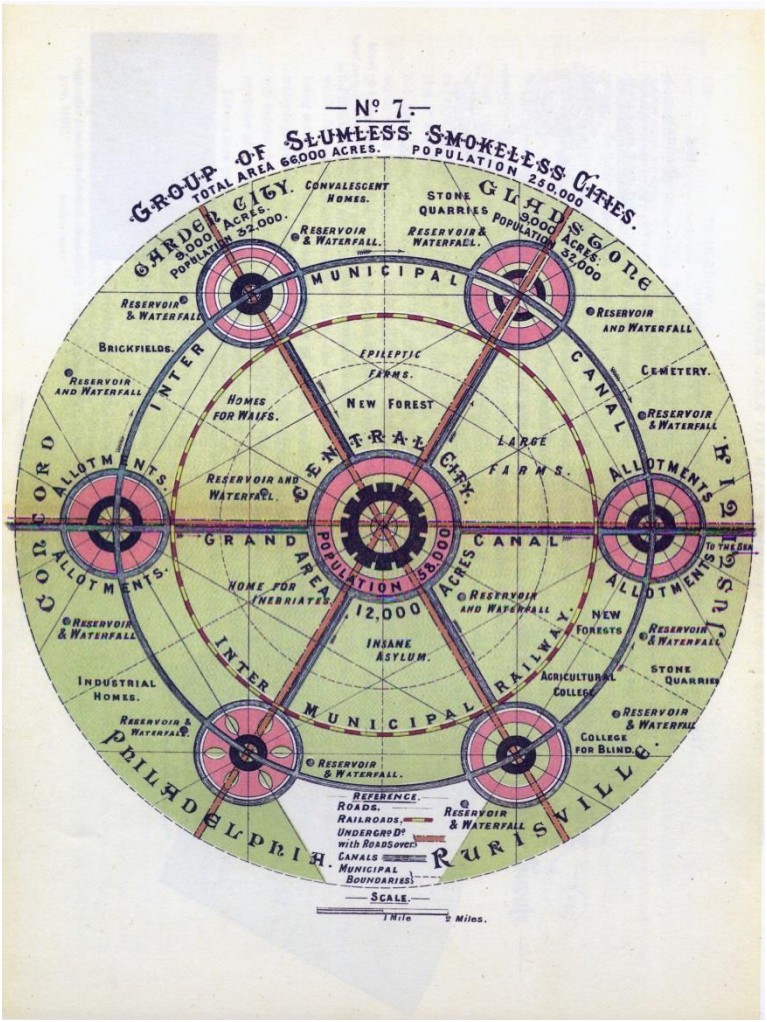

c Social Cities consist of several Garden Cities separated by greenbelts, but connected by a system of railways.

Fig. 2.1 The Diagrams of Garden Cities and Social Cities

(Source: Hall, P., Hardy, D., Howard, E. and Ward, C. ,2003)

His physical diagrams **(Fig. 2.1a, b)** illustrated that each Garden City of 1000 acres supporting a population of 32,000 was encircled and contained by a permanent greenbelt of 5000 acres. Each city comprised six equal wards enveloped by 120-foot wide boulevards. A belt of green, upwards of three miles long followed. This belt was called the Grand Avenue and was designed to divide each ward into two separate parts with different functions. A long line of frontage of the Grand Avenue was deliberately arranged in crescents, in an attempt to enlarge its splendid width (Howard, 1898/1965). This indicates that the wide boulevards and green spaces in fact functioned as the clearly defined boundaries of each ward and of each Garden City.

Howard also proposed a new pattern for a large city, termed *Social Cities* **(Fig. 2.1c)** in his book. This model depicted a group of the Garden Cities, separated by the permanent green belts, linked by the means of a rapid transit system to enable the inhabitants of each Garden City to be able to reach the neighbouring cities in five minutes by train. He envisaged that the future development of a large city, such as London, '*must inevitably follow – the planning and building of town clusters – each town in the cluster being of different design from the others, and yet the whole forming part of one large and well-thought-out plan*' (ibid, 1898/1965: 139). Here, the towns meant the Garden Cities that were well bounded and separated by the green belts, and functioned as the parts belonging to the larger city. This idea of a Social City has heavily influenced the spatial layout of city plans proposed by other practitioners and theorists, such as Stein's Regional City (1942), Abercrombie's Greater London Plan (1944) and Peter Calthorpe's concept of Regional City (2001). Those plans will be discussed in due course.

Raymond Unwin, one of the greatest figures of the Garden City movement, clarified further how the parts of the Garden City were spatially organised. In a paper of *On Distribution* published in the Town Planning Institute Journal (1920-1921), he said '*I believe that the proper distribution of the parts of the city and the clear definition of its various areas would do much to secure this (localisation of life) … it will be found that the proposed distribution will largely depend on the proper apportionment of open space around each area, and that this open space will serve two main purposes … and it will give a degree of definition to the area and separation from other areas which will emphasise the locality as a defined unit. Referring to the importance of defining areas, I may perhaps quote what I wrote in 1919 that these (green) belts can well define our parishes or our wards*.' (Quoted from Mumford, 1954: 262). Although Unwin mainly intended to relate the urban parts to daily life at the local level, he explicitly provided a spatial means of defining those urban areas, such as parishes and wards and by relegating the green belts and open spaces as their boundaries he separated them from each other.

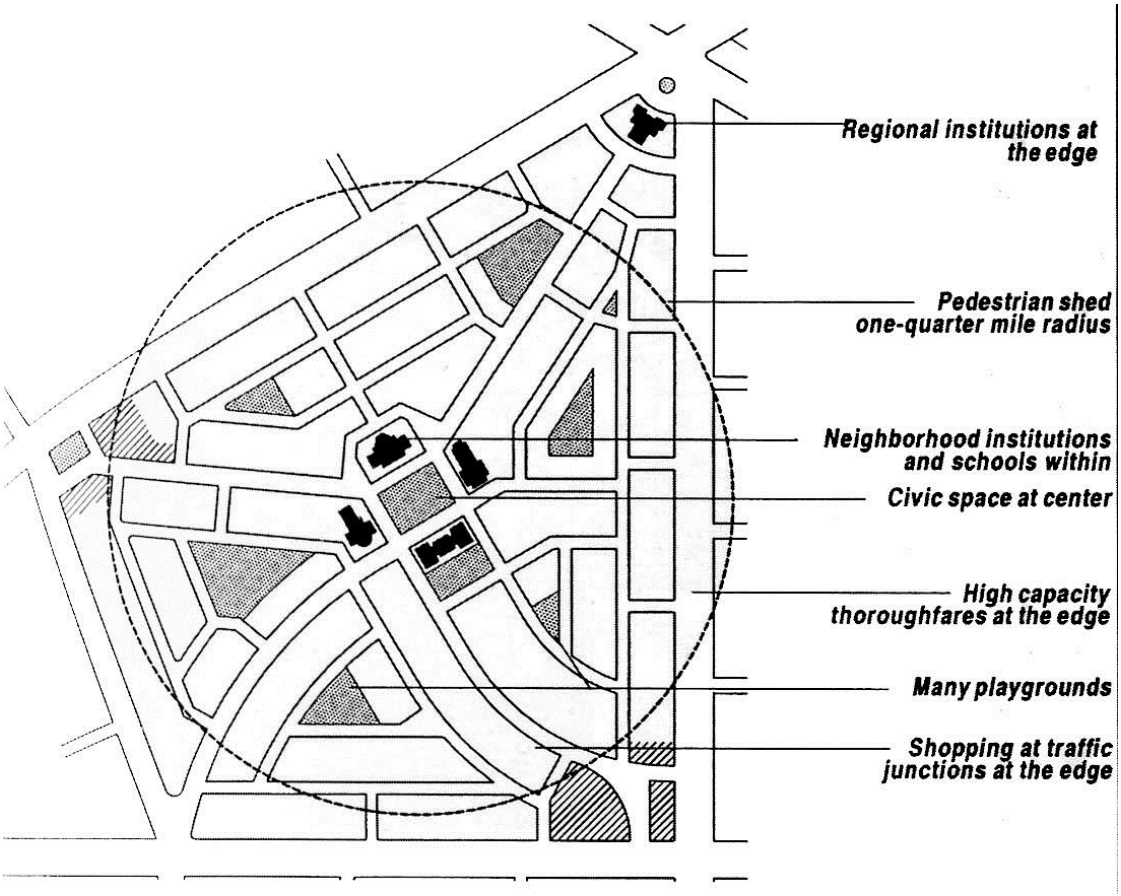

Fig. 2.2 Perry's Neighbourhood Unit. It is the five-minute walk catchment area bounded by the arterials. (source: Neal, 2003)

2.2.2 Neighbourhood Unit

Influenced by the Garden City movement, Clarence Perry, during the 1920s, proposed a new physical form for a modern urban area, called the *neighbourhood unit* (Abercrombie, 1944; Mumford, 1954; Johhson, 2002; Lawhon, 2009). He (1929) organised the neighbourhood unit around several spatially oriented ideas **(Fig. 2.2)**. First, arterial roads were consciously placed around, not through, each neighborhood unit, so that the major arterials defined and distinguished the place of the neighborhood, and by design, the unwanted through-traffic was eliminated from the neighbourhood. Second, the internal streets, arranged hierarchically and expressed in a curvilinear form, were distinctly different from those arterial roads as at the unit boundary. In this way, the internal structure was designed to discourage through traffic and enhance the safety of pedestrians. Third, the neighbourhood unit was sized to be the catchment

area of an elementary school and/or civil institutions located at the geometric centre of the neighbourhood unit. The distance from the school and/or the civil institutions to the edge of the neighbourhood was only about one-quarter of a mile and roughly a five-minute walking distance, so that residents could walk no more than a few minutes to reach the school and/or the civil facilities, without having to cross any major arterial roads.

To Perry (1929), the neighbourhood unit was *more than* just a local urban area to live. To him it was a unit, a well defined part of a city as a whole and an essential organ of a city, used to construct a city on a larger scale. As Mumford (1954) argued, Perry's neighbourhood unit led to a major change in the basic unit of physical planning, '*from the city-block or the avenue, to the more complex unit of the neighborhood, a change that demanded a reapportionment of space for avenues and access streets, for public buildings and open areas and domestic dwellings: in short, a new generalized urban pattern*' (1954: 260).

Perry proposed one way of describing how an urban part is spatially structured. It included two spatial factors: *1) the arterial roads as the boundaries of the neighbourhood unit; 2) the five-minute walking distance to the centre of the neighbourhood unit.* The former delineates the neighbourhood unit; and the latter measures the size of the neighbourhood unit. He did not however clarify the spatial way in which all the units were combined to form a city, but seemed to imply that the arterial roads encircling the units served to separate them, but also functioned to mechanically combine them into the whole city.

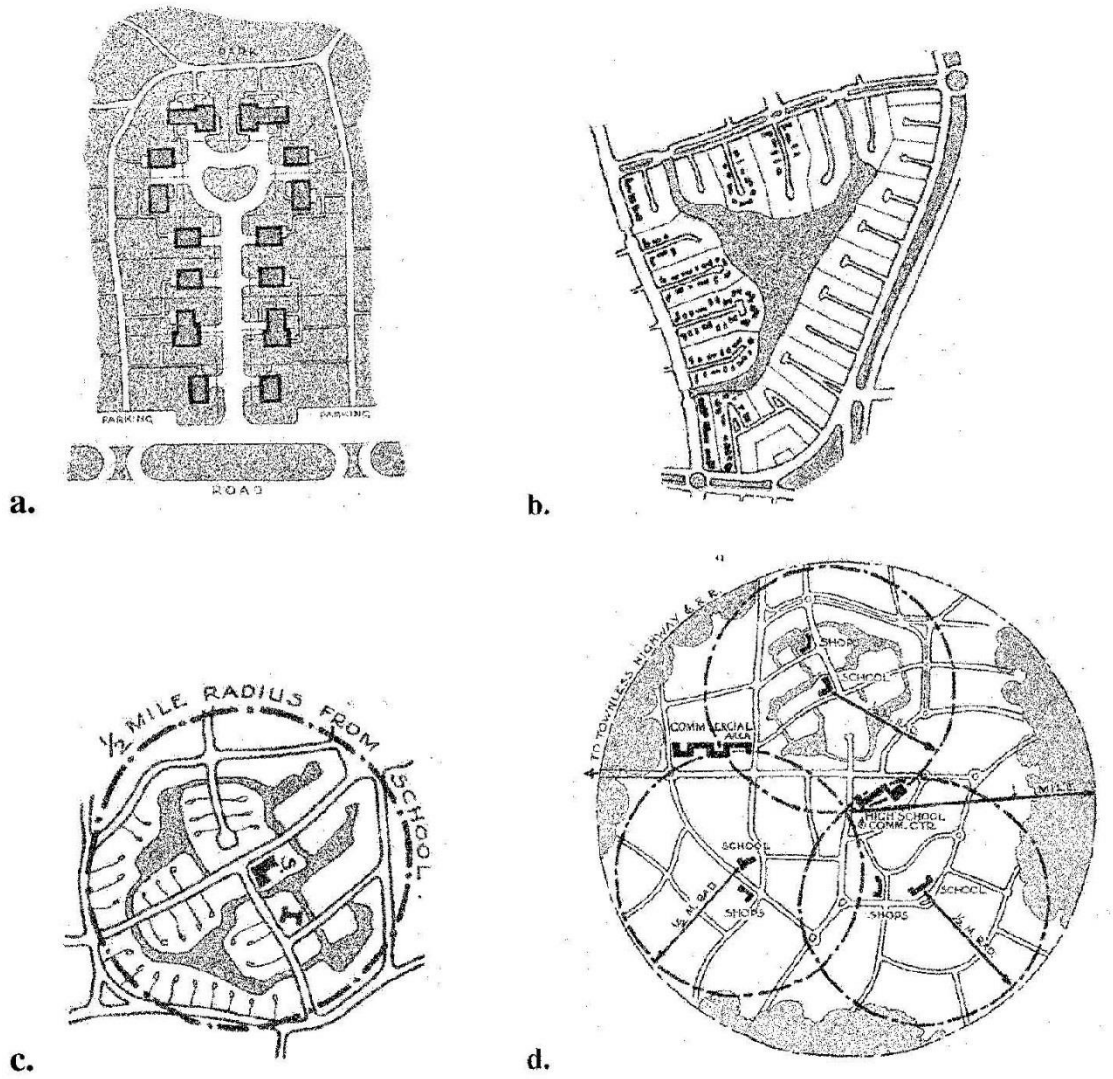

Fig 2.3 The General Plan of the Radburn Idea: a) a group of houses assembled around a wide cul-de-sac; b) a superblock with a centre green park; c) a neighborhood constituted by superblocks; d) a town aggregated by three neighbourhood.

(Source: Stein, 1942, quoted from Larsen, 2005)

2.2.3 Radburn Ideal and Regional City

Collaborating with Perry, Stein refined a system of street hierarchy, and then applied it to illuminate how the planned neighbourhoods were linked together to form urban districts, towns and cities at a regional scale (Stein, 1942, 1951; Mumford, 1954; Lawhon, 2009). Stein and Wright first designed a planned community named Radburn, in 1928 on 2 square miles for a

population of 25,000, with an aim of showcasing a new form of city for the motor age (Stein, 1942, 1951). In the Radburn project, they proposed an idea of the *superblock* **(Fig. 2.3)**. The superblock described several houses that were grouped around a 30-foot wide cul-de-sac to form a cluster of houses, each of which was then connected to an access road branching off the 60-foot-wide main roads that served as the superblock boundary. The clusters of houses were arranged around a central garden, the backbone of the planned neighbourhood. The cul-de-sacs on the garden side of the houses were connected to footpaths, which ran across the central garden. The living and sleeping rooms of the houses faced inwards towards the garden areas, while the service rooms faced vehicle access roads. The superblocks, enclosed by main roads, aggregated to form the town of Radburn. In this uniquely planned development the footpaths for pedestrians were linked together and ran across the main roads by underpass or overpass, so that there was a separation of pedestrian and vehicular traffic. This was maintained on a larger scale in the form of a town. This hierarchy of streets, together with the superblocks connected by parks and open spaces and manifest in the Radburn project, was known as the *Radburn Idea* (Stein, 1942, 1951). Mumford (1954) claimed that the Radburn Idea enhanced the urban system as a result of integrating a vehicular road plan with the fuller use of pedestrian streets and public open spaces. In general, the superblocks were spatially separated from the main roads accommodating automobiles, but at the same time linked together by the tree-lined footpaths and open spaces.

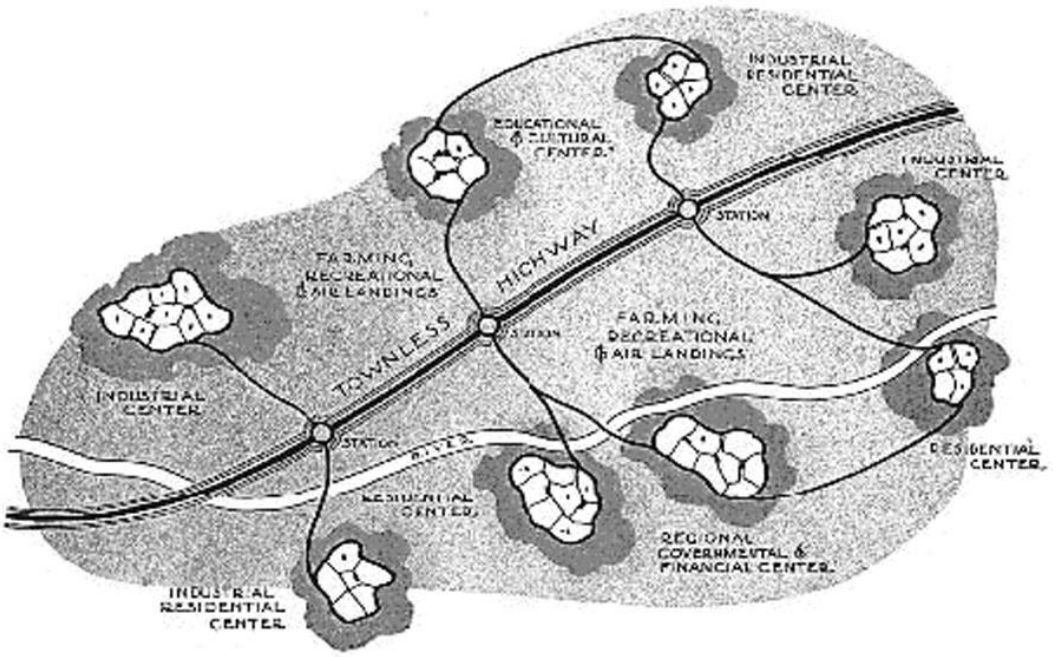

Fig 2.4 The Diagram of Stein's Regional City. It is a cluster the Radburn-like towns separated by the greenbelts, but connected by the townless highway. (Source: Stein, 1942, quoted from Larsen, 2005)

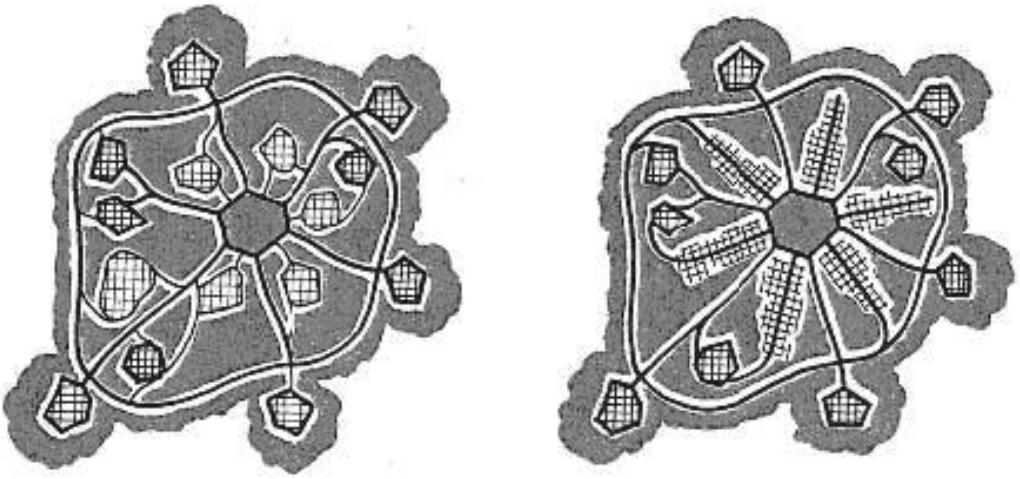

Fig 2.5 Two Proposals for Regenerating the Existing City into the Regional City.
(Source: Stein, 1942, quoted from Larsen, 2005)

During the 1930s, Stein further explored the spatial relationship between the superblocks, the Radburn-like towns, cities and region, and proposed the concept of the *Regional City* (Stein, 1942; Birch, 1980; Larsen, 2005, 2008). In his view, the superblocks, though varying in form so

as to effectively adapt to topography, were linked together by central gardens to form Radburn-like towns, and then those towns, surrounded by the greenbelts like forests, farms and recreational areas, were connected by a system of highways, called *the townless highway*, offering access to the towns via interchange stations, but not penetrating the towns **(Fig. 2.4)**. The educational, community, shopping and industry institutes were relegated to the geometric centre of those towns, and the size of each town was determined by the five-minute walking distance to those central institutes. In this way, a multi-centre metropolis, or a regional city, was expected to become an alternative to the existing big industrial city, as Stein (1942) asserted.

Stein further outlined a radical proposal **(Fig. 2.5 Left)** for reconstructing the existing central districts of cities that literally required the densest areas and slums to be replaced with gardens and parks, according to his Regional City concept (Stein, 1942; Larsen, 2005). He suggested that the city centre should be replaced by a large central park, and the existing main streets then reconstructed to create the townless highways which connected the redeveloped areas contained by the green spaces. In his less favoured alternative **(Fig. 2.5 Right)**, some of towns were allowed to be developed alongside the major highways, but still bounded by green space. With regard to spatial layout, he in fact borrowed the idea of Social Cities proposed by Howards and replaced the rail links between the Garden Cities with a system of highways. The Radburn-like towns were still clearly defined and contained by greenbelts, but expected to be linked by a hierarchy of roads.

Fig 2.6 Community Survey of London.

(Source: Forshaw and Abercrombie, 1943, 1944)

2.2.4 Tripp's precinct and Abercrombie's London Plan

In the UK, the Scotland Yard officer, Alker Tripp developed the concept of the traffic free precinct encircled by arterial roads onto which traffic flows concentrated. This was conceived as a new layout that protected a safe town life. In the book titled *Town Planning and Road Traffic*(1942), he discussed a new urban structure in which the central area was enclosed by an arterial ring road to which the arterial radial roads would lead from outside the town, a network of sub-arterials was arranged between the radials and within the ring, and the traffic free precincts, served by the local roads, were located between the sub-arterials. Like Stein, he also completely separated pedestrian and vehicular spaces by forbidding any contact between the ordinary pedestrian and the moving traffic on any arterial and sub-arterial roads. As a result, all precincts were segregated and bounded by the traffic arterials without any frontage development. '*On the one hand is the picture of town life in an ordered series of safe and*

sequestered precincts wherein every avocation is peacefully pursued in safety, and on the other is the present picture of those same activities missed up with a jumble of traffic, which means exposure to sudden death everywhere' (Trip, 1942:142).

This precinct idea, together with the neighbourhood unit and the Garden City movement, had been adopted in Abercrombie's London Plan as a solution to creating a completely new structure for London, but with the emphasis on identification of the existing communities (Forshaw and Abercrombie, 1943, 1944; Mumford, 1954). Abercrombie (1944). This at first distinguished the existing area structure of London **(Fig. 2.6)**, via the community and open space survey, and concluded that many of these communities can be traced back to the original villages which existed at the beginning of the twentieth century. On this basis, he carefully planned a hierarchical road network, combined with an open space system, running within the gaps between the existing communities and villages. The precincts were maintained or re-planned as residential communities, business or industry precincts. These precincts had clearly defined entry points at specific locations from the sub-arterial roads that clearly defined those precincts. The shopping centres would be arranged within the precincts rather than along the arterial or sub-arterial roads. The whole structure of this plan, Abercrombie suggested, was not only to reduce traffic congestion for efficiency, but also to provide quiet precincts for all social activities away from the noise, dust and danger of the main roads that had threatened London at the time. As a result, his London plan was in fact expressed as a series of more strictly defined areas.

2.2.5 Discussion

In effect, all these ideas and plans, more or less, implied a similar spatial expression of the part-whole relation. Urban parts are arranged as self-contained and pedestrian friendly areas, which would be physically confined or separated by boulevards, greens or arterial roads, and then simply and mechanically combined one by one into the whole city, but each part appearing as an island against the background of green or vehicle movement. At the level of neighbourhood, Howard's ward was spatially defined by wide boulevards. Perry's neighbourhood unit, Stein's

superblock, Tripp's precinct and Abercrombie's community area were all distinguished by the arterial roads acting as area boundaries, except Stein's superblocks which were spatially linked by the footpaths across the central green parks. At the level of town, both Howard's Garden Cities and Stein's Radburn-like towns were contained and surrounded by greenbelts, although the Garden Cities were connected by the railway to form Social Cities, and the Radburn-like towns linked by the townless highways to develop regional cities. All these works emphasised the idea of a *clear boundary*, either with a natural (e.g. a river) or artificial barrier (e.g. a busy road), that seemed to bound and separate urban parts. These studies did not however elaborate on whether the area boundary is able to act as a connector integrating and linking urban parts together.

2.3 Area boundary discussed after the 1950s

The concept of clear area boundaries had been widely criticised after the 1950s. The following section will continue to review the notions of area boundary discussed in other works since then.

2.3.1 Semillattice structure and thick boundary

In his seminal paper: *A City is Not a Tree*, Alexander (1965) argued against the idea that a city would be constituted by the compartmented and disassociated units with clear boundaries because this did not capture the functional complexity of a living city. He classified two ideal urban structures: a *tree* structure in which for any two parts belonging to the whole system, either one is wholly contained in the other, or else they are totally separated; and what he called a *semilattice* structure in which any two parts are overlapped and the common elements shared by these two parts also belong to the whole. In his view, Abercrombie's London Plan, for example, is a tree structure mechanically aggregated by the separated units, but a living city should have a semilattice structure. Thus, the Abercrombie Plan for London, he pointed out, implied the concept that any smaller elements within any one of those planned communities belong together so tightly that they only interact with the elements in other communities through

the medium of the communities to which they themselves belong. But this, he asserted, did not reflect the functional reality of London as a big city, in which people living in one community worked in a factory that was very likely to be in another community. He thought that the catchment areas of the smaller elements, such as elementary schools, grocery and youth clubs, within a community covered different sizes areas and therefore would be overlapped beyond the boundary of the community to form a semilattice structure (Alexander, 1965). Although he addressed that the failure to give physical expression of the semilattice structure had resulted in a vital consequence, functionally and socially, he did *not* clarify what the spatial form of such semilattice structure would be. He went on to discuss the psychological reasons why designers insisted on using a tree-like structure.

In a later text, Alexander (1977) abstracted 253 detailed patterns for regions, cities, towns, neighbourhoods, buildings and even a building's particular detail. This was developed as a language used to construct city or metropolis and based on the idea that larger patterns should be generated from the grass roots and each pattern should be connected to the other patterns, so that an overview of a whole project as the customised language would be generated by the interaction of the patterns. The patterns, he asserted, are the observed phenomena of buildings and/or cities that have been distilled from their own building and/or planning efforts. He did not however go on to illuminate the spatial mechanism for generating and aggregating those patterns, but instead assumed that a good city could be synthesized from all of them. For example he pronounced that the larger patterns of a metropolis consisted of a number of different smaller patterns of subcultures, '*each one strongly articulated, with its own spatial territory, its own values sharply delineated, and sharply distinguished from the others*' (Ibid: 48), under his assumptions that a group with a specific life style or cultural characteristic should correspond to a bounded space to protect its idiosyncrasies, by analogy to the differentiation of an ecological species being determined by the geographic isolation. In the same way, the patterns of subculture consisted of various smaller patterns of self-contained neighbourhood of not more than 300 yard across. Here, he seemed to present the tree-like structures that he opposed in his early paper.

Meanwhile, he (1977) returned to the concept of the semilattice structure by proposing the idea of '*thick boundary*'. This concept, when discussing neighbourhood boundaries, described the wide swathes of land with public facilities or commercial activities shared by several neighbourhoods. For him, the 'thick boundary' of neighbourhood was expected to function like a cell wall in its transactions with its surroundings. In order to form such a boundary, he addressed the feature of restricted access into the neighbourhood: the number of streets and paths leading to the interior of the neighbourhood was reduced, so that those few points where access was possible would become important. Meanwhile however those restricted points were enlarged to accommodate public meeting places for the common functions shared by several neighbourhoods. For example, the 'thick boundaries' would include a park, collector roads, small parking lots, a shopping street and a playground. In this sense, the neighbourhood boundaries, as he argued, not only acted to protect one individual neighbourhood, but also served to unite all neighbourhoods on a higher scale.

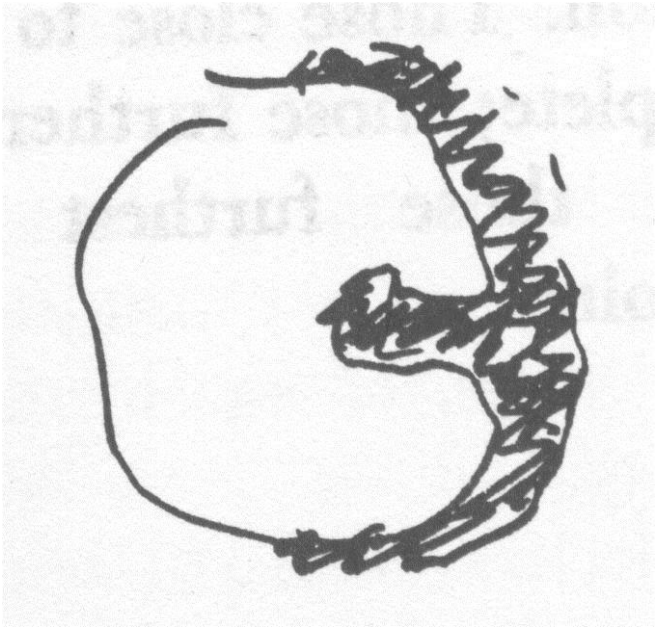

Fig 2.7 A Partial Horseshoe Pattern. Urban centre outside one neighbourhood would bulge into the geometric centre of the neighbourhood, and at the same time, extending itself along the neighbourhood boundary and thus forming a partial horseshoe hatched in black.
(Source: Alexander, 1977)

He further related the concept of ‘thick boundary’ to the neighbourhood centre. With respect to the neighbourhood centre partly defined according to housing density, he illustrated a rather simple pattern, the eccentric nucleus. The neighbourhood centre laid on the thick boundary for each neighbourhood which was closest to the nearest larger urban centre, under the assumption that there was only one larger centre. Furthermore, this neighbourhood centre would bulge into the geometric centre of the neighbourhood, and at the same time, extending itself along the thick boundary and thus forming a partial horseshoe pattern **(Fig. 2.7)** in terms of its location within the city. Alexander treated the ‘thick boundaries’ pattern as the overlapped areas of the semilattice structure which he discussed in the paper *A city is not a Tree*, yet he still did not accurately clarify either the physical expression of the semilattice structure, or the spatial mechanism to generate the ‘thick boundary’. In fact, he proposed *another kind of cellular structure* in which all cells are not only defined by, but also combined together by, the ‘thick boundaries’. The functional facilities are shared by several neighbouring cells.

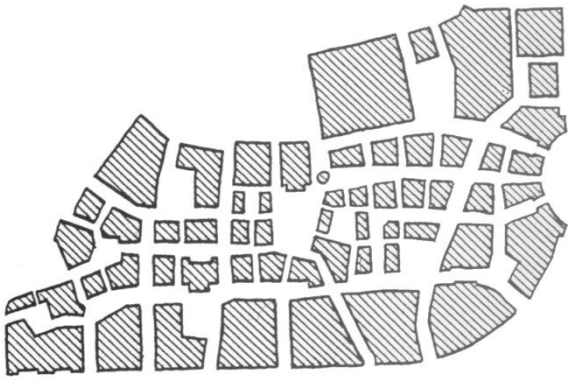

Fig 2.8 Urban Quarter with Smaller Central Blocks and Larger Peripheral Blocks.
(Source: Kier, 1977, 1998)

2.3.2 The cities within the city

By investigating how the historic quarters in the pre-industrial cities worked, Leon Kier (1977, 1998) proposed the idea of ‘*the cities within the city*’, denoting mixed-use urban areas, called urban quarters. In his article he integrated all functions of urban life, formal and informal, public

and private, in an attempt to criticize the mono-functional areas with clear boundaries developed in the first half of the twentieth century. He asserted that a city should only be constructed in the form of urban quarters that have the qualities of the whole city. Each urban quarter should include its own centre, periphery and readable boundary, and in this sense, each quarter was 'a city within a city', integrating all urban functions, such as for dwelling, working and leisure.

He then elaborated on how an urban quarter was spatially organised. Each quarter was built within a territory and dimensioned on the basis of a maximum of a 10 minute walk and no larger than 35 hectares; each quarter had at least one square and one high street at the centre and would never extend more than 900m in any direction. The boundary of the quarter was still coupled by boulevards, avenues, parkways, public gardens and golf courses. He then began to describe an urban quarter in relation to the geometric feature of its spatial layout. It was structured in a clear hierarchy of streets and squares to generate a regular grid, an irregular grid or a coherent mixture of both, in which the central blocks should be smaller than the peripheral blocks, **(Fig. 2.8)** so that a denser network around the central square would be created. This would introduce a sense of centrality in terms of the number of street corners, shop frontages, entrances and so on. In the street network of each quarter, cul-de-sacs and one-way streets would be avoided at all costs. Kier (1998:129) even argued that '*the number of street corners is an indicator of urbanity; the number of cul-de-sacs is an indicator of the absence of urbanity.*'

He further suggested that a borough was formed by four quarters, a city comprised a certain number of boroughs, and a metropolis consisted of several cities, so that an extended family of urban quarter, borough, city and metropolis finally created a multi-centre pattern of 'cities within the city'. The boroughs were distinguished by promenades with good connections to paths and tracks for walks in the surrounding areas. The cities were separated by greenbelts, such as parks, valleys, forests and agriculture lands. Here he implied that urban quarters and boroughs could be treated on a different scale from urban areas, and he also addressed the idea of area boundaries with good connections.

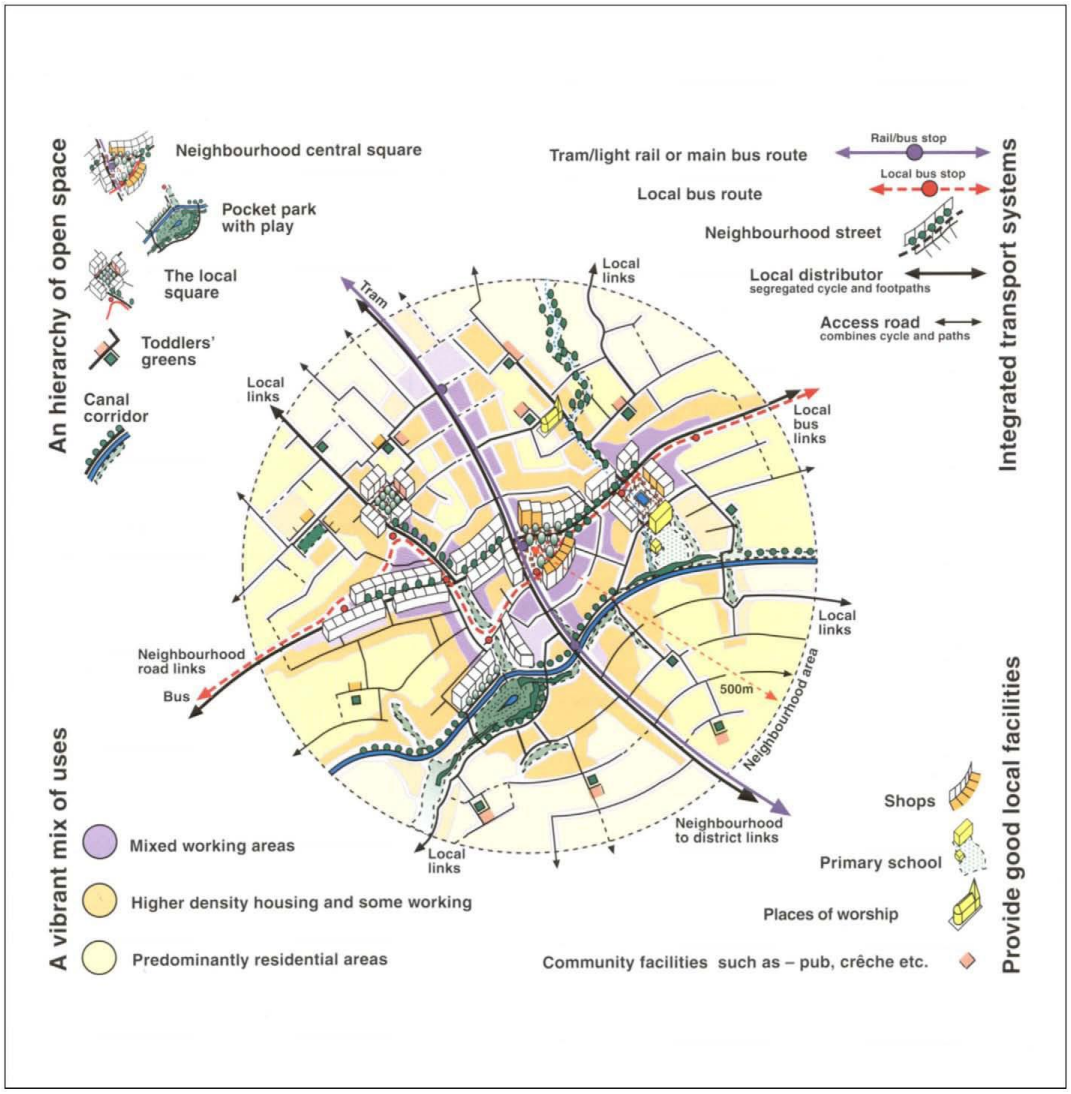

Fig 2.9 A Diagram of Urban Village.

(Source: UTF, 1999, 2002)

2.3.3 Urban village movement

Later, Krier's idea of '*the cities within the city*' had been embraced and developed in the Urban Village Group, of which Krier was a foundation member (Thompson-Fawcett, 1998, 2000). The formation of this Group was initiated by the Prince of Wales who was '*hoping we can encourage the development of urban villages in order to reintroduce human scale, intimacy and a vibrant street life*' (HRH The Prince of Wales, 1989: 4) in the introduction to his book of *A Vision of Britain: A Personal View of Architecture* (Neal, 2003; Rodwell, 2007). The philosophy and principles of a urban village concept, published in the *Urban Village Report* by Aldous (1992), argued for well-designed, compact, mixed use and mixed tenure urban areas, with minimal car

dependency. The urban village construct was supposed to be relatively self-sufficient in terms of the residents' needs for working, shopping, recreation and community life. In the late 1980s, Krier was already masterplanning Poundbury on the outskirts of Dorchester. Poundbury was the first development in the UK to be seen as a urban village according to the morphological principles elaborated in his article of '*a city within a city*' (Franklin and Tait, 2002).

In both theory and practice, urban villages were seen as a new model for innovative development in green or brownfield[11] sites, as well as urban regeneration in the existing developed areas of historic cities. Some parts of London and Paris still function in many everyday respects as a series of urban villages (Aldous, 1992; Neal, 2003; Rodwell, 2007). The spatial structure of the urban village **(Fig. 2.9)** was characterised by a mixed use community in a catchment area of a 500 metres radius around a public square incorporating transit stop and civic and commercial facilities, so that every facility was distributed within walking distance. A readable arrangement of public facilities, local squares, parks, local bus routes, streets, and footpaths radiate out from small blocks surrounding the central square to larger blocks on the periphery of urban village. Public transit, like light rail and bus routes, went through the village centre, and the mixed use land was developed along the pubic transit. At the regional level, a poly-centric grouping of villages was created by the link of public transit (Neal, 2003). All those descriptions about the spatial structure of urban villages were illustrated by the diagrams in the report of the Urban Task Force, *Towards an Urban Renaissance* (UTF, 1999, 2002; Neal, 2003).

[11] Brownfield site means abandoned or underused industrial and commercial land available for re-use and redevelopment.

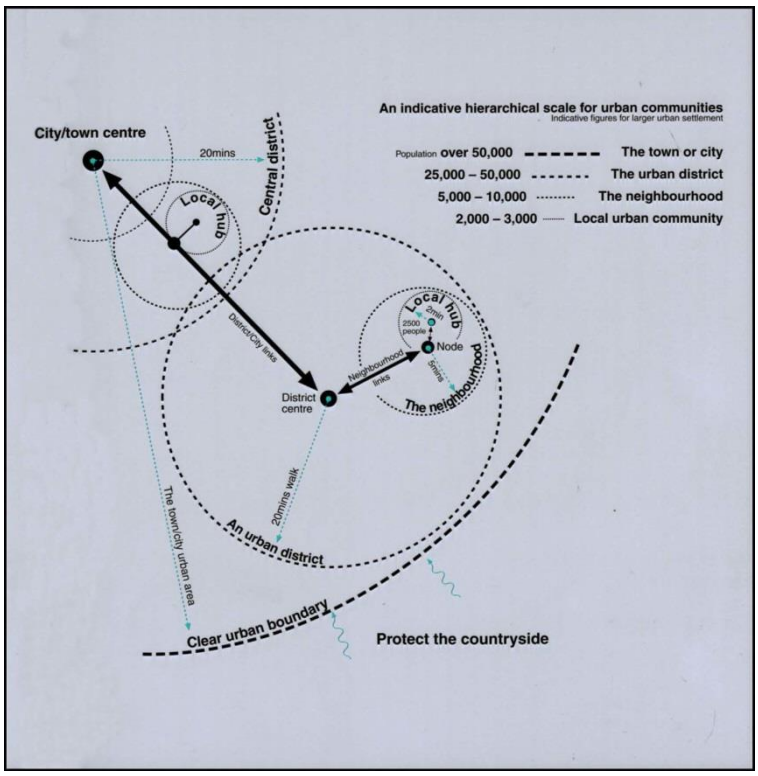

a A hierarchical scale of urban areas defined in terms of walking distance from centre to edge.

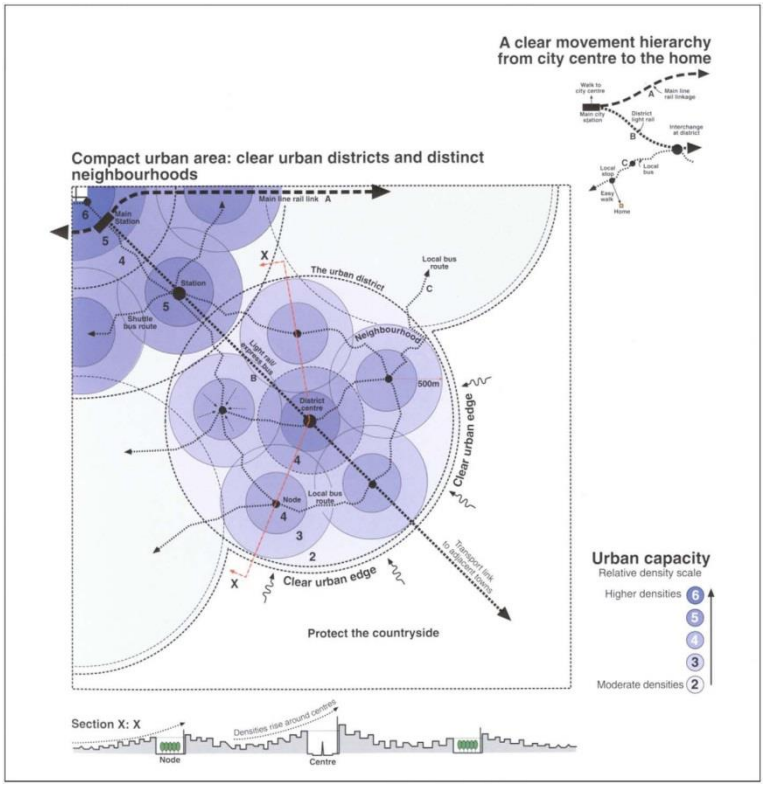

b A hierarchical scale of urban areas defined with regards to density (measured by the number of dwellings per hectare) from centre to edge.

Fig 2.10 A Hierarchical Scale of Urban Areas (Source: UTF, 1999, 2002)

A hierarchical scale of urban areas **(Fig. 2.10a and b)**, consisting of local urban community, neighbourhood, urban district, city and town or city, was further discussed in the report (UTF, 1999, 2002). On the one hand, all kinds of urban areas were defined with regard to *a fixed metric distance to the centres*. For example, the local community covered a two-minute walking distance catchment, the neighbourhood a five-minute walking distance catchment and the district a twenty-minute walking distance catchment. And all those urban centres were linked by public transit. On the other hand, urban areas were also defined in terms of *density*, measured by the number of dwellings per hectare, from centre to edge. Each area was structured in concentric bands of density, with higher densities around public transport centres, and lower densities at the less connected edges. The diagram also demonstrated that the boundaries of neighbourhood and/or districts overlapped each other, but cities were clearly bounded by greenbelts as a way to reduce low density development in the surrounding rural area.

2.3.3 New urbanism

It is striking that in North America in the same period we begin to find a very similar spatial model underlying the ideas about urban parts and the whole we associate with new urbanism. From the 1980s until now, a group of architects, builders and urban designers have promoted an influential and growing movement, generally called *New Urbanism*, which encompasses the Traditional Neighbourhood Development (TND) or Neotraditional Town Planning (NTP) developed by Andres Duany and Elizabeth Plater-Zyberk (1994, 1999, 2002) and the Transit-Oriented Design (TOD) synchronously articulated by Peter Katz, Peter Calthorpe, Doug Kelbaugh and Daniel Solomon (Katz, 1994; Calthorpe, 1994; Calthorpe and Fulton, 2001). We will review the TND and TOD models respectively in due course. In general, this movement, based on the return to pre-industrial urban forms and typologies, aimed to tackle the challenges of '*disinvestment in central cities, the spread of placeless sprawl, increasing separation by race and income, environmental deterioration, loss of agricultural lands and wilderness, and the erosion of society's built heritage*' by developing a new language of physical design (The Charter of The New Urbanism, 1996: 1). It reaffirmed the well-defined, mixed-use local area,

termed *neighbourhood* in the Charter, as the basic building block of the liveable districts and cities, a network of places rather than functional zones[12].

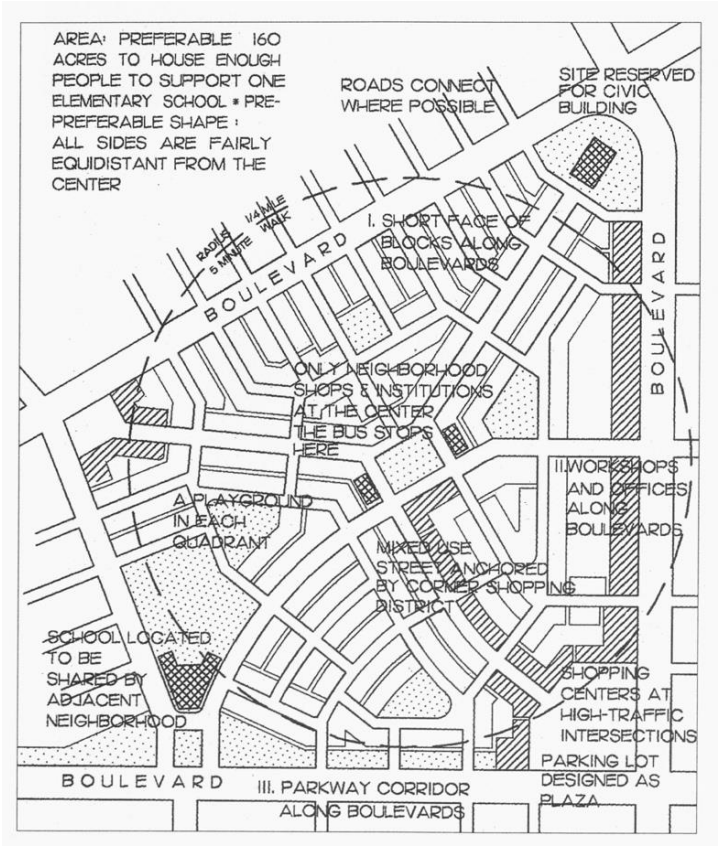

a The Diagram of the Traditional Neighbourhood Development (TND) Drawn in 1994 (Source: DPZ, 1999)

[12] Functional zoning, in general proposed in the Athens Charter of CIAM (the International Congress of Modern Architecture), means that a city would be rigorously divided into different functionally specialized zones, such as living zone, working zone, recreation zone and so on, in order to make functional zones and the whole city more efficient, rational and hygienic. For detail, see Le Corbusier (1947) Concerning Town Planning. London: The Architectural Press. pp.61-65.

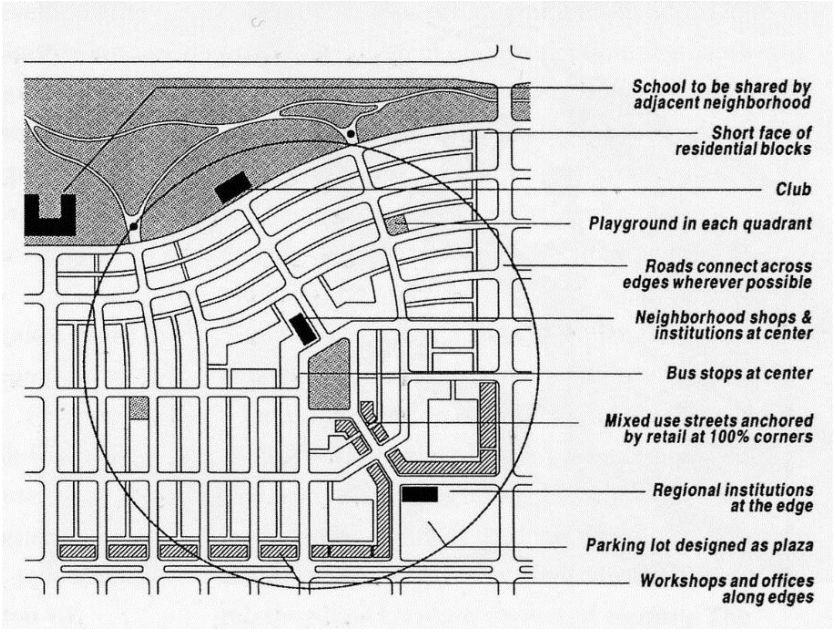

b The updated version of the Traditional Neighbourhood Development (TND) illustrated in 2002 (Source: DPZ, 2002)

Fig 2.11 Two Versions of the Traditional Neighbourhood Development

The TND attempted to update Perry's neighbourhood unit by moving primary schools and more local institutes to the edge of the unit and in the meantime intensifying the internal grid. This has been demonstrated by the diagrams **(Fig. 2.11)** which are illustrated in the *Lexicon of New Urbanism* (DPZ, 1999, 2002). Compared to the diagram of Perry's neighbourhood unit **(Fig. 2.2)**, the diagram of the TND developed in 1994 and 2002 still shows that the neighbourhood covered a similar sized area, bounded by main roads and scaled to a five-minute walking distance. However, the boundaries of the TND were connected to more alleyways and lanes planned within the neighbourhood; a mixed use main street, with a higher percentage of local shops and business, leaded from a corner of neighbourhood to the central park. An increased area of land along each boundary was reserved for retail units and offices, in order to make these boundaries more active. In particular, a bus stop was placed at the centre of a neighbourhood and the bus route was organised to link several neighbourhoods together, or extend to the regional centre.

The version of the TND developed in 2002 further intensified the internal structure and supported a morphological transition from rectilinear streets at the urban centre to curvilinear

roads toward the rural edge. The new version of the TND was still however spatially defined by the active boundaries or the five-minute walking distance from centre to edge. In the view of Duanny and Plater-Zyberk (1994, 1999, 2002), the TND was characterised by both the centre and the boundary. The former was always a public space or an important street intersection, associated by post office, meeting hall, day-care centre, shops, workplaces, or religious and cultural institutions; and the latter might be defined by natural forest, farms, orchards, woodland, wetland, very low density residential use, public open land, parks, schoolyards, high traffic thoroughfares, railway, boulevards or main streets, in terms of the location of neighbourhood in a region.

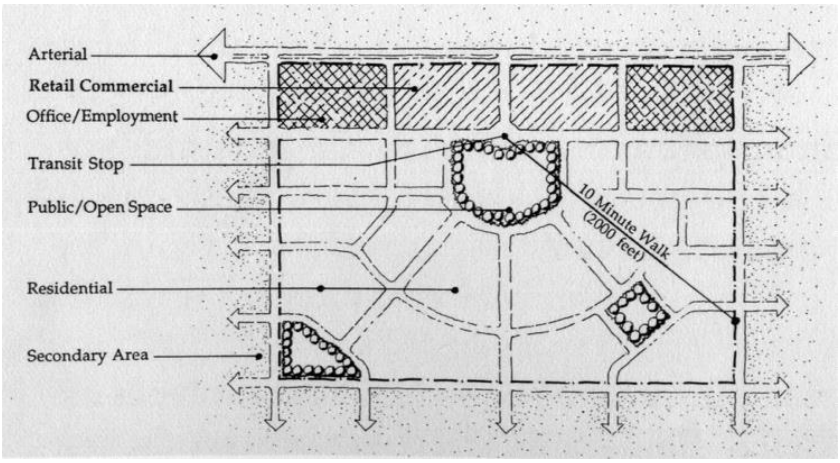

Fig 2.12 The Diagram of the Transit Oriented Community. It was developed along the arterial and around a transit stop. (Source: Katz, 1994)

The *Transit Oriented Development* (TOD) **(Fig. 2.12)** embodied various similar ideas as the TND concerning pre-industrial urban forms, but it had evolved from the concept of the *Pedestrian Pocket*, meaning the idea of a small town or village structured primarily around public transit, such as a light rail station, with the needs of the pedestrian in mind and to enable residents of one pocket to travel conveniently to other pockets and to big cities (Kelbaugh, 1989). Once again, the idea of the five- or ten-minute walking distance from centre to edge determined the size of the TOD. Each transit stop catalyzed a neighbourhood planned for high density development and organized around pedestrian friendly high streets, squares or parks. The boundaries of the TODs varied in character: In rural districts, the boundaries were usually

defined by green belts; in towns and cities, they were often arterial ways or transit lines (Calthorpe, 1994; Calthorpe and Fulton, 2001).

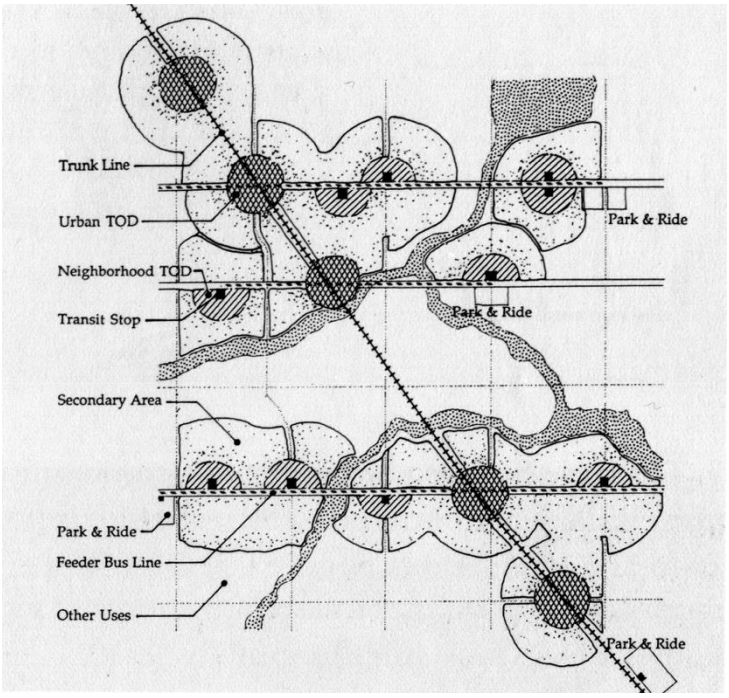

Fig 2.13 The Diagram of Katz and Calthorpe's Regional City. Various communities, neighbourhoods, districts, towns and cities are linked by the transit lines. (Source: Katz, 1994)

Based on the concept of the TND and the TOD, an urban district was expected to be built via groups of neighbourhoods; a town or city was aggregated by several urban districts. Corridors, ranging from arterials to wildlife trails, rivers or rail lines, acted as the connectors or the separators of neighbourhoods, districts and cities (DPZ, 1994, 2002; Calthorpe, 1994, 2001). *The neighbourhood, the district and the corridor* were treated as the three essential elements of development and regeneration in a metropolis, and in particular the corridor characterised by its visible continuity was considered as the most important element in the formation of the metropolis. On this basis, Calthorpe (2001) further formulated the idea of *Regional City*[13] **(Fig. 2.13)**, meaning a constellation of neighbourhoods, towns, cities and suburbs linked by *light rail*.

[13] Calthorpe's concept of Regional City is slightly different from Stein's idea of Regional City reviewed in section 2.2.3, because Calthorpe addressed that neighbourhoods, towns and cities were linked by light rail, but Stein proposed that towns were connected by a system of highways.

Calthorpe's theory shares remarkable similarities with Howard's concept of Social Cities, where a cluster of independent Garden Cities would also be linked by rails.

2.3.4 Discussion

In summary, Alexander's semi-lattice structure (1965, 1977), Krier's urban quarter (1977, 1998), the Urban Village movement (Aldous, 1992; UTF, 1999, 2002; Neal, 2003) and the New Urbanists' models (DPZ, 1994, 2002; Calthorpe, 1994, 2001), all evaluated that a living city cannot be constructed through clearly bounded areas, and then attempted to give emphasis on the *overlapped or accessible* boundaries in which shared facilities and services are located. Morphologically speaking, Alexander addressed the idea of *'thick boundary'* in that wide swathes of public spaces, associated with public facilities and institutes, were arranged between the limited roads leading to the internal structure of neighbourhoods, as well as the concept of the *eccentric nucleus* that the neighbourhood centre was located on the 'thick boundary'. Krier's urban quarter, the Urban Village Movement and New Urbanism concentrated on *a fixed walking distance from centre to edge, the permeable and active boundaries of neighbourhood and the well-bounded central square with public transit stop*, in an attempt to spatially characterise neighbourhood and its relation to the urban whole. In addition, Krier differentiated the urban quarters by *the gradient of the block size from centre to edge*, and the Urban Village movement marked out urban areas, ranging from neighbourhood, district to city, according to *the variation of development density from centre to edge.* The New Urbanism movement addressed *the corridors, ranging from boulevards and light rail to rivers*, as the connectors in sustaining urban areas. All the ideas seemed to imply the interconnectivity, rather than the separation, between urban parts.

2.4 The continuous urban grid

A handful of texts after the 1950s *explicitly* argued that a city is *a continuous network* and urban parts cannot be mainly determined by their boundaries or centres, although those works also discussed the features of area boundary or centre. The following section will review such works.

2.4.1 Street neighbourhood

In Jane Jacob's book titled *The Death and Life of Great American Cities*, she called for the abandonment of conventional ideas such as the neighbourhood unit, and argued that urban areas in cities were '*significantly defined only by their fabric and the life and intricate cross-use they generate, rather than by formalistic boundaries*' (Jacob, 1961: 193). In her view, any idea of neighbourhoods as cosy, inward-looking and self-contained units was harmful to cities. This she argued was because the residents in a city would move around the whole city and would choose from the entire city for friends, job, recreation, entertainment, and even education sometimes, and thus the neighbourhood units, as the parts of the city, would not work without this fluidity of use and choice throughout the city as a whole. She also pointed out that urban citizens usually understood and emphasised with the concept of neighbourhood, because they cared about the street or district where they lived and at least used some common facilities or services within a fragment of the city, during their daily lives. A city, she argued, was not an accumulation of repetitious neighbourhoods or towns, and paradoxically a stable urban neighbourhood was physically, socially and economically generated by the fluidity and mobility of cross-use through the entire city (ibid, 1961).

She then explained further the part-whole relation in forming a living neighbourhood, in spite of that her focus was obviously the socio-economic aspects of urban parts and the whole. The neighbourhoods were classified into three kinds: *street neighbourhoods* (defined as physical, social and economic continuities on streets but at small scale), *districts* (serving a population of 100,000 or more in big cities), and *the city as a whole*, because the urban individuals were assumed to simultaneously operate and manage at street scale, on district scale and in the neighbourhoods of the city as a whole (ibid: 117-129). But these three sorts of neighbourhoods, defined by Jacobs, were supposed to have different functions and complemented each other to form a real city. The street neighbourhoods were supposed to have functions for enhancing urban safety through public surveillance, cultivating continuity of public life, building social trust and helping assimilate children into responsible and tolerant urban life. The neighbourhood as the whole city was considered as the source from which administrative and policies were made, different communities of interest were formed and economic activities were raised. The

neighbourhoods of the districts were expected to mediate the functions between the street neighbourhoods and the neighbourhood as the entire city. For example, the districts would help distribute the resources of the whole city to the individual streets, or would turn the experiences of street life into a policy for the whole city.

On these grounds, she finally outlined a simple procedure for *physically* designing the neighbourhoods of the districts and then strengthening their individual identities. First, the living and safe streets should be created; second, these streets should be constructed and connected into a *continuous network* to form a district; third, open spaces and public buildings should be properly allocated in the network, in order to intensify and knit together mixed use land rather than isolate different uses or districts and neighbourhoods.

In addition, Jacobs pointed out that the boundaries of conventional neighbourhood units or their adaptations, whether formed by arterial roads, industrial parks, institutions, green spaces, or any other massive use of special land, usually inclined to create dead ends for most users, and consequently, the streets connected to the boundaries would get no or less uses from the people inside the units. As a result, it generated a dead barrier between the units, and this deadness would be further extended into the internal areas of the units along the streets adjoining the streets next to the boundaries, until a heavily used attractor was met. She proposed a number of solutions for the problem of dead boundaries: high density of population near boundaries; especially short blocks close to boundaries; extreme fluidity of street usage across boundaries; mixtures of land usage and in the age of buildings on boundaries (ibid: 259-269). However, Jacobs did not clarify further the spatial mechanism of a urban network in generating urban parts at different scales, but addressed the social and economic variables.

2.4.2 Sequential continuity

The idea that urban parts can be characterised in relation to a continuous urban network is endorsed by other writers, such as Kevin Lynch. He however openly opposed the idea that a city is only composed of segregated urban units. In the study of the legibility of the cityscape,

meaning '*the ease with which its parts can be recognized and can be organized into a coherent pattern*' (Lynch, 1960: 2-3), Lynch (1960, 1981) gave a spatial dimension to the differentiation of urban areas, named *districts* in his book. He argued that the 'district' was one of five elements for people to use to structure their city. The other elements consisted of path, edge, node and landmark. Districts are conceived as a two-dimensional entity, which people can mentally go inside or outside, and which are identifiable as having homogeneous characteristics, such as physical appearance, noise, and even the feel of getting lost. He spoke about the typical features with which to recognize districts and the clues which are continuous throughout the whole structure of the districts and discontinuous elsewhere. These clues would be generated by spatial characteristics, such as the narrow sloping streets of Beacon Hill, or by building type, such as the swell-front row houses of the South End, or by typical building feature, like the white stoops of Baltimore, or by *a continuity of colour, texture, or material, of floor surface scale or facade detail, lighting, planting, or silhouette* (ibid: 103-104). If the combination of three or four such features appeared and overlapped throughout a district, this unified district might be distinguished immediately. He further argued that the continuity of physical features within a district may coincide with certain kinds of social activities and uses, ensuring a sense of the district.

Apart from such continuity, he indicated that most people would point out the approximate location of a district boundary. Some boundaries may be hard and precise, such as a motorway, riverside or green park; the others may be soft, uncertain and permeable, such as the border between a shopping zone and an office district in a downtown area. In addition, some districts may have a strong centre with a gradient of physical characteristics which fade away. He argued either boundaries or centres had less to do with constituting a district, whilst limiting or strengthening its identity. A good city has a *continuous* network, rather than a series of bounded cells (Lynch, 1981:401).

Like Jacobs, Lynch (1960, 1981) also asserted that people can identify urban areas of a city, because they move around in the city and function within it. He also gave further explanation in terms of spatial relations. In his view, an urban area sensed as a whole would be demarked by *the network of sequences*, meaning a sense of interconnectedness or intervisibility at any level

or in any direction among five types of elements, namely paths, edges, nodes, districts and landmarks. '*District may join to district, by juxtaposition, intervisibility, relation to a line, or by some link such as a mediating node, path or small district. Beacon Hill is linked to the metropolitan core by the spatial region of the Common, and therein lies much of its attraction. Such links heighten the character of each district, and bring together great urban areas*' (Lynch, 1960: 104-105). Thus, the pattern of a whole district would be gradually developed and conceived by sequential experiences, reversed and interrupted, so that each part would flow from the next to form a sense of wholeness, which Lynch called *sequential continuity* (ibid:115). On these grounds, Lynch (1981) asserted that the sense of urban area may stem from the organised sequences within the continuous fabric as a whole rather than within the well-bounded neighbourhoods. It seemed that Lynch was attempting to analyze the formation of urban areas and the part-whole relation from the perspective of sequential linkages and directional relations within the street network. He did not provide a precise way of illuminating and measuring those sequential links and directional relations within the continuous network.

2.4.3 Study area

Regarding this issue, we can return to Rossi (1984: 63) who also argued that urban part, identified as the *study area* in his book, can be defined and interpreted by comparison to other larger elements of the overall urban fabric, such as the street system. The study area, he further clarified, was *an abstraction*, in terms of the spatial context of the whole city, as well as the history of the city. For example, in order to characterise one urban part, it was useful to investigate the physical surroundings that demarcated its immediate urban context, and the historical events that coincided with the development of the part. On the one hand, the whole city emerged from the process of integrating its different study areas over the years; on the other hand, the different areas obtained their own features embodied in form and space, but understood by the evolution of the whole city. In this sense, '*the study area always involves a notion of the unity both of the urban whole as it has emerged through a process of diverse growth and differentiation, and of those individual areas or parts of the city that have acquired*

their own characteristics' (Ibid: 64). He in particular stressed that the concept of the study area had *no* relation to Perry's neighbourhood unit or any sociological implications.

In his view, the formation of the study areas can be identified through their location within the whole city, their imprint on the ground, their topographic constraints, as well as their physical appearance which he saw as representing a consistent mode of living, involving a whole historical transformation. He claimed that each study area, identified from the whole structure of a city, reflected one moment in the history of urban growth or renewal. This would be identified by the typological and social homogeneity of the area and would be composed of a similar type of building accommodating persons who had the collective memory and shared a similar way of life.

Each study area, he argued, had its own characteristics, morphologically, historically and possibly also linguistically, and which could be manifested in the mass and density of the study area. He imagined that the city was distinguished by those characteristic areas, rather than simply functional zones. The study areas would also be used to construct the complex, but objective urban whole. As a result, the relationships between the study areas, he emphasized, cannot be interpreted as a kind of functional interdependence, but rather as the reaction to the entire urban structure that had evolved over the years. In other words, the different features of the study areas mainly depended on the historical process through which the whole city came into existence. Here, he in fact added a temporal dimension for describing urban parts and their relationship to the whole. Although Rossi's characterisation clearly also has a spatial dimension, he again gave no clear or explicit account of the role of spatial structure in the formation of urban parts, but gave priority to physical and historical characteristics of these urban parts.

2.5 Space Syntax

Although the ideas of Lynch and Rossi are very suggestive of a more complex definition of urban area and its relation to the whole city, neither really suggest the methods for rigorously describing what spatial structure as a continuous network is and how to clarify by what means precisely urban parts relate to the continuous network, in terms of space. It was left to the space

syntax movement to begin to open up this question. It was Hillier's establishment of a theory of space as configuration and a series of related methodologies, called space syntax, (Hillier and Hanson, 1984; Hillier, 1996) which shed a new light on the spatial relationship of urban parts and the whole, as well as area differentiation.

Hillier (1984, 1988, 1991, 1993, 1996) argued that urban parts are not local things, but are created by the whole city. First, he offered a valuable insight into the spatial definition of the continuous spatial network. For him, the spatial network of a city is *not* an inert background of human behaviours, but *a historic record of the spatial ordering and structuring driven by human activities*. He made a fundamental proposition of space that a physical city is an object whose spatial form is also a social ordering. This suggests that social patterning has spatial logic, and also that spatial patterning has a social content (Hillier and Hanson, 1984: 9). For example, '*encountering, congregating, avoiding, interacting, dwelling, teaching, eating, conferring are not just activities than happen in space. In themselves they constitute spatial patterns*' (Hillier, 1996: 29). In his view, space constitutes a form of social patterning, which is driven by social activities through history.

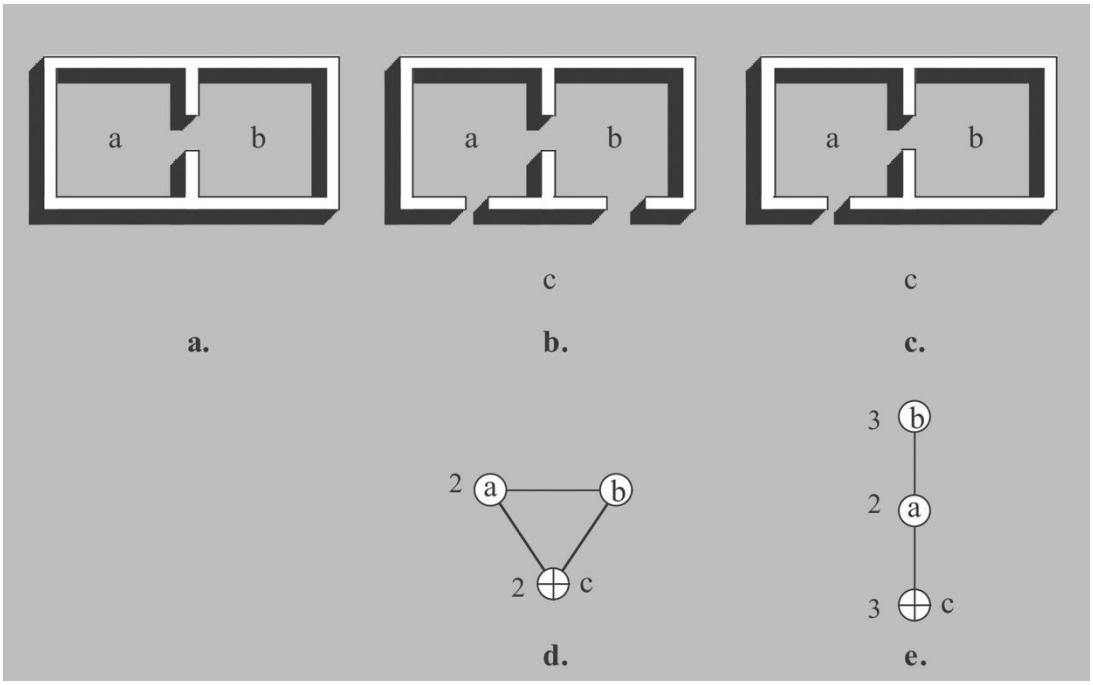

Fig.2.14 A Simple Example to Explain the Concept of Configuration.

(Source: Hillier, 1996:34)

He, then argued that the relationship between spatial and social patterning usually lies at the level of the complex system of spatial and social relations, rather than at the level of the individual spatial or social element. In order to precisely describe such complex relations, he developed a new concept of *configuration*, that is: '*relations taking into account other relations*' (Hillier, 1996: 1), and then explained this notion by showing a simple example. **Fig 2.14a** shows that cell a is connected to cell b through an entrance. The relationship of cell a and cell b is simply symmetrical because cell a is a neighbour of cell b, and meanwhile, cell b is a neighbour of cell a. This suggests that the relationship of any pair of neighbouring elements in a system is simple. **Fig 2.14b** shows that both cell a and b are further connected to a third space, c, through entrances. Fig **2.14c** illustrates that only cell a is connected to another space c through an entrance. In **Fig 2.14b**, we can go to either a or b from c, but in **Fig 2.14c**, we have to go to b through a from c. With regards to c, the relation of a and b is different in these two figures. In **Fig 2.14b**, the relation of a and b is symmetrical with regards to c, but in **Fig 2.14c**, the relation of a and b is asymmetrical with regards to c. This is a configurational relationship in the sense that this connection between a and b is defined by the simultaneous presence of c (Hillier and Hanson, 1984: 147-149; Hillier, 1996:33-35). Thus, the configurational relationship, as Hillier (1984, 1996) clarified, is defined by at least a third element, and perhaps all other elements, within an entire system. The configuration therefore addresses a set of relationships among the elements, all of which are interrelated in the whole network, rather than a simple relationship between two elements.

Hillier (1984, 1996) also proposed that the configurational properties of a system can be simply represented by a graph, called a *justified graph* in his books. A justified graph is produced in such way that a selected node as a root is put at the base, and then any other nodes at one depth from the root are aligned horizontally above it, any other nodes at two depths from the root above those at one depth, and so on until all levels of depth from the root are accounted for (Hillier and Hanson, 1984: 106). For example, **Fig 2.14d** is a justified graph representing the configurational relation of a, b and c with regard to c as the root. Obviously, **Fig 2.14d** and **Fig 2.14e** simply illustrate the different configurational properties between **Fig 2.14b** and **Fig 2.14c**, with regard to the element c.

Then he (1984, 1996) further developed a series of syntactic variables at different radii to objectively and rigorously describe the different configurational properties found at different scales. One of the important variables is *integration* measuring how close each spatial element is to all other elements within a system. The higher integrated an element is the closer it is to all the other elements. The next chapter will elaborate on those syntactic measures and look into the technical details. The following will continue to use the concept of configuration, in the general sense, to understand the spatial properties of the continuous structure of an urban grid.

Based on a large number of empirical studies, Hillier (1983, 1984, 1987a, 1987b, 1988) found a strong and significant correlation between the configuration of an urban grid, measured by integration and the movement rate. He then suggested that the spatial configuration at the more globalised level, rather than at the individual level, is the primary factor that can be used to predict movement. For him, urban network is configured in order to produce co-presence, encounter and avoidance by creating and channelling the urban movement. In this sense, the movement within an urban grid can be treated as a functional product of spatial configuration of the grid, rather than a result primarily caused by local properties, such as those which were supposed to constitute the overlocalised, well-bounded, inward looking and repetitive urban cells that had been adopted in 20th century urban design (Hillier, 1984, 1988, 1996). He (1993: 32) then termed the movement determined by the grid configuration itself as *natural movement*.

In his view, the cellular territory ideas, used by some other theorists and designers to conceptualise the spatial formation of urban parts and the whole, in fact are based on the territorial idea that a hierarchical nesting of identical levels of spatial organization corresponds to various levels of social organsiation, such as individuals, families, clusters of neighbours, neighbourhoods and so on (Hillier and Hanson, 1984, Hillier et al, 1988, 1993). But those cellular ideas tend to fragment the continuous urban grid into well-defined but over localised areas which lack a natural movement through the global network, and as a consequence they often become dramatically underused. This may result in physical and social degeneration for those bounded zones (Hillier et al, 1993).

Hillier then (1996) proposed that the part-whole structure of a city, in general, is shaped by the *movement economies* process that urban structure considered as a spatial configuration mainly determines urban movement, both vehicular and pedestrian, impacting on patterns of land use and building densities that give the feedback on movement and its relation to the urban structure. This process maximizes *the multiplier effects* on the evolution of well-functioning cities. Some land uses, such as commercial and retail, are attracted to the locations with a higher rate of the natural movement, while other lands uses like residential are drawn to the quieter places with a lower rate of natural movement. The locations occupied by the first kind of land use then attract more movement, and this in turn attracts more movement-seeking uses and new buildings, creating higher density developments. This has the multiplier effect, built on the basic relationship between urban structure and movement, and then results in a seamless network of higher and lower density areas (Hillier, 1996).

Hillier (1996) continued to elaborate. He identified that the good urban areas are spatially structured as *the interfaces* between different scales of natural movement and that are shaped by different scales of spatial configuration. Greater distance journeys tend to occur on globally integrated roads; whilst more localized journeys on locally integrated streets. The structure of the whole city acts as a spatial means to mix together different scales of journeys to maximize contact, and the urban areas constituting the city can be understood by the relationship between more localised and more globalised movements primarily determined by the urban structure.

On this basis, he concluded, '*places are not local things. They are moments in large-scale things, the large-scale things we call cities. Places do not make cities. It is cities that make places. The distinction is vital. We cannot make places without understanding cities*' (Hillier, 1996: 151). Meanwhile, he also argued that the concept of space that has underpinned the traditional cellular ideas are '*too static and too localised*', but the configurational concept of space is '*dynamic and global*' (Hillier, 1996: 153). For him, the formation of the urban areas can be detected by the relation between different scales of configuration.

Later, in the paper titled *Centrality as a Process*, Hillier (1999) further tackled the question of how the pattern of attraction inequalities in an urban grid, meaning the pattern of centres and subcentres that pervade the urban grid, is generated by the movement economy process with its spatio-temporal dimension. Although this study sought to investigate urban centres, rather than urban areas, it gave some clues how to define urban areas in a syntactic way.

He first identified that the live centres – the centres that benefit from movement – are not only the products of a urban network that determines the locations of these centres at the global level, but also shaped by the local process of *grid intensification*, meaning that the reduction of block size to reduce the average metric distance from all points to all others in a spatial network, so that local interaccessibility and metric trip efficiency are optimised. As a result, a live centre is usually characterised by a compact and convex shape, with several strategic links extending to the more global structure.

Through analysing and comparing several *ideal* layouts, he (1999) identified that a grid, formed from smaller central blocks and larger edge blocks, has a lower metric mean distance from all points to all others than a regular grid with uniform blocks, if holding total land coverage and travellable distance constant. Then, he further clarified that the local grid intensification of the live centre also comes from the process of optimizing its global attraction with regards to the entirely urban network. In this sense, *configuration*, he argued, produces *attraction* considered as a centre or subcentre. However, he did not continue to characterise the pattern of centres and subcentres in the real urban grid through the spatial process of metric integration (meaning how metrically close each space is to all others), but highlighted that this was one course for future study, at the end of the paper (Hillier, 1999).

These centres and subcentres on different scales, Hillier (2001) ascertained, are usually linked together to form a foreground urban network embedded into a background network of primarily residential space. This *dual structure* of urban form, he (2001) proposed, is driven by two forces: the micro-economic and the socio-cultural forces. On one hand, the foreground network, associated with the micro-economic activity of market, exchange and trading, is mainly constituted by the longer lines to form the strategic structure of a city. Its spaces are more

visually integrated at the global level to maximise natural co-presence and visual contact in those spaces. On the other hand, the background network, dominated by socio-cultural events, is largely produced by a large number of shorter and less integrated streets that are structured to restrict natural co-presence, which varies according to the different socio-cultural customs. They in fact generate the larger areas of background space in the *interstices* of the foreground network (Hillier, 2001).

In his view, both the foreground network of linked centres and the background network of residential areas are produced by locally placing, sizing and shaping blocks, which are governed by the spatial laws, such as a law of *centrality* (meaning that a block located at the centre of a space will increase the distance from all locations to all others more than one located peripherally), as well as a law of *compactness* (meaning that the more compact a block or group of blocks, the less will be increased in the distance from all locations to all others in the surrounding space) (Hillier, 2001). He suggested that the dual networks come into being whenever a block is locally added into a system, locally longer street should be preserved, but at the cost of creating shorter streets. To some extent, this in fact showed a bottom up process to create the kind of the part-whole structure. The theory of dual structure however increasingly focuses on the formation of centres, and does not explicitly deal with urban areas and their boundaries.

With Yang, Hillier et al (2007, 2010) further discovered a *patchwork* of local areas, meaning that each patch acquires similar syntactic values and so similar colouring, seemingly representing some differentiation of the background urban network into semi-discrete areas. The similar kind of patchwork was also detected by Dalton (2006, 2007). The methodological details of these two works will be reviewed in next chapter. The patchwork phenomenon, Hillier (2007, 2010) suggested, results from the local distortions in urban space induced by the placing, shaping, orienting and scaling of urban blocks at the local level, and reflects the way in which we talk about urban areas conceived at different scales. Compared to the foreground network that arises from the visual effects of the placing and shaping physical structures at the global level, the background network, partitioned into semi-discrete areas, is metric and local, as it is captured by the local metric properties. The patchwork phenomenon, he addressed,

demonstrates that the area structure of the city depends on the configuration of the urban grid. Along the syntactic line, Blanchard and Bolchenkov (2009) adopted mathematical way of exploring community structure by diffusion processess that the movement of particles from an area where their concentration is high to an area having a lower concentration. In fact they argued that the community structure can be mathematically captured by quantifying the global property of the street with respect to other streets in urban network.

2.6 Discussion

This chapter suggests that the spatial definition of urban areas varied much in the aforementioned literature. The works before the 1950s, such as Howard's Garden City and Perry's neighbourhood unit, focused on *well-defined and clear boundaries*, such as greenbelts and arterial roads, which were mainly applied to separate urban areas. Many works after the 1950s, such as Alexander's thick boundary structure, Krier's urban quarter, the Urban Village movement and the New Urbanists' models emphasize *the permeable boundaries* with the spatial links or overlapping between areas, which were considered as the spatial tool for aggregating urban parts into a consolidated city or region. Among these works, a handful of writers, such as Jacob, Lynch and Rossi, argued that urban parts in general relate to *a continuous urban network*. However, all literature which addresses the urban network, except space syntax studies, have not explicitly dealt with the question of how spatial structuring works in the formation of the continuous urban network and how exactly this relates to the urban parts.

All the studies which concentrated on space syntax, suggested that urban parts can be considered as the products of the spatial configuration of an urban network as a whole, but also are shaped by their local features. In the syntactic view, the spatial definition of urban areas involves *three* factors: local features, global configuration, and the interface between the different scales of configuration which in turn determine the different scales of natural movement. But *how exactly are those factors measured and analysed in the existing syntactic studies? What kinds of methods have been deployed by these syntactic studies to study urban areas and their relations to the whole? Have they quantitatively revealed the nature of area*

boundaries in terms of space? In order to tackle these questions, the next chapter will continue to review the existing syntactic techniques used to study urban areas.

Chapter Three: A Review of Syntactic Techniques and a Diagnostic Study

3.1 Introduction

Following the review of space syntax theories concerning urban parts and the whole, conducted at the end of the previous chapter, this chapter focuses on the methodological aspect of the space syntax. It aims to explore the way in which the area boundaries might be quantitatively described and identified in relation to the continuous urban network of which the areas are parts. It starts by reviewing the basic syntactic techniques for representing and analysing a continuous urban network, as well as the existing syntactic techniques for describing and detecting urban areas in terms of spatial configuration. This evaluation will be employed to identify new dimensions to be investigated and prepare the ground for developing a methodological framework for this research.

A diagnostic study of two large-scale projects: Canary Wharf in London and Brindleyplace in Birmingham is then looked at, based on this student's primary study of those two developments (Yang, 2005). This study is conducted to elaborate further on the typical syntactic procedure for studying urban areas and additionally begin to explore new techniques for investigating the boundaries of the projects. These two projects are selected because they have different spatial development strategies. One strategy effectively prioritised spatial segregation into its surrounding areas and the other prioritizing integration. This study will therefore enable us to make a comparative study on the project boundaries and then go on to develop more general ideas of area boundaries that might be applied in the following chapter.

It focuses on three related questions: do the different spatial strategies result in the different spatial layouts of the projects with regards to their surrounding as a continuous spatial network? How far do the projects impact on, and are affected by the surrounding areas in terms of space

and movement pattern? And does the two-way process of interaction between the internal and the external affect the spatial boundaries of those two projects and of their surrounding areas?

3.2 Space syntax measures and techniques

3.2.1 Basic syntactic techniques for representing and analysing urban grid

How exactly is a continuous urban network represented and measured in a syntactic way? As developed in *the Social Logic of Space* (Hillier and Hanson, 1984: 90-93), the syntactic presentation of the spatial network of a settlement was set up based on the following ideas: the spatial network of the settlement is defined by the aggregation of solid elements like houses, public buildings and so on and is represented as one continuous space. This is presented in black in **Fig. 3.1a**; any a point in the spatial structure, such as point y highlighted in **Fig. 3.1b**, is both the part of linearly extended spaces, represented by the doted lines in **Fig. 3.1b**, in *one* dimension, and the part of an extended *convex space* (meaning the space within which each pair of persons can directly see each other[14]), denoted by the hatched area in **Fig. 3.1b**, in *two* dimensions. Thus, the spatial structure of the settlement is objectively represented as an *axial map*, meaning the least set of the longest straight lines of visibility and/or permeability which passes all the convex spaces and makes all axial links[15]. **Fig. 3.1c** illustrates an example of an axial map of Gassin in the Var region of France, originally shown in *the Social Logic of Space* (1984: 91 and 109). Any a linear space, represented by an axial line, can be described in terms of its complex relation to all others, namely its configurational relation. The axial map therefore simultaneously represents all the configurational relations in the continuous structure of the settlement.

[14] Mathematically speaking, a two-dimensional space is a convex, if every point on the straight line segment joining any pair of points within the space is also within the boundary of the space. For detail, see Hillier, B. and Hanson, J. (1984), pp.97-8.

[15] Axial map also can be defined as the minimal set of axial lines such that the set taken together fully surveils the system, and that every axial line that may connect two otherwise-unconnected lines is included. It can be objectively produced. See Hillier and Hanson (1984), pp. 17, 91and 99, and Turner, A., Penn, A., and Hillier, B. (2005), An algorithmic definition of the axial map, *Environment and Planning B: Planning and Design*, volume 32, p. 425- 44.

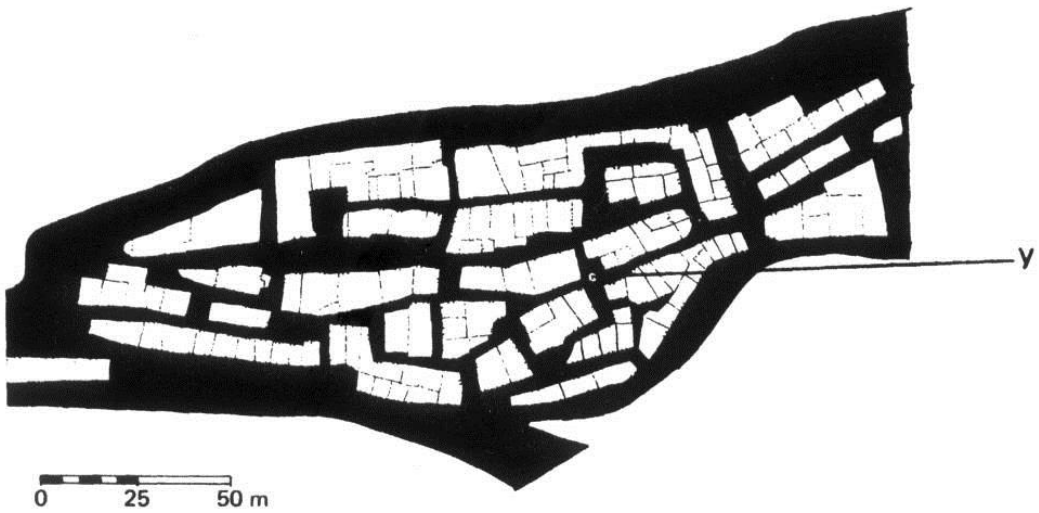

a. The black represents a continuous spatial network

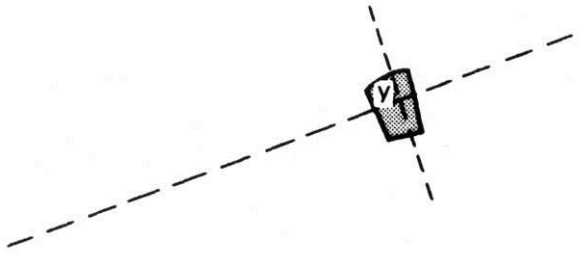

b. Point Y is both the part of the linear extension of spaces, denoted by the doted lines, and the part of the two-dimension extension of space, indicated by the shaded convex.

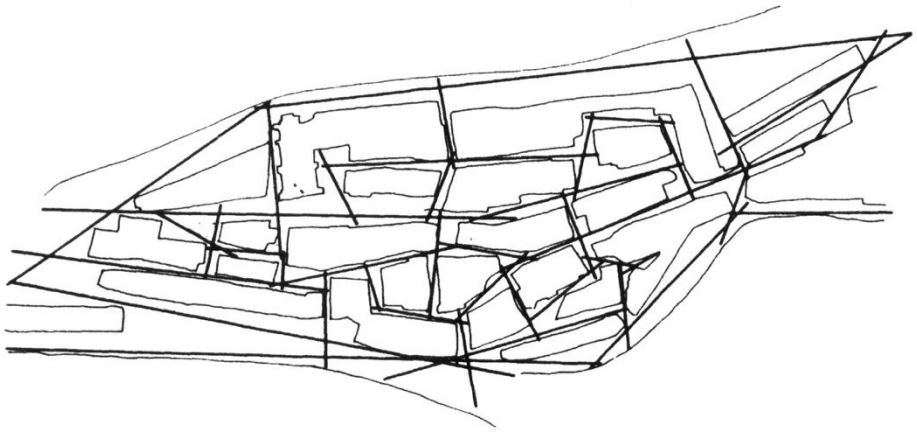

c. An axial map is constituted by the least set of the longest straight lines of visibility and permeability which passes all open spaces and makes all axial links.

Fig. 3.1 The Syntactic Presentations of the Spatial Network of Gassin in the Var Region of France (source: Hillier and Hanson, 1984: 91)

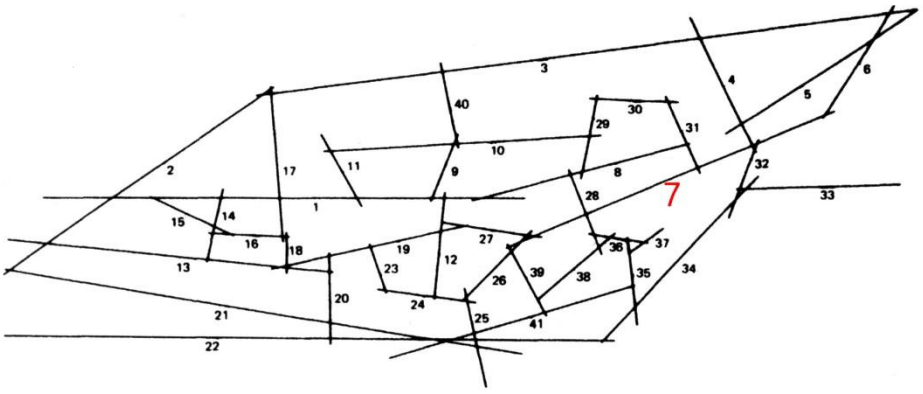

a. Each axial line is assigned a reference number (source: Hillier and Hanson, 1984: 91).

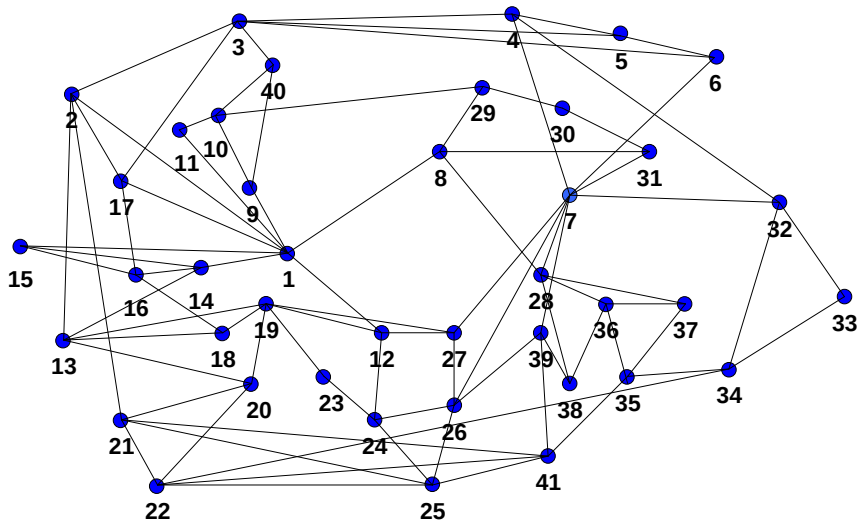

b. The above axial map can be converted into a graph in which the axial lines are represented as nodes and the intersections of the lines as links.

Fig.3.2 The Transformation of An Axial map into A Topological Graph

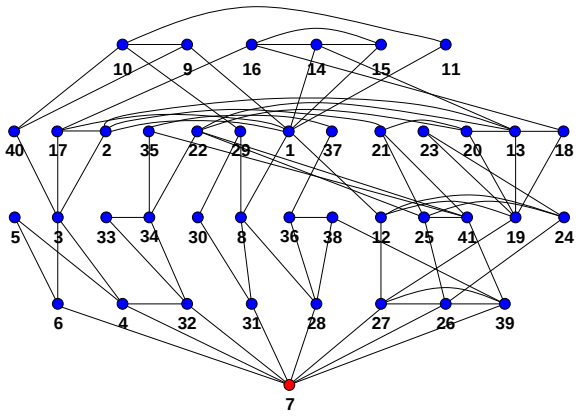

a. The spatial graph seen from the point of the view of line 7.

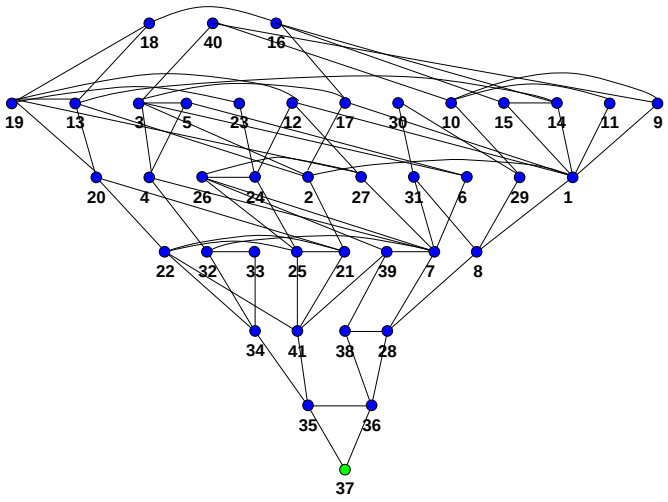

b. The spatial graph seen from the point of the view of line 37.

Fig. 3.3 The J-graphs of Lines 7 and 37. The difference in the configurational relation between spaces can be easily found by justifying the graph in the following way: a selected node, as the root (such as Line 7 or 37), is put on the baseline, the nodes one depth away from the root are horizontally aligned immediately above the root, the nodes two depth away from the root above those one depth away, and so on until all other nodes are taken into account in terms of their depth from the root (Hillier and Hanson, 1984).

In order to illuminate and analyse the configurational relations, the axial map is converted into a *graph* in which *axial lines are represented as nodes (or vertices) and the intersections of the lines as links (or edges)* **(Fig. 3.2)**. As reviewed in **Section 2.5** of the previous chapter, the difference in the configurational relations between spaces can be easily found by justifying the graph in the following way: a selected node, as the root, is put on the baseline, the nodes one depth away from the root are horizontally aligned immediately above the root, the nodes two depths away from the root above those one depth away, and so on until all other nodes are taken into account in terms of their depth from the root (Hillier and Hanson, 1984: 106). For example, **Fig. 3.3a and b** showing the two justified graphs – denoted as J-graphs – of **Fig. 3.2b** visualise the different configurational properties of two individual spaces, represented by line 7 and line 37 in the axial map of Gassin **(Fig. 3.2a)**. This suggests that these two individual spaces can be differentiated in terms of the way in which they are connected to all other spaces

of the settlement and according to the distance to them. In this sense, the J-graph, which is one form used to represent the spatial network, can be used to illustrate the complex configurational relations between each specified space and the contextual structure in which that space is embedded.

Based on the above objective presentations of the network of space, several syntactic measures were developed to quantitatively describe the configurational properties of space[16]. One of the most important variables is *depth* which measures how many necessary topological steps from the root line are needed to go through to another given line as a destination. For example, as **Fig. 3.3a** shows, the topological depth from the root line 7 to one destination line 10 is 4.

When the values of depth to the root line from all other lines are added up, the sum, denoted by *total depth*, expresses the configurational property of the whole network with regard to that specified root space[17]. For example, the total depth of line 7 is 97 **(Fig.3.3a)**, whilst that of line 37 is 157 **(Fig.3.3b)**. This quantitatively describes that the whole spatial network, looked at from line 7, seems to become 'shallower' than the same structure observed from line 37, so that it differentiates line 7 from line 37 regarding the way in which they are connected to all other spaces. In theory, the most depth exists when all spaces are arranged in a unilinear sequence way from the root space, and the least exists when all spaces are directly linked to the root (Hillier and Hanson, 1984).

On the basis of the concept of depth, the variables of *connectivity* and *integration* were introduced in the quantification of the spatial configurations at different scales. The variable of connectivity measures the number of the spaces directly connected to a root space, in order to capture the most localised feature of that root space. The variable of integration, roughly expressed as the reciprocal of the *normalised total depth* (meaning the total depth without the

[16] For the detailed procedure for analysing an axial map, see Hillier and Hanson (1984), p97-123.
[17] Total depth is also seen as a universal distance from the root point, which shows a generalization of the idea of depth/distance. For the details, see Hillier (1996), pp.104-108.

effect of system size[18]), measures how topologically close a space is to all other spaces. The shallower the total depth of a space the more this space intends to be integrated into the spatial network as a whole. The deeper depth a space is, the less this space is integrated. The most integrated line is the shallowest in the spatial network; the least integrated is the deepest.

An axial map can be indexed and coloured according to the integration values, so that the underlying configurational patterns can be highlighted and understood in a more intuitive way. The warmer the colour of the axial line, the higher the integration value, and vice versa. For example, the red line represents the highest integration value and the dark blue line represents the lowest integration value, in other words, the most segregation. An example is illustrated in **Fig. 3.5** of the diagnostic study conducted later.

The variable of integration itself can be measured at different scales. The integration at the infinite radius, denoted as integration Rn and usually named *global integration*, measures the normalised total depth of a given line to all other lines within the system. However, the integration at global level might also be calculated at the radius-radius, meaning that the integration analysis is made at the mean depth of the whole structure from the most integrated line, in order to optimise the globality of the analysis, but minimize the *edge effect* (the edge effect occurs when the spatial features of the lines near to the edge become more segregated because they are partly cut off from the immediate surroundings outside the edge). This measure is called the *radius-radius integration*[19].

The integration at the radius of 3, denoted as integration R3 and usually called *local integration*, measures the normalised total depth of a given line to the surrounding lines up to three topological steps away[20]. In general, we can measure the integration value at any a radius of k (integration Rk), that is, the reciprocal of the normalised total depth of a given line to the lines up

[18] Total depth is substantially affected by the number of nodes in the graph representing the spatial structure of a settlement. Both theoretical and empirical normalization methods were offered and clarified in the book of *the Social Logic of Space* to eliminate the bias caused by the system size, so that total depth or integration can be compared across different sized systems. For the details, see Hillier and Hanson, 1984: p108-113.

[19] For detailed definition of the radius-radius integration, see Hillier, 1996, p163.

[20] The root line is considered to have the first step, so that in the DepthMap, the integration R2 in fact means the integration at the radius of 3, namely the local integration.

to k steps away, to capture the configurational properties of spatial network at any a given radius.

In syntactic analysis, the global integrated core of a large settlement can be found by highlighting 10% of the most integrating lines at the infinite radius, and it is manifested by a *deformed wheel*, consisting of a hub of lines somewhere centre, spokes reaching out from the hub towards the periphery in all main directions, and rims or part of the periphery of the site (Hillier, 1983; Hillier, 1989; Hillier and Hanson, 1984; Hillier, 1987, 1996). In addition, the most integrated line at the radius n is termed *global integrator*, potentially associated to a major centre; whilst, the most integrated lines at the radius of 3 are named *local integrator*, potentially related to local centre (Hillier and Hanson, 1984: 115, 124-5; Hillier, 1996: 120-2).

Another basic variable is *choice*, formulated to assess how likely each space is chosen as part of the simplest or shortest routes from all spaces to all other spaces in a spatial network (Hillier el al, 1987a and b). It in fact measures how often a space is passed through by the simplest or shortest routes, and therefore it can be used to predict the though-movement potential[21]. This describes the potential of all movement passing through a specific space. The variable of choice also can be measured at different radii, which suggests different scales of through-movement potential.

The more complex syntactic measures were developed in the existing syntactic studies to capture the interfaces between local and global syntactic properties of a spatial network. The local property that can be directly seen from a specific space is usually measured by the connectivity of that space; whilst, the global property that cannot be seen from that space is obtained by computing integration Rn. *Intelligibility* is calculated by the degree of the linear correlation between connectivity and global integration (or integration Rn), in order to measure the degree to which what can be seen and experienced locally in the system allows the large-scale system to be learnt without conscious effort (Hillier et al, 1987a; Hillier, 1996). An

[21] The relation of choice and potential of through-movement has been discussed in Hillier, B., et al (1987a), Creating Life: Or, Does Architecture Determine Anything? Architecture et Comportement/Architecture and Behaviour , 3 (3) 233 - 250. pp.237.

intelligible urban network is one in which can easily be used to capture the global structure from local properties (ibid). In a similar way, another variable of *synergy*, calculated by the degree of the linear correlation between integration R3 and Rn, is also used to identify the relation between local conditions and global structure, and empirically has an effect of lessening the influence of system size (Hillier et al, 1993). In general, the variables of intelligibility and/or synergy can be applied to illuminate the degree to which urban parts relate to the larger-scale system in which it is embedded (Hillier, 1996: 71 and 129). We will further review the detailed technique in the next section.

Recently, a new syntactic model, based on an axial map, has been developed to represent the structure of space and in order to investigate and understand the geo-topological, metric and configurational features on a *finer* scale (Turner, 2001, 2004; Dalton, 2001, 2003; Hillier and Iida, 2005). The analysis unit is defined as the line segment between intersections of axial lines, and so the axial map is broken at the intersections to generate the *segment map*[22]. The spatial network is then converted into a graph in which the segments are denoted as nodes and the intersections of the segments as links. The segment analysis of spatial configuration varies with the definition of distance from one segment to another (Hillier and Iida, 2005; Hillier, 2009). Metric distance is defined as the shortest physical distance along the lines between the mid-points of the origin and destination segments; topological distance, or fewest turn distance, is seen as the number of changes of direction necessary to be taken from one segment to another one; and angular distance, or least angle distance, is considered as the sum of angular changes that are made on a least angular change route[23]. This allows the different ways of representing and analysing spatial network with regards to the metric, topological and angular distances.

Several key variables are deployed to conduct segment analysis. Segment connectivity measures the number of segments directly connected to the root segment; and segment length is defined as metric length of a segment. The basic geometric feature of a city can be examined by those two measures. And recent researches (Hillier and Iida, 2005; Hillier, 2009) show both

[22] For the detailed procedure, see Turner, 2001, 2004, and Hillier and Iida, 2005.
[23] For the mathematical definition of the different types of distance in the segment analysis, see Hillier, B. and Iida, S. (2005), Network and psychological effects in urban movement, In: A.G. Cohn and D.M. Mark (Eds.): *COSIT 2005, LNCS 3693*, 475–490. pp.482.

angular choice and angular total depth are useful in predicting movement. The former measures how many least angular paths between every pair of segments, and the latter gauges the cummulative total of the least angular paths to a selected segment as root. And metric radius has been demonstrated to be effective, so that segment analysis is typically run at a series of metric radii, rather than topological or angular radii (Hillier, 2009: K01, 4). In addition, node count in the segment analysis is usually defined as the number of segments encountered with a constricted metric radius.

3.2.2 The existing syntactic methods of investigating urban areas

The above review of the basic syntactic techniques then poses more specific questions: *how can the spatial features of a pre-given area (whose boundaries are defined in terms of other socio-economic or physical variables), such as named area, be rigorously described in a syntactic way? And, is it possible to disaggregate an urban network as a whole into the sort of discrete parts in terms of their configurational relations?* This *first* question aims to characterise the pre-given area; whilst the *second* one seeks to spatially detect urban parts that are embedded within the whole network. These two questions are related to each other. The first question will help us understand the spatial properties of urban areas in relation to the way those areas and their surroundings are structured. The responses to this question will allow us to explore the second question.

We start by reviewing the existing syntactic methods for tackling the above two questions. As we mentioned at the end of the last section, a segment map has only been developed recently, and even fewer techniques for investigating urban parts, based on the segment map, had been proposed at the time when this student began to conduct this research. This section will therefore focus on reviewing those techniques based on the axial map.

We first discuss the techniques that have applied to describe and characterise pre-given areas. The extensive studies usually describe a pre-given area by simply averaging the basic geometric and syntactic values of all the axial lines *within and across* the boundary of that area,

so that they were able to investigate and understand syntactic properties of that area as a whole, or explore whether and how those spatial properties of that area relate to other socio-economic or functional factors at the area level (Hillier et al, 1987a; Peponis, 1989; Hillier, 1996, 1999; Vaughan, 1997; Karimi, 1997; Hillier and Greene, 1999; Kasemsook, 2003). The local spatial features of a pre-given area are usually measured by several variables, such as *mean line length* (the average of metric length of the axial lines of an area), *mean connectivity* (the average of connectivity of the axial lines of an area) and *mean integration R3* (the average of integration R3 of the axial lines of an area); whilst, the global spatial characteristics are often captured by *mean integration Rn* (the average of integration Rn of the axial lines of an area) and/or *mean radius-radius integration* (the average of the radius-radius integration of the axial lines of an area).

More complex measures have been developed to describe a pre-given area with regards to the whole structure of a town or city. Based on the study of 25 areas selected from 6 Greek towns, Peponis et al (1989) suggested that if the mean integration Rn of an urban area, taking account of the context of the whole town, is higher than the mean integration Rn of the town of which the area is the part, the area appears more distinct. He called the ratio of those two variables *the definition of the local area*. Later, in the study of 17 informal settlements in Santiago de Chile, Hillier and Greene (1999) proposed another measure of *local spatial advantage* (LSA).This variable was calculated by dividing the mean integration Rn of a settlement (whose boundaries were defined by socio-economic data) in the context of a 7-km local system into the mean integration Rn of the whole 7-km system and thus captured the extent to which a settlement occupies a strategic place in its contextual structure. The higher the LSA value is, the more the settlement is integrated into its metric context defined by 7-km.

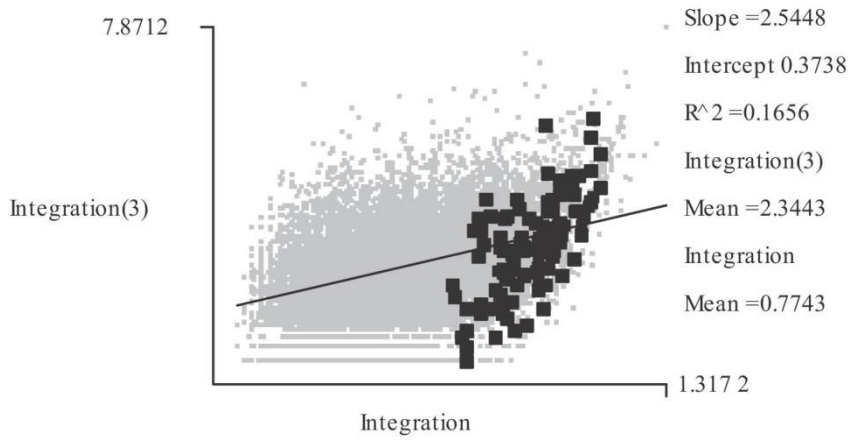

Fig. 3.4 The Scattergram of the City of London in the Context of Great London. The black dotes represents the axial lines of the City of London, and the grey dotes denotes the axial lines of Great London of which the City is a part. (source: Hillier, 1996: 172)

The more widely used technique of describing a pre-given area was developed by Hillier (1987a, 1996) to characterize urban areas by measuring the values of *intelligibility* and *synergy*, both of which were reviewed in the previous section. The higher the value results in areas which have a good spatial relation with the whole structure, and vice versa. Hillier (1996) further advanced a method for visualising the extent to which an area is spatially distinguished from the whole city, by comparing the pattern of intelligibility (or synergy) of that area to that of the whole city of which the area is a part. The intelligibility (or synergy) patterns of the area and the whole city are shown by plotting connectivity (or integration R3), on the vertical axis, against integration Rn, on the horizontal axis in the same scattergram. **Fig. 3.4** shows an example of the synergy scattergram of the City of London in the context of Great London (Hillier, 1996: 172). The more the area forms a linear scatter, the more that area is well-defined. The steeper the slope of the regression line of the area across the regression line for the whole city is, the more the local integration is stronger than the global, then the more the area is distinctive[24]; the more the points representing the area lie on the regression line for the whole city, the more that area relates to the main grid of the whole city, but not forming a distinctive area[25]. Hillier (1996) also gave a caveat that a clutch of the connected axial lines with very low global integration

[24] For other cases, see Hillier, 1996, p171-172.
[25] The examples have been illustrated in *Space is the Machine*. See Hillier, 1996, p177.

would not function as an area, because the formation of an area also depends on a good integration at the global level.

All the above methods focus on the measures calculated at the extreme radius: integration at Rn (or radius-radius) and connectivity (or integration R3), and did not explore the syntactic values at the medium radii that might play a role in characterising pre-given areas. A handful of studies however have examined the syntactic values at some medium radii.

Hillier (1996) first demonstrated that local areas in Chicago are characterised by the correlation between connectivity and integration Rn, those in London by the correlation between integration R3 and Rn and those in Shiraz by the correlation of R6 and Rn. Thus, he argued that the different cities have different ways of structuring their local area buildings. In the study of Iranian old cities, Karimi (1997) also suggested that the mean integration R5 of an area is best to describe local structures of the Iranian old cities, and plotting integration R5, rather than integration R3, against integration Rn to illustrate three distinctive areas – city spine including bazaar complex, central quarter and residential quarters – whose regression line is steeper than the regression line for a whole city. This in fact raises the questions: *do the different pre-given areas in the same city have the different ways of structuring their local layout with regards to their contexts found at different scales? If so, can we describe a pre-given area in terms of a whole range of configurational relations between the internal and the external structures, ranging from its immediate surroundings to the whole city of which it is a part?* We will tackle these questions by carrying out a diagnostic study in the second part of this thesis.

We continue by reviewing other existing techniques for detecting urban areas from a continuous network. We first look at two studies. In a study of towns in Greece, Peponis (1989) proposed that sub-areas in the towns can be articulated by decomposing the spatial structure of the towns along the spaces with higher choice Rn, in the expectation that the boundaries of those sub-areas should have more through movements measured by choice than their internal spaces. The decomposition procedure was conducted as follows: several spaces with the higher choice values were highlighted to show the choice core; the decomposition started by cutting along the

highest choice line; when the choice core bifurcated, the cut was carried out so as to maximize the total choice value but minimizing the total number of necessary cut-lines.

Read (1999, 2003, 2005) later studied Dutch cities and asserted that those cities usually comprised of both a global supergrid (that usually accommodating higher speed and intensity of movement) and local grids (those containing lower speed and intensity of movement), self-similar but operating at different scales, and further argued that the vertical jumping between the supergrid and the local streets which he called 'vertical ecology'[26], according to the differentiation between quicker and slower space-time rhythms and experiences, will help us achieve a better understanding of urban parts and the whole in contemporary cities. He proposed two techniques to explain this biplex urban structure. One was the *integration gradient map*, picking out the streets with higher integration values relative to the other streets proximate to them and then tracing the streets of higher integration gradient based on integration R3 or Rn through urban grid, as a way to highlight the supergrid. The other was the *area integration map*, indicating the concentrations of higher integration R3 through giving a line the average of integration R3 values of all the lines within a topological distance of two or three (or within a fixed metric distance) from this line, in order to illuminate the local areas.

The above two studies focused on identifying the area boundaries by indexing syntactic values and then decomposing the urban network along those boundaries. But a linear space with higher integration or choice values, considered as the area boundaries in the above two studies, might be a high street acting as an active space traversing a whole consolidated area, or might be an expressway bypassing or bounding an area. In other words, in many cases it is difficult to distinguish whether a linear space is a connector of smaller parts belonging to one area, or a separator of two different areas, according to its integration or choice values. It then poses two related questions: *what is the nature of an area boundary? And can we decompose an urban grid and then detect urban areas by using other syntactic methods?*

[26] For details, see Read, SA (2005). Flat city; a space syntax derived urban movement network model. In A van Nes (Ed.), *proceedings of 5th international space syntax symposium*. Amsterdam: Techne Press, 341-357.

A number of studies gave some clues. Based on the study of several areas in London, such as Barnsbury, St. Peter's Street Area, City of London, Highgate and Islington, Hillier (1987a, 1989) first suggested that urban areas can be identified by using the technique of optimizing the correlation between movement rates and integration Rn (calculated in the different scales of the contextual areas). This technique started by conducting a movement survey *in* and *around* an observed area to collect movement data. The observed area was then embedded in the different sized contextual areas as the reference areas, and the integration values were respectively read from those different systems; the correlation between integration values and movement rates had been respectively carried out until the best correlation was found. For example, as the reference area of Barnsbury became much larger, the correlation deteriorated markedly; but as the reference area of St. Peter's Street area became smaller, the correlation became less significant. The sub-areas, marked out by optimizing the reference area to generate the best correlation, were termed as *natural areas*, in the sense that they, argued by Hillier (1987a: 243), were different from the 'neighbourhood units'[27] defined by Perry in 1929, but emerged from a continuous and well integrated urban network. Hillier did not decompose the urban network along the area boundaries defined as the linear spaces with higher choice or integration values, but identified urban areas in terms of *the change in the correlation between spatial configuration and movement rate, as the contextual structures vary*.

Following this line, Raford (2004, 2005) with Hillier, further developed the technique of what he termed the *correlation contour map*, which seeks to define an area by mapping the overlapped or separated contour lines, with regards to the degree of correlation found between movement rates and spatial variables within the area enclosed by a contour line. Using this method he distinguished urban areas in the fragmented urban context of downtown Boston. The correlation contour map was produced as follows. Regression analysis was conducted, coupled with the gate inclusion and exclusion process, to explore the statistical correlation between spatial variables, such as local integration (defined as integration R4 in Raford's study) and the number of topological steps to the nearest transit stations, and the observed movement rates at a cluster of selected gates. Starting with a small cluster of gates that had the best statistical

[27] Section 2.2.2 in the previous chapter reviewed Perry's concept of neighbourhood unit.

correlation, a new gate nearest to that cluster of gates were added and another round of the regression analysis was then processed with all input variables to calculate the correlation. If the correlation still remained relatively strong a new gate was included; if not, the new gate was excluded. The other new gates were tested and included until no other new gate can be added to keep a relative strong correlation. This formed an area enveloped by a contour line, within which all gates had a strong correlation. Then, new gates were further added in this way to generate another contour line with a less strong correlation. This correlation process allowed the possibility of several overlapped or discrete contour peaks which represented Hillier's natural areas. Raford further produced different correlation contour maps for the different types of people, such as local residents and tourists. He suggested that the different user groups interpreted their own boundaries of those areas in different ways. This technique allows us to investigate the nature of area boundaries, though it, like Hillier's previous study, still partly relies on the functional dimension of movement to identify urban areas. The diagnostic study conducted later will test this method with the aim of examining the boundaries of the projects.

More recently, Dalton (2006, 2007) developed a purely spatial technique for detecting and simulating urban areas based on axial map, and called it *point intelligibility (or synergy) mapping*. Point intelligibility mapping was processed as follows: a fixed subsystem connected to each root line, such as the closest 90 lines to the root, was first defined, and intelligibility value of this subsystem was assigned to each root line; the axial map was then coloured in terms of the intelligibility values. As a result, it illustrated a kind of patchwork pattern, in that the clusters of neighbouring lines seemed to have the same colour. Each patch may represent a neighbourhood. The point synergy mapping worked in the same way, except replacing the variable of intelligibility by the variable of synergy. As for each same sized subsystem selected around each root line, the synergy value of the subsystem was computed and assigned back to the root lines for later visualisation. Through these two techniques, he (2007) argued that the area boundaries caused by the configuration of spaces can be detected and illustrated, and this can influence our understanding of neighbourhood in terms of physical structure. This study implies that the syntactic relation between local conditions and more globalised structuring might be used to understand the formation of area boundaries.

Moreover this study focused on the comparison between the sub-systems of the same size, because the sub-systems picked out by the same radius – that being simply seen as a tool for selecting the axial lines up to a fixed depth away from a root line to constitute a sub-system to be analysed around the root – perhaps have different numbers of axial lines, but some smaller sub-systems might have very high intelligibility or synergy values only due to their small size; and so that the size effect needs to be eliminated (Dalton, 2006, 2007). This however demonstrates the other side of the same coin: that the same size sub-systems perhaps have different radii. To investigate the role of radius in detecting urban areas from a continuous network is also vital. As discussed earlier, this thesis seeks to explore how to define urban areas in terms of the way they interact with their contexts ranging from the immediate surroundings to the whole network. It is *radius* that can be used to select the various contexts in one consistent way. The diagnostic study of this chapter (Yang, 2005) was however carried out at the time when Dalton was developing this technique for detecting urban areas and as a consequence this study did not use his technique.

The previous chapter mentioned that Hillier (2007, 2010), with Yang, developed another method (based on segment map) for detecting and illustrating urban areas, in which the student participated. The diagnostic study was also conducted at the same time when Hillier was developing that technique, and so the study did not use that technique either. Hillier's method will be reviewed in the next chapter and will be applied in the latter chapters, because the author has been involved in Hillier's works.

In addition, Blanchard and Volchenkov (2009), borrowing the idea of space syntax, sought to detect communities in a continuous urban network by the first-hitting time which quantifies the expected number of steps a random walker starting from the origin street needs to reach the destination for the first time. A numerical measure, called the Cheeger constant, was then used identify whether or not an urban network had a "bottleneck". If the Cheeger constant is small but positive, then a "bottleneck" exists in the sense that there are two large clusters of neighbouring streets with few links between them. If the Cheeger constant is large, any possible division of the network set into two clusters has "many" links between those two subsets. Following the similar aglormism, Law (2017) adopted the Modularity Optimisation algorithm on the street-

network dual graph to identify Street-based Local Area, defined as a local area with street-based, topological/configurational membership. The Modularity calculates the difference between observed number of edges within a subgraph and the expected number of edges. The greater the observed number of edges relative to expected, the higher the modularity. In fact, Law also sought to detect the bottlenecks in the continuous urban network.

From the above review of those syntactic techniques, it can be suggested that understanding *the nature of area boundaries* is key to decomposing urban networks into the different parts. *Is it possible to distinguish the boundaries of an area by investigating the syntactic relations between its internal layout and the surroundings at different radii?* The following pilot study makes a first step towards tackling the above question through a comparative study of two large-scale developments, Canary Wharf in London and Brindleyplace in Birmingham.

3.3 The diagnostic study of Canary Wharf and Brindleyplace

3.3.1 Different spatial strategies of the two projects

We at first review the spatial strategies employed for developing Canary Wharf and Brindlyplace, respectively, in order to give an informative background of this comparative study. Canary Wharf, located in Greater London's poorest Borough of Tower Hamlets and to the east of the City of London, was originally announced in 1985. Initially this new development was to cover 71 acres in the north of the Isle of Dogs (Brownill, 1990). Brindleyplace, lying in the poorest area of Ladywoods and to the west of the city centre core (artificially segregated by the notorious Birmingham Ring Road), was originally proposed for private development in 1987 and planned to cover 17 acres of mixed-use redevelopment (Holyoak, 1999). **Fig 3.5** displays the location of the two projects in their urban contexts.

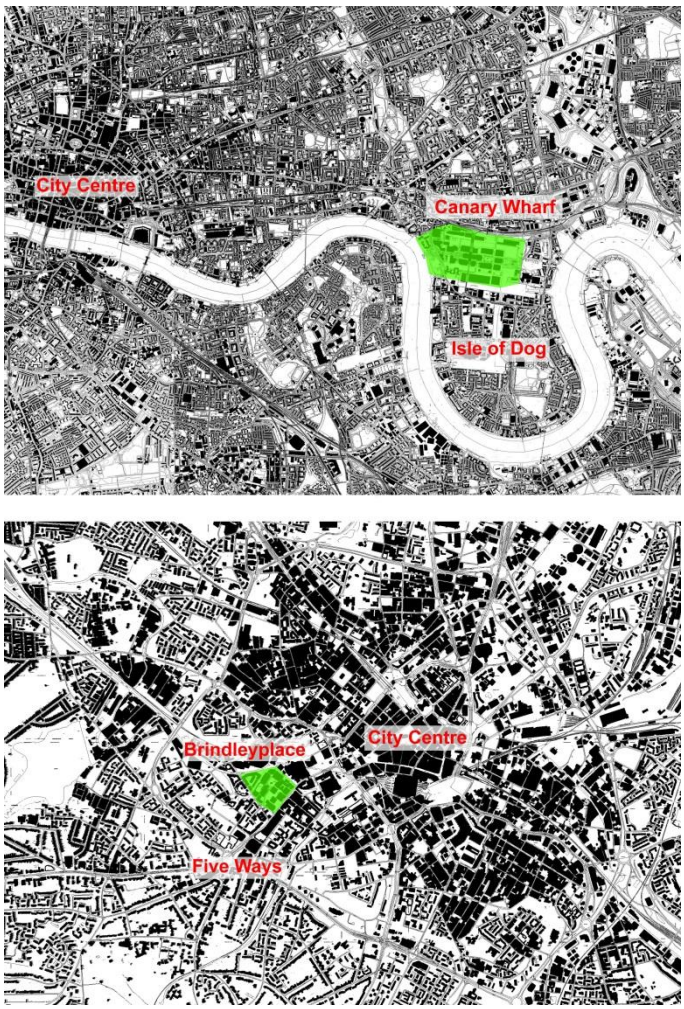

Fig. 3.5 Locations of Canary Wharf and Brindleyplace

Top: Canary Wharf, located in the poorest Borough of Tower Hamlets and to the east of the City of London.

Bottom: Brindleyplace, lying in the poorest area of Ladywoods and to the west of the city centre core.

Both developments confronted the problem of how to deal with spatial connections to the surrounding areas. Initially both tried to create new urban centers on derelict brownfield sites, but both also adopted different spatial strategies. The regeneration of Canary Wharf, as a major part of the London Docklands Development, started with the planning policy of deregulation[28] in

[28] Canary Wharf, as an Enterprise Zone, 'was designated in April 1982 and lasted for ten years. There were no planning controls (with minor exceptions), rates (property taxes) were paid by Government and capital investments could be written off against a company's tax liability'. See LDDC, 1997: A Strategy for Regeneration.

the early 1980s. The London Docklands Development Corporation (LDDC)[29], a quango agency set up by the UK Government in 1981 to regenerate the dockland areas of East London, put an emphasis on flexible market-led development and had *no* concrete spatial framework for the whole district of which Canary Wharf is located at the centre (Gordon, 2004). The London Docklands Development Corporation had been criticized often for creating a fragmented urban environment and failing to achieve social regeneration in the surrounding area since the beginning of the regeneration process (Brownill, 1990; Brian, 1992; Foster, 1999). Although Canary Wharf had a masterplan and design guidelines produced by Skidmore Owings and Merrill (SOM, 1987a and b) to ensure 'continuous and high quality open space alternatives' *within* the site, the masterplan, together with the expressway (Aspen Way) designed and constructed on the north of the site, was considered as *a welcome barrier* to the adjoining poor area of Poplar (Edwards, 1992).

In contrast, Brindleyplace was located in the Broad Street Redevelopment Area (BSRA) announced in 1984, where both the local authority and the city council always had a spatial framework to maximize the accessibility to the BSRA (Birmingham City Council, 1994). This was partly due to the lessons learned from the notorious ring road around the urban centre core, which was believed to have destroyed the vitality of Birmingham. The regeneration of Brindleyplace was expected to be achieved by the market-led strategy so that the development priorities could be continuously changed, within the context of a flexible design framework, as new opportunities in the market came along. Thus, the masterplan was constantly reviewed and adjusted according to the change of market. The masterplan at each stage, with the emphasis on optimising its accessibility to the surrounding areas, was considered as one way to give confidence to investors in any future development (Holyoak, 1999; Madelin, 1999; Healey, 1999). As for Terry Farrell's masterplan that acted as the basis for the final masterplan, Hillier with his colleagues gave a spatial and movement analysis at the urban level and this played a critical role in the revised masterplan to intrinsically and seamlessly link the site with the neighbouring areas (Holyoak, 1999). The case of Brindleyplace was appraised to offer a model

[29] For a detailed introduction of LDDC, see LDDC, 1997.

for creating a piece of real city, '*which adds a new location to the mix of places which compose the city*' (Healey, 1999: 105).

Brindleyplace attempted to spatially integrate with its surroundings, whilst Canary Wharf sought to be spatially segregated from its neighbouring areas. *Did such different spatial strategies result in different spatial structures of the two projects? How did they spatially and functionally interact with their adjoining areas, and does such interaction matter for the nature of their boundaries?*

3.3.2 Methodology

We then set up a syntactic methodology framework to tackle the above questions. An analysis of the two projects and their immediate surroundings in 1991 and 2004 was conducted, in order to compare their spatial structures before and after the developments. We selected the year 1991 and 2004 due to the following reasons. First, the second phase of the large-scale development of Canary Wharf did not start in 1991, although its first development phase was almost finished – but almost no tenants moved to the site – in and around that year; the construction of Brindleyplace project had not begun until 1992. Second, the offices and shops in both Canary Wharf and Brindleyplace were only fully rented out after the year 2000. Third, the pedestrian movement data for the two projects within and outside the project site in 2004 were available; and the pedestrian movement data of Brindleyplace in 1991 was also available.

The movement data for Brindleyplace in 1991 was obtained from the Space Syntax Lab which was involved in this urban regeneration project (Hillier et al, 1991). The pedestrian movement data within and outside the development site was collected on weekdays by the Space Syntax Lab in 1991[30]. The data included 11 observation gates within the site and 142 gates outside. But the movement data for Canary Wharf in 1991 was not available. For example, **Fig. 3.6a**

[30] For the detailed procedure to conduct movement survey of Brindleyplace in 1991, see Hillier, B and Penn, A and Grajewski, T and Jianming, X (1991) Brindleyplace, Birmingham: the UCL study of the potential of the site and the Farrell masterplan, UCL.

demonstrates the locations of gates and the movement pattern (where red denotes higher movement and blue indicates a lower value).

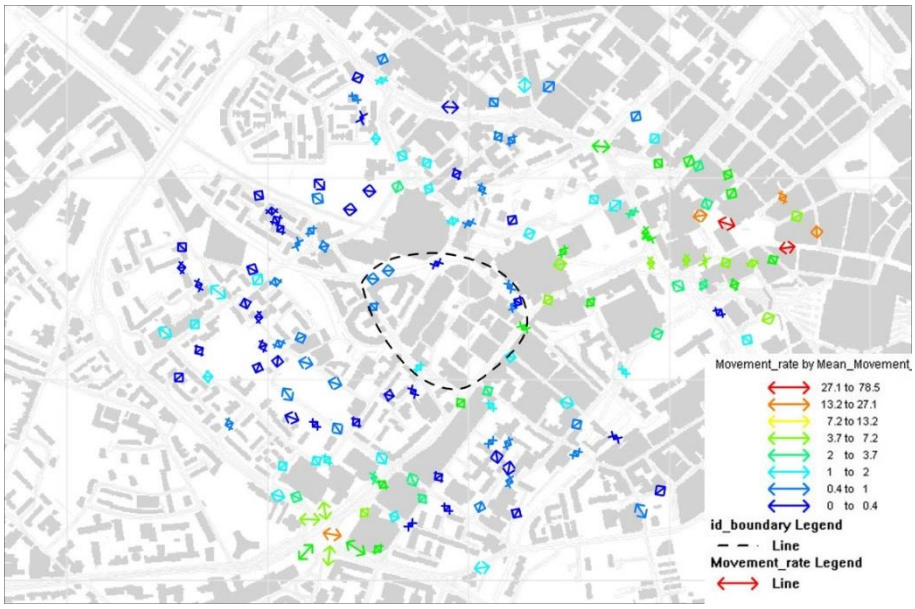

a The location of gates and the movement pattern of Brindleyplace and the nearest surroundings in 1991 (the site boundary represented by the black doted line). Red denotes high rate movement; and blue indicates low rate movement.

This image was produced according to the movement data in the report of Brindleyplace, Birmingham: the UCL study of the potential of the site and the Farrell masterplan (Hillier et al, 1991)

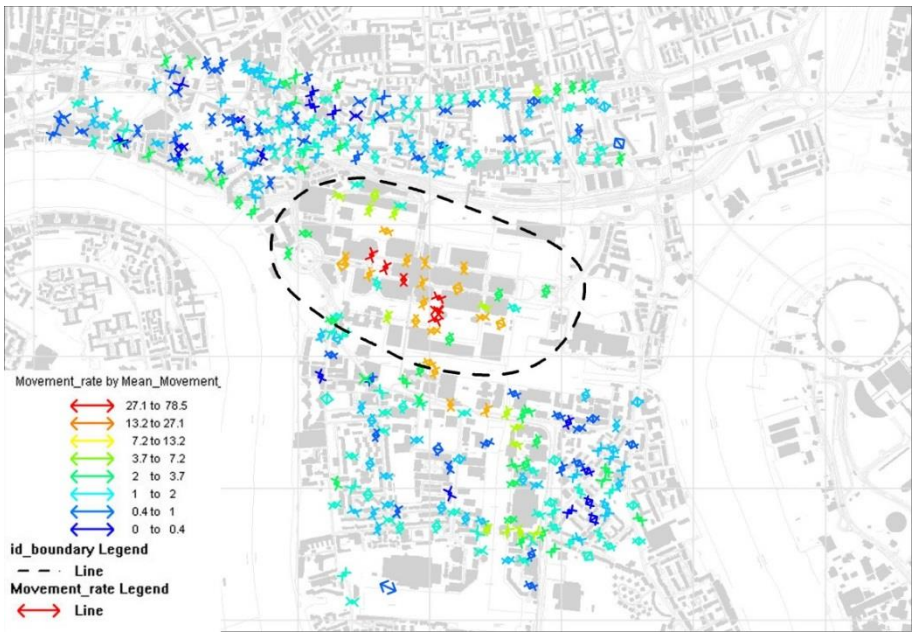

b The location of gates and the movement pattern of Canary Wharf and the nearest surroundings in 2004 (the site boundary represented by the black doted line). Red denotes high rate movement; and blue indicates low rate movement.

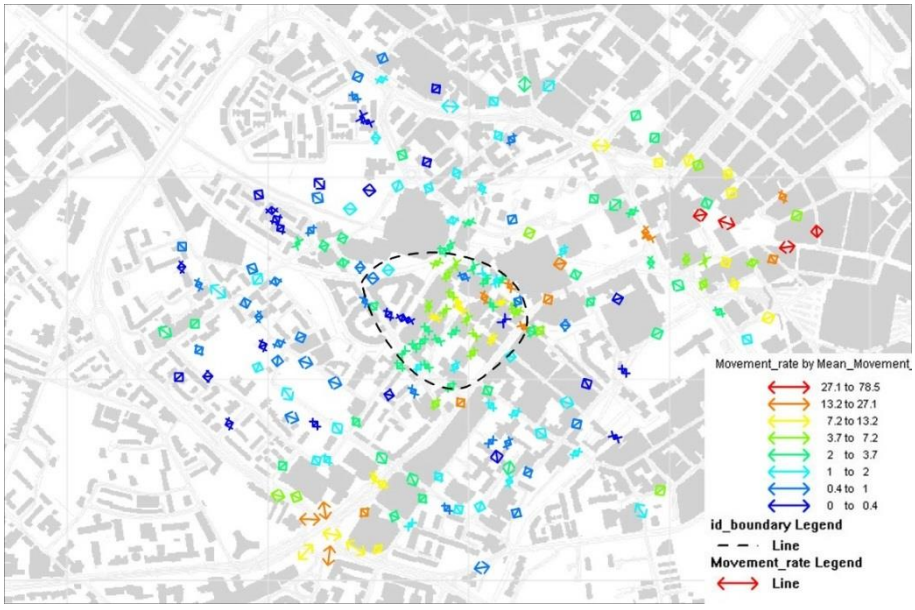

c The location of gates and the movement pattern of Brindleyplace and the nearest surroundings in 2004 (the site boundary represented by the black doted line). Red denotes high rate movement; and blue indicates low rate movement.

Fig. 3.6 Locations of Gates and Movement patterns in Canary Wharf and Brindleyplace

The pedestrian movement survey of both Canary Wharf and Brindleyplace was conducted by the student on a couple of sunny workdays in August, September and October 2004. For Canary Wharf, the observation was carried out at 318 gates among which 38 gates were located within the project site. For Brindleyplace, the observation was made at 203 gates amongst which 46 gates were located within the project site. All the gates were counted from 8am to 6pm with 5 rounds and each of them was observed for 5 minutes within each round. The movement data collected in the five rounds for each gate were averaged to get an overall movement pattern. For example, **Fig. 3.6b** and **c** display the location of those gates and their movement patterns (where red denotes higher movement and blue indicates lower value).

Then, the axial maps of the two projects with their surroundings in 1991 and 2004, respectively, were drawn to represent their spatial structures before and after the development. As for those maps, the ratio of the area of the project site to the area of the context in which the project is embedded is kept almost identical (about 6%) to ensure that the same proportion of the contextual structure was taken into account for the analyses in the two cases. **Fig. 3.7** shows the unprocessed axial maps in 2004, in which red lines denote site boundaries, and blue lines represent their nearest surrounding areas and where the movement surveys were made. The project sites together with the nearest surroundings are located at the centre of the axial maps, so that the edge effect[31] is minimised.

[31] The edge effect occurs when the spatial features of the lines near to the edge become more segregated because they are partly cut off from the immediate surroundings outside the edge. This was reviewed in **Section 3.2.1**. For detail, see Hillier (1996), p163.

.

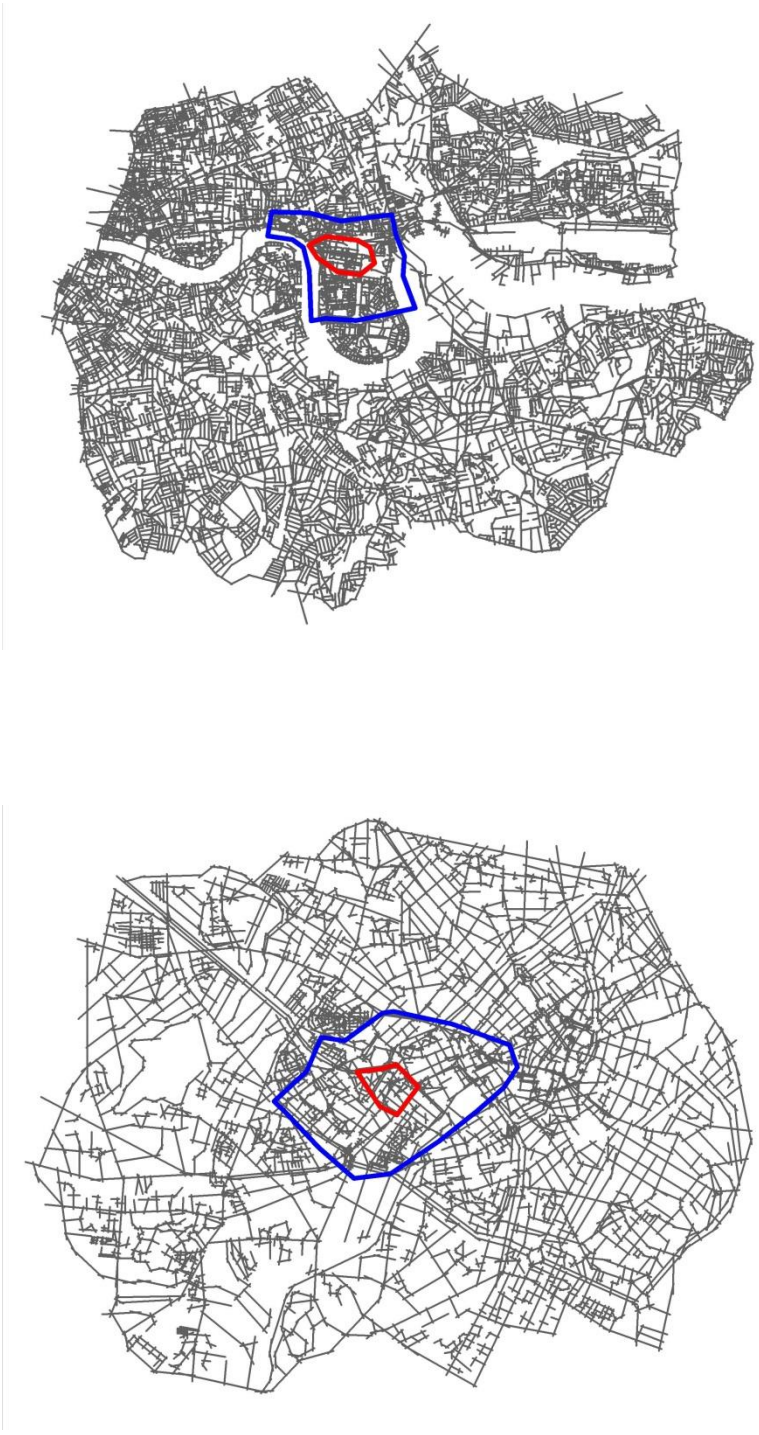

Fig. 3.7 The Unprocessed Axial Maps of Canary Wharf and Brindleyplace in 2004

Top: the map of Canary Wharf; **Bottom**: the map of Brindleyplace.

In the two maps, red lines represent the boundary of the project site and blue lines denoting the boundary of the nearest surrounding areas within which the pedestrian movement survey was conducted.

The axial maps, associated with the movement data for the two projects, set the baseline for further analyzing the two projects. The axial maps of the two projects in 1991 and 2004 were processed, respectively, and then maximum syntactic value, such as the maximum of integration Rn, of the lines crossing each gate was assigned to the gate one by one.

The explorable analysis includes *two* parts. The first part is about the *spatial comparison of the two projects*. The axial maps of the two projects were coloured according to the values of integration Rn and R3, as a way of showing and comparing the patterns of global and local integration for each project before and after the development. For each project before and after the development, the same colour ranges were used so that a visual comparison can be made. Red indicates more integrated spaces, and blue denotes more segregated spaces. In particular, red, orange and yellow denote 10% of the most integrated lines, locally and globally, termed *local integrator* and *global integrator* respectively, as reviewed in **Section 3.2.1**. They represent the potential of local and global centres respectively and are called as *spatial integrator* in general. To compare the integration patterns before and after the development allows us to primarily investigate whether different spatial strategies resulted in different spatial transformations.

We then examined the catchment areas constituted by the axial lines up to a fixed depth away from the axial line with the highest integration R3 values within the project, called *site integrator*, representing the local spatial centre of project. For each project, those catchment areas were compared before and after the development, in order to see how far the spatial centre of each project spatially influenced the surrounding areas.

Moreover, we proposed a new syntactic technique for illustrating the way the project interacts with the contexts, ranging from its immediate surroundings to the whole city of which it is a part. As reviewed in **Section 3.2.2**, the variables of intelligibility and synergy can be applied to measure the relationship between local conditions of an area and the global configuration of the area; and this suggest that these two variables can be used to examine the extent to which an area is spatially embedded into the whole city. Following this line, we suggested two measures: *intelligibility Rk*, defined as the R-square of the linear correlation between connectivity and

integration Rk (integration at a given radius of k), and *synergy Rk*, defined as the R-square of the linear correlation between integration R3 and integration Rk. They measure how far an area is embedded into the context selected by a fixed radius of k (between and including the most localized radius and the most globalised radius). A series of intelligibility Rk or synergy Rk on the vertical axis plotting against radius k on the horizontal axis, what we called *the increasing radius intelligibility or synergy* (Yang, 2005) These were expected to give a thorough account of the effect of the interaction between the projects and their multi-scale contexts with an increase of radius. We examined the increasing radius intelligibility and synergy of the two projects after the development.

Furthermore we examined the internal layout of each project – only comprising of the axial lines within and intersecting with the project boundary – without taking account of their contexts, named *the project independently* in this thesis. Then, as for each project after the development, *the project independently* was compared with the same internal layout embedded into the contextual structure, called *the project within the context*, by conducting a linear correlation between integration Rk of the project independently and that of the project within the context, with increasing radius of k. The greater the correlation at a specific radius, the more that project is embedded into the surroundings at that radius, and vice versa. This enables us to explore the radius at which the contexts significantly influence the projects in a syntactic way.

The *second* part focused on *an analysis of spatial configuration and movement pattern* in the two projects by using the technique of correlation contour map (reviewed in **Section 3.2.2**), in order to achieve a better understanding of the nature of project boundaries. First, we produced and compared the correlation contour maps of the two projects after the development. Within each *contour peak*, the correlations between the spatial configuration and the movement rates were optimised. As reviewed in **Section 3.2.2**, Hillier (1987) suggested the concept of natural area of which the spatial configuration *best* predicts the movement rates. Thus, the boundaries of the natural areas can be represented by the lines of contour peaks, termed *natural boundaries* in this chapter. This helps us to explore whether and how the project boundaries relate to the natural boundaries.

Then, we overlaid *the 5% global and local integrators*, meaning the 5% most integrated lines at Rn and R3 respectively, on the correlation contour maps to visually examine whether and how those strong integrated spaces, perhaps within and outside the project areas, relate to the natural boundaries, if identified, of the projects and of the surrounding areas.

Finally, since we obtained the movement data of Brindleyplace in 1991, we further produced a correlation contour map before the development, and then compared it to the contour map after the development, in order to investigate the project boundaries in relation to the transformation of the natural boundaries, if found, in Brindleyplace and its surroundings. However, we had no movement data for Canary Wharf before the development, so we did not conduct such a comparison for this project.

Integration R3 in 1991 Integration R3 in 2004

Integration Rn in 1991 Integration Rn in 2004

Fig. 3.8 The Spatial Patterns of Canary Wharf Before and After Development

It illustrates the locally and globally spatial integration patterns of Canary Wharf and the nearest surrounding areas, before and after the development, respectively. Each colour scale represents the same value between the cases before and after the development in an attempt to make an accurate comparison. The red, orange and yellow lines represent the 10% most integrating spaces. The black doted lines denote the boundary of the project site.

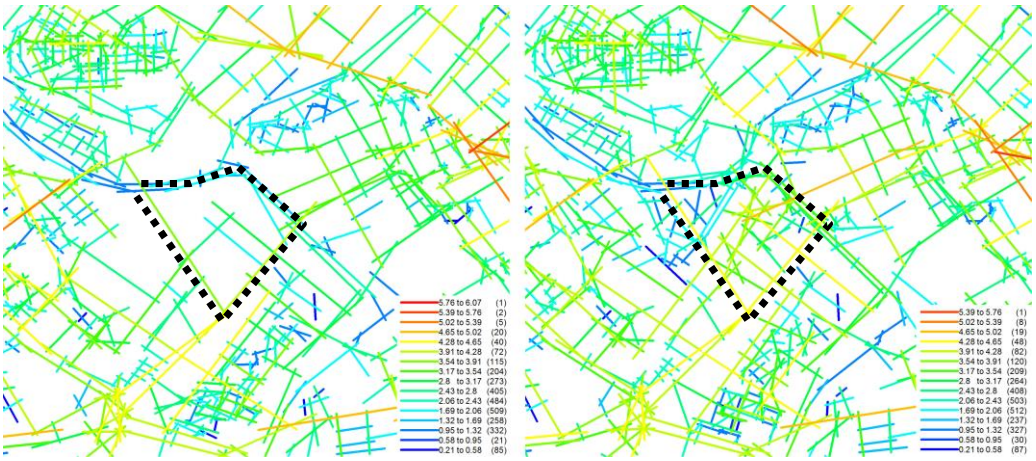

Integration R3 in 1991 Integration R3 in 2004

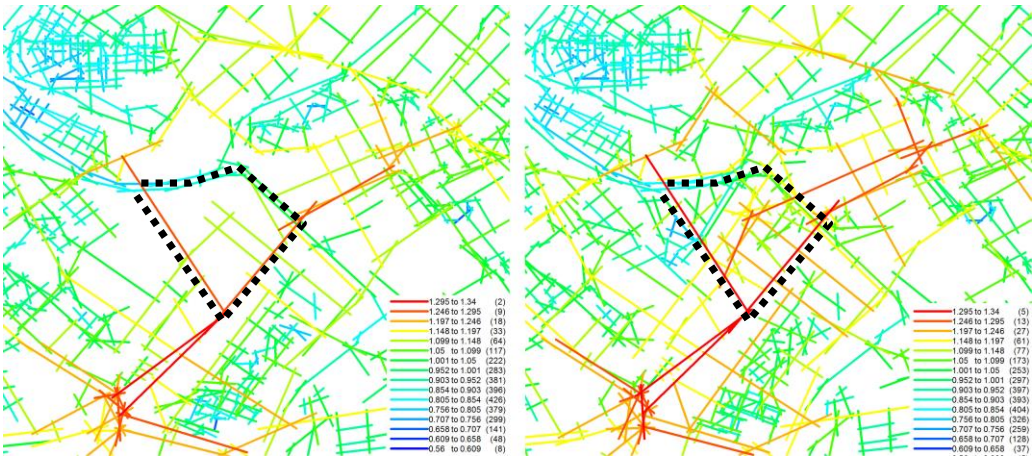

Integration Rn in 1991 Integration Rn in 2004

Fig. 3.9 The Spatial Patterns of Brindleyplace Before and After Development

It illustrates the locally and globally spatial integration patterns of Brindleyplace and the nearest surrounding areas, before and after the development, respectively. Each colour scale represents the same value between the cases before and after the development in an attempt to make an accurate comparison. The red, orange and yellow lines represent the 10% most integrating spaces. The black doted lines denote the boundary of the project site.

3.3.3 The spatial interaction between the internal and the external

This section presents the findings in the spatial analysis of the two projects, with the aim of revealing how far they were spatially embedded into their surroundings, under the different spatial strategies for development discussed in **Section 3.2.1**.

Spatial transformations before and after the development

The local and global integration patterns of the two projects in 1991 and 2004 **(Fig.3.8 and 3.9)** visually demonstrate that both projects and their immediate contexts experienced the different spatial transformations. Before the development, there were *no* global or local integrators, coloured in red, orange or yellow, within their respective sites. However, in their immediate

surroundings, several stronger lines in warmer colour, at both local and global radii, were found. This suggests that before the development, the internal layouts of the two projects had *not* been spatially structured, and so did not generate either global or local integrators indicating the potential centres.

After the development however the internal structure of Canary Wharf (shown in **Fig. 3.8**) had two light yellow lines - representing North Colonnade and South Colonnade - at the local radius, which suggests that it gained the relative weak local integrators at the geometric centre, but still did not obtain a global integrator. However, the global integrators at its north surrounding areas seemed to become a bit weaker, as the red lines decreased; but several lines at its north and south surroundings became more yellow at the local radius. This demonstrates that the regeneration of Canary Wharf had not improved spatial integration within and outside the site at the global scale, although a relative weak local centre appeared within the site and the local centres at the surrounding areas became a bit stronger.

In contrast, after the development, the Brindleyplace project (shown in **Fig. 3.9**) gained stronger global and local integrators, denoted by the red, orange or yellow lines, both within and outside the project site; and some integrators at the immediate surroundings even penetrated into the geometric heart of the site. Furthermore, these global integrators formed a strong deformed wheel (the concept of deformed wheel has been reviewed in **Section 3.2.1**), linking the project site to its surroundings in all main directions. The local integrators, coloured in orange and yellow, within and around the site also constituted a weaker and incomplete deformed wheel, in particular linking the project site with the city centre core to the east. This suggests that the regeneration of Brindleyplace has generated a more coherent spatial structure integrating the site into its surroundings, locally and globally.

The relation between the site integrator and the immediate surrounding areas

How far did the site integrators (the most integrated line at 3 within the project site, as **Section 3.3.2** defined), representing the local spatial centre for both projects impact on the surroundings, before and after the developments? **Fig. 3.10**, for example, shows the catchment areas constituted by the axial lines 3 and 9 depths away from the site integrator of Canary

Wharf, before and after the development. The catchment areas seem not to increase significantly after the development, and this suggests that the regeneration of Canary Wharf did not improve the spatial relation between the project centre and the surrounding area.

However, **Fig. 3.11**, for example, shows the catchment areas constituted by the lines both 3 and 7 depths away from the site integrator of Brindleyplace, before and after the development. It demonstrates that the catchment areas extended to the northeast after the development, and this indicates that the regeneration of Brindleyplace significantly improved the spatial connections between the project centres and the surrounding areas to the northeast.

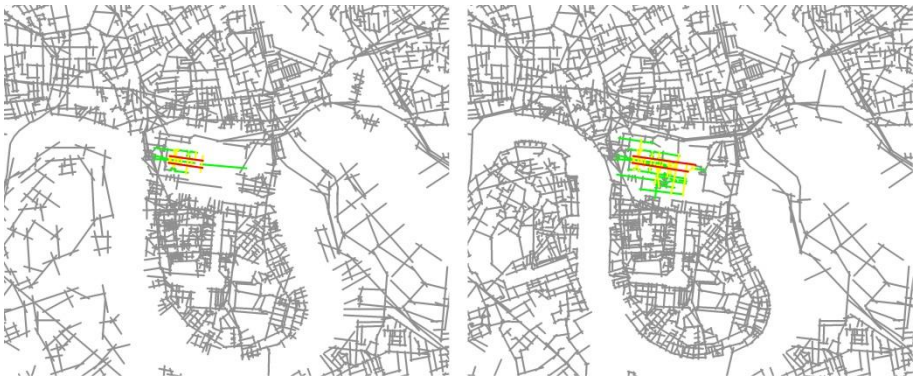

Canary Wharf in 1991 Canary Wharf in 2004

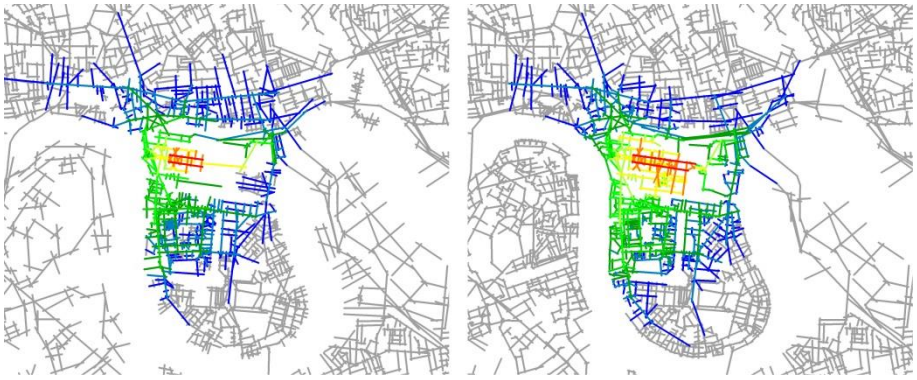

Canary Wharf in 1991 Canary Wharf in 2004

Fig. 3.10 The Catchment Area 3 and 9 Depths from the Site Integrators of Canary Wharf

Top: the catchment areas 3 topological depths from the site integrators, before and after the development, respectively (Red denotes the site integrators, green indicates the edge of the catchment);

Bottom: the catchment areas 9 topological depths from the site integrators, before and after the development, respectively (Red denotes the site integrators, blue indicates the edge of the catchment).

Brindleyplace in 1991 Brindleyplace in 2004

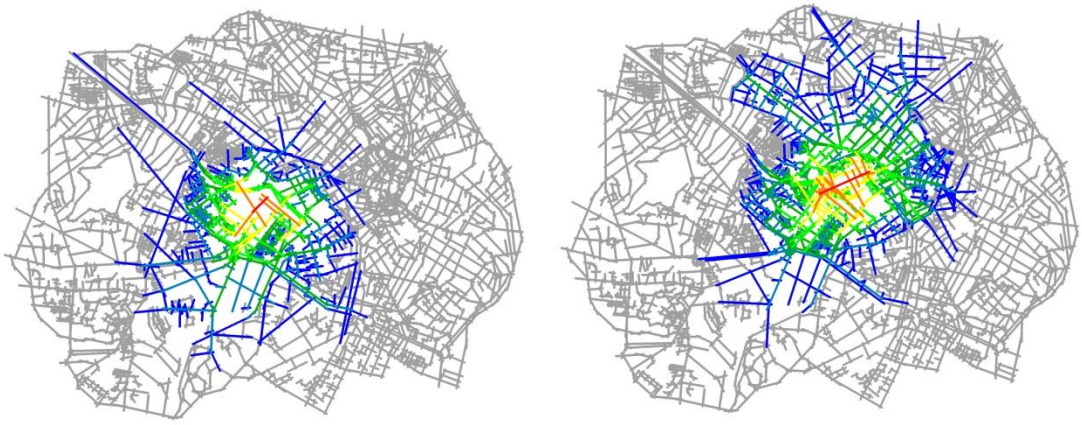

Brindleyplace in 1991 Brindleyplace in 2004

Fig. 3.11 The Catchment Area 3 and 7 Depths from the Site Integrator of Brindleyplace

Top: the catchment areas 3 topological depths from the site integrators, before and after the development, respectively (Red denotes the site integrators, green indicates the edge of the catchment);

Bottom: the catchment areas 7 topological depths from the site integrators, before and after the development, respectively (Red denotes the site integrators, blue indicates the edge of the catchment);

Table 3.1: The Size of Catchment Areas k Topological Depths from Site Integrator (CW: Canary Wharf; BP: Brindleyplace: CW_increase: the percentage of increase of the catchment area of Canary Wharf)

Case	3-depth (acres)	5-depth (acres)	7-depth (acres)	9-depth (acres)
CW 91	37	81	213	494
CW 04	50	136	252	527
CW_ increase	135%	168%	118%	107%
BP 91	57	252	695	1258
BP 04	134	491	804	1526
BP_ increase	235%	195%	116%	121%

In addition, **Table 3.1** shows that the size of the catchment areas 3, 4, 7 and 9 depths from the site integrators of Canary Wharf and Brindleyplace, before and after the development, respectively. The catchment areas of Canary Wharf are much smaller than those of Brindleyplace at the radius of 3, 4, 7 and 9, in 1991 and 2004, in spite of Canary Wharf of 71 acres being much larger than Brindleyplace of 17 acres. The percentage of increase of the catchment areas in the Canary Wharf project is lower than that of Brindleyplace at the radius of 3, 5 and 9. Although the increase percentage of Canary Wharf at 7 (118%) is slightly higher than that of Brindleyplace at 7 (116%), the increase in area of Brindleyplace at 7 (109 acres) is much larger than that of Canary Wharf at 7 (39 acres). This finding supports that the Bridleyplace project in general was more spatially integrated into its surroundings.

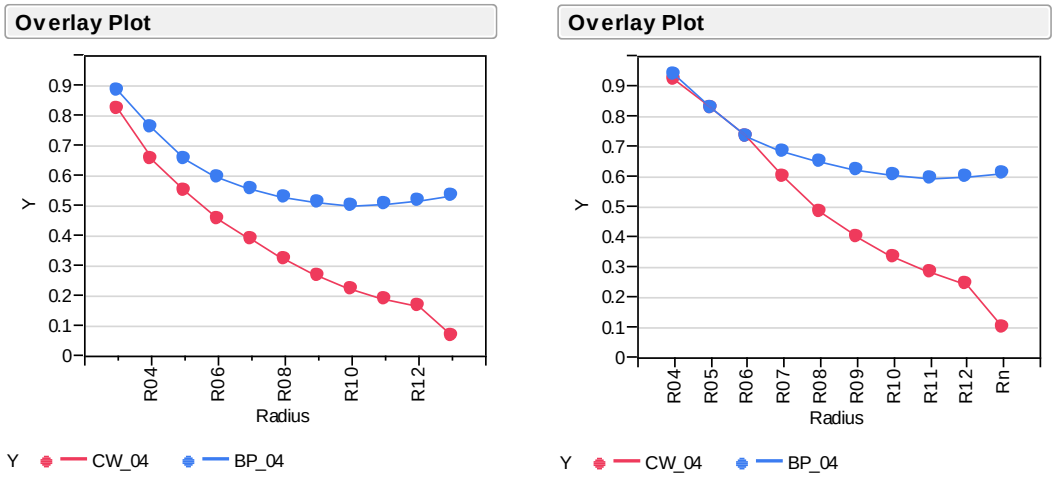

the increasing radius intelligibility the increasing radius synergy

Fig. 3.12 The Scattergrams of Increasing Radius Intelligibility and Synergy of Canary Wharf and Brindleyplace within the Contexts After Development

(CW_04: Canary Wharf in 2004; BP_04: Brindleyplace in 2004.)

How were the projects spatially embedded into the surroundings with increasing radius?

How far or at what scale were the two development sites spatially integrated into or segregated from their surrounding areas? **Fig 3.12** shows the scattergrams of increasing radius intelligibility and synergy (elaborated in **Section 3.3.2**) for the two projects after the development. The intelligibility and synergy curves of Brindleyplace both remain relative higher and more stable, but those of Canary Wharf drop sharply. This illustrates that Brindleyplace gained higher intelligibility and synergy values across radii; but Canary Wharf only had high intelligibility values (more than 0.5) at the radius of 3 to 5, and high synergy values (more than 0.6) at the radius of 4 to 7. It suggests that the Canary Wharf regeneration only advanced its relation to the more localised surroundings. The Brindleyplace regeneration, in contrast, created a good relationship between the internal layout and the contextual structures ranging from its immediate surroundings to the whole city.

Table 3.2: The R-square Values of the Correlation of Integration Rk of the project independently and that of the Same Project within the Context of the Whole City (CW: Canary Wharf; BP: Brindleyplace).

Radius	2	3	4	5	6	7	8	9
CW_ 04(R2)	0.758	0.734	0.651	0.556	0.414	0.223	0.116	0.058
BP_ 04(R2)	0.718	0.772	0.796	0.804	0.799	0.752	0.694	0.640

The above findings have been supported by conducting the correlation between the integration Rk values of *the project independently* – that only consists of the lines within and across the project boundary without taking account of the surroundings, as defined in **Section 3.3.2** – and those values of *the project within context*. **Table 3.2** shows the R-square[32] values of Canary Wharf and Brindleyplace at the radius of 2 to 9, after the development. In general, the values of Canary Wharf drop down with increasing radius. However, it has higher values at the radius of 2 to 5, but decreases dramatically after 5. This suggests that the internal layout of Canary Wharf was more spatially segregated from its contextual areas at the radius of larger than 5.

However, the R-square values of Brindleyplace remain above 0.7 from the radius 2 to 7, and slowly decrease from 7 to 9. This confirms that the Brindleyplace regeneration intended to spatially integrate the surroundings with its internal layout, and thus improve the spatial relations between the internal and the external across different scales.

From the above spatial analyses carried out in **Section 3.3.3**, it can be suggested that the spatial structuring of the two projects, guided by the different spatial strategies, determined the degree to which the projects were spatially embedded into their multi-scale surrounding areas. We will consider the following question: *do the different syntactic interactions between the internal and the external structures affect the nature of the boundaries of the two projects?*

[32] R-square is a statistical measure of how well a regression line approximates real data points. An R-squared of 1.0 (100%) indicates a perfect linear relationship, but an R-square of 0.0 means no linear relationship.

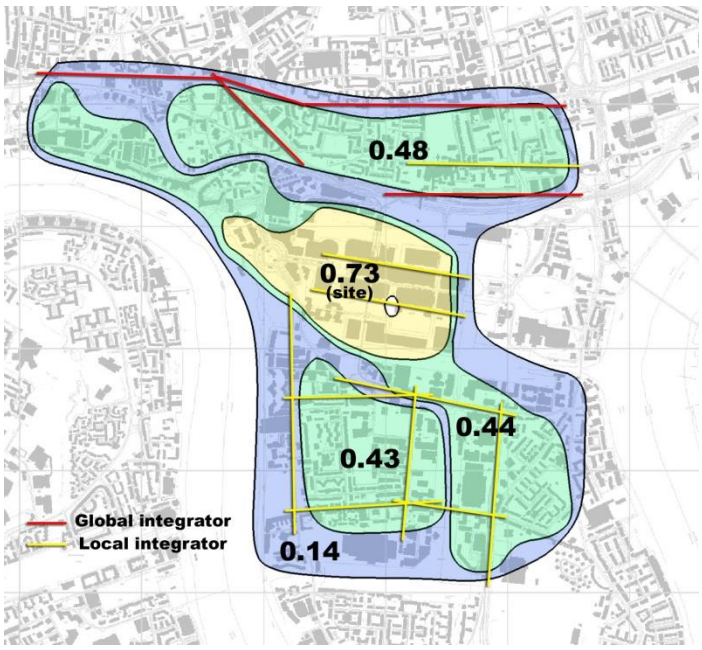

Fig. 3.13 The Correlation Contour Map, Superimposed by the 5% Global and Local Integrators, of Canary Wharf and the Surroundings in 2004

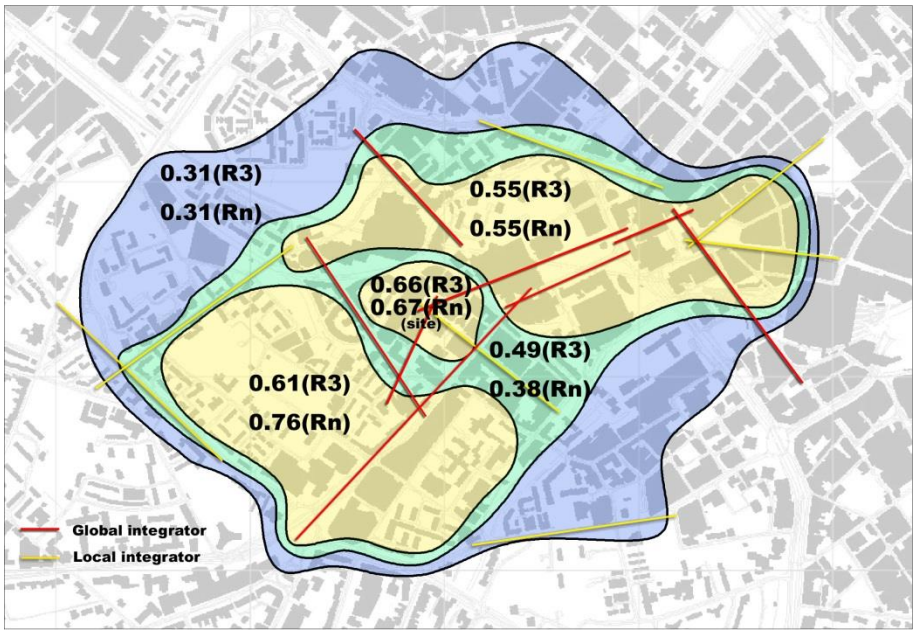

Fig. 3.14 The Correlation Contour Map, Superimposed by the 5% Global and Local Integrators, of Brindleyplace and the Surroundings in 2004

3.3.3 Natural boundaries of the two projects

In order to tackle the above question, we explore the *natural boundaries* – defined in **Section 3.3.2** as the boundaries (or the contour peak lines) within which the correlation of movement rates and spatial configuration is optimised – for each development.

The correlation contour maps of the two projects after the development

The correlation contour maps of Canary Wharf and Brindleyplace after the development reveal the different features of the natural boundaries of the two projects and of the surroundings **(Fig. 3.13 and 3.14)**. At first glance, the contour map of Canary Wharf has one contour peak, with an R-square over 0.5, generated by optimizing movement rates and local integration; whilst, the contour map of Brindleyplace has three contour peaks, with an R-square over 0.5, created by optimizing movement rates and global or local integration. This suggests that the natural boundaries of Canary Wharf are shaped by the local spatial properties. In comparison, the natural boundaries of Brindleyplace and of its surrounding areas are influenced by both the global and local spatial configurations.

On the one hand, **Fig. 3.13** shows that the Canary Wharf project, as a contour peak, has the highest correlation of 0.73 between integration R3 and movement rates, except for an outlier in front of the main entrance of Jubilee Station. If adding the factor of the topological depth from this main entrance to all other lines into the correlation calculation through the technique of the multi-regression model[33], Canary Wharf even gains a slightly higher correlation of 0.76. This demonstrates that the movement rates inside the project site were sustained by the local structure, as well as the supplementary factor of the tube station as one major attractor. With the regard to the fact that the main entrance of Jubilee Station is only one depth away from the site integrator, it can be suggested that the local configuration of Canary Wharf plays an important role in shaping the movement patterns within the natural boundaries.

[33] Multi-regression model is to learn more about the relationship between several independent variables (eg. integration and topological depth to a tube station) and a dependent variable (eg. movement rate).

When taking account of the neighbouring areas to the northwest and the southeast, the R-square dropped down to 0.44 and a second-tier contour appeared. When more gates outside this second-tier contour were then added, the R-square sharply decreased and reached 0.14 (meaning no correlation at all). But two other second-tier contours, one with an R-square of 0.48 to the north and the other with an R-square of 0.43 to the south, were found, and they might relate to the areas of Poplar and Millwall. To some extent, it demonstrates that Canary Wharf, represented by the contour peak with the highest correlation, was relatively isolated from Poplar and Millwall, both of which are denoted by the second-tier contours. And it suggests that the pedestrian movement within the site of Canary Wharf, corresponding to its self-sustained spatial layout, has no relation to its surrounding areas. This implies that the natural boundary of Canary Wharf is *hard* with regards to its surrounding areas.

On the other hand, **Fig. 3.14** shows that Brindleyplace has three contour peaks, representing Brindleyplace itself with an R-square of 0.662 locally and of 0.674 globally, the city centre core to the east with an R-square of 0.55 both locally and globally, and Five Ways to the southwest with an R-square of 0.61 locally and of 0.76 globally. Taking account of the three peaks as a whole, the R-square decreased to 0.49 locally and 0.38 globally, but they still remain moderate. When all other gates in the further surroundings were included, the R-square dropped to 0.31 both locally and globally; but they were not the worst, compared to the R-square of 0.14 in the case of Canary Wharf. To a large extent, this suggests that the three areas as the peaks, including the project of Brindleypalce, were less separated from each other and their surroundings, locally and globally, compared to the contour map of Canary Wharf. In other words, the Brindleyplace regeneration was making progress in integrating the spatial structures of the project site, the city centre and Five Ways into a whole and bringing the movements together at different directions and scales. In this sense, compared to the natural boundary of Canary Wharf only generated at the local radius, the natural boundary of Brindleyplace created at both local and global radii seems *softer* according to its surrounding areas.

How do the natural boundaries relate to spatial integrators?

We progress by looking a whether the natural boundaries of the two projects relate to the pattern of the spatial integrators - representing the pattern of potential centres, as discussed in **Section 3.3.2** - that usually sought to combine the spaces together? **Fig. 3.11 and 3.12** also show the 5% spatial integrators, both locally and globally, superimposing over the contour maps. The local integrators within the project site of Canary Wharf seemed to be circumscribed within the contour peak line representing its natural boundary (**Fig. 3.13**). The other integrators at the surroundings, either locally or globally, did not penetrate into the contour peak representing Canary Wharf. Three clusters of integrators were visually separated by the correlation contour 'valley' with the weakest R-square of 0.14. This suggests that those integrators inside and outside the project site failed to form a continuous integration core to spatially integrate this project into the surroundings, which resulted in the *hard* natural boundary of Canary Wharf.

In contrast, the spatial integrators within the site of Brindleyplace were interconnected with the integrators at the surroundings to form an integration core, penetrating the natural boundary of Brindleyplace as a contour peak and linking that contour to other surrounding contour peaks, denoting the city centre core and Five Ways (**Fig. 3.14**). As a result, the three contour peaks were combined together to form a larger second-tier of contour with the moderate correlation, which suggests *soft* natural boundaries. In fact, it can be implied that the softer natural boundary of Brindleyplace results from the strong and continuous integration core passing through the natural boundaries of the neighbouring areas.

The above analysis suggests that the formation of natural boundaries of the two projects are related to the features of the integration core constituted by the most integrated spaces, as well as the degree to which spatial configuration impacts on the movement pattern.

The transformation of the natural boundaries in the case of Brindleyplace

In addition, the transformation of the natural boundaries of Brindleyplace and of its surrounding areas, before and after the development, supports the above finding. **Fig. 3.15** displays two

contour maps of Brindleyplace before the development, one of which is produced by the correlation between integration R3 and movement (**Top**), and the other generated by the correlation between integration Rn and movement (**Bottom**). The former illustrates that one contour peak, with an R-square of 0.59, covered the city centre core and the areas to the north of the project site, and the latter shows that one contour peak, with an R-square of 0.71, covered Five Ways and the areas to the west of the site. They indicate that the movement in the city centre core had a better correlation with the local integration, but the movement in Five Ways had a better correlation with the global integration. It can be concluded that the movement pattern in the city centre core was more influenced by local spatial structure; but the movement pattern in Five Ways was more shaped by global spatial configuration. This suggests that the Brindleyplace project and its surroundings were spatially fragmented before the development, and so resulted in separating the movements at the global and local levels. As a result, the natural boundary of the city core was distinguished according to local configuration, but the natural boundary of Five Ways was marked out according to global configuration. But the project site seemed not to form a natural area, and this supports the previous finding that the site had no structure before the development (shown in **Fig. 3.9)**.

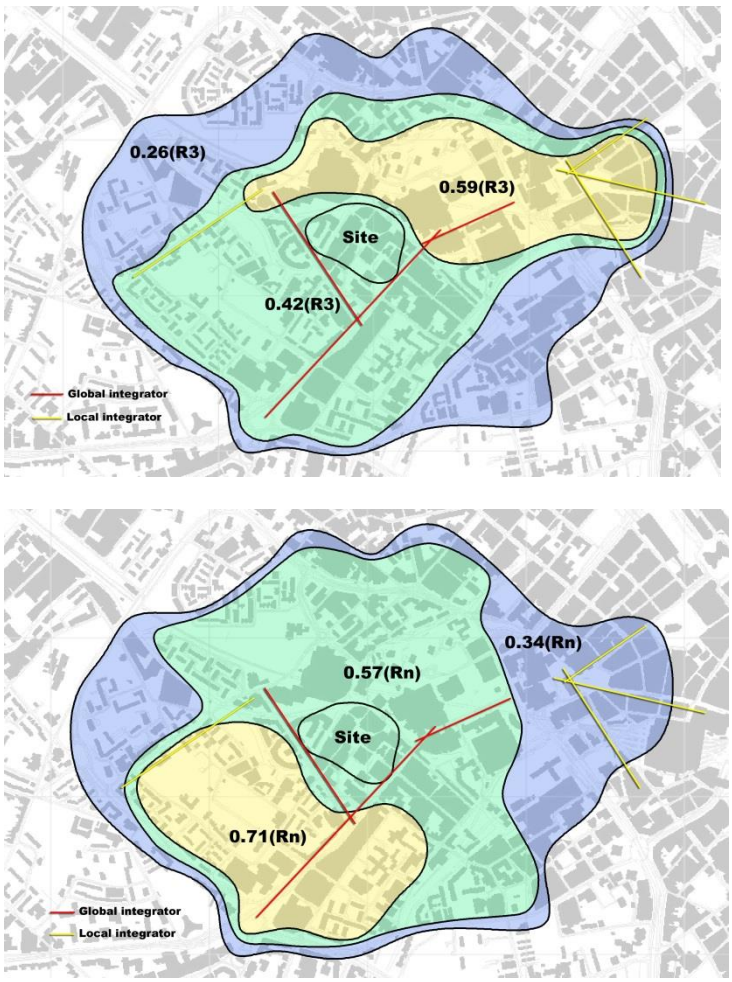

Fig. 3.15 The Correlation Contour Map, Superimposed by the 5% Global and Local Integrators, of Brindleyplace and the Surroundings in 1991

Top: the map produced by the correlation between integration R3 and movement rate;

Bottom: the map generated by the correlation between integration Rn and movement rate.

The distribution pattern of the 5% spatial integrators, illustrated by **Fig. 3.15**, also suggests the kind of spatial fragmentation. The global integrator, Broad Street, was located in the middle of the contour peak with a better correlation between global integration and movement (**Bottom**); whilst, the local integrator, New Street, was within another contour peak with a greater correlation between local integration and movement (**Top**). The global and local integrators were separated from each other, and they corresponded to the disconnected global and local natural areas, representing Five Ways and the city centre core, respectively.

After the development, three contour peaks, showed in **Fig 3.14**, emerged at both global and local levels, and meanwhile, the global and local integrators came to intersect each other to form a strong integration core, linking the three peaks together. It suggests that the Brindleyplace regeneration had been progressively woven into its fragmented contextual areas at the global and local scales, and then mixing and influencing the movement flows at both the local and global levels to create a new integrated area with a softer natural boundary. Meanwhile, it also can be argued that the spatial structuring of the Brindleyplace project itself also spatially and functionally impacted on the formation of surrounding areas, in the sense that the natural boundaries of the city centre core and Five Ways were sustained and shaped by the enhancement of the spatial configurations, in particular the formation of a strong integration core at both global and local radii, after the development. This implies that the boundary of the area scale project is not a pre-given and static barrier, but something marked by a *change* in spatial configuration within and outside the project, as well as its influence on the variation of movement pattern.

3.4 Discussion

There are two main findings in the above diagnostic study. First, the two projects can be spatially characterised and distinguished according to the way in which they interact with their contextual structures, ranging from the nearest surroundings to the whole city of which they are a part. For example, the scattergrams of the increasing radius intelligibility (or synergy) of the two projects **(Fig 3.12)** illustrate that Canary Wharf is more segregated from its surrounding areas at the radius of larger than 7, but Brindleyplace is relatively more integrated with its contexts across radii.

Second, the different patterns of natural boundaries – created by optimising the correlation between integration and movement rate – of the two projects, shown by the correlation contour mapping **(Fig. 3.13 and 3.14)**, relate to the different pattern of distribution of spatial integrators. The natural boundary of Canary Wharf is *hard*, mainly corresponding to the disconnected integrators within and outside the project site; but the natural boundary of Brindleyplace is *soft*,

linked to the natural boundaries of the surrounding areas by a stronger integration core constituted by the interconnected spatial integrators within and outside the project site.

The evidence outlined above suggests that to understand the nature of the spatial boundary, account has to be taken of the spatial configuration of the surrounding contexts, and its relation to the internal structure of the development. This then leads to the argument that the notion of area boundary is *not* simply a local idea, but is to do with how the spatial configuration of an area is related to the larger urban context of which it is a part.

It then can be conjectured that boundaries of an area might be investigated by detecting a change in the configuration of the area with regards to its multi-scale contextual structures, such as the change illustrated in the scattergram of the increasing radius intelligibility **(Fig 3.12)**, or the change in the pattern of global and local integrators of Brindleyplace before and after the development, which sustain, if not determine, the transformation of the natural boundaries shown in the correlation contour maps **(Fig. 3.14 and 3.15)**.

This kind of change can be considered as *the discontinuity in the way the spaces belonging to urban areas – that are spatially generated as parts of the whole - interact with the surroundings with increasing scale*, rather than a physical barrier locally enclosing and separating urban parts. It can be argued that area boundaries might be a manifestation of *those discontinuities in urban network*, meaning urban network being spatially partitioned into various discrete parts with regards to the syntactic relation between the generated parts and their multi-scale contexts. This raises a general question: *is it possible to measure and clarify those discontinuities in urban network with regards to spatial configuration?*

Chapter Four: Methodology

4.1. Introduction

In the previous chapter we showed evidence that the project boundaries of the two major developments are at least influenced by the way in which the projects spatially and functionally interact with their contextual structures at different scales; but one project has a much stronger *discontinuity* in the interaction between project site and the surroundings with an increase of radius, for example, showing a significant change in the creasing radius intelligibility **(Fig 3.12)**, than the other. So next we ask if there can be a syntactic method for identifying discontinuities in terms of space, and in this way arriving at a spatial definition of urban area. Since the j-graph identifies the pattern of connection of the graph outward from each line or segment considered as the root of the graph, we can ask first whether the study of the j-graph can bring to light discontinuities in its outward growth. The simplest way is to examine the relation between the radius of the j-graph and the sum of lines or segments encountered at that radius (called node count). The conjecture would be that any significant change in the pattern of growth in number of nodes can perhaps represent a kind of discontinuity in the line or segment graph.

This chapter takes two steps to explore this conjecture. First, it visually examines the pattern of growth in number of nodes from the perspective of a root axial line in the London case, and then investigates the mathematical relation between radius and node count of each line (or segment), based on the cases of London, Beijing and the London Docklands. The three cases were chosen due to their different geometric layouts[34]: London is an irregular structure developed over hundreds of years; Beijing is more like a traditional orthogonal structure evolving for hundreds of years; but most parts of the London Docklands comprise various large area-scale projects that had been planned and constructed since the 1980s. This enables us to set the experimental analyses in more complex contexts and gain a general understanding of the pattern of growth in number of nodes.

[34] The later empirical chapters and their appendices will further give a detailed introduction of urban parts of these three districts.

Second, an ideal example of axial map, associated with its representation of j-graph, is deployed to theoretically explore whether we can detect a significant change in the growth pattern of nodes, and examine whether the significant change, if identified, denotes the discontinuity in the axial map. Then, the project of Canary Wharf is re-examined to experimentally investigate whether we can identify a dramatic change in the growth pattern of a group of lines, because the project, as the previous chapter highlighted, has been spatially segregated from the contexts. This will help us clarify the concept of discontinuity in terms of the change rate of node count.

Based on the ideas developed in the above studies, it further explores the techniques for detecting the discontinuities in urban fabric, if existed, by conducting the experimental studies on these three cases of London, Beijing and the London Docklands. And more experimental studies on other cities, such as Birmingham, Chicago and Amsterdam, are further carried out to allow us to get more general results, because these cities selected from different parts of the world also have different geometric features.

The techniques expected to be developed in these experimental studies are then compared to Hillier's techniques for spatially differentiating urban areas (Hillier, et al, 2007, 2010), in order to elucidate the theoretical relationship between these techniques. This enables us to establish a synthesised framework for investigating the spatial mechanism involved in the formation of area structure, such as named area structure, in the later empirical chapters. It ends by addressing how the next two empirical chapters are organised according to the conceptual ideas embodied in the proposed methodology framework.

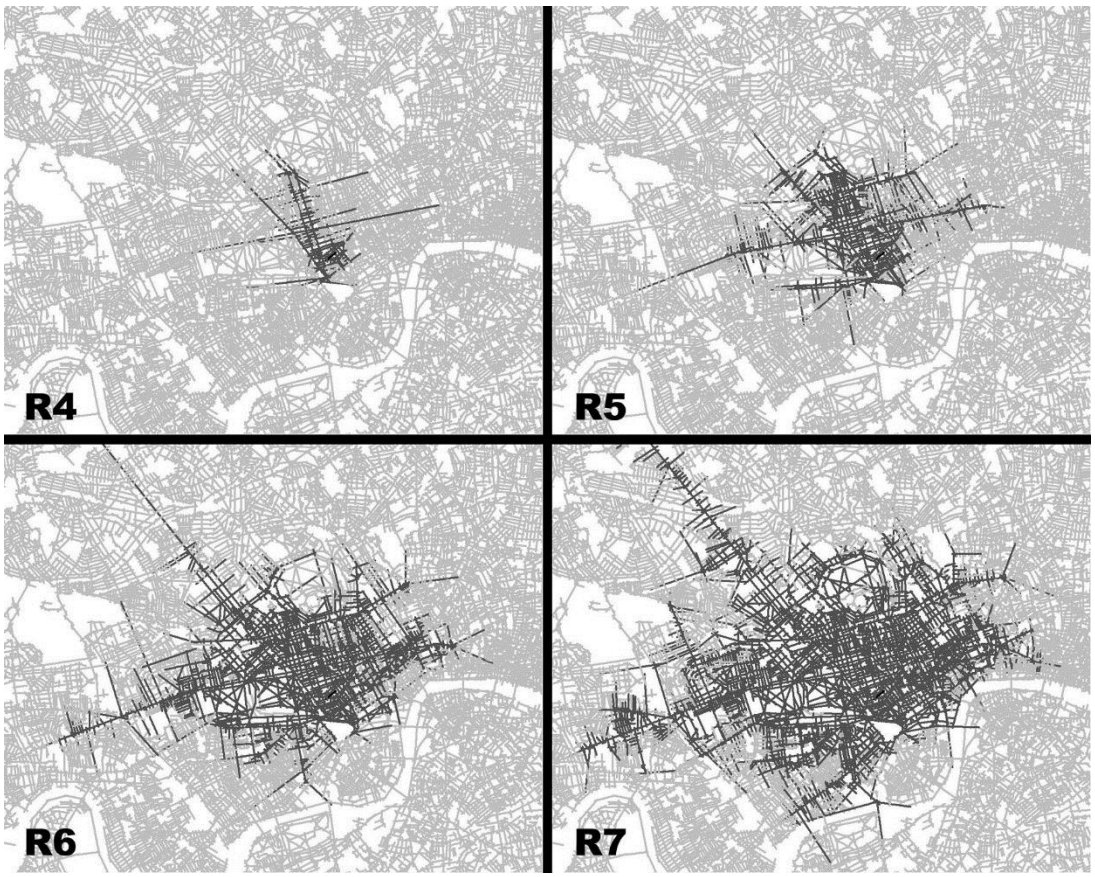

Fig. 4.1 The Axial Lines (Coloured in Dark Grey) up to 4, 5, 6 and 7 Topological Depth Away from A Root Line. It illustrates an embeddedness trajectory on which the root line is gradually embedded into its surroundings, regarding to its topological depth to them, from the radius of 4 through 5 and 6 to 7.

4.2 Embeddedness trajectory

4.2.1 The definition of embeddedness trajectory

Let us first visualise the number of the lines encountered with increasing radius, from the point of view of an axial line as a root, in order to intuitively explore how the root line is spatially embedded into the surrounding areas as radius increases. For example, we randomly selected a root line in the axial map of London, calculated its step depth meaning the topological depth

from the root to all other destination lines,[35] and then highlighted all the lines found up to 4, 5, 6, or 7 topological depths away from the root line, respectively **(Fig. 4.1)**. Dark grey represents the lines encountered up to the topological radius of 4, 5, 6, or 7, respectively.

In fact, **Fig. 4.1** compiles a sequence of images, which approximately illustrate the kind of trajectory on which the root line is gradually embedded into its surroundings, regarding to its topological depth to them, from the topological radius of 4 to 7. This trajectory, based on axial map, is called the *topological embeddedness trajectory* in this thesis. We raise this idea based on the axial map, because we usually investigate the topological relations of axial lines. However, if we examine metric properties of a spatial network, we often represent the spatial network by segment map[36]. Thus, on the ground of the segment representation, the *metric embeddedness trajectory* is defined as the trajectory on which any a segment is progressively embedded into the contextual segments, regarding to its metric distances to them, with an increase of metric radius. The idea of *the embeddedness trajectory*, either topological or metric, enables us to examine and visualise the relationship between any a space itself, represented as either an axial line or a segment, and its contextual structures found at different scales.

Then, *can we develop a method for mathematically describing the embeddedness trajectory of a line (or segment) in general?* The following analyses will be conducted based on three real cases of London, Beijing and the London Docklands. This methodology chapter however aims to develop the syntactic techniques for exploring and differentiating urban areas (which might be applied to the latter empirical chapters), rather than seeks to give an in-depth study of urban areas in these three cases. The latter is an objective of the later empirical chapters.

[35] For the procedure to calculate step depth, see Turner (2004), Depthmap 4, A Researcher's Handbook, p25.
[36] For the review of segment map, see the end of Section 3.2.1 in the previous chapter.

a. The unprocessed London axial map

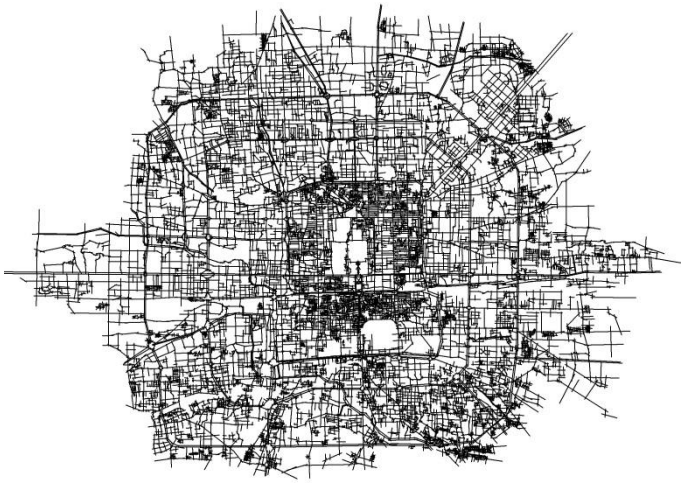

b. The unprocessed Beijing axial map

c. The unprocessed the London Docklands axial map

Fig.4.2 The Unprocessed Axial Maps of London, Beijing and the London Docklands. They have different geometric layouts.

The axial map of London we used is the same as the axial map of Greater London[37] within the North and South Circular roads, of which the historic central district of London is located at the centre. The axial map of Beijing was drawn based on the Beijing Map 2003 (BJISM, 2003) and covering the historic old district and the surroundings within the 4th Ring Road. The axial map of the London Docklands, based on the OS Land-line Map of London in 2004, is an extension map of Canary Wharf, shown in chapter three **(Fig.3.7 Top)**. The original map of Canary Wharf was extended northwards approximately to the roads of A104 and A12, and southwards to the roads of A205 and A20, in order to cover more contextual areas of the Docklands; and the London Docklands is placed at the map centre. **Fig. 4.2**, respectively, shows the unprocessed axial maps of the three regions. The axial maps (and segment maps), respectively, were processed to give the values of node count Rk - meaning the number of the lines (or segments) encountered up to the radius of k, as introduced earlier - to all lines (and segments).

The axial maps of London and Beijing both have the radius-radius[38] of 10, so that the tested topological radius range for these two cases was restricted from 1 to 10, in order to reduce the edge effect[39] in conducting the analysis of the embeddedness trajectories. And since the radius-radius of the London Docklands is 19, the tested topological radius range was given from 1 to 19.

As for the segmental analysis, the tested metric radius range begins at 400m and ends at 8,000m, with an interval scale of 100m, because the metric system radius (defined as the average metric distance from the geometric centre of the segment model to the edge) of the three segment models approximates 10,000m, and so the segment analysis at the radius of lower than 10,000m, such as 8,000m, is least influenced by the edge effect (that the analysis of segments at the edge of the segment map is also affected by their location at the edge of the segment map).

[37] For the detailed definition of the axial map of Greater London, see Hillier (1996), p161-62.
[38] The radius-radius is equal to the mean depth of the whole structure from the most integrated line. For detail, see Section 3.2.1 in chapter three, or Hillier (1996), p163.
[39] The analysis of spaces along the periphery of the axial map is always affected by their location at the system edge. For detail, see Section 3.2.1, or Hillier (1996), p163.

Then, the linear regression analysis between the logarithm of node count and the logarithm of radius, within the radius range of 1 to the radius-radius (or metric system radius), was performed for each axial line (or segment) in the three cases, respectively, by using the statistical software of JMP[40]. If the two variables had a strong linear correlation, represented by an almost straight regression line with a high R-square[41], their relationship could have been mathematically expressed as follow:

$$\ln(NC_k) = \alpha \times \ln(k) + \beta \qquad k \in [a,b] \qquad (4.1)$$

where NC_k denotes node count, α indicates the slope of the regression line, k means radius, β is a constant, and $[a,b]$.is the radius range within which a linear regression line with a high R-square is verified.

Then, the equation **(4.1)** can be transformed as:

$$NC_k = H \times k^{\alpha} \qquad k \in [a,b] \qquad (4.2)$$

where α is power law exponent, equal to the slope of the regression line, and H is a constant.

This means that node count could have a power-law relation with radius, if a linear regression line, with a high R-square, was found within a range of ‘a’ to ‘b’.

[40] JMP is statistical discovery software that contains basic statistical analyses, plus automated analytic techniques for data mining and predictive modeling. See http://www.jmp.com/software/pro/.
[41] R-square is a statistical measure of how well a regression line approximates real data points. An R-squared of 1.0 (100%) indicates a perfect linear relationship, but an R-square of 0.0 means no linear relationship.

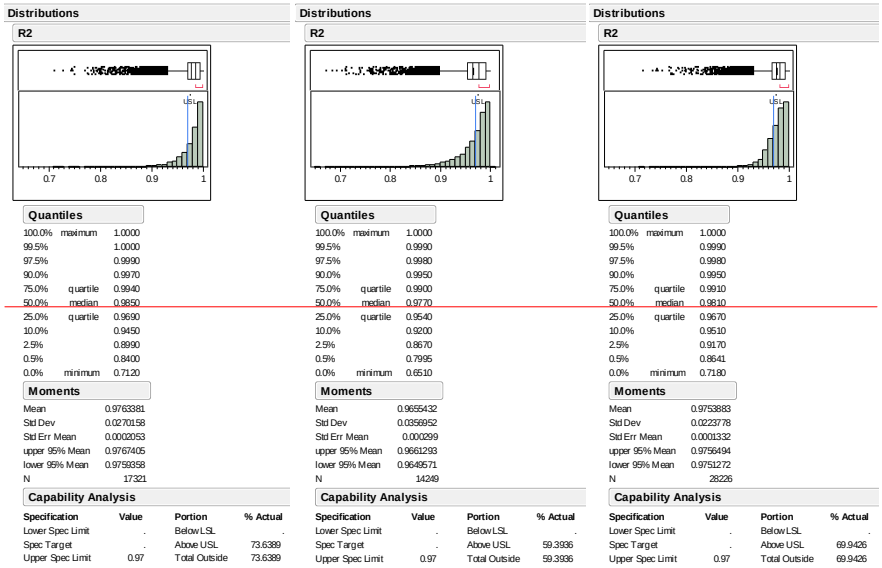

Fig. 4.3 The Approximated Power-law Relation between Node Count and Radius within the Tested Radius Ranges for More than Half of the *Axial Lines* in London, Beijing and the London Docklands (from left to right)

Top: the distribution patterns of the R-square in correlating node count and radius

Bottom: the distribution patterns of power-law exponent α

Red line highlights the median value respectively.

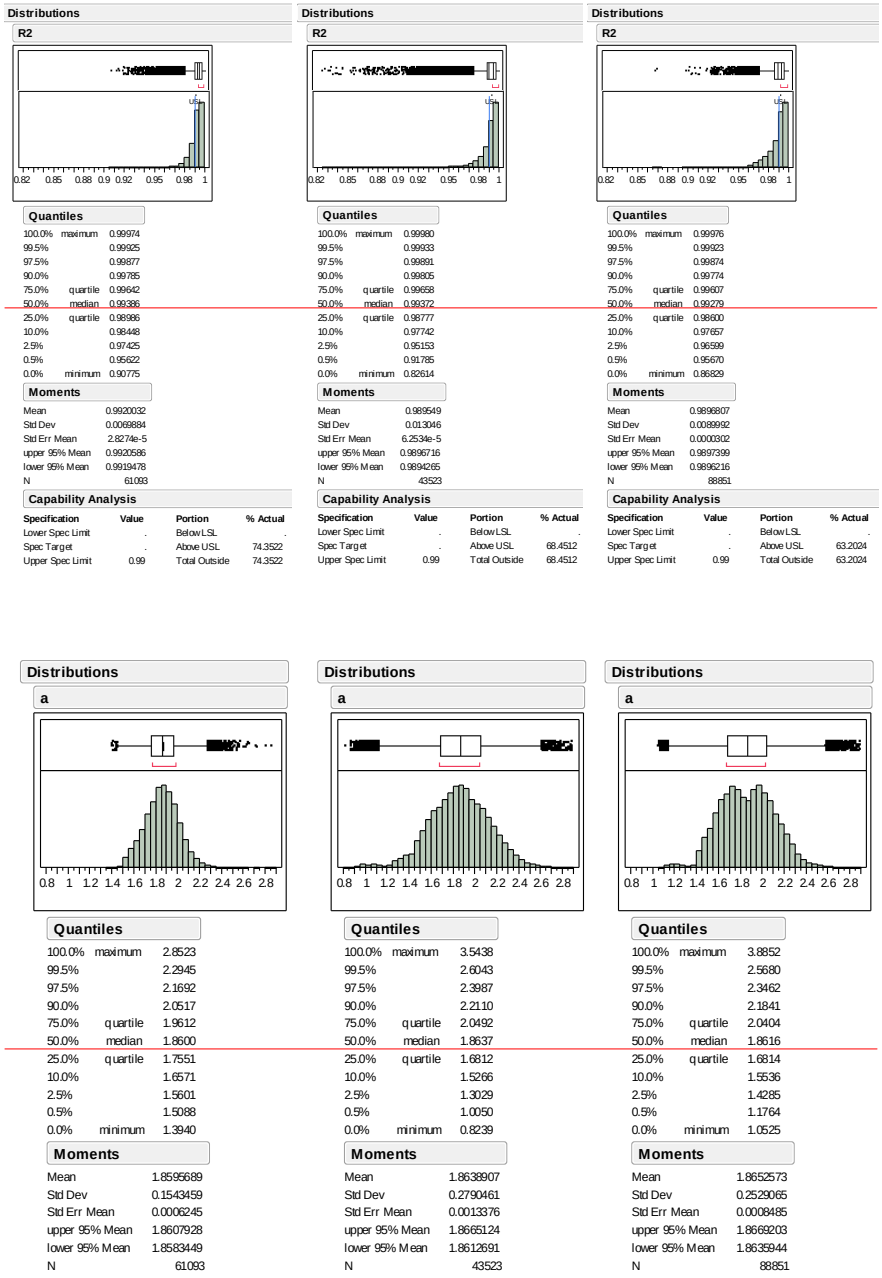

Fig. 4.4 The Approximated Power-law Relation between Node Count and Radius within the Tested Radius Ranges for More than Half of the *Segments* in London, Beijing and the London Docklands (from left to right)

Top: the distribution patterns of the R-square in correlating node count and radius

Bottom: the distribution patterns of power-law exponent α

Red line highlights the median value respectively.

The axial analyses suggest that more than half of axial lines in each case have an approximated power law relation between node count and radius[42] (Yang and Hillier, 2007). **Fig. 4.3** shows the distribution patterns of the R-square and the power-law exponent values of all the axial lines of the three cases, respectively. **Fig. 4.3 Top** indicates that the median of the R-square values of the London map is 0.985, the median of Beijing is 0.977, and the median of the London Docklands is 0.981. If the R-square is set above 0.97, 73.6 percent of the lines in London, 59.4 percent in Beijing and 69.4 percent in the London Docklands have a power law relation between node count and radius, within their constricted ranges. If the R-square is set above 0.90, all the lines of the three cases have an approximate power-law relation between these two variables. This suggests that most topological embeddedness trajectories, within the range of 1 to the radius-radius, in the three cases are approximately governed by power laws.

And the segment analyses also demonstrate that in these cases power law governs the metric embeddedness trajectories of more than half of segments within the range of 400m to 8000m. **Fig. 4.4** illustrates the distribution patterns of the R-square and the power-law exponent values of all the segments in the three cases, respectively. **Fig. 4.4 Top** shows the median of the R-square of London is 0.9939, the median of Beijing is 0.9937 and the median of the London Dockland is 0.9928. If the R-square is constricted above 0.99, 74.4 percent of the segments in London, 68.5 percent in Beijing, and 63.2 percent in the London Docklands have a power law relation between node count and metric radius within the constricted range. If the R-square is set to 0.90, each segment in these three cases has an approximate power-law relation. This result seems to be *stronger* than that generated from the above axial analysis.

However, we should remind the readers that the power-law function between node count and radius, found in the above axial and segment analyses, was *statistically approximated* within the range of 1 to the radius-radius (or metric system radius) for each line (or segment), because, for example, the R-square of 0.9 means that approximately 90% of variation in the two variables

[42] Park (2007) also studied the axial model of London and reached a similar conclusion. See Park,H. (2007) The Structural Similarity of Neighbourhoods in Urban Street Networks:A Case of London. In: Kubat, A.S. and Ertekin, O. and Guney, Y.I. and Eyuboglu, E., (eds.) 6th International Space Syntax Symposium, 093-1-18, pp.093-10.

can be explained by power law. The recent research shows that the embeddedness trajectories, either topological or metric, can be more precisely described by the two-parameter Weibull function in a statistical way (Yang and Hillier, 2012). This analysis however is out of the scope of this thesis, and so it will not be further explained.

4.2.2 The discontinuity along the embeddedness trajectory

Is it there any a discontinuity found along the embeddedness trajectory, where the relation between node count and radius changes significantly? At first, we use an ideal example to approach this question. Since any an axial map can be transformed into a j-graph, we can explore the embeddedness trajectory by constructing the j-graph. **Fig. 4.5 Top** shows an ideal example of axial map. When this system is observed from a root line in red (denoted as R), it can be converted into a j-graph **(Fig. 4.5 Bottom Left)** of which the red line is the root node. It has six layers and the number of the nodes at each layer varies with increasing radius, so that the *shape* of the j-graph in effect approximately illustrates how the root is progressively embedded into its contextual nodes, according to its topological depth to them, as radius rises up. The sum of the encountered nodes dramatically drops down from the 3rd to the 4th layers, which indicates the kind of *discontinuity* between the 3rd and the 4th layers in the j-graph. This demonstrates that the root node is more spatially segregated from the other nodes beyond the 3rd layer.

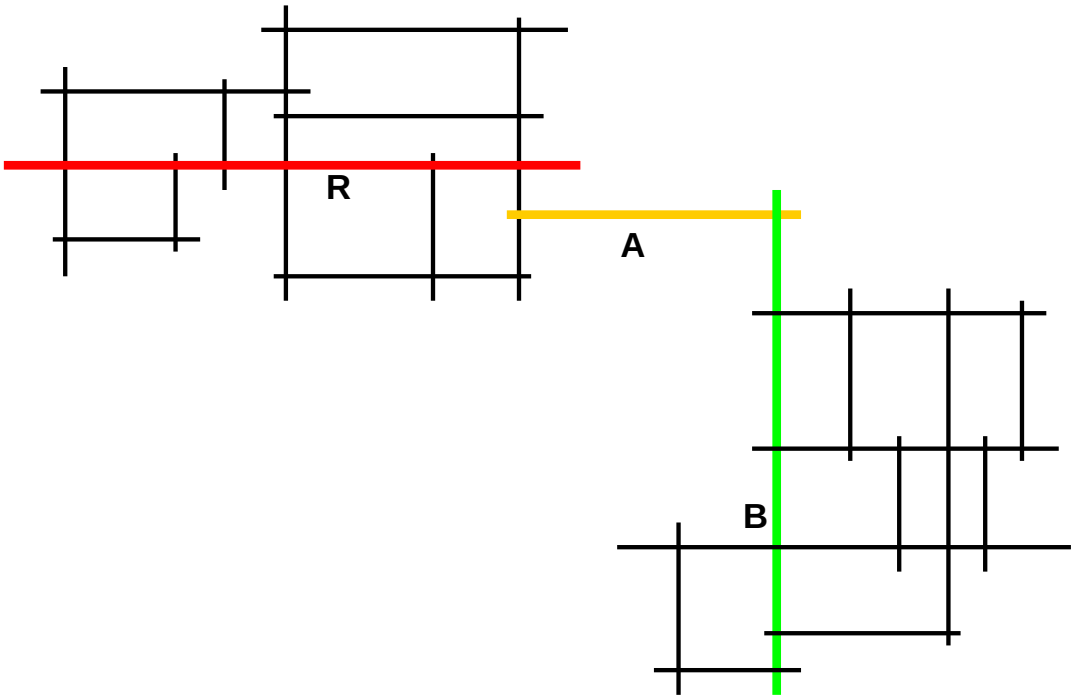

An ideal example of axial map

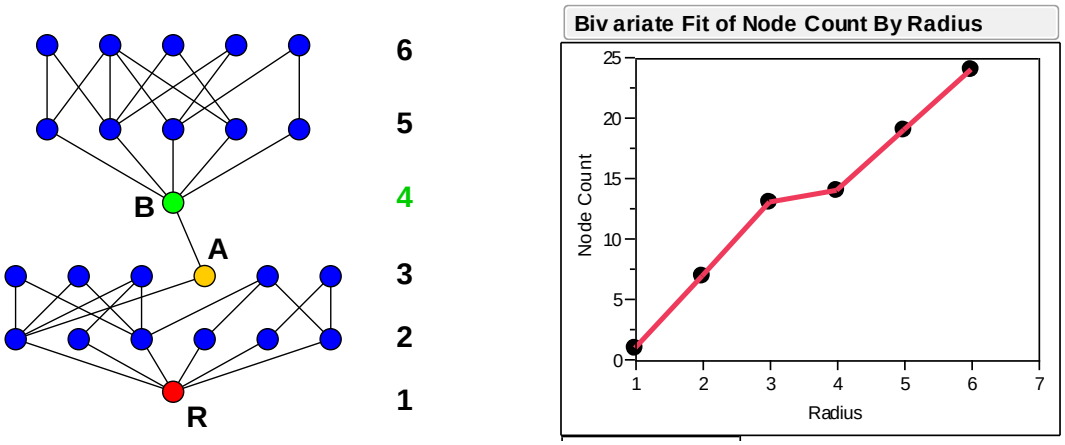

Left: A j-graph converted from the top axial map, if observing the system from the red line (R); **Right**: the scattergram of plotting node count Rk of the left J-graph, on the y-axis, against radius on the x-axis.

Fig. 4.5 A Discontinuity Detected in An Ideal Axial Map. The discontinuity can be captured by illustrating the dramatic change in node count values between the radius of 3 and of 4. Both the j-graph and the scattergram of node count against radius demonstrate how node count varies with the increasing radius.

The discontinuity found between the 3rd and the 4th layers in the j-graph also can be detected by plotting radius, on the x-axis, against node count of the root (the red line), on the y-axis **(Fig. 4.5 Bottom Right)**. The scattergram demonstrates that the radius 3 is a critical point, because the node count value significantly decreases from the radius of 3 to 4. And it shows that the shape of the curve in the scattergram corresponds to the shape of the j-graph, and so that the curve in fact represents the embeddedness trajectory. In this way, the discontinuity along the embeddedness trajectory in this ideal example can be examined by plotting node count against radius.

And meanwhile, the nodes at the 2nd and 3rd layers **(Fig. 4.5 Bottom Left)**, topologically closer to the root, have to be connected to the other nodes beyond the 3rd layer via the link between node A and B; but this link implies the discontinuity where the sum of the encountered nodes decreases significantly. Thus, the nodes at the 2nd and 3rd layers would encounter more deep nodes beyond the 4th layer, and so they are more spatially segregated from these deep nodes. To some extent, it explains why the area constituted by the axial lines up to three depths away from the root (the red line) seems to be more spatially separated from the other lines (**Fig. 4.5 Top**).

This gives us a clue to the way of spatially defining urban area in terms of the discontinuity found along the embeddedness trajectory. If a group of neighbouring spaces, represented by lines or segments, had such discontinuities along their embeddedness trajectories, it could have suggested

that they were spatially segregated from the contexts at the point where the discontinuities were identified. But this is a conjecture at this stage.

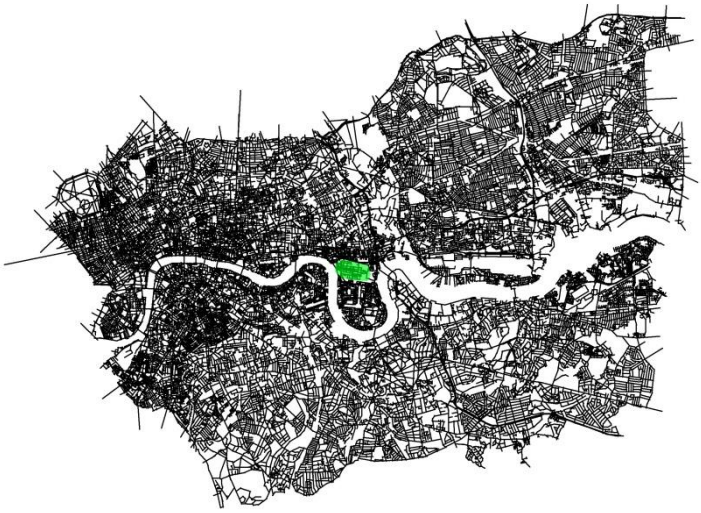

Fig.4.6 The Location of Canary Wharf. It is shaded by the green and is located at the unprocessed axial map of the London Docklands.

4.2.3 A simple experiment to investigate small variation in the power-law relation between node count and radius

Then, we start to examine whether a group of lines or segments constituting a pre-given area, on average, have any a discontinuity along their embeddedness trajectories, by conducting an experimental study of the Canary Wharf project. Both axial and segment representations were used to investigate the conjecture proposed at the end of last section, because we did not know which representation was useful for exploring the discontinuity of a group of neighbouring spaces.

In order to take more surrounding areas into account and avoid the edge effect[43] as far as possible, we selected the axial map of London Docklands (introduced in Section **4.2** and illustrated in **Fig. 4.2**), which covers more areas than the axial map of Canary Wharf displayed in the previous chapter (**Fig.3.5**). And Canary Wharf is still placed at the centre of the Docklands map (**Fig.4.6**). Then the axial and segment analyses were conducted respectively. For the axial analysis, we averaged the node count values of all the axial lines within and

[43] See footnote 6.

intersecting with the project boundary. The mean node count values– called *mean topological node count* – at different topological radii ranging from 1 to 40 denote a series of topological node count of Canary Wharf as a whole.

For the segment analysis, we averaged the metric node count values of all the segments within and on the project boundary. These mean node count values – termed *mean metric node count* – at different metric radii, ranging from 400m to 8000m with an interval scale of 100m, represent a series of metric node count of Canary Wharf.

As **Section 4.2.1** discovered, most of axial lines (and segments) in the London Docklands have an approximated power-law relation between node count and radius. Thus, we created the scattergram plotting the logarithm of the mean topological (and metric) node count of Canary Wharf, on the vertical axis, against the logarithm of the radius, on the horizontal axial (**Fig. 4.7 Top and Bottom**), termed *the log-log radius plot*, to see whether group of the lines (and segments) representing Canary Wharf have a power law relationship between these two variables.

Fig. 4.7 Top Left and Bottom Left, respectively, show that the data points as scattered in the log-log radius plots (based on the axial and segment analyses, respectively) do not form a perfect straight line, in spite of the fact that mean topological and metric node count variables, respectively, have an approximate power-law relation with radius, with an R-square of 0.9918 (**Top Left**) and 0.9871 (**Bottom Left**).

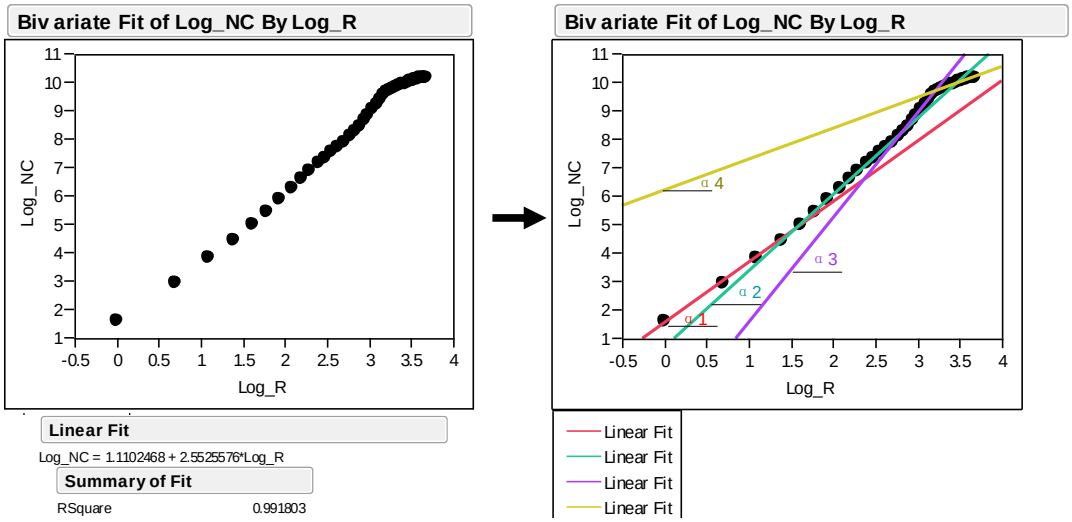

(**Based on axial analysis**)

Left: the scattergram plotting the logarithm of mean node count against the logarithm of radius, where a linear correlation was found within a radius range of 1 to 40, with an R-square of 0.9918;

Right: the stronger linear correlations were identified within four radius ranges respectively (for example, α1denotes the slope of the regression line found within the first radius range of 1 to 7)

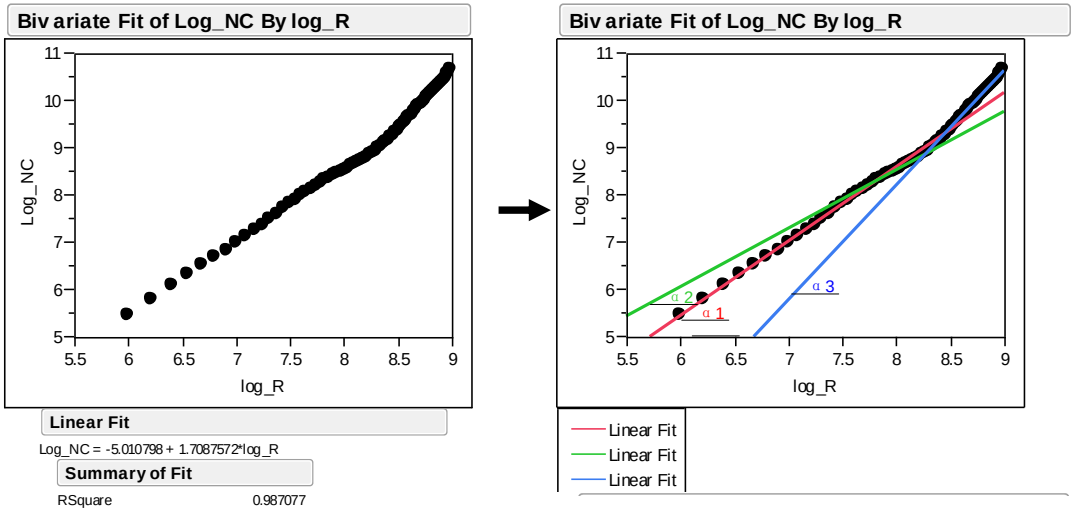

(**Based on segment analysis**)

Left: the scattergram plotting the logarithm of mean node count against the logarithm of radius, where a linear correlation was found within a range of 400m to 8000m, with an R-square of 0.9871;

Right: the stronger linear correlations were identified within four radius ranges respectively (for example, α1denotes the slope of the regression line found within the first radius range of 400m to 2700m)

Fig.4.7 A **Strong Power Law Relation between Mean Node Count of Canary Wharf and Radius Found within Smaller Radius Ranges, Based on the Axial and Segment Analysis**. The inflexion points on the curve of the log-log radius plot suggest the discontinuities along the embeddedness trajectory, where node count changes significantly.

We then seek out to explore smaller variations in these power-law relations. The regression analysis was conducted, coupled with the data points (as scattered in the log-log radius plot) inclusion and exclusion process, to explore a stronger correlation between the logarithm of node count and the logarithm of radius, within some specific radius ranges. Based on the axial analysis, we explain this procedure. Starting with the first two data points located at the bottom left of the log-log radius plot, a third data point nearest to them was added, and the linear regression analysis was then processed to calculate the correlation. If the R-square is above 0.999, a fourth data point nearest to the first three points was included and tested to see whether it could keep a strong regression line with an R-square above 0.999. Following this way, the other new points were tested and included until a kth new point could be added to decrease the R-square below 0.999. This showed a stronger power-law relationship found within the radius range of 1 to k-1. Then, the first (k-2) points were excluded, and another round of testing and inclusion (and exclusion) was carried out. It started with the (k-1)th, kth and (k+1)th points to explore whether we could find a stronger correlation, with an R-square above 0.999, within another radius range of k to m (m>k).

Table 4.1a The Slope of the Regression Line of α (that is equal to the power-law exponent) and the Corresponding the Radius Range, Based on the Axial Analysis of Canary Wharf.

(For example, Radius Range 1 denotes the first radius range of 1 to 6 within which a linear regression line appears with an R-square over 0.999; α1 of 2.123 indicates the slope of the regression line that is equal to the power-law exponent)

Area Name	Radius Range 1	α 1	Radius Range 2	α 2	Radius Range 3	α 3	Radius Range 4	α 4
Canary Wharf	1,6	2.123	6,17	2.672	17,25	3.679	25,40	1.088

Table 4.1b The Slope of the Regression Line of α (that is equal to the power-law exponent) and the Corresponding the Radius Range, Based on the Segment Analysis of Canary Wharf.

(For example, Radius Range 1 denotes the first radius range of 400m to 2700m within which a linear regression line appears with an R-square over 0.999; α1 of 1.575 indicates the slope of the regression line that is equal to the power-law exponent)

Area Name	Radius Range 1	α1	Radius Range 2	α2	Radius Range 3	α3
Canary Wharf	400-2700	1.575	2700-3700	1.237	3700-8000	2.419

We report the result of axial analysis at first. **Fig. 4.7 Top Right** shows that the perfectly linear regression lines appear within four constricted radius ranges, with an R-square over 0.999. The slope of each regression line is denoted as α. As **Table 4.1a** demonstrates, the α varies from 2.123 to 2.672, 3.679 and 1.088, respectively corresponding to the consecutive radius ranges of 1 to 7, 7 to 17, 17 to 25, and 25 to 40. This suggests that a stronger power law relation between mean topological node count and topological radius is found within smaller topological radius ranges.

The log-log radius plot has three inflexion points at the radius of 7, 17 and 25, where the regression lines significantly change their directions on the embeddedness trajectory. It suggests that the mean topological node count changes sharply at these three inflexion points. In this sense, the inflexion points imply the kind of discontinuities where the lines representing Canary Wharf, on average, encounter a very large number of new lines, or a very small number of new lines. In addition, the radii of 7 and 17 are lower than the radius-radius of 19, which means that the discontinuities found at the radius of 7 and 17 are not affected by the system boundary.

Then, the similar result was found in the segment analysis. **Fig. 4.7 Bottom Right** illustrates three perfectly linear regression lines appear within smaller metric radius ranges, with an R-square over 0.999. The slope of the regression line varies from 1.575 to 1.237 and 2.419, respectively corresponding to the constricted radius range of 400m to 2700m, 2700m to 3700m, and 3700m to 8000m **(Table 4.1b)**. This suggests that a power law relation between mean metric node count and metric radius is found within smaller metric radius ranges.

It also indicates that two inflexion points are respectively identified at 2700m and 3700m in the log-log radius plot. These points suggest the discontinuities, where the sum of the contextual segments encountered by Canary Wharf, on average, changes dramatically. And both 2700m and 3700m are smaller than the metric system radius of 8000m, so that these discontinuities marked out at these two radii are not affected by the system boundary.

The axial and segment analyses both suggest that although the embeddedness trajectory of Canary Wharf, within a wider range, is roughly governed by power law, several small parts of the trajectory, defined by narrower ranges, are expressed by the stronger power law relations between node count and radius. The inflexion points, as shown in the log-log radius plots, represent the discontinuities along the embeddedness trajectory of Canary Wharf. This seems to offer a method for describing what a pre-given area is, in relation to its multi-scale contexts, but it needs be further tested in the later empirical chapters.

These analyses also raise a key question: *do all the lines or segments representing an area have similar discontinuities found along their individual embeddedness trajectories?* If so, we might be able to highlight that area by illustrating these similar discontinuities on axial (or segment) map. Following this line, it might be possible to simulate the area structure by detecting and then illustrating the discontinuities along the embeddedness trajectory of all the lines (or segments).

However, a group of lines (or segments) denoting an area perhaps has several discontinuities (represented by inflexion points in the log-log radius plot) along their embeddedness trajectories. For example, that group of lines representing Canary Wharf, on average, has three inflexion points denoting the discontinuities (**Fig. 4.7 Top Right and Table 4.1**). And the different groups of lines (or segments) perhaps might have different discontinuities marked out at different radii. Technically speaking, it is not easy to create a single map to visualise all the discontinuities identified at all the different radii. Besides which, it is perhaps useful to simulate the area structure at each single radius, in such a way as to generate linear structure such as integration core[44] at each single radius (**Fig. 3.4)**, so that we can examine the area structure at each single radius.

To overcome this difficulty, we re-examine the inflexion points representing the discontinuities of Canary Wharf, as shown in the log-log radius plot (**Fig. 4.7)**. Since the inflexion points demonstrate that node count changes significantly at these points, they also suggest that node count at the radii between any two consecutive inflexion points does not vary dramatically. This in fact reflects two sides of one coin, or two related features of an embeddedness trajectory. Thus, we shift our attention to the part of the embeddedness trajectory, bounded between any two consecutive inflexion points, where a stronger power-law can be verified within the small radius range. And the power-law exponent, equal to the slope of the regression line, suggests the kind of consistent *pace* at which Canary Wharf is spatially embedded into the contexts within that small range. If all the lines (or segments) constituting an area, such as Canary Wharf, had similar power-law exponents within a constricted range, we could have distinguished that

[44] As reviewed in Section 3.2.1, the integration core is constituted by the 10%, 25% or 50% most integrated lines. For detail, see Hillier and Hanson (1984), p115.

group of lines (or segments) from the contextual structure by comparing their power-law exponents - calculated within that range - with those of their contexts. This gives a clue to simulate the kind of area structure at each radius.

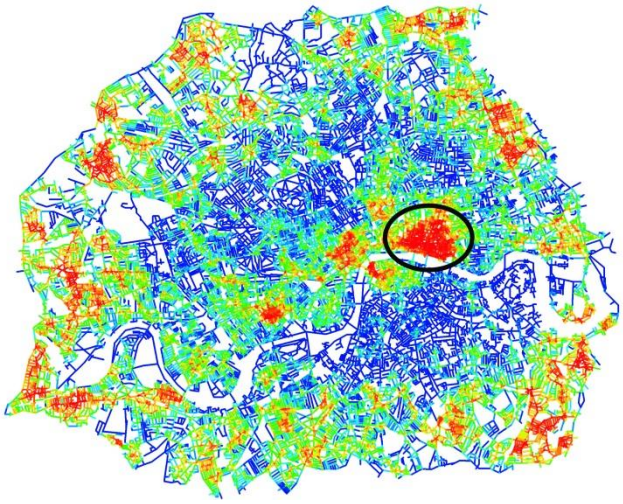

The City of London highlighted by the black circle

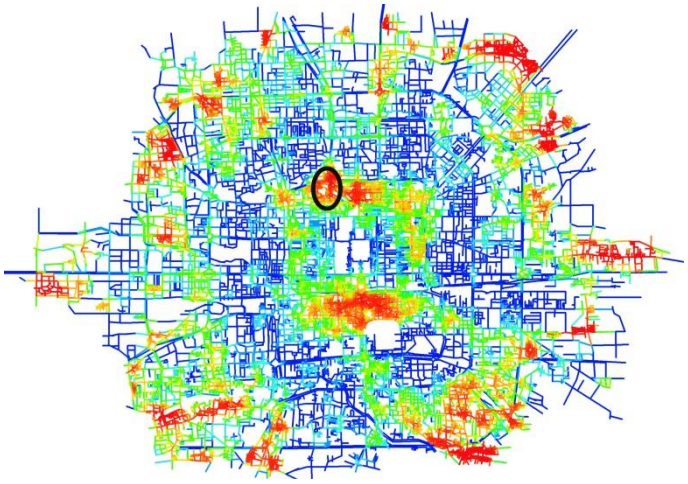

The Shichahai District highlighted by the black circle

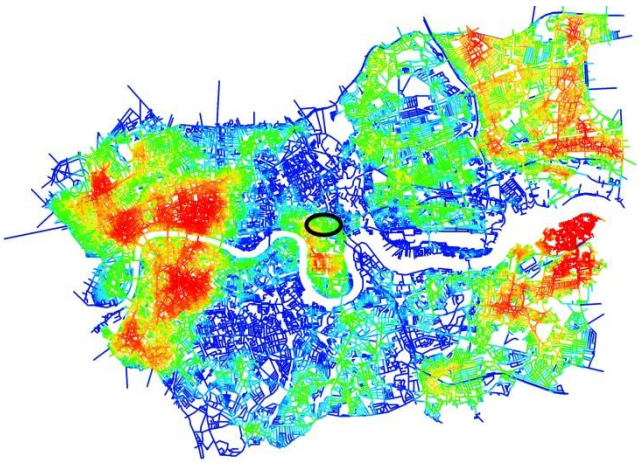

Poplar highlighted by the black circle

Fig. 4.8 The Patchwork Patterns of London, Beijing and the London Docklands (from top to bottom). They are created by the power-law exponent in the relation between node count and metric radius within the radius range from 400m to 8000m with a 100m interval, for the cases of. Red indicates the smallest exponent, and blue denoting the largest exponent.

4.3 A method of generating the periodic patchwork pattern

4.3.1 The clue to create the kind of patchwork pattern

Let us conduct another simple experiment. **Section 4.2** pointed out that most of the *segments* in London, Beijing and the London Docklands, on average, have a stronger power-law relation between node count and radius, found within a wider range[45], than most of the *axial lines* in these regions, respectively, so that the power-law exponents produced in the segment analysis can be used to more precisely describe the corresponding embeddedness trajectories than those exponents produced in the axial analysis. Thus, in this experimental study we focus on the segment analysis.

Now we seek out to visualise the data of power-law exponents generated in the segment maps to see whether groups of neighbouring segments have similar power-law exponents within the

[45] As section 4.2 elaborated, the wider radius range for segment analysis starts at 400m and ending at 8000m; and that for axial analysis is kept between 1 and the radius-radius.

wider metric range of 400m to 8000m. As for these three cases, the power-law exponent values, calculated by the software of JMP[46], were assigned back to each segment in the Mapinfo Professional[47], and then coloured in term of the exponent values. These values were divided into 16 bands, each of which was represented by one colour. Red indicates the lowest exponent values and dark blue denotes the highest values. The result shows *the kind of patchwork pattern*, meaning that several groups of neighbouring segments acquire the similar exponent values, and so shaded in the similar colours and surrounded by the discontinuities where the values change significantly (**Fig. 4.8**). To a large extent, this suggests that some groups of neighbouring segments have similar average paces at which they are spatially embedded into the surroundings. But the patches generated at the edge of the system are greatly influenced by the system boundary, because the segments constituting these patches have a complete discontinuity at the system edge, beyond which they cannot acquire any other segments at all. In this sense, the patches located at the edge of the system are not fully created by the structuring of urban network, but are influenced by the system boundary. Thus, we should focus on the patches located at the centre of the systems.

At first sight, some patches even seem to relate to named areas. For example, the City of London was coloured in red, the Shichahai area of Beijing shaded in red, and Poplar in the London Docklands coloured in green (**Fig. 4.8**). However, the patchwork patterns created in the three cases seem coarse. This is perhaps due to the reason that they were created by a wide radius range of 400m to 8000m. As discussed earlier, within this wide range, the power-law exponents were produced with an R-square around 0.9, which suggests 10% variations cannot be explained by power laws. However, **section 4.3.2** indicates that it is possible to obtain stronger power-law relation within narrower radius ranges. For example, all the segments of Canary Wharf, on average, have a stronger power law relation between node count and radius within the narrower ranges of 400m to 2700m, of 2700m to 3700m, and of 3700m to 8000m (with an R-square above 0.999, respectively). *Can we generate the fine-scale patchwork*

[46] JMP is statistical discovery software that contains basic statistical analyses, plus automated analytic techniques for data mining and predictive modeling. See http://www.jmp.com/software/pro/.
[47] The Mapinfo Professional is the mapping software produced by Mapinfo Corporation. See http://www.pbinsight.com/products/location-intelligence/applications/mapping-analytical/mapinfo-professional.

patterns by visualising the power-law exponents produced within the narrower ranges bounded by two inflexion points?

However, it is highly possible that each segment (or line) has a power law relation within different narrower ranges, and so all of them have different inflexion points found at different radii. But now we seek to produce the kind of patchwork pattern in terms of the power-law exponent values generated at each single radius. It is impossible to generate one image (the same as **Fig. 4.8**) to visually represent the pattern of power-law exponents found within the ranges bounded by the different inflexion points at the same time.

Thus, we seek to interpret power-law exponent in another way. The power-law exponent is, in fact, equal to the slope of the regression line of the logarithm of node count against the logarithm of radius with a fixed radius range **(Fig.4.7)**. The regression line generated within that radius range can be approximated by a regression line, with the same slope, produced within any a very narrow range belonging to that radius range. In this way, we can calculate the power-law exponent within a very narrow radius range. Of course, within a very narrow radius range, the power-law correlation cannot be verified, because the sample size is very smaller. However, the slope of the regression line, found within the very narrower range, still measures *the change rate of node count*, regardless of the verification of power law relation. And the dramatic change in node count also can be detected by calculating the slope of the regression line within a very narrow range. Thus, we propose a conjecture that *the patchwork pattern in urban network can be discovered by comparing the slopes of the regression lines found within very narrow radius range*. The next section will investigate this conjecture.

4.3.2 The definition of embeddedness

First, we give a mathematical definition of the slope of the regression line produced in the log-log radius plot **(Fig.4.7)**. When we calculate the slope of the regression line verified within a very narrow radius range, such as one topological depth in axial analysis, or 600 meters in segment analysis, we in fact approximate the derivative of the logarithm of node count in respect to the logarithm of radius. If the variable of radius is denoted by k and the width of the very narrow range denoted by σ, the derivative at k, approximating to the slope of the

regression line from (k - σ) to k, can measure the change rate of node count at that specific radius of k. As **section 4.2.2** suggests that the embeddedness trajectory of a line (or segment) can be illustrated by the log-log radius plot, the derivative of the curve shown in the log-log radius plot, in effect, measures the derivative of the embeddedness trajectory. The latter can be used to capture the *pace* at which that line (or segment) is spatially embedded into its surroundings at a given radius. Thus, this derivative, called *embeddedness,* is expressed by the product of the function of node count and radius:

$$Emd(k,\sigma) = \alpha(k,\sigma) = \frac{\ln NC_k - \ln NC_{k-\sigma}}{\ln k - \ln(k-\sigma)} \qquad (4.3)$$

where $Emd(k,\sigma)$ denotes embeddedness of a line (or segment) at the radius of (k-σ) to k; $\alpha(k,\sigma)$ denotes the slope of the regression line found at the radius of (k-σ) to k in the log-log radius plot; and NC_k denotes node count of the line (or segment) at the radius of k.

For any an axial map, since the smallest width of range σ is one topological depth, the *topological embeddedness* of an axial line at a radius of k is defined as the slope of the regression line found at the radius of k-1 to k in the log-log radius plot.

$$Emd(k) = \alpha(k) = \frac{\ln NC_k - \ln NC_{k-1}}{\ln(k) - \ln(k-1)} \qquad (4.4)$$

where Emd(k) denotes *topo-embeddedness* of a line at a radius of k, measuring the pace at which the line is topologically embedded into the context at the radius of k; $\alpha(k)$ indicates the slope of the regression line found at the radius of (k-1) to k; and NC_k means node count at k.

If the topo-embeddedness values of all the axial lines, read from the same axial map, are only compared to each other at a fixed radius of k, the value of ($\ln k - \ln(k-1)$) in fact is the same for each line, because k is a constant. Thus, the equation can be simplified into the following format:

$$Emd(k) = \alpha(k) \sim \ln\left(\frac{NC_k}{NC_{k-1}}\right) \sim \frac{NC_k}{NC_{k-1}} \qquad (4.5)$$

This transformation indicates that the topo-embeddedness Rk can be measured by dividing node count at k by node count at (k-1), without causing any change in the rank order of the topo-embeddedness Rk. In this way, the topo-embeddedness Rk is approximated by the change rate of node count between the two consecutive radii.

As for segment model, the variable of radius also can be considered to increase discretely, because the variation in metric radius is at least larger than the length of the shortest segment encountered[48]. As a result, node count of any a segment as a root also increases in a discrete way, and the smallest increase in radius is denoted as σ . Thus, the *metric embeddedness* of a segment at a radius of k is defined as the slope of the regression line found at the radius of (k-σ) to k in the log-log radius plot. The equation for *metric embeddedness* is developed in such a way as to calculate topo-embeddedness, aiming to approximate the pace at which a segment is *metrically* embedded into its contextual structure at a given metric radius.

$$Emd(k,\sigma) = \alpha(k,\sigma) \sim \frac{NC_k}{NC_{k-\sigma}} \qquad (4.6)$$

where, $Emd(k,\sigma)$ denotes metric embeddedness of a segment at a radius of k, approximating the change rate of node count of the segment from metric radius of (k-σ) to k, and σ is the smallest width of metric radius range, or interval scale, such as 600m, if assuming that radius increases discretely with equal interval; and NC_k denotes node count at k.

[48] For the detailed procedure to calculate metric radius in the segment model, see Turner (2004), Depthmap 4, A Researcher's Handbook.

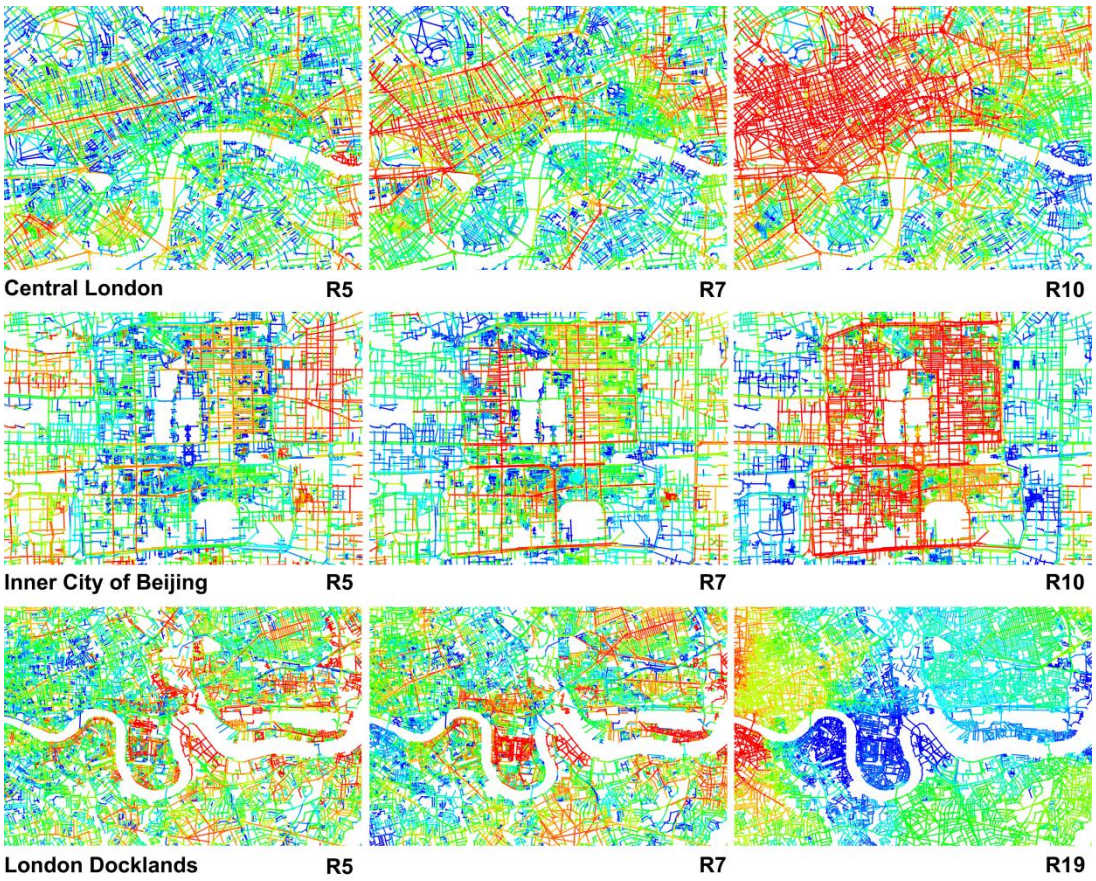

Fig. 4.9 The Patchwork Patterns of London, Beijing and the London Docklands Generated by Topo-embeddedness.

It respectively illustrates the images of London and Beijing at the radius of 5, 7 and 10, as well as the images of the London Docklands at 5, 7 and 19. Red indicates the smallest topo-embeddedness values, and blue denoting the largest topo-embeddedness values.

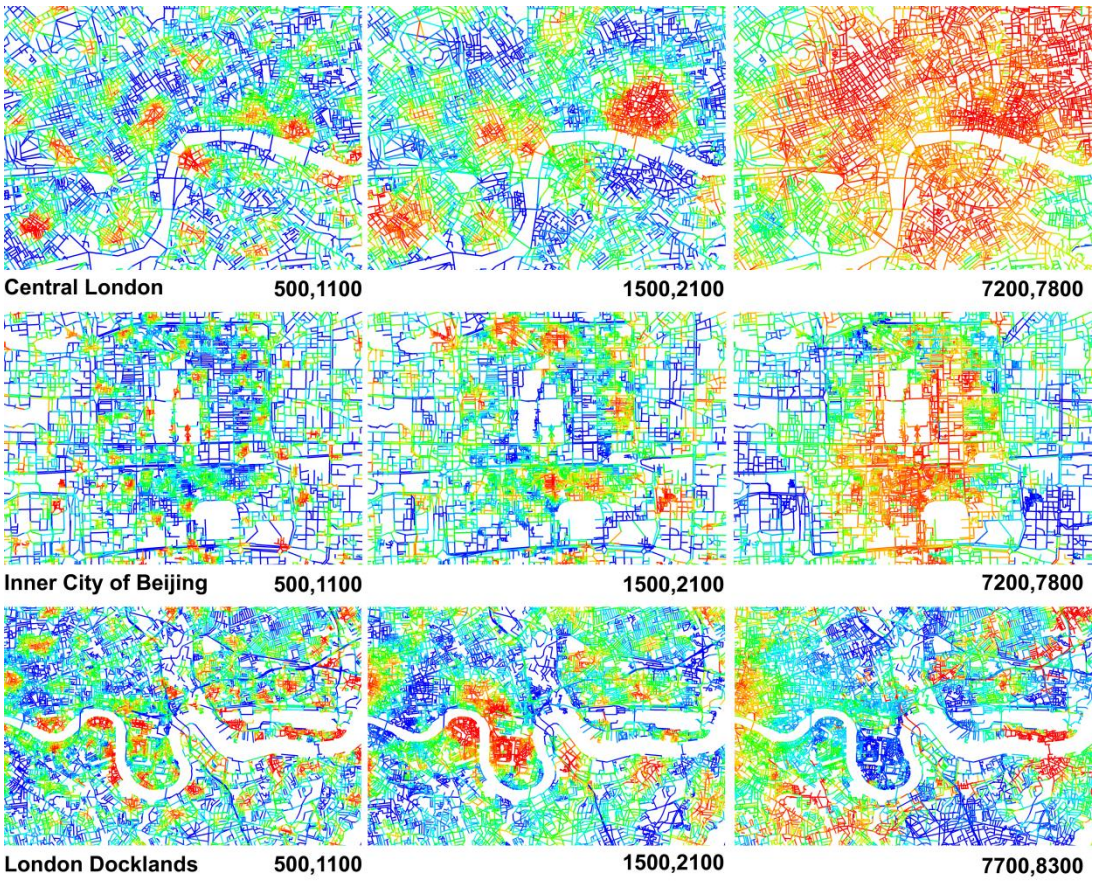

Fig. 4.10 The Patchwork Patterns of London, Beijing and the London Docklands Generated by Metric embeddedness

It respectively shows the images of London and Beijing at the radius of 1100m, 2100m and 7800m, as well as the images of the London Docklands 1100m, 2100m and 8300m. The interval scale is 600m. Red indicates the smallest metric embeddedness values, and blue denoting the largest metric embeddedness values.

4.3.3 The discovery of the periodic patchwork pattern

Then, *do groups of neighbouring lines or segments tend to have similar topo- or metric embeddedness values? Or, can we detect the discontinuities in spatial network, where these values change sharply, so that we can create the spatial pattern similar to the patchwork pattern generated in* ***Section 4.3.1*** *(****Fig. 4.8****)?* We set out to formulate a method for tackling the above questions. The method, based on axial map for example, is explained as follows. First,

$Emd(k)$ (topo-embeddedness) is calculated and then assigned back to each axial line in the DepthMap[49], and then the axial map is exported out and then imported into the Mapinfo Professional[50]; then, each axial line is coloured from red to dark blue, according to the $Emd(k)$ values, within 16 bands based on equal count. The red indicates the lowest values, and the dark blue denotes the highest values. As for segment model, the same method is deployed to index and colour all the segments according to metric embeddedness.

We applied the above method to the three cases of London, Beijing and the London Docklands, respectively. **Fig. 4.9** illustrates the images of London and Beijing, coloured according to the topo-embeddedness values at the radius of 5, 7 and 10, as well as the images of the London Docklands at the radius of 5, 7 and 19, respectively. These images focus on the central part of the three cases, in order to avoid the edge effect discussed in section **4.3.1**. They show *the patchwork pattern* as similar as what displayed in **Fig. 4.8**, in that groups of neighbouring lines tend to have similar colouring (meaning the similar values of topo-embeddedness), and surrounded by discontinuities where values and so colours change. In addition, the patches marked out vary with an increase of topological radius, and larger areas seem to be identified by higher radii.

Fig. 4.10, respectively, shows the images of London and Beijing, coloured with regard to the metric embeddedness at the radius of 1100m, 2100m and 7800m with an interval scale of 600m, as well as the images of the London Docklands at 1100m, 2100m and 8300m also with an interval of 600m. These images illustrate the stronger periodic patchwork patterns, compared to those generated by the topo-embeddedness (**Fig. 4.9**). They also demonstrate that smaller patches created at lower radius are merged together to form larger patches at higher radius. The later empirical chapters will give an in-depth examination of the spatial properties of the periodic patchwork patterns of these three cases.

[49] The DepthMap developed by Tuner, A. of UCL is a single software platform to perform a set of spatial network analysis. See http://www.vr.ucl.ac.uk/depthmap/

[50] The Mapinfo Professional is the mapping software produced by Mapinfo Corporation. See http://www.pbinsight.com/products/location-intelligence/applications/mapping-analytical/mapinfo-professional.

The similar patchwork patterns were also found at different radii, when we tested this technique on various cities, such as Amsterdam, Chicago, and Birmingham **(Fig. 4.11 and 4.12)**. This kind of patchwork patterns seems to be a general phenomenon found across cities. It suggests that such periodic patchwork phenomenon mathematically created by topo- or metric embeddedness, by and large, can be seen as a regularity revealed by manipulating spatial data in a syntactic way. This periodic patchwork phenomenon can be arguably considered of as a created phenomenon, defined by Hacking (1983), that a noteworthy discernible regularity under definite circumstances is revealed, represented or created by designing and doing experiments. As Hacking (1983) suggested, the created phenomena, such as the Josephson effect of superconduction[51], did not exist until people created certain kinds of device and technology. Such kind of phenomena isolated, purified and produced in the man-made devices, he asserted, are embodied by the way of making these devices, and so they are '*the keys that unlock the universe*' (ibid: 227-8). On this ground, he argued that the created phenomena are '*the centre pieces of theory*' (ibid: 220). In this sense, we argue that the discovery of the patchwork phenomenon represents *a regularity of the discrete area-like structure* across scales and cities, and at least *mathematically* reflects the reality of the periodic patchwork pattern of urban network. This will help us achieve a better understanding of the part-whole problem that will be further explored in the latter chapters.

[51] It is a phenomenon of supercurrent across a device consisting of two superconductors separated by a thin insulator. For detail, see Hacking (1983), p228.

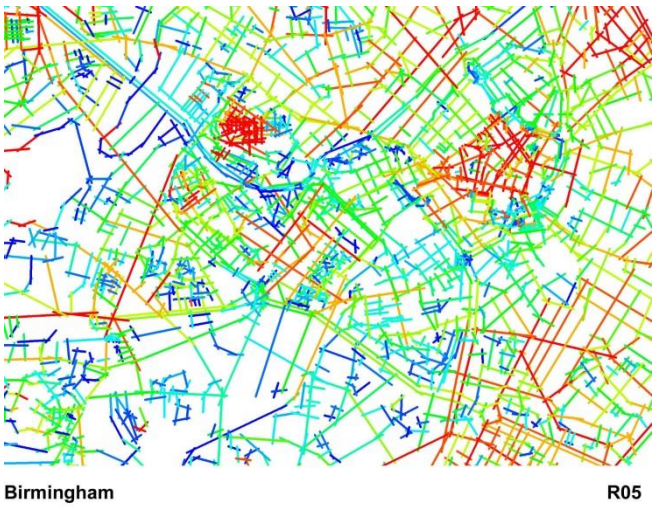

Fig. 4.11 The Patchwork Patterns of Birmingham (R5), Amsterdam (R5) and Chicago (R4) Created by Topo-embeddedness.

Red indicates the smallest values, and blue denoting the largest values.

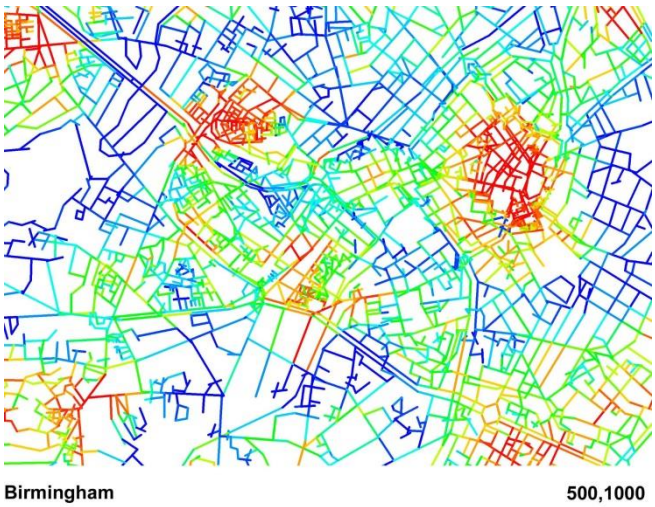

Fig. 4.12 The Patchwork Patterns of Birmingham (at 1000m), Amsterdam (at at 1800m) and Chicago (at 3000m) Created by Metric Embeddedness.

Red indicates the smallest values, and blue denoting the largest values.

4.3.4 The conjecture of spatial discontinuity

The periodic patchwork patterns (**Fig. 4.9 - 4.12**) show that urban network, represented by either axial or segment map, is divided into the discrete patches, each of which is surrounded by discontinuities where the values of embeddedness change significantly. This illustrates the kind of discontinuity in spatial network, called *spatial discontinuity* in this thesis. Then, does such spatial discontinuity really reflect the discontinuity in the pattern of connection of the graph (representing axial or segment map) outward from each node (denoting line or segment) considered as the root of the graph, the latter represented by the *discontinuity along embeddedness trajectory*? To tackle this question will enable us to clarify whether and how the created patches are affected by their external structures.

As we discussed in the previous sections, the discontinuity along embeddedness trajectory captures a significant change in the way a line (or segment), or a group of lines (or segments) representing a pre-given area, is spatially embedded into the contexts with increasing radius. This gives a description of *individual* space or area in relation to *varying radius*. In contrast, the spatial discontinuity of an urban network however indicates that when all the lines (or segments) of the whole network are simultaneously embedded into the surroundings at a given radius, the different groups of neighboring lines (or segments) being embedded at almost same paces are surrounded by the discontinuities, where the surrounding lines (or segments) are embedded at a different pace. This addresses the emergent properties of *the network as a whole*, but at *a specific radius*.

These two concepts however are related together. If each individual line (or segment) has no discontinuity along its embeddedness trajectory, it means that all the lines (or segments) are embedded into the surroundings at a consistent pace as radius increases. However, if any pair of lines (or segments), such as ‘A’ and ‘B’, are embedded at different paces, can each of them keep a consistent - though not necessarily the same - pace with increasing radius? No. This is due to the reason that, for example, when ‘A’ encounters ‘B’ at a certain radius, ‘A’ must be embedded into the further context (selected beyond that radius) at the same pace as ‘B’, because at that moment we observe these further contexts of ‘A’ from the perspective of ‘B’.

Thus, it suggests that if there was no discontinuity along embeddedness trajectory, all lines (or segments) of the whole network could have been embedded at the same pace, and so that the network could have not been partitioned into the different parts according to the variation of their paces. Theoretically speaking, it leads to *the conjecture of spatial discontinuity*, that the pattern of spatial discontinuities of urban network as a whole arises from the discontinuities along the embeddedness trajectories of all the individual spaces, where the pace at which each individual is embedded into the surroundings is altered dramatically. This will be empirically investigated in the later chapters.

4.4 Another method of creating the periodic patchwork phenomenon

As reviewed in earlier chapters, the similar periodic patchwork phenomenon, based on segment model, has been discovered by Hillier (2007, 2010). His new technique is described as follows. As for each segment as a root, metric mean depth – meaning the average metric distance from all segments to all other segments, see **Section 3.2** – up to a specific metric radius of k, denoted as MMD Rk, is calculated and then assigned back to each segment in the DepthMap[52]; and then all the segments are indexed and coloured according to the MMD Rk values. When the colour range from red to dark blue is adjusted in the DepthMap, the patchwork pattern also emerges. The red indicates the smaller MMD Rk and the dark blue representes the larger MMD Rk. Or, after the MMD Rk values are given by the DepthMap, the segment data can be imported into the Mapinfo Professional[53], and then grouped into 16 bands, with regard to the MMD Rk values sorted by the equal count, and coloured from red to dark blue. The same periodic patchwork pattern also can be generated.

[52] See footnote 16.
[53] See footnote 17.

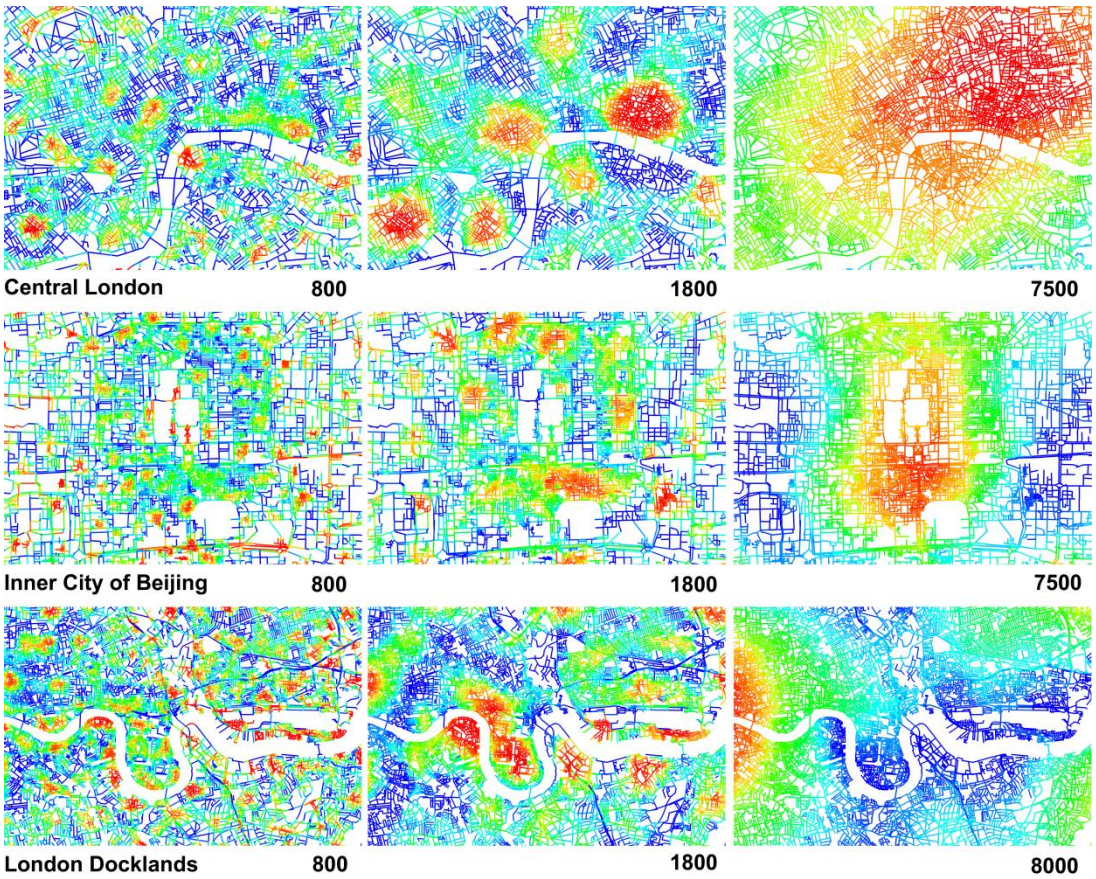

Fig. 4.13 The Patchwork Patterns of London, Beijing and the London Docklands Generated by Metric Mean Depth.

It, respectively, illustrates the images of London and Beijing at the radius of 800m, 1800m and 7500m, as well as those of the London Docklands at 800m, 1800m and 8000m. Red indicates small values, and blue denoting large ones.

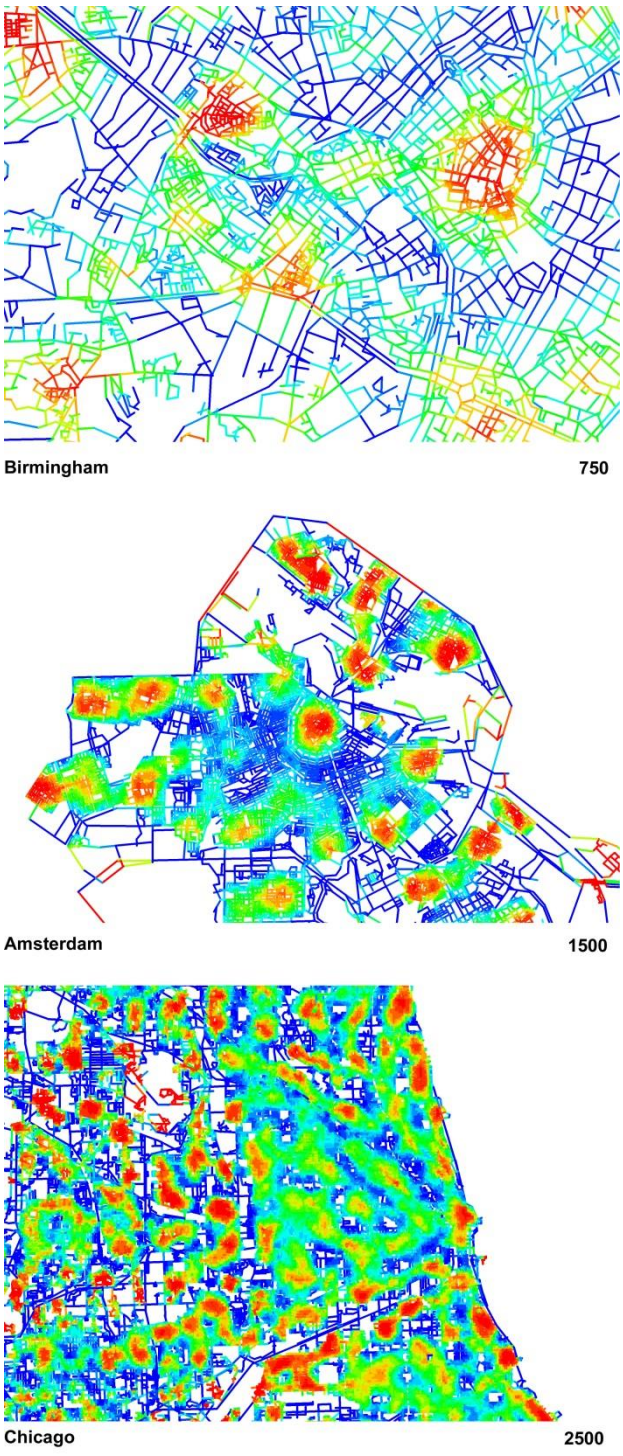

Fig. 4.14 The Patchwork Patterns of Birmingham, Amsterdam and Chicago Generated by Metric Mean Depth.

It, respectively, shows the patchwork patterns of Birmingham at 750m, Amsterdam at 1500m, as well as that of Chicago at 2500m. Red indicates small values, and blue denoting large ones.

For example, **Fig. 4.13**, respectively, illustrates the patchwork patterns of London and Beijing at 800m, 1800m and 7500m, as well as those of the London Docklands at 800m, 1800m and 8000m. As the same as we did in **section 4.3.1**, we still focus on the central districts of these three regions, in attempt to avoid the edge effect[54]. In general, **Fig. 4.13** also shows that larger radius identifies larger patches.

Then, we seek out to visually compare the patchwork patterns generated by MMD (**Fig. 4.13**) with those created by metric embeddedness (**Fig. 4.10**). The patchwork patterns of the three cases, generated by the MMD at 800m and 1800m (**Fig. 4.13**), respectively, are almost the same as those created by the metric embeddedness at the radius ranges of 500m to 1100m, and of 1500m to 2100m (**Fig. 4.10**). However, the patchwork patterns of London and Beijing, produced by the MMD at 7500m, are not very similar to those generated by the metric embeddedness at the range of 7200m to 7800m; and the patchwork pattern of the Docklands, created by the MMD at 8000m, seems to be different from that generated by the metric embeddedness at the range of 7700m to 8300m. This suggests that if the radius is not very large, the patchwork patterns generated by MMD seem to be almost the same as those created by metric embeddedness. However, we are concerned that it is likely a coincidence, because we just test three cases.

Then we further examine the cases of Birmingham, Amsterdam and Chicago as well. **Fig. 4.14** shows the patchwork patterns created by the MMD R750m in Birmingham, the MMD R1500m in Amsterdam, as well as the MMD R2500m in Chicago, respectively. These images, respectively, are almost the same as those created by the metric embeddedness of 500m to 1000m in Birmingham, of 1200m to 1800m in Amsterdam, as well as of 2000m to 3000m in Chicago **(Fig. 4.12)**. This suggests that at relatively low or medium metric radius, the visually identical patchworks can be *empirically* generated by both MMD and metric embeddedness.

[54] The analysis of spaces along the periphery of the axial map is always affected by their location at the system edge. For detail, see Section 3.2.1, or Hillier (1996), p163.

This in effect raises the questions: since the variable of MMD perhaps focuses on the internal layout, but the variable of metric embeddedness seems to gives a priority to the external structure, *why do these two variables empirically yield the similar periodic patchwork patterns at relatively low radii? What is the relationship between these two variables?* Park (2007, 2010) examined the mathematical relation between these two variables in Appendix 1[55] of the paper written by Hillier (2007, 2010), and concluding that the two measures mathematically give the same results, if the relation between node count and radius is governed by power law. And then, we also conducted a mathematical investigation on the relation between the two variables, regardless of the verification of the power law relation, from the perspective of analytic geometry. **Appendix A** elaborates on the detail of this analysis. In general, it suggests that MMD at a fixed radius is a function of the change rate of node count between two specific metric radii, that is, metric embeddedness. As a result, MMD at a fixed radius and metric embeddedness within a constricted radius range will mathematically generate the same periodic patchwork patterns, if we choose an appropriate radius range for calculating metric embeddedness.

Since the two variables, one of which is expected to capture the contextual structure, theoretically produce almost the same patchwork patterns, *is it possible that the patches created by these two variables are empirically impacted on by their contextual structures?* In order to tackle this question, we need to further examine and compare the created patches by conducting more empirical studies of urban areas in the later chapters. This helps us to understand the nature of spatial discontinuity.

[55] For detail, see Hillier, B. et al (2010) Metric and Topo-geometric Properties of Urban Street Networks: Some Convergences, Divergences and New Results, *The Journal of Space Syntax*, 258-79, p. 258-9.

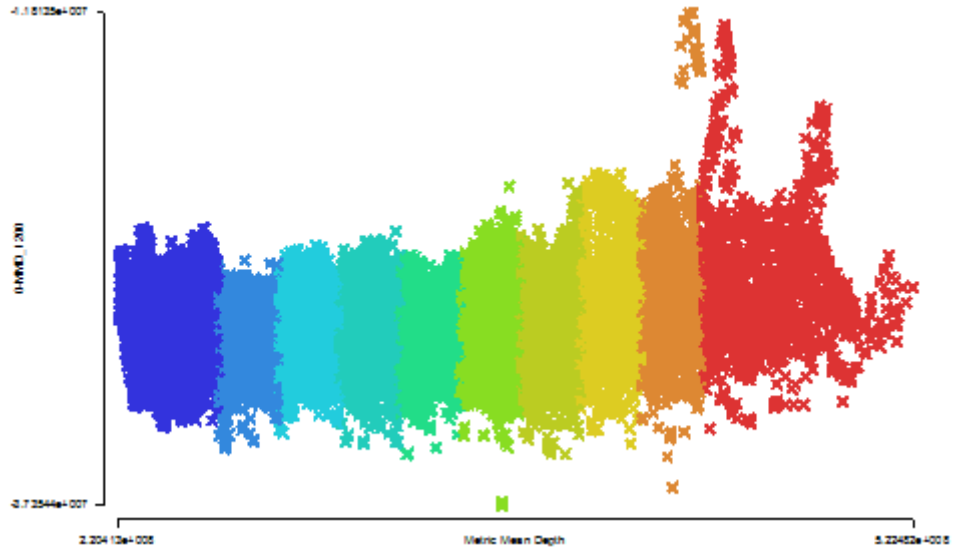

a. The mountain scattergram at 1200m

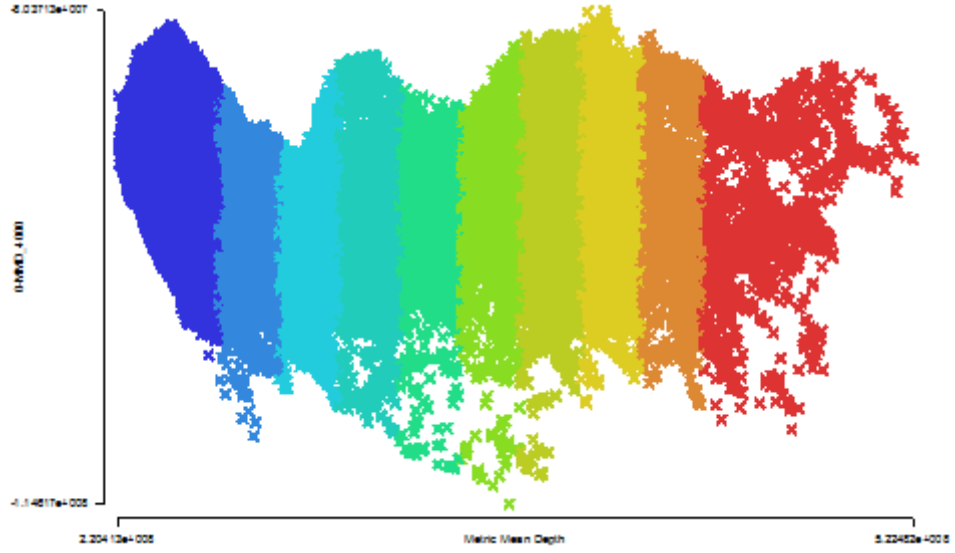

b. The mountain scattergram at 4000m

Fig. 4.15 Two Mountain Scattergrams (plotting the reciprocal of MMD Rk, on the vertical axis, against the MMD Rn, on the horizontal axis) of London at 1200m and 4000m.

The peaks and troughs appear in the two scattergrams.

4.5 The method of exploring area structure

The discovery of the periodic patchwork pattern also poses other key questions: *what is the morphological mechanism accounting for the emergence of the periodic patchwork pattern? And, does the created phenomenon of the periodic patchwork give a heuristic approach to understand the area structure of city, such as the named area structure?* These questions will be investigated in the latter empirical chapters, but this section tries to explore the possible methods for approaching these questions.

First, we review the latest syntactic techniques of investigating the spatial mechanism for generating the periodic patchwork pattern, together with the theoretical concepts underlying them, and explore a possible new dimension. In fact, the created patchwork pattern can be considered of as the kind of periodic structure emerging from the spatial structuring of urban network, which relate to some fundamental theoretical ideas of space syntax. As Hillier (1996, 2001) clarified, the locally placing of physical objects, such as the barring process[56] investigated in chapter 8 of *Space is the Machine*, induces global change in spatial configuration, and so creating the configurational structure, such as integration core[57] (reviewed in **Section 3.2.1**); and in this sense, the disposition of objects brings about the distortion in space. On these grounds, Hillier and Yang (2007, 2010) argued that the periodic patchwork pattern, representing the kind of metric distortion in space, also results from the placing and shaping objects in space.

To establish this argument, another new technique of representing and exploring the periodic patchwork pattern was then generated by MMD Rk. In the DepthMap[58], a scattergram is drawn by plotting the reciprocal of MMD Rk, on the vertical axis, against the MMD at the infinite radius (MMD Rn), on the horizontal axis; and the result expresses the local metric configurational structures (measured by 1/MMD Rk) of sub-networks picked out by the radius of k against the metric configurational pattern of the whole network. We then discovered a new phenomenon

[56] The barring process is a series of placing and/or moving bars in a cellular complex to see how each cell gains depth, and what kind of cellular configuration result. For example, more centrally placed bars create more depth gain than peripherally placed bars. For the detail of barring process, see Hillier (1996), p287-99.
[57] For detail, see Hillier and Hanson (1984), p115.
[58] See footnote 16.

that the peaks and troughs, meaning the rise and fall of the MMD Rk patterns on the vertical axis, appear in the scattergram, termed the *mountain scattergram*. For example, **Fig.4.15 a and b**, respectively, show two examples of the mountain scattergrams of London at 1200m and 4000m, and this demonstrates the periodic structures of London at the two radii.

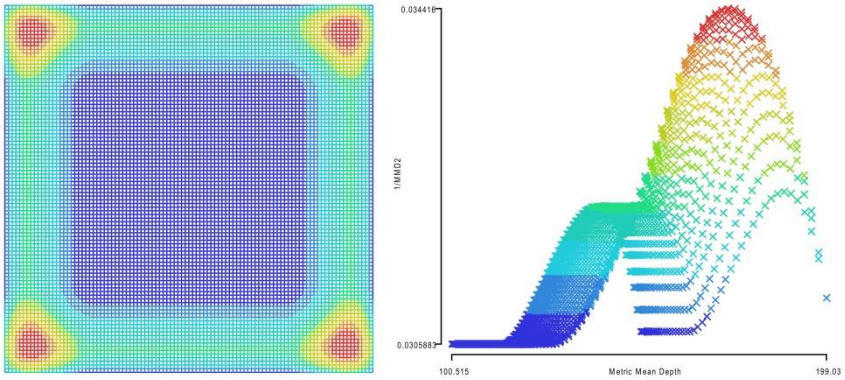

a. Left: the patchwork pattern of a square grid, created at a radius of a quarter of the diameter of the grid, denoted as MMD R2;

Right: the mountain scattergram plotting 1/MMD R2 against MMD Rn

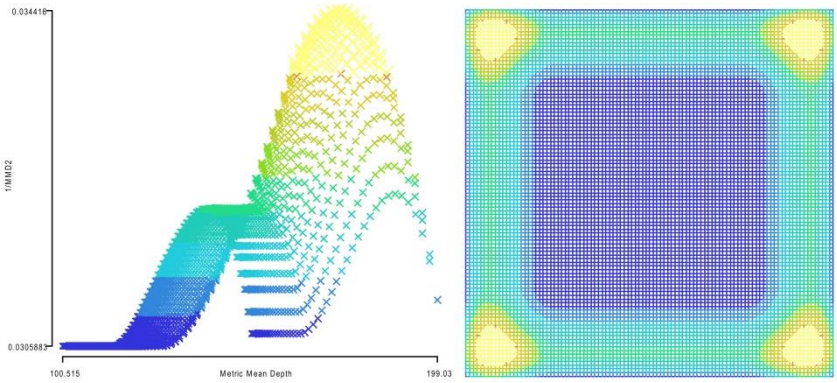

b. Left: the rightmost peak was selected and then highlighted by the bright yellow;

Right: then the four red patches with the lowest MMD R2 were simultaneously shaded in the bright yellow.

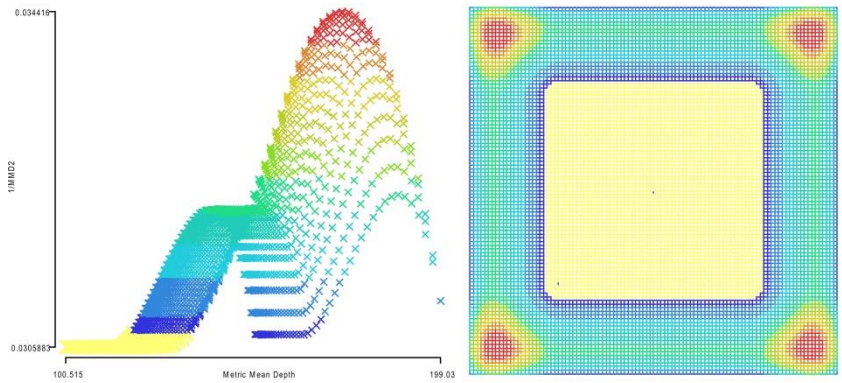

c. Left: the leftmost trough was selected and then highlighted by the bright yellow;

Right: then the central blue patch with the highest MMD R2 was simultaneously shaded in the bright yellow.

Fig. 4.16 Hillier's Experiment of A Simple Square Grid (source: Hillier et.al. 2007, 2010).

Hillier and Yang (2007, 2010) then examined a simple square grid with a boundary by applying this new technique to see whether the boundary, considered as the first partitioning of this system, generates the periodic structure in the grid[59]. For example, based on the segment analysis, **Fig.4.16a Left** shows the patchwork pattern of that square grid, created at a radius of a quarter of the diameter of the grid, denoted as MMD R2 in his paper. Red indicates the lowest MMD R2, and blue denotes the highest MMD R2. Four red patches were found near four corners, because, as he clarified, these segments near the corner acquired the shallow segments all around at that specific low radius, but the grid boundary prevented these segments to acquire the deeper segments (in that there is no segments encountered beyond the grid boundary). But the segments located at the centre were able to obtain the deeper segments at that radius.

This can be revealed by the mountain scattergram plotting 1/MMD R2 against MMD Rn (**Fig.4.16a Right**), coupled with the corresponding patchwork pattern at R2. For example, when the rightmost peak in the scattergram was selected and then highlighted in bright yellow, the four red (corner) patches with the lowest MMD R2 were simultaneously shaded in bright yellow

[59] For detail, see Hillier, B. et al (2010) Metric and Topo-geometric Properties of Urban Street Networks: Some Convergences, Divergences and New Results, The Journal of Space Syntax, p258-79.

(**Fig.4.16b**); and, when the leftmost trough was selected, the central blue patch with the highest MMD R2 was simultaneously highlighted in bright yellow (**Fig.4.16c**). This indicates the rightmost peak represents the four red patches, and the leftmost trough denotes the central patch. We also can reverse the above procedure: to first select the patches in the grid and then to see whether they are represented by peaks or troughs. It confirms the findings shown in **Fig. 4.16 b and c**. As we pointed out, the peaks and troughs, illustrating the fluctuation of the MMD R2 patterns, represent the metric distortion introduced by the boundary into the grid. Moreover, we also used this technique to demonstrate how the placing and shaping multi-objects induce the metric distortions in space by investigating the systems with more partitions[60].

If a created patch could be represented by a peak or a trough at a radius of k, the morphological properties of that patch could have been interpreted in terms of the shape of the peak or trough. This is due to the following reason. The summit of the peak has the lowest MMD Rk (because the reciprocal of the MMD Rk is plotted on the y-axis) and the rest has the higher MMD Rk, so that the *peak* demonstrates that the MMD values *rise up* from the metric centre of that patch to its surroundings. In contrast, the bottom of the trough has the highest MMD Rk and the rest has the lower values, so that the *trough* indicates that the MMD Rk values *fade away* from the metric centre of that patch to its surroundings. Thus, if a peak or a trough was associated with a patch, the peak could have suggested that the corresponding patch had a metrically integrated centre with lower MMD Rk, but the trough could have implied that the corresponding patch was surrounded by the metrically integrated edge.

Then, *does the above possible interpretation of peak-trough pattern exactly relate to the locally placing of physical objects (discussed at the beginning of this section)?* As reviewed in **Section 2.5** in chapter two, Hillier (1999) also proposed the theory of *grid intensification*, meaning the reduction of block size to reduce mean distance from all points to all others in an urban network[61], and this casts a light on the morphologic interpretation of the peak-trough pattern as shown in the mountain scattergram. As he (ibid) clarified, a grid with central smaller blocks and

[60] See footnote 23, or Hillier et. al. (2007, 2010).
[61] For detail, see Hillier (1999) *Centrality as a process accounting for attraction inequalities in deformed grids,* Urban Design International, 3/4, 107-127.

edge larger blocks has lower MMD, but a grid with central larger blocks and edge smaller blocks has higher value. This in fact suggests two kinds of morphological motifs: *the centre-to-edge motif*, meaning a grid is more intensified in the centre than at the edge; and *the edge-to-centre motif*, indicating a grid is more intensified at the edge than in the centre. The former is more metrically integrated, and the latter metrically segregated.

These two motifs relate to the peaks and troughs. The peak with a more metrically integrated summit can be interpreted as the centre-to-edge motif with more integrated and intensified centre; and the trough with a more metrically segregated bottom can be treated as the edge-to-centre motif with more integrated and intensified edge. This suggests that the peak-trough pattern can be interpreted in terms of the locally placing of the different sized blocks. As discussed in the previous paragraph, the mountain scattergram can be applied to investigate whether the created patches have any corresponding relationship with the peaks or troughs. If such relation was verified, we could have use the technique of the mountain scattergram, in the light of the theory of gird intensification, to explore the morphological mechanism for generating the periodic patchwork pattern.

Second, we continue to review and explore the syntactic techniques for investigating the functional implications of the created patches. Perhaps the simplest way is to make a *visual* comparison between the created patches and the pre-defined areas like named areas, as the same as Hillier and Yang (2007, 2010) and Yang and Hillier (2007) did. If they had the visual correspondent relationship, it could have meant that the periodic patchwork pattern might have the functional implications, and so that it could have served as a tool for investigating the area structure like named area structure.

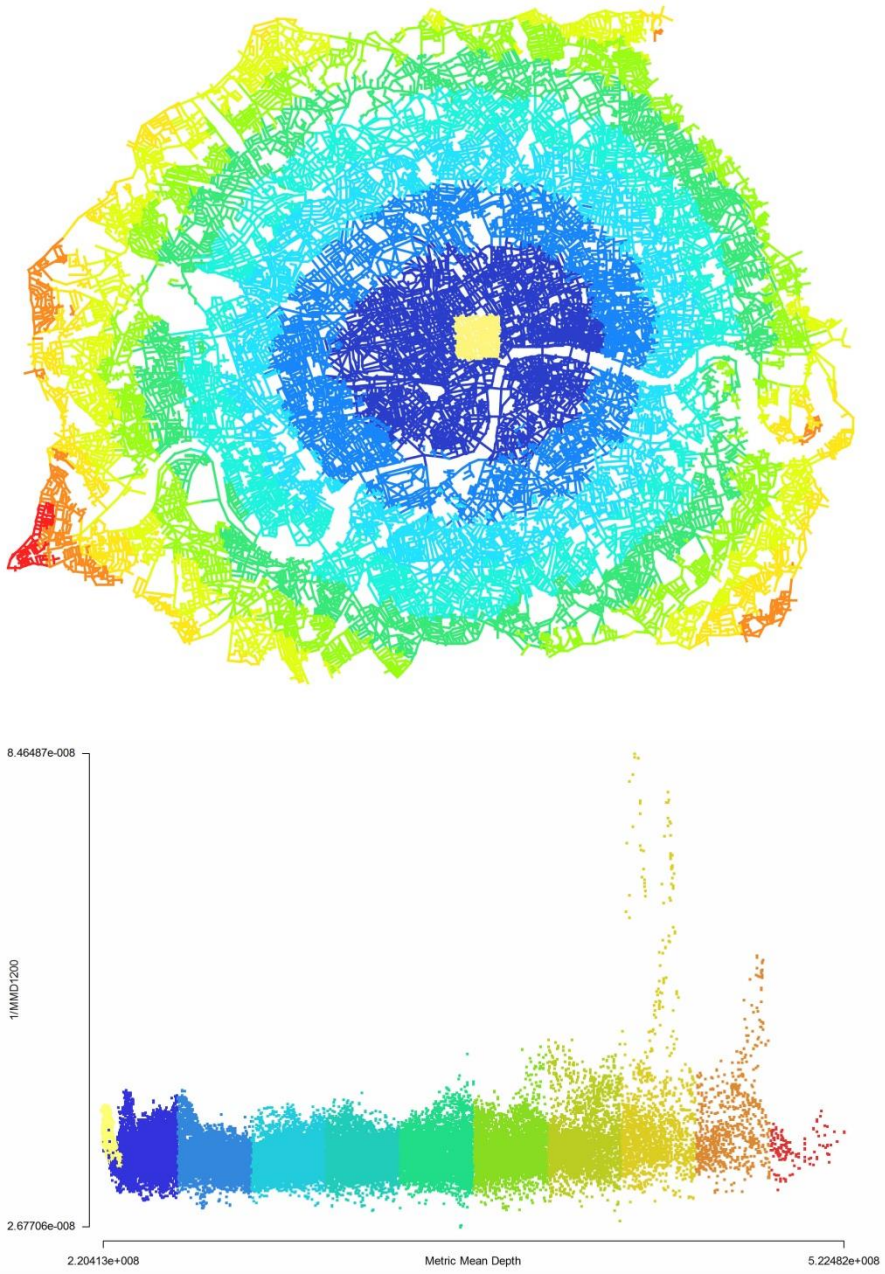

Fig.4.17 An Analysis of A Pre-defined Area by Using the Mountain Scattergram

Top: to select a pre-defined area (coloured in yellow) in the segment map of London

Bottom: the corresponding yellow peak appeared at the left end of the mountain scattergram of 1/MMD at 1200m against MMD Rn.

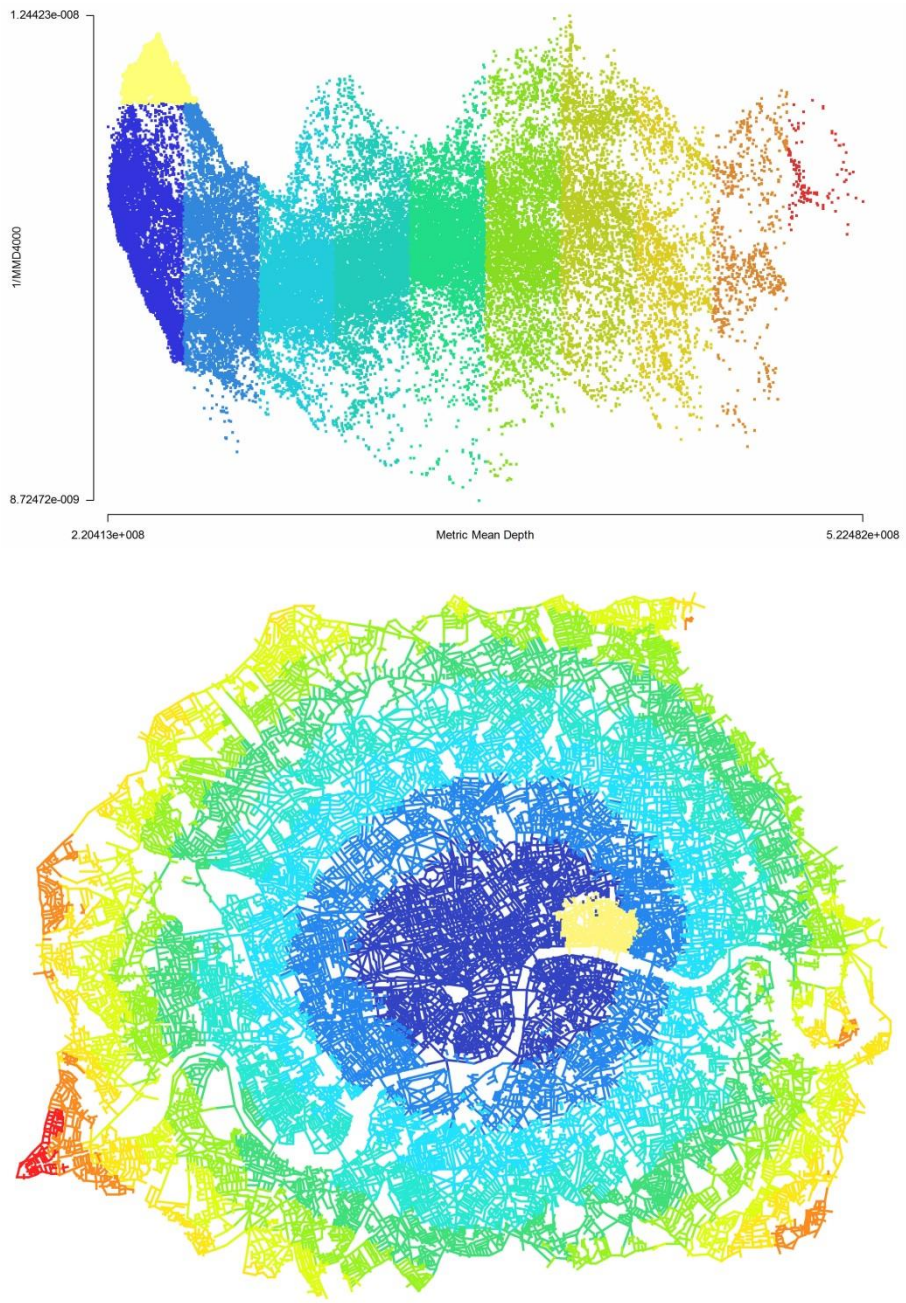

Fig.4.18 An Analysis of the Peak-trough Pattern by Using the Mountain Scattergram

Top: to select a peak (coloured in yellow) in the mountain scattergram of 1/MMD at 4000m against MMD Rn;

Bottom: the City of London being simultaneously highlighted in yellow in the segment map of London

Hillier et al (2007, 2010) also suggested that the technique of mountain scattergram can be used to investigate the named area structure[62]. We use an example of London to explain the analysis procedure and then explore new dimensions in the light of the theory of grid intensification (as discussed earlier). On one hand, we can examine how a pre-define area is represented in the scattergram, aiming to study its morphological feature with regard to the whole network in which it is embedded. For example, an area was selected from the segment model of London, and it was immediately highlighted in bright yellow **(Fig.4.17 Top)**; a series of mountain scattergrams were then produced at the radii from low to high until the selected area was first identified as a peak or a trough; and the result showed it was identified at 1200m (**Fig.4.17 Bottom**). This allows us to explore the scale at which a pre-defined area spatially, or perhaps functionally, behaves.

And meanwhile, if a pre-defined area could be represented as a peak (or trough), we also can investigate morphological properties of the area with regards to the shape of the peak (or trough). As discussed in the first part of this section, the peak denotes the centre-to-edge motif, whilst the trough indicates the edge-to-centre motif. Thus, if that area was represented by a peak, it could have been interpreted as an area having a grid-intensive centre; and if it was denoted by a trough, it could have been thought as an area surrounded by the grid-intensive edge.

On the other hand, instead of selecting an area in the segment model, we selected a peak, for example, in London's mountain scattergram of 1/MMD at 4000m against MMD Rn (**Fig.4.18 Top**). The City of London was simultaneously highlighted in bright yellow in the window of the segment model **(Fig.4.18 Bottom)**. In this way, we can investigate how the peak-trough pattern, another way of representing the periodic patchwork pattern (if identified), relate to the named area structure for example, and so this might reveal the functional meaning of the created patches.

[62] For detail, see Hillier, B. et al (2010) Metric and Topo-geometric Properties of Urban Street Networks: Some Convergences, Divergences and New Results, The Journal of Space Syntax, p258-79.

In addition, as reviewed in **Section 2.5**, Hillier (1999) clarified that a locally intensified centre, or a compact and convex shape, arises from the micro-economic process minimising metric distance among all points (measured by MMD) and meanwhile maximising access to all points. Although he focused on the live centres[63] that accommodate retail, markets, catering, entertainment and other activities benefiting from movement, rather than urban areas such as named areas, the method of interpreting the variable of MMD also can be applied to study urban areas. This can be combined with the technique of mountain scattergram to explore whether the micro-economic process that optimises the MMD relates to the spatial formation of area structure.

4.6 Discussion: a methodology framework

All the syntactic methods, discussed in the previous sections of this chapter as well as the previous chapter, can be put together to establish a methodology framework for investigating and identifying urban areas in terms of spatial configuration, with the emphasis on the interaction between internal layout and the multi-scale contexts.

One group of the techniques aims to describe *what exactly a pre-defined urban area (such as a named area) is in relation to the way the area is embedded into the surrounding contexts with increasing radius*. Thus, they are called the *descriptive techniques*, and comprise the increasing radius intelligibility/synergy developed in the previous chapter and the log-log radius plot discussed in this chapter. However, the former is conducted only on the basis of axial map, and the latter is based on both axial and segment maps. Since the segment map is a finer-scale representation, and, as **Section 4.3.3** showed, the patchwork pattern is stronger in the format of segment map, the latter chapters will not use the increasing radius intelligibility/synergy, but only deploy the log-log radius plot.

[63] Section 2.5 has reviewed the idea of live centre. For the detailed definition of live centre, see Hillier, B. (1999) *Centrality as a process accounting for attraction inequalities in deformed grids*, Urban Design International, 3/4, 107-127.

Another group of the techniques seeks to explore *whether area structure can be detected, illustrated and simulated*, aiming to explore the spatial mechanism involved in generating the area structure. Thus, they are called the *generative techniques*. Basically they include two methods of creating the *periodic patchwork pattern* by indexing the embeddedness or metric mean depth (MMD) values at different radii, as well as one method of producing the *peak-trough pattern* by illustrating the mountain scattergram.

As defined in **Section 4.3.2**, the variable of embeddedness, based on axial or segment representation, measures the change rate of node count between radii, and seems to give emphasis on the contextual structure. However, the variable of MMD, discussed in **Section 4.4**, calculates metric distance from all segments to all others up to a certain radius (only based on the segment model), and so seems to focus on the internal structure. But **Section 4.4** showed that both variables produce the similar patchwork patterns at relatively low or medium radii; and MMD can be mathematically explained by metric embeddedness (**Appendix B**), although more empirical studies should be conducted in the latter chapters.

On these grounds, we can make a visual comparison between the patches, mathematically created by these two variables, and pre-defined areas, in order to qualitatively explore the functional implication of the created patches, as well as the spatial dimension of the area structure.

As **Section 4.5** explained, the mountain scattergram, also created based on the segment model, offers a method of transforming the periodic patchwork pattern into the peak-trough pattern, and then examining the geometric and metric features of the created patches against the metric pattern of the whole network of which they are the parts, in the light of the theory of *grid intensification*[64]. We can use it to scrutinize the morphological relation between the created patches and the whole periodic structure, so that we can pave a way for revealing the spatial mechanism for generating the periodic patchwork pattern. Moreover, it also can be applied to

[64] It has been reviewed in section 2.5. For detail, see Hillier (1999) *Centrality as a process accounting for attraction inequalities in deformed grids,* Urban Design International, 3/4, 107-127.

investigate whether the peak-trough pattern has any relation to the pre-defined areas, such as named areas, as a way of exploring the functional aspect of the periodic patchwork patterns.

The above descriptive and generative techniques not only constitute the principal elements of a methodology framework for studying the empirical cases in the next two chapters, but also offer a conceptual structure to organise these chapters. The empirical studies of urban parts and the whole will be carried out in the next two chapters. Chapter five will conduct a comparative study of named areas selected from the historic central districts of London and Beijing. In each case, nine named areas will be selected. **Sections 5.2** will explain the criteria for selecting them, and will illustrate the predefined boundaries of those named areas as well as the two central districts. Chapter six will then investigate eight new development areas (delineated by the London Docklands Development Corporation[65]) and other sixteen smaller areas in the London Docklands. **Section 6.2** will clarify the criteria for selecting those areas, and will highlight the boundaries of those areas and the London Docklands as a whole.

First, both chapters will apply the descriptive technique to the sample areas. The objectives are not only to describe what the named areas or the newly developed areas are, in terms of their interaction with the multi-scale contexts, but also to test the descriptive technique on the different types of the cases.

The basic syntactic variables and techniques, reviewed in **Section 3.2**, will also be applied to illustrate a spatial profile of these areas selected from the different districts and provide an informative background for the comparative study. For the axial analysis, node count Rk of each area (or district) is defined as the arithmetic mean of the node count values of all the axial lines enveloped within, intersecting with and just passing by the area boundary (or the district boundary), as described in **Section 4.2.3**. Axial line length, connectivity and integration Rk of each area (or district) are defined in the same way. We will also use the variable of intelligibility

[65] The London Docklands Development Corporation was set up on 2nd July 1981, under the provisions of s.136 of the Local Government, Planning and Land Act 1980, to secure the development of London Docklands. For detail, see the London Docklands Monographs (1997), or http://www.lddc-history.org.uk/index.html.

and synergy, defined in **Sections 3.2.1 and 3.3.3**, to describe the relationship between local condition and global structures.

As for the segment analysis, syntactic value of each area (or district) is defined as the arithmetic mean of these syntactic values of all the segments enveloped within, and just passing by the area boundary (or the district boundary). We will deploy the variables of segment length, segment connectivity, angular choice, angular total depth, node count and metric mean depth, reviewed in **Section 3.2.1**. The variables of angular choice and angular total depth were not normalised[66], and so would have been affected by system size. Thus we will focus on node count at different radii, rather than other variables.

Second, both chapters will use the generative techniques to seek to investigate and simulate the area structures in the real cities, and so will attempt to tackle the conjecture of spatial discontinuity, set out in **Section 4.3.4**, that the discontinuities in a spatial network stem from the way in which each individual space is embedded into contexts with an increase of radius. This then leads to formulate a conceptual model of theoretically investigating spatial mechanism of generating parts and the whole, which will be discussed in the final chapter. The more detailed introduction of the methods for studying these three empirical cases will be given in chapter five and six, respectively.

[66] A way of normalizing angular choice and angular total depth to allow for comparison across cities of different size and shape was subsequently proposed by Hillier and Yang (2012).

Chapter Five: Spatial Discontinuity in the Central Historic Districts of London and Beijing

5.1 Introduction

The preceding methodology chapter summarised two kinds of syntactic techniques: *descriptive techniques* for illustrating what a pre-given area is, in terms of its embeddedness trajectory through which the area is gradually embedded into its multi-scale contextual structures, ranging from the immediate surroundings to the whole network of which it is a part; and *generative techniques* for creating the *periodic patchwork pattern* – meaning a kind of mathematical patchwork in which patches acquire similar syntactic values which show as similar colours surrounded by the discontinuities where values and so colours change – across radii. Chapters five and six, using those techniques, conduct an empirical study of the contrasting pre-given areas, including historic named areas and newly developed areas.

The analysis in each chapter is conducted in three phases, each of which is designed to answer a different, but related, question regarding the spatial definition of urban areas. First, it attempts to investigate whether the pre-given areas, such as named areas, can be described and characterised regarding their spatial relations to contexts with increasing radius, with the aim of detecting whether the multi-scale contextual structures would perhaps be involved in spatially defining urban areas; second, it examines the relationship between the created patches and the pre-given areas, in order to explore whether the periodic patchwork pattern can serve as an objective framework of investigating urban areas in relation to the whole network; and third, it explores what kind of geometric and spatial mechanism could account for the formation of the area structure represented by the periodic patchwork pattern (if their relationship is verified in the second phase), and make the first step towards understanding the part-whole problem raised at the beginning of this thesis.

In this chapter, the above questions are investigated by studying the two contrasting cases of the north part of Central London and the Inner City of Beijing. There are two reasons for selecting these two cases. First, both historic districts have various distinctive named areas with similar size; second, they have undergone different spatial transformation processes[67]; third, they have visually different geometric layouts. Thus, the comparative study of these two cases perhaps might suggest some generalised results for the spatial structure of historic named areas.

5.2 Background

This section gives a brief introduction to the named areas in the historic central districts of London and Beijing, respectively, in order to provide a background for this empirical study. As many writers (Clout and Wood, 1986; Hall, 1989; Morris, 1994; Kostof, 1999; Hebbert, 1998) argued, Central London always resisted a grand overall design, and evolved in a rather more piecemeal fashion throughout history. It has been often characterised as a collection of villages or distinct places highlighted by a set of area names[68]. In contrast, many researchers (Liang, 1952; Liu, 1980; Hou, 1998; Fu, 1998; Liang 2005) pointed out that the Inner City of Beijing was originally planned and constructed according to a grand scheme[69] based on a regular grid, and the current named areas are closely related to the original gated quarters[70], in spite of having experienced incremental reconstruction, adjustment and modification throughout its long history. **Appendix C1** gives a more detailed review of the spatial transformations of Central London and the Inner City of Beijing, as well as their relationship to the named area structures.

[67] For more details, see Appendix C of the introduction of Central London and the Inner City of Beijing.
[68] For the evolvement of area name in London, see Mills, A. D. (2010) A Dictionary of London Place-Names, Oxford University Press, Pxi-xxii.
[69] A conceptual plan of capital city, elaborated in the Confucian etiquette framework in the Zhou Dynasty (1027 - 256 BC), was used to guide the construction of the Inner City of Beijing, which has been reviewed in Appendix C1. Or, see Liu Dun Zhen (1980) Chinese Architecture History, China Architecture and Building Press (in Chinese).
[70] During the Yuan Dynasty (1271 - 1368), the city Dadu (current Beijing) was divided into 50 gated quarters - called Fangs – physically defined by the main roads and the archways called Paifangs. And most main roads enveloping those gated quarters have not been dramatically changed, and some quarter names still have survived today. See Appendix C.

5.2.1 The named areas selected in the central district of London

The district of Central London studied in this thesis, illustrated in **Fig. 5.1**, is the same as the congestion zone of London (implemented on 19 February 2007)[71], broadly bounded by Marylebone Road, Euston Road and Pentonville Road to the North, City Road, Commercial Street and Bishopsgate to the East, Tower Bridge Road, New Kent Road and Kennington Lane to the South and Vauxahall Bridge Road, Grosvenor Place and Park Lane to the West. This district approximately corresponds to the central district of London defined in Abercrombie's London Plan of 1944[72]. This chapter focuses on the areas to the north of the Thames River, called *the central district of London*. It comprises three parts: the City of London (the financial and business centre), Westminster (the political and cultural centre), and the West End (the commercial and entertainment centre)[73]. They form the vital historical core of London being made up of many distinct named places, such as Mayfair, Soho, Bloomsbury etc (Clout and Wood, 1986; Sheppard, 1998; Mills, 2010).

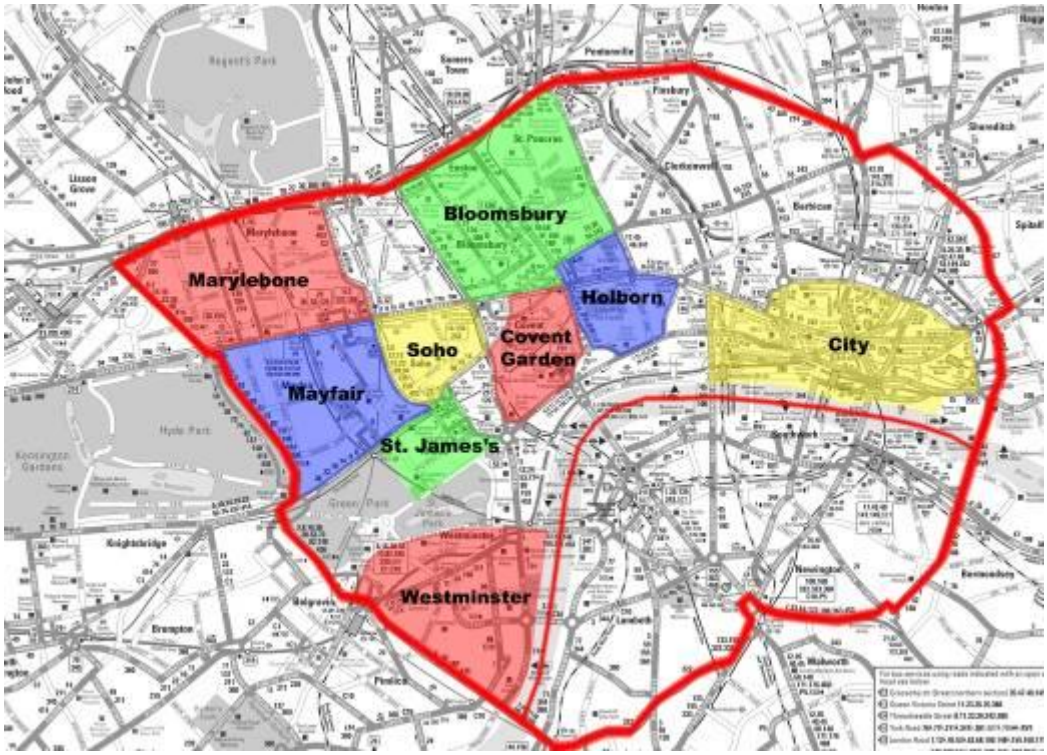

Fig. 5.1 The Boundary of Central London and the Locations of Nine Named Areas Studied in This Chapter. Thick red lines denote the boundary of Central London

[71] See http://www.tfl.gov.uk/tfl/roadusers/congestioncharge/whereandwhen/#section-2.
[72] For the description of the central district of London in the Abercrombie's London Plan, see Forshaw and Abercrombie, 1943, p22.
[73] For description of those three parts, see footnote 6.

Fig. 5.2 The Great Estates of Marylebone and Mayfair between the 18th and 19th Century. (source: GLC (1968) Greater London Development Plan: Report of Studies, Greater London Council, p258)

Marylebone includes four parts: 64. Hope; 78. Lloyd-Lisson; 99. Howard de Walden; 100. Portman

Mayfair includes eight parts: 3. Audley; 6. Berkeley; 26. Conduit Mead; 33. Curzon; 53. Grosvenor; 79. Maddox-Pollen; 80. Burlington; 120. Sutton

According to the area boundaries informally defined in The London Gazetteer (Willey, 2007), nine named areas in this central district are selected as the study areas, the City[74], Westminster[75], Marylebone[76], Mayfair[77], Soho[78], Bloomsbury[79], Covent Garden[80], Holborn[81] and St. James's[82], all of which are shown in **Fig. 5.1**. The last seven areas, extracted from the West End, have different characters associated with different land uses (Mills, 2010). Marylebone -

[74] See Willey, R. (2007) London Gazetteer, Chambers Harrap, P101-02.
[75] Ibid, P546-57.
[76] Ibid, P316-17.
[77] Ibid, P317-18.
[78] Ibid, P446-47.
[79] Ibid, P48.
[80] Ibid, P119-20.
[81] Ibid, P243.
[82] Ibid, P423.

sometimes called Marylebone Village - roughly bounded by Oxford Street to the south, Regent's Park to the north, Edgware Road to the west and Portland Place to the east, is mainly residential, with some medical offices. It was primarily developed between the 18th and the 19th century, in which the majority of the part to the west of Marylebone High Street was constructed by the Portman Estate and the part to the east of Marylebone High Street was owned by the Howard de Walden Estate[83] **(Fig. 5.2)**. Mayfair, bounded by Hyde Park to the west, Oxford Street to the north, Green Park to the south and Regent Street to the east, is a vibrant place for fashionable residence, exclusive shopping, luxury hotels, private banks and the most expensive offices. This area was developed between the mid 17th century and the mid 18th century by a variety of landlords, such as the Grosvenor Estate, the Berkeley Estate, Maddox-Pollen and Burlington **(Fig. 5.2)**. Soho is a multicultural area for commerce, culture and entertainment, as well as a residential area for both rich and poor. It is surrounded by Oxford Street to the north, Regent Street to the west, Shaftesbury Avenue to the south, and Charing Cross Road to the east. Bloomsbury, associated with arts, education and medicine, is roughly bounded by Euston Road to the north, Gray's Inn Road to the east, High Holborn to the south and Tottenham Court Road to the west. Covent Garden has been famous for shopping and entertainment since the 1500s. It became a retail centre in the 1980s, enclosed by High Holborn, Kingsway, The Strand and Charing Cross Road. Holborn is a concentration of the surviving Inns of Court and legal professional and media offices, bordered by Fleet Street to the south, Southampton Row Kingsway to the west, Theobalds Road to the north and Gray's Inn Road and New Fetter Lane to the east. St. James's is an area for commercial offices with some of the highest rents in London, exclusive houses, art galleries and membership only clubs, bounded to the north by Piccadilly, to the west by Green Park, to the south by The Mall and St. James's Park and to the east by The Haymarket. It was developed as an exclusive residential area for aristocrats (Clout and Wood, 1986; Sheppard, 1998). Most areas mentioned above are bounded by important streets, but also have often more important streets passing through them. As a result, there is not a simple answer to the question as to how those areas are spatially defined.

[83] For the estates in Central London in the 18th and 19th century, see GLC(1968) Greater London Development Plan: Report of Studies, Greater London Council, p258.

5.2.2 The named areas selected in the central distinct of Beijing

Beijing Inner City, a 38 sq km district, is encircled by the Second Ring Road to the north, west and east, as well as Chang'an Avenue[84], the ten-lane road bypassing Tian'an Men Square, to the south **(Fig. 5.3)**. We call it *the central district of Beijing* in this thesis. Like the central district of London, this district is also the historic core of the capital city, and comprises the current political, cultural, commercial and financial centres.

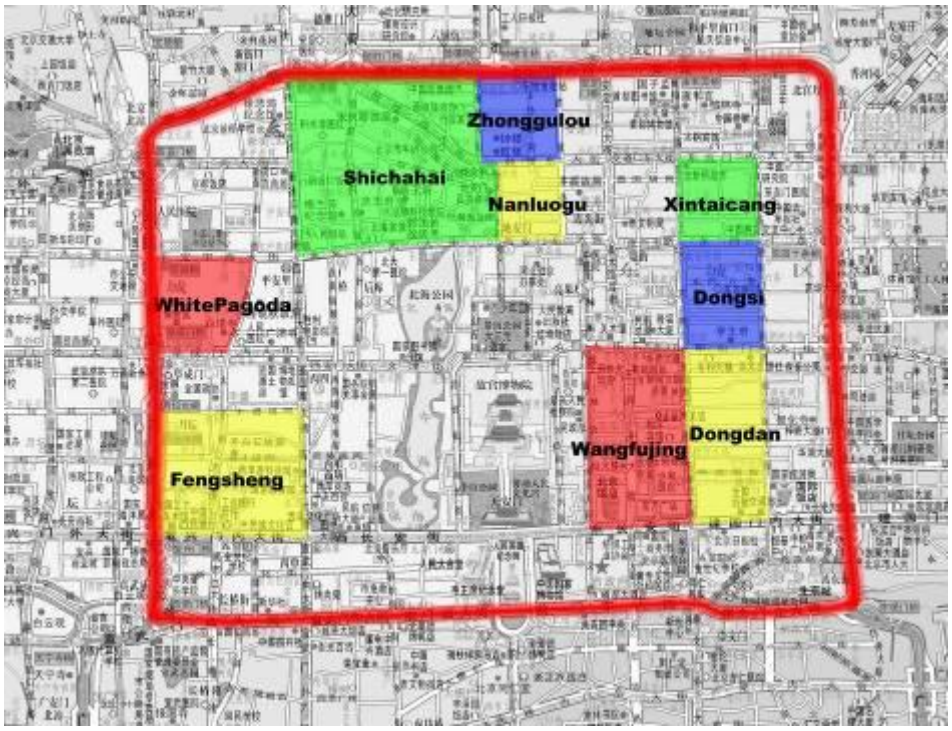

Fig. 5.3 The Boundary of the Inner City of Beijing and the Locations of Nine Named Areas Examined in This Chapter. Thick red lines denote the boundary of the Inner City.

According to the boundaries of named areas highlighted in the Beijing Administrative Map Collection (BCAB and BSMI, 2005), we selected nine named areas: Wangfujing[85], Dongdan[86],

[84] Both the Second Ring Road and Chang'an Avenue were built along the former city wall of the Inner City after the 1960s. See Appendix C.
[85] See BCAB and BSMI (Beijing Civil Affair Bureau and Beijing Surveying and Mapping Institute) (2005), Beijing Administrative Map Collection, Hunan Map Publisher. (in Chinese) p8.
[86] Ibid, p13.

Dongsi[87], Xintaicang[88], Nanluogu[89], Zhonggulou (Bell Tower and Drum Tower)[90], Shichahai[91], White Pagoda[92] and Fengsheng[93] **(Fig. 5.3)**. Each area has a different character and function, though all of them are mixed use areas. Wangfujing is a vibrant area for commerce (with the highest rents), retail, luxury hotels, exclusive courtyards and clubs, as well as colleges. It is approximately bounded by Dongsi West Street to the north, Chang'an East Avenue to the south, Yan He Street to the west and Dongsi South Street and Dongdan North Street to the east. In the Ming Dynasty, this area was an exclusive residential quarter for princes and princesses. Dongdan is a mixed use area, which includes commerce, retail, administrative offices and residence, roughly encircled by Changyangmen Nei Street, Changyangmen South Street, Jianguomen Street and Dongdan North Street. Dongsi is an area for commerce, catering, new offices and residence, bordered by Dongsishi Lane, Changyangmen North Street, Dongsi North Street and Changyangmen Nei Street. Xintaicang is mainly for residence, with some smaller businesses, bounded by Dongzhimen Nei Street, Dongsi North Street, Dongsishi Lane and Dongzhimen South Street. It was the north part of Xisi area in history. Nanluogu is a concentration of the luxury court yard houses, with the Academy of Drama and a hospital compound, bounded by Gulou East Street, Di'anmen Wai Street, Di'anmen East Street and Jiaodaokou South Street. Zhonggulou is for residence and catering, enveloped by Andingmen Street, North Luogu Lane, Guluo East Street and Old Gulou Street. It was a commercial market in history. Shichahai is a concentration of luxury clubs, cultural facilities, entertainment, catering and a hospital as well as exclusive courtyard houses. It is enclosed by Deshengmen East Street to the north, Old Gulou Street and Di'anmen Wai Street to the east, Di'anmen West Street to the south, and Xinjiekou Street to the west. Whitepagoda is a mix of the Tibetan Buddhism Temple, open markets, culture facilities, new estates, the exclusive banks and the court yard houses, bounded by Fuchengmen North Street, Ping'anli West Street, Zhaodenglv Road, and Fuchengmen Nei Street. Fengsheng is a place of banks, retail, administrative offices and residential housing, surrounded by Fuchengmen Nei Street, Taipingqiao Street, Xuecai Lane, and Xisi South Street.

[87] Ibid, p12.
[88] Ibid,,p11.
[89] Ibid,p10.
[90] Ibid, p10.
[91] Ibid, p20.
[92] Ibid, p19.
[93] Ibid, p19.

5.3 What are the named areas in terms of their contexts?

5.3.1 The morphological differences between the two cities (and their central districts)

Before studying the named areas, we first quantitatively examined whether the whole maps of London and Beijing (or their central districts), as the contexts of those named areas, have different geometric and syntactic features. We sought to provide an informative background for investigating the named areas in due course. The axial maps of both London and Beijing (**Fig 5.4**), comprising those named areas, were drawn to represent their spatial structures in a consistent way, and then segmented into segment maps. Both axial maps have the radius-radius[94] of 10 and both segment maps have the metric system radius[95] of around 9900m. The central districts (including those named areas) of London and Beijing (denoted by dotted lines in **Fig. 5.4**) are respectively located at the centre of the axial (or segment) maps. The central district of London has a minimum buffer distance (meaning the minimum metric distance from the edge of this district to the edge of map of London) of 7000m, whilst the central district of Beijing has a minimum buffer distance of 8000m. This buffer distance was built to avoid the biases introduced by the edge effect[96].

[94] The radius-radius is equal to the mean depth of the whole structure from the most integrated line. For detail, see Section 3.2.1 in chapter three, or Hillier (1996), p163.
[95] Metric system radius is defined as the average metric distance from the geometric centre of the segment model to the edge. See Section 4.2.1.
[96] The analysis of spaces along the periphery of either axial or segment map is always affected by their location at the system edge. For detail, see Section 4.2.1, Section 3.2.1, or Hillier (1996), p163.

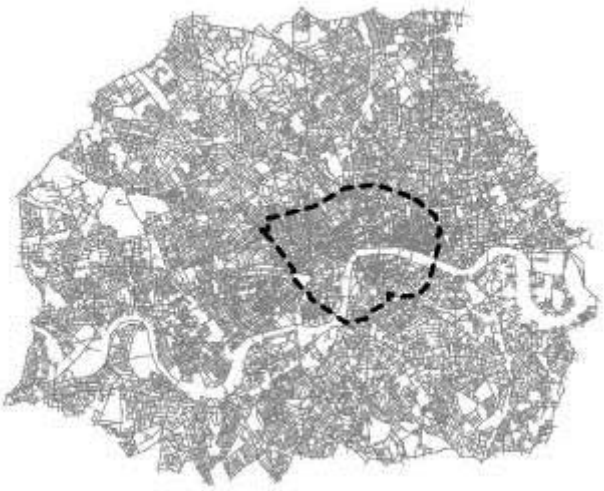

The unprocessed Central London axial map (the central district of London highlighted by dotted lines)

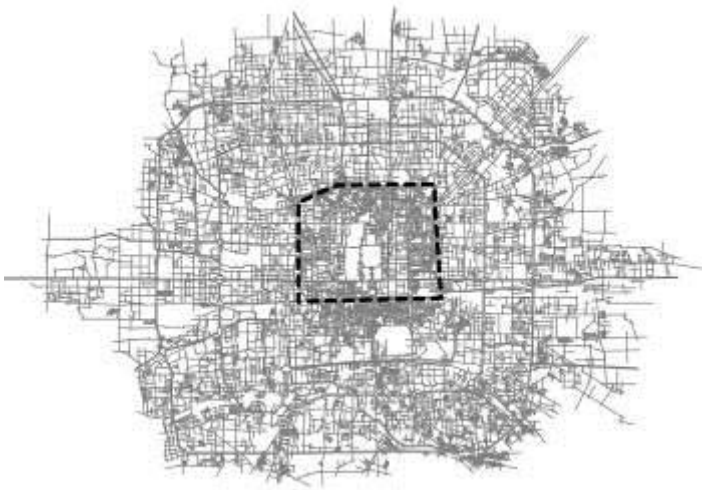

The unprocessed Beijing axial map (the central district of Beijing highlighted by doted lines)

Fig. 5.4 The unprocessed axial maps of London and Beijing.

The primary analysis was conducted by comparing the basic geometric and syntactic values, such as axial line length, segment length, axial line connectivity, segment connectivity, axial integration and intelligibility[97] (summarised in **Table 5.1**), of the two cities and their central districts. It demonstrates the following points. First, London (and its central district) has a denser grid than Beijing (and its central district) in terms of segment length. As **Table 5.1** shows,

[97] Section 3.2 reviewed those syntactic measures.

London has a smaller mean segment length (66m) than Beijing (98m); and the central district of London also has much smaller mean segment length[98] (44m) than that of Beijing (70m). As smaller mean segment length of a district roughly indicates that the district has larger number of smaller blocks, this suggests that London (and its central districts), on average, has smaller blocks than Beijing (its central districts), and so the former is more metrically intensified.

Table 5.1 The Basic Geometric and Syntactic Values of London and Beijing (as well as of their central districts).

(Ax_M_Len: the mean of axial line length; Seg_M_Len: the mean of segment length; Ax_M_Conn.: the mean of axial line connectivity; Seg_M_Conn.: the mean of segment connectivity; M_Int.Rn: the mean of integration Rn; M_Int.R10: the mean of integration R10)

	Ax_M_Len (m)	Seg_M_Len(m)	Ax_M_Conn	Seg_M_Conn.	M_Int. Rn	M_Int. R10	Intelligibility Rn
London	285	66	4.2	4.4	0.808	1.250	0.086
Beijing	353	98	3.7	4.2	0.827	1.241	0.042
Central district of London	253	44	5.6	4.8	1.051	1.482	0.200
Central district of Beijing	247	70	3.5	4.2	1.002	1.425	0.140

[98] However, the smaller mean segment length of London (and its central district) might be caused by a factor of *trivial rings* meaning that the tiny segments generated by several intersecting axial lines, because the axial map of London seems to have more non-right angle intersections usually associated with more trivial rings. In order to test this conjecture, we calculated the number of the segments less than 0.1m, 0.5m, 1m, 2m and 4m, respectively, and then computing the percentage of those tiny segments in the two cases, respectively. Although London has more trivial rings than Beijing, the London and Beijing maps have almost the same percentage of the trivial rings: less than 0.1m, 0.5m, 1m, 2m and 4m, respectively. This shows that those trivial rings have not significantly affected the above result.

Second, the central district of London, on average, maintains a higher degree of visual continuity of streets than the central district of Beijing. This is unexpected, because the central district of Beijing seems to have a more rectangular form than that of London, and so we intuitively assume that the former has a larger amount of long and continuous streets represented by axial lines. However, **Table 5.1** quantitatively shows that the central district of London has a slightly longer mean axial length (253m) than the central district of Beijing (247m) (**Table 5.1**), although the former has much shorter segments. To some extent, this implies that the named areas in London, on average, would perhaps be better visually connected to their surrounding areas (via those longer streets) than those in Beijing, due to the fact that the central district of Beijing has a lot of short alleys, called Hutong, inside the blocks.

Third, London (or its central district) is much better connected at local scale than Beijing (or its central district); and meanwhile, the central district of London is more integrated at a global scale. For example, London has a higher mean axial and segment connectivity (4.2 and 4.4 respectively) than Beijing (3.7 and 4.2 respectively); and the central district of London also has higher mean axial and segment connectivity values (5.6 and 4.8 respectively) than that of Beijing (3.5 and 4.2 respectively), shown in **Table 5.1**. London (1.250) is slightly more integrated than Beijing (1.241) at the radius-radius (R10); and in particular, the central district of London (1.051 and 1.482 respectively) is more integrated than that of Beijing (1.002 and 1.425 respectively) at both the infinite radius and the radius-radius (R10). This indicates that London is better spatially structured than Beijing in terms of connectivity and integration, although the former is a more irregular grid.

Fourth, London (or its central district) has a better relationship between local conditions and global configuration, based on the axial analysis. As **Table 5.1** displays, London (or its central district) has a higher intelligibility Rn value (0.086, or 0.200) than Beijing (or its central district) (0.042, or 0.140). To some extent, perhaps this hints that the London areas, as the local entities, might be better embedded into the whole urban network, but this needs to be investigated in next section.

In general, the above analysis demonstrates that London (or its central district) is geometrically and syntactically different from Beijing (or its central district). Then, *how far are those named areas in the two cases spatially embedded into the geometrically and syntactically different networks as their contexts, respectively?*

5.3.2 The embeddedness trajectories of the named areas

So next, we sought to examine the named areas in the two cities. Based on the unprocessed axial maps, **Fig. 5.5** and **5.6** respectively illustrate the boundaries[99] of those named areas. Then, we illustrated the embeddedness trajectory[100] of each named area, by using the descriptive technique of the log-log radius plot for all the axial lines (and/or segments) making up an area. This aims to investigate whether we can numerically describe the way in which the named areas are spatially embedded into the surroundings with increasing radius.

[99] For the definition of the boundaries of the named areas, see section5.2.1.
[100] For the definition of the embeddedness trajectory, see Section 4.2.

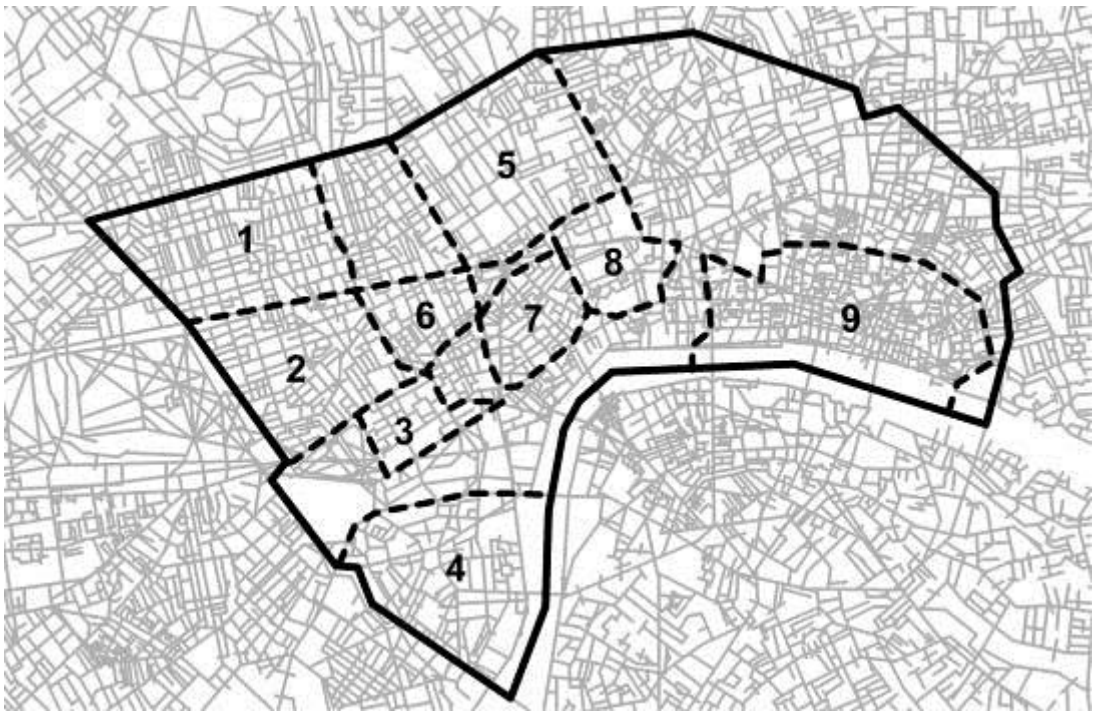

Fig. 5.5 The Axial Map of the North Part of Central London (called the central district of London later), Superimposed by the Boundaries of the Nine Named Areas.

1. Marylebone; 2, Mayfair; 3. St.James's; 4. Westminster; 5. Bloomsbury; 6. Soho; 7.Covent Garden; 8. Holborn; 9. The City

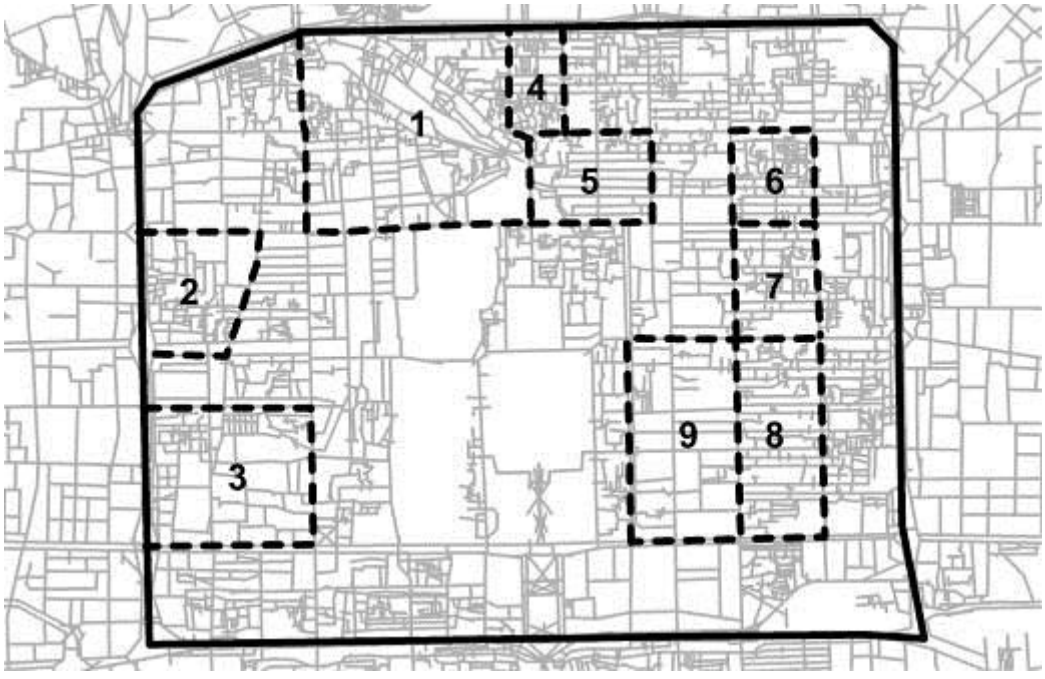

Fig. 5.6 The Axial map of the Inner City of Beijing (called the central district of Beijing later), Superimposed by the Boundaries of the Nine Named Areas.

1. Shichahai; 2, Whitepagoda; 3. Fengsheng; 4. Zhonggulou; 5. Nanluogu; 6. Xintaicang; 7.Dongsi; 8. Dangdan; 9. Wangfujing

As discussed in **Section 4.2.3**, the log-log radius plot can be applied to investigate the mathematical relationship between mean node count of each area and topological (or metric) radius within relatively narrower radius ranges. Based on the axial map, we use an example of Westminster to briefly explain the procedure for producing the log-log radius plot (**Fig. 5.7**). We start by exploring whether the first three data points (located at the bottom left of the log-log radius plot, see **Fig. 5.7**) have a strong correlation between the logarithm of radius and the logarithm of node count (with an R-square of 0.999). When a strong correlation was not found, we excluded the first data point and then included the fourth point as a new point, seeking to test whether the second, third and fourth points have a strong correlation. When a strong correlation was detected, new points nearest to the fourth point in the log-log plot would be included respectively until the R-square decreased below 0.999. A strong correlation above 0.999 was then found within a relatively narrower range of 2 and 12, excluding the range of 1 to 2. Another round of testing and inclusion (and exclusion) was carried out for the other new points and a strong correlation was also found within another narrower range of 12 to 17 (**Fig. 5.7**). The slope of the regression line (found within each small range) is equal to the power-law exponent (denoted by α); and the end point of the small range denotes an inflexion point in the log-log plot. The power-law exponent (approximating the embeddedness pace defined in **Section 4.3.2**) in effect measures the *pace* at which an area is spatially embedded into the surroundings within a narrow range; and the endpoint of the small range suggests a discontinuity along the embeddedness trajectory, where the sum of the encountered lines, measured by node count, changes dramatically. Bearing in mind that a line can be drawn crossing the first and second points, although this does not mean of course that a power-law relationship is verified across the whole range. However, we still call the slope of that linear line as the first exponent and denote it as α1, because as with power-law exponent, that slope still denotes the change rate of node count at the radius of 1 to 2.

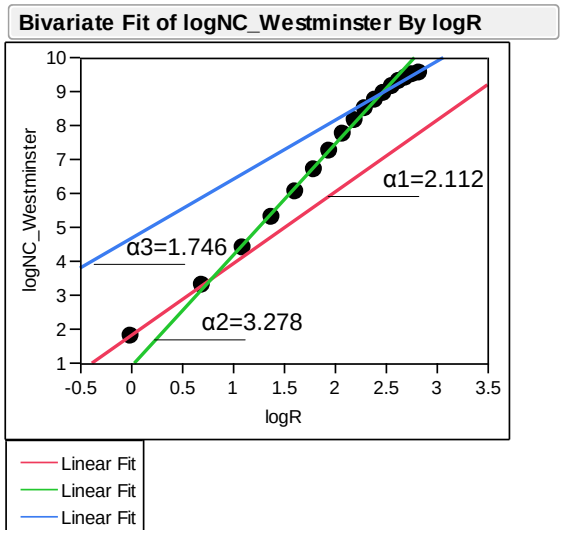

Fig. 5.7 The Log-log Radius Plot of Westminster. A strong correlation between the logarithm of radius and the logarithm of node count (with an R-square of 0.999) was found within smaller ranges of 1 to 2, 2 to 12, and 12 to 17. The values of α1, α2 and α3, respectively, denote the slopes of the regression lines found within those smaller ranges, and these slopes are equal to power-law exponents (α1 does not mean power law exponent, because the smaller range is too narrow).

The above technique was also applied to all the other named areas in the two cases respectively. The log-log radius plot analysis, based on the axial maps, was conducted within the topological radius range of 1 to 20; and the analysis, based on the segment models, was then carried out within the metric radius range of 400m to 9,900m, with an interval scale of 100m. Compared to the radius-radius (10 topological depths) or the metric system radius (around 9,900m) of the two cities, the endpoints of the whole range (such as 20 topological depths or 9,900m) are large enough to be used to test this descriptive technique.

Topological embeddedness trajectories (based on the axial maps)

For topological analysis, **Fig. 5.8** illustrates all the log-log radius plots of the London areas; whilst, **Fig. 5.9** shows all the plots of the Beijing areas. Each plot has three regression lines with different slopes (denoted by red, green and blue lines respectively). They respectively demonstrate that each named area, either in London or in Beijing, has a power law relation between mean node count and topological radius within the constricted topological radius

ranges. And the discontinuities along the embeddedness trajectories were highlighted by the intersections of those regression lines. For each area, this means that the embeddedness pace changes dramatically at certain radii.

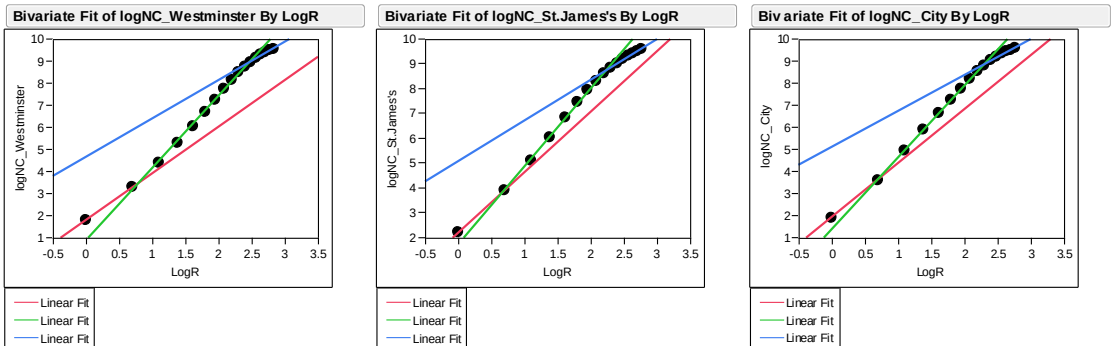

a. Westminster b. St. James's c. The City

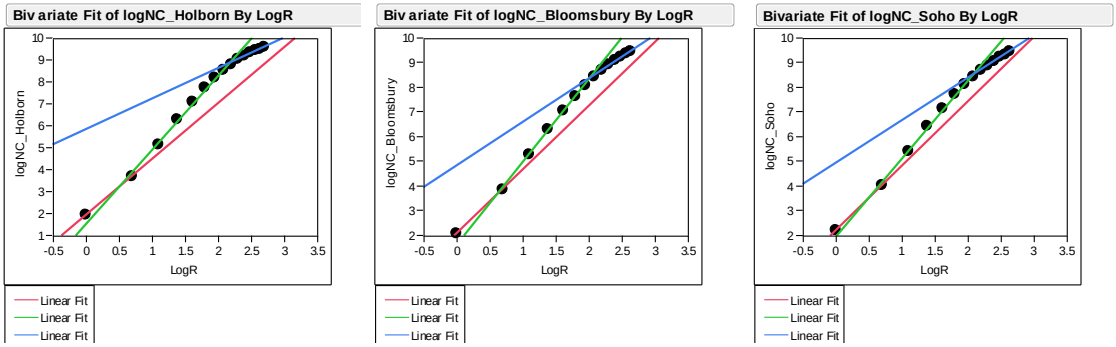

d. Holborn e. Bloomsbury f. Soho

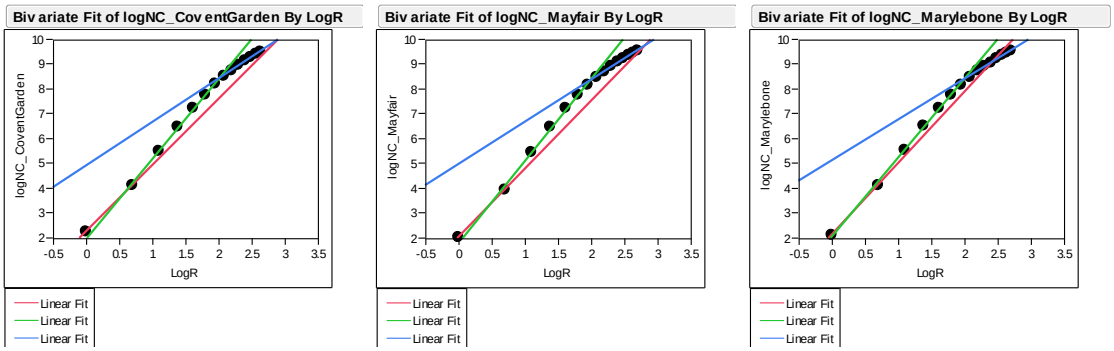

g. Covent Garden h. Mayfair i. Marylebone

Fig. 5.8 The Topological Embeddedness trajectories of the London Areas (based on the axial maps). Red, green and blue lines respectively indicate the regression lines generated within the constricted radius ranges.

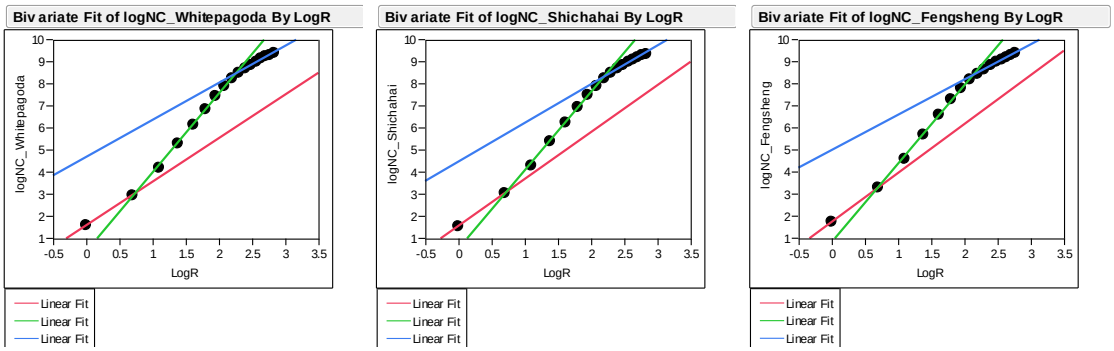

a. Whitepagoda b. Shichahai c. Fengsheng

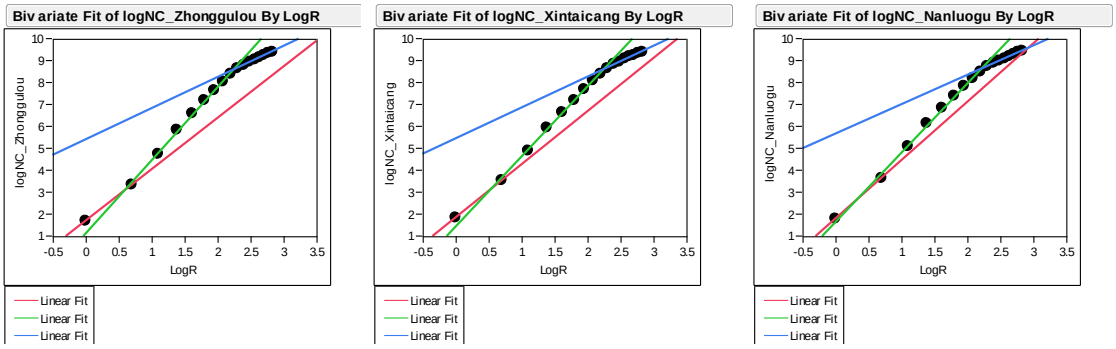

d. Zhonggulou e. Xintaicang f. Nanluogu

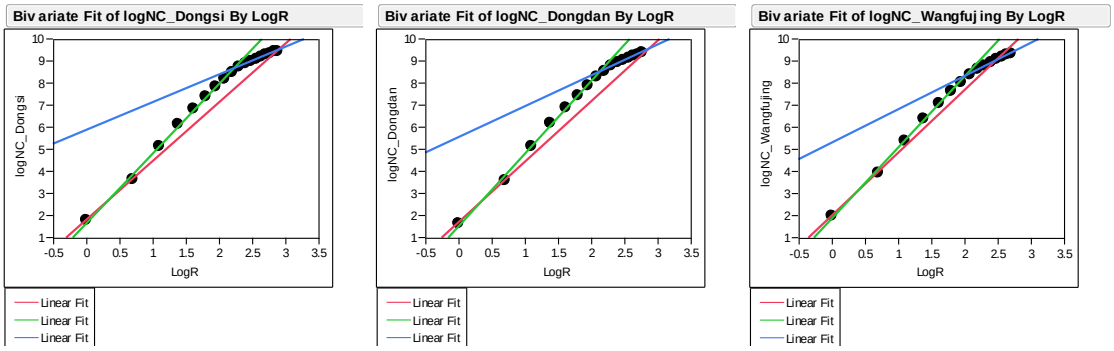

g. Dongsi h. Dongdan i. Wangfujing

Fig. 5.9 The Topological Embeddedness trajectories of the Beijing Areas (based on the axial maps). Red, green and blue lines respectively indicate the regression lines generated within the constricted radius ranges.

And meanwhile, **Tables 5.2 and 5.3** respectively summarise power-law exponents (denoted as α) as well as the corresponding radius ranges (denoted as radius range), and this in fact numerically illustrates the topological embeddedness trajectories of the named areas. At first sight, all the named areas in each case have three radius ranges (corresponding to the three regression lines shown in **Fig. 5.8 and 5.9**); and the endpoint of the first range is 2, the endpoint

of the second range is around the radius-radius of 10 and the endpoint of the third rang is around 17. This demonstrates that the first two discontinuities are least influenced by the system edge, but the third one is likely affected by the system edge.

Table 5.2 The Power-law Exponents (denoted as α) and the Corresponding Topological Radius Ranges of the London Areas (based on the axial analysis).

Mean of α in each range* indicates the arithmetic mean of α within each radius range for all the named areas, although those areas do not have the equal width of the range 2 and 3. The mean values of α1, α2 and α3 roughly show how the power-law exponent varies with increasing radius range.

The table is sorted by α1 in an ascending order. But α1 indicates the difference in the logarithm of node count between the radius 1 and the radius 2, rather than the power-law exponent within the first radius range, because that first range is too narrow to verify the power-law relation.

Area	Radius Range 1	α1	Radius Range 2	α2	Radius Range 3	α3
Westminster	1,2	2.112	2,12	3.278	12,17	1.746
St.James's	1,2	2.438	2,10	3.153	10,16	1.635
City	1,2	2.444	2,10	3.267	10,16	1.634
Holborn	1,2	2.553	2,10	3.366	10,15	1.769
Bloomsbury	1,2	2.582	2,8	3.347	8,14	1.703
Soho	1,2	2.606	2,9	3.150	9,14	1.723
Covent Garden	1,2	2.660	2,8	3.216	8,14	1.746
Mayfair	1,2	2.743	2,8	3.307	8,15	1.696
Marylebone	1,2	2.864	2,8	3.173	8,15	1.643
Mean of α in each range	Radius Range 1	2.556	Radius Range 2	3.251	Radius Range 3	1.699

Table 5.3 The Power-law Exponents (denoted as α) and the Corresponding Topological Radius Ranges of the Beijing Areas (based on the axial analysis).

HM 15 means the harmonic mean of exponents from 1 to 15.

Area	Radius Range 1	α1	Radius Range 2	α2	Radius Range 3	α3
White Pagoda	1,2	1.978	2,10	3.563	10,17	1.752
Shichahai	1,2	2.122	2,9	3.559	9,17	1.632
Fengsheng	1,2	2.219	2,9	3.545	9,16	1.588
Zhonggulou	1,2	2.343	2,10	3.328	10,17	1.421
Xintaicang	1,2	2.414	2,10	3.203	10,17	1.401
Nanluogu	1,2	2.650	2,10	3.171	10,17	1.335
Dongsi	1,2	2.654	2,10	3.151	10,18	1.253
Dongdan	1,2	2.752	2,9	3.297	9,16	1.391
Wangfujing	1,2	2.835	2,8	3.210	8,15	1.508
Mean α in each range	Radius Range 1	2.447	Radius Range 2	3.336	Radius Range 3	1.458

In order to feel how these discontinuities look like in the axial map, we randomly selected two areas in London to visualise their discontinuities. For example, **Fig. 5.10** displays the distribution patterns of the three discontinuities of Westminster and Mayfair. The first discontinuity was found at the edge of their immediate surroundings (coloured in red), the second identified at the edge of their large-scale contexts (coloured in blue), and the third marked out at the edge of their further contexts (coloured in black). Morphologically speaking, **Fig. 5.10** also demonstrates that the context of each named area is approximately partitioned into three levels of contexts – namely the immediate surroundings, the large-scale contexts and the further contexts reaching the system edge – in terms of the discontinuities. And meanwhile, **Tables 5.2 and 5.3** show that the first discontinuity of all the areas were found at 2, and this implies that they all have the same *topological* relationship with their immediate surroundings

with respect to the values of topological depth. Perhaps this might relate to the fact that all those named areas are located at the well developed central districts and have been evolved for a long period of time.

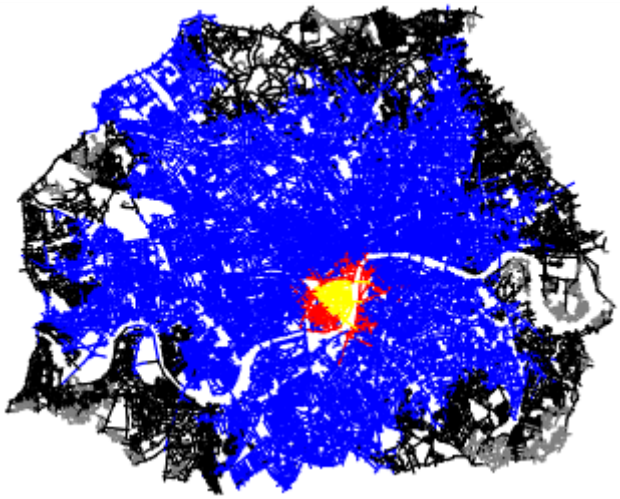

a. Westminster. Yellow denotes the axial lines belonging to Westminster; red indicates the radius range of 1 to 2; blue means the radius range of 2 to 12; black represents the radius range of 12 to 17; and grey indicates the rest of the context area.

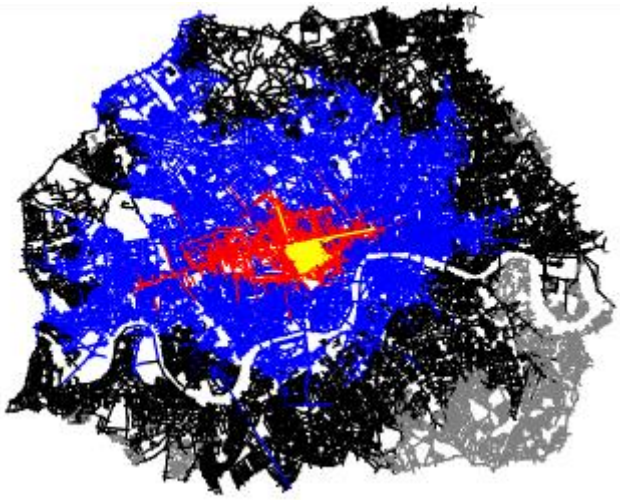

b. Mayfair. Yellow denotes the axial lines belonging to Mayfair; red indicates the radius range of 1 to 2; blue means the radius range of 2 to 8; black represents the radius range of 8 to 15; and grey indicates the rest of the context area.

.

Fig. 5.10 The Spatial Discontinuities along the Topological Embeddedness trajectories of Westminster and Mayfair, Respectively.

However, **Fig. 5.10** also shows that the contexts of the two areas seem to be partitioned into the different patterns. For example, Westminster has small sized immediate surroundings than Mayfair, perhaps because Mayfair is better connected to the immediate surrounding areas, so that it can access to relatively wider immediate surroundings. This in fact can be captured by their first exponents expressing the paces at which they are embedded into the immediate surrounding areas. And in general, the exponents (denoted as α in **Tables 5.2 and 5.3**) were generated within the radius ranges bounded by the endpoints representing the discontinuities, so that the exponents in turn can be used to reflect the character of the discontinuities, with respect to the different levels of contexts they separate. Therefore, we then move to investigate their exponents.

Tables 5.2 and 5.3 also show the mean of exponents in each radius range for all the areas in both cases respectively. On average, each case has moderate mean exponent in the first range, high mean exponent in the second range, and low mean exponent in the third range. This indicates that those areas, in general, are topologically embedded into the immediate surroundings at a moderate pace, and then into the larger-scale contexts at a quick pace, and finally into the further contexts at a slow pace (because they reach the system edges above the radius-radius of 10).

Since the third exponents are affected by the system edges, we focus on the first two exponents. At first sight, the named areas in each case have the different exponents in either the first or the second range. This indicates that they are topologically embedded into either the immediate surroundings or the large-scale contexts at *different* paces. In other words, this reflects that each area has different immediate surroundings (and/or their large-scale contexts) with respect to their topological embeddedness paces.

Moreover, **Fig. 5.11** (**Left**) shows that no correlation between the first and the second exponents was found for the London areas (with an R-square of 0.025). This demonstrates that the paces at which the London areas are topologically embedded into the two levels of contexts are not interdependent. In other words, when any a London area is topologically embedded into the first level of context at a quick pace, this does not mean that that area is embedded into the

second level of context at a slow or quick pace. This suggests that the discontinuities found between the two levels of contexts are different in terms of the relationship between the two levels of contexts, and so that the London areas can be distinguished in terms of those discontinuities.

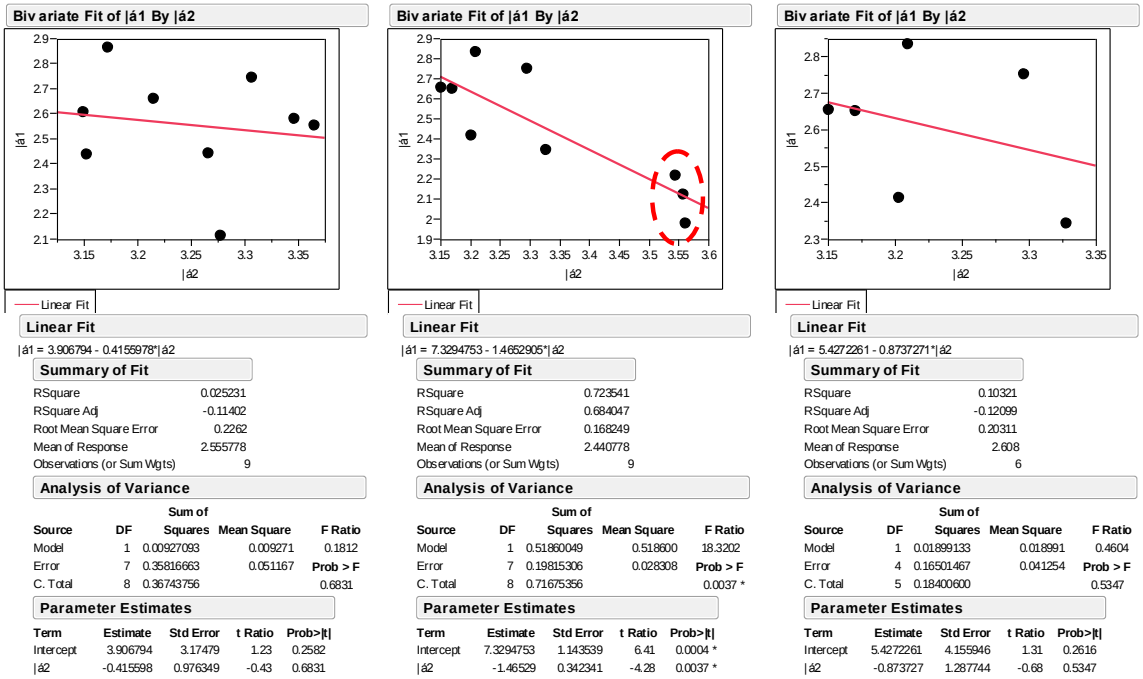

Left: No correlation between the first and the second exponents in the London case;

Middle: A strong correlation between the first and the second exponents in the Beijing case (but this is affected by three outliers highlighted by a red dotted circle);

Right: No correlation in the Beijing case, if three outlier points are excluded.

Fig. 5.11 The Correlations between the First and the Second Topological Exponents in London and Beijing Respectively (based on the axial maps).

Fig. 5.11 (**Middle**) however displays a strong correlation between the first and the second exponents verified for the Beijing areas (with an R-square of 0.724), but this strong correlation seems to be affected by three outliers situated at the left right corner of the scattergram. This is due to the reason that the three outlier areas (namely Whitepagoda, Shichahai and Fengsheng) are topologically embedded into the immediate surroundings at a much lower pace, but embedded into the large-scale contexts at a much higher pace, and the regression line was therefore influenced by their extreme values. When they are excluded, no correlation was found

for the other Beijing areas, with an R-square of 0.103 (**Fig. 5.11 Right**). This also suggests that the paces at which those Beijing areas (except for the outliers) are topologically embedded into the two levels of contexts are not interdependent, and so that they can to some degree be marked out with respect to the topological discontinuities found between the two levels of contexts.

Metric embeddedness trajectories (based on the segment maps)

Then we, based on their segment maps, moved to investigate metric embeddedness trajectories in both cases, respectively illustrated in **Fig. 5.12 and 5.13**. In contrast to the topological embeddedness trajectories shown in **Fig.5.8 and 5.9**, the metric embeddedness trajectories seem much *straighter* in the log-log radius plots, and this suggests that all the named areas roughly have a power-law exponent between mean node count and metric radius within an overall radius range of 400m to 9900m. It also implies that those areas are metrically embedded into their surroundings in a more consistent way.

However, each metric embeddedness trajectory is still slightly bended, so that a stronger power-law relationship can be identified within relatively smaller radius ranges, which are represented by red, green or blue regression lines shown in **Fig.5.8 and 5.9**. The intersections of the consecutive regression lines indicate the discontinuities along the metric embeddedness trajectories, although the difference in slope of the regression lines seems relatively small. This still suggests the contexts of those areas are partitioned into the different levels of parts with respect to the way they are metrically embedded into the contexts.

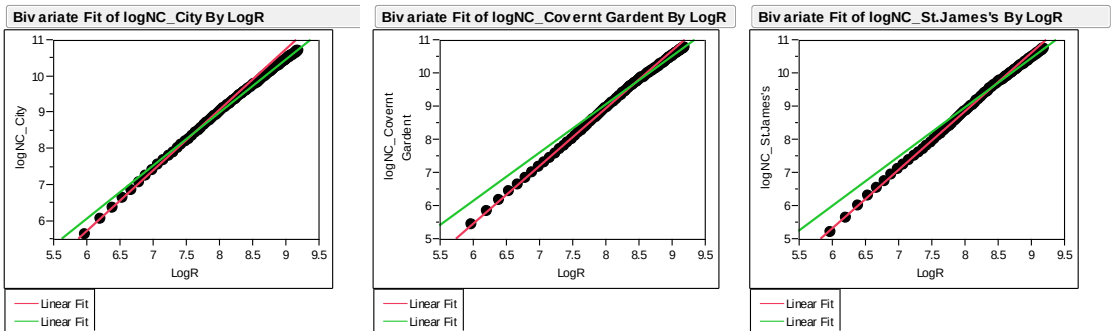

a. The City b. Covent Garden c. St. James's

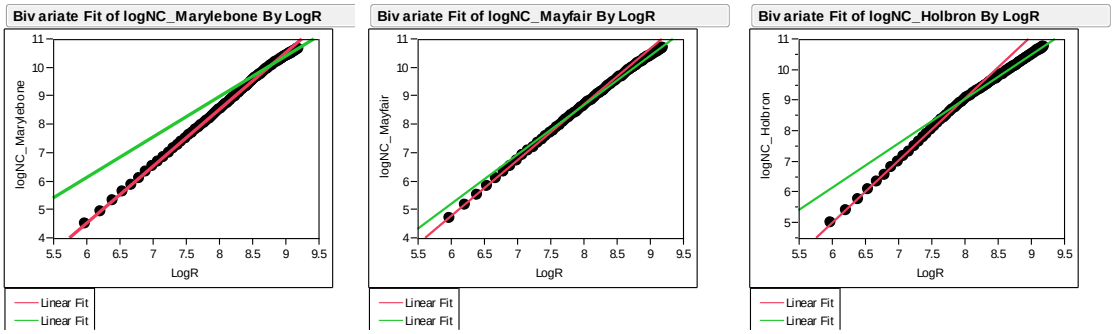

d. Marylebone e. Mayfair f. Holborn

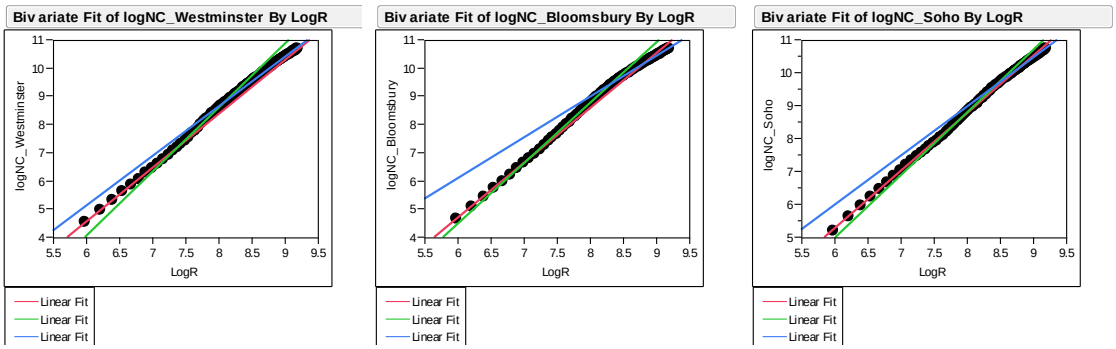

g. Westminster h. Bloomsbury i. Soho

Fig. 5.12 The Metric Embeddedness trajectories of the London Areas (based on the segment maps). Red, green and blue lines respectively indicate the regression lines generated within the constricted radius ranges (some plots only have two regression lines).

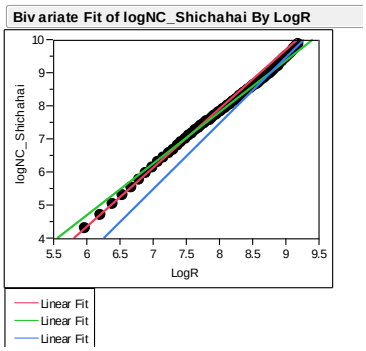

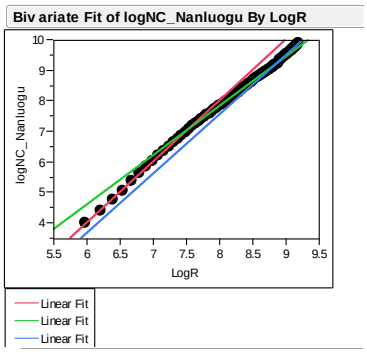

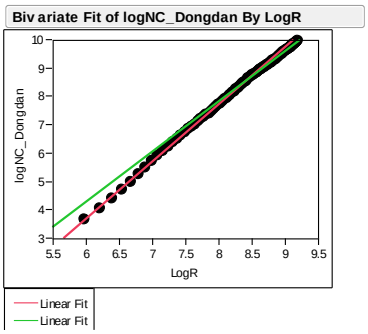

a. Shichahai b. Nanluogu c. Dongdan

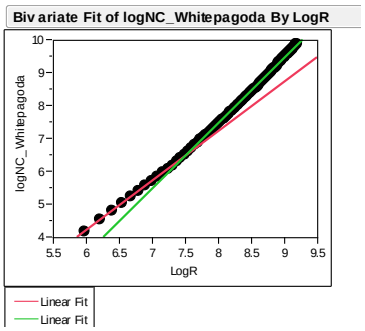

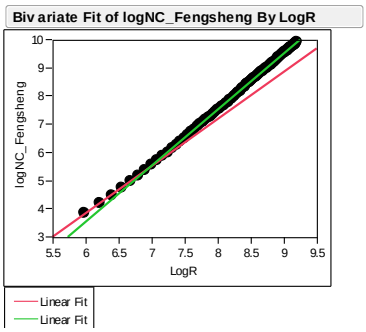

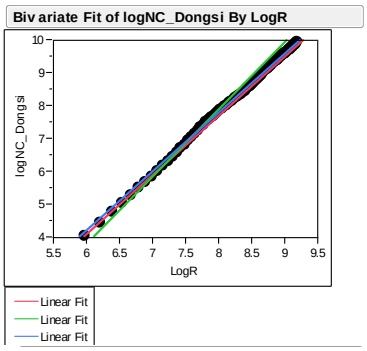

d. Whitepagoda e. Fengsheng f. Dongsi

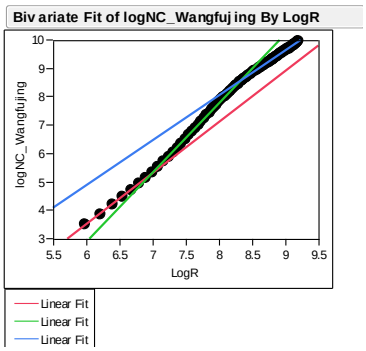

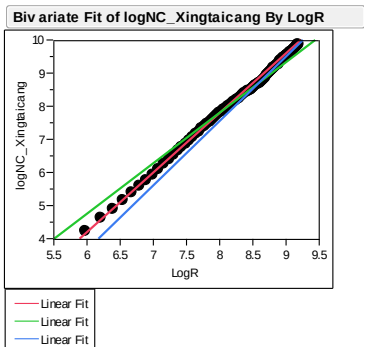

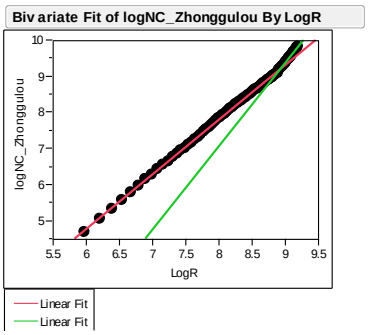

g. Wangfujing h. Xintaicang i. Zhonggulou

Fig. 5.13 The Metric Embeddedness trajectories of the Beijing Areas (based on the segment maps). Red, green and blue lines respectively indicate the regression lines generated within the constricted radius ranges (some plots only have two regression lines).

And meanwhile, **Tables 5.4 and 5.5** respectively summarise power-law exponents (denoted as α) as well as the corresponding radius ranges (denoted as radius range), and this in fact numerically illustrates the metric embeddedness trajectories. In contrast to the topological embeddedness trajectories, not all the named areas in each case have three metric radius ranges, and in particular, the endpoints of the first metric ranges are not similar to each other.

This demonstrates that their discontinuities along the *metric* embeddedness trajectories were found at more varying radii, than the topological embeddedness trajectories, in spite of the fact that the metric trajectories themselves seem much straighter (as mentioned earlier). Since metric radius of the whole system in each case is around 9900, this suggests that the first two radius ranges are least affected by the system edges. Therefore it indicates that the named areas in both cases are metrically embedded into their contexts at least at two levels. However, some areas, such as Marylebone in London and Zhonggulou in Beijing, have wider first radius ranges, and so their first level of contexts not only include the immediate surrounding areas, but also comprise the large-scale contexts. But the endpoints of the first radius ranges (or the startpoints of the second ranges) still denote the discontinuities found between the two levels of contexts.

Table 5.4 The Power-law Exponents (denoted as α) and the Corresponding Metric Radius Ranges of the London Areas (based on the segment analysis).

Area	Radius Range 1	α1	Radius Range 2	α2	Radius Range 3	α3
City	400- 1800	1.679	1800- 9900	1.464		
Covent Garden	400- 4100	1.736	4100- 9900	1.453		
St.James's	400- 4800	1.767	4800- 9900	1.485		
Marylebone	400- 6500	1.997	6500- 9900	1.426		
Mayfair	400- 2500	1.964	2500- 9900	1.736		
Holborn	400- 2800	2.038	2800- 9900	1.447		
Westminster	400- 1800	1.909	1800- 3100	2.269	3100- 9900	1.752
Bloomsbury	400- 1400	1.941	1400- 4100	2.135	4100- 9900	1.448
Soho	400- 2100	1.748	2100- 4200	1.905	4200- 9900	1.493
Mean value	Radius Range 1	1.859	Radius Range 2	1.699	Radius Range 3	1.550

Table 5.5 The Power-law Exponents (denoted as α) and the Corresponding Metric Radius Ranges of the Beijing Areas (based on the segment analysis).

Area	Radius Range 1	α1	Radius Range 2	α 2	Radius Range 3	α 3
Shichahai	400- 2400	1.777	2400- 7300	1.562	7300-9900	1.991
Nanluogu	400- 2000	2.007	2000- 7400	1.616	7400-9900	1.934
Dongdan	400- 4700	2.019	4700- 9900	1.767		
WhitePagoda	400- 1600	1.507	1600- 9900	1.990		
Fengsheng	400- 1000	1.669	1000- 9900	1.996		
Dongsi	400- 1400	1.800	1400- 2600	2.043	2600- 9900	1.796
Wangfujing	400- 1000	1.798	1000- 4400	2.440	4400- 9900	1.581
Xintaicang	400- 3100	1.793	3100-5800	1.521	5800- 9900	1.953
Zhonggulou	400- 7300	1.511	7300-9900	2.301		
Mean value	Radius Range 1	1.791	Radius Range 2	1.868	Radius Range 3	1.826

We then move to examine their power-law exponents calculated within the constricted ranges, because as discussed earlier, the exponents (besides the radius ranges) also reflect the feature of the discontinuities. We first observed the mean exponent of each case to capture an overall but average picture. **Tables 5.4** shows that the mean exponents of the London areas decrease from 1.859 to 1.699 and then 1.550, with an increase of radius. This indicates that the London areas *on average* are metrically embedded into the different levels of contexts at decreasing paces, although three areas (Westminster, Bloomsbury and Soho) are embedded into the first level of context at a quicker pace than the second level of context. In contrast, **Tables 5.5** displays that the mean of the exponents of the Beijing areas increases from 1.791 to 1.868 and then decrease to 1.826, with an increase of radius. This demonstrates that the Beijing areas *on average* are metrically embedded into the second level of contexts at a quicker pace, although some areas, such as Shichahai, Nanluogua and Dongdan, are metrically embedded into their first level of contexts at a quicker pace. To some extent, it might suggest that the London areas *on average* have a better metric relationship with the immediate surroundings than the Beijing areas.

However, at the level of individual areas, all the areas in each case have different exponents for each level of context. In particular, **Fig. 5.14 Left** shows that no correlation between the first and the second exponents for the London areas (with an R-square of 0.025); and meanwhile, **Fig. 5.14 Right** displays that a very weak correlation between the first and the second exponents for the Beijing areas (with an R-square of 0.232). This demonstrates that in each case, the paces at which the named areas are metrically embedded into the first level of contexts have no relationship with the paces at which they are embedded into the second level of contexts. In this sense, it suggests that both the London and the Beijing areas have the different discontinuities found between the two levels of contexts, and those areas therefore can be characterised and differentiated according to their metric relationships to the two levels of contexts.

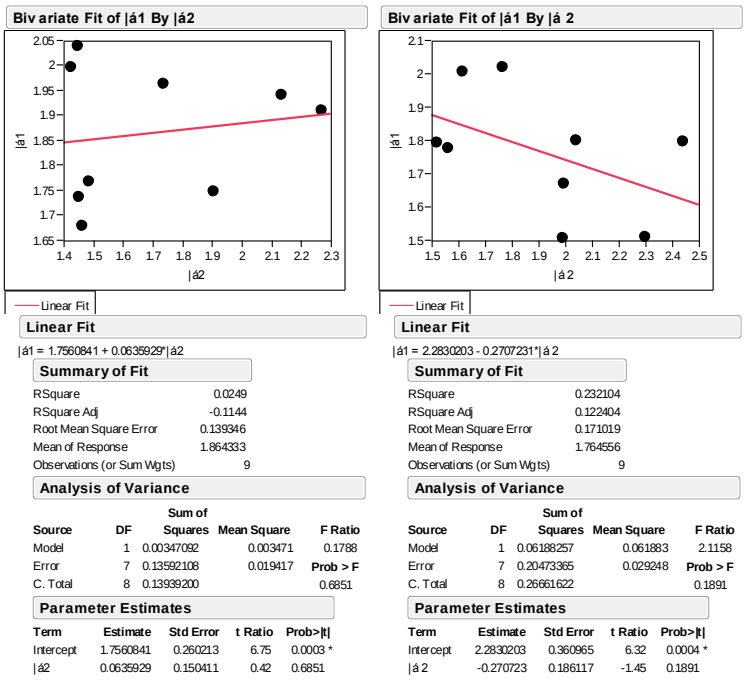

Left: No correlation between the first and the second exponents in the London case;

Right: a very weak correlation between the first and the second exponents in the Beijing case.

Fig. 5.14 The Correlations between the First and the Second Metric Exponents in London and Beijing Respectively (based on the segment maps).

In this sense, it can be argued that the multi-scale contexts of those named areas (besides their internal layouts) need to be taken into account when spatially describing those areas. This leads

to a question: *can we simulate those named areas in relation to their contexts?* To tackle this question might allow us to visualise the spatial formation of those named areas from the point of view of the continuous spatial network as a whole.

5.4 Do the created patches relate to the named areas?

Since the previous chapter demonstrated that the periodic patchwork patterns – in which the patches are surrounded by the discontinuities where the syntactic values change significantly – can be mathematically created in the cases of London and Beijing, we then moved to investigate whether the named areas in the two cases correspond to the created patches. The previous chapter revealed that the variables of metric embeddedness pace and metric mean depth (MMD) generate a much stronger patchwork phenomenon than topo-embeddedness pace, and further experiments confirmed this, so that this section focuses on the patches generated by metric embeddedness pace and MMD respectively.

5.4.1 The visual relationship between the named areas and the patches created by metric embeddedness pace

We first made a comparison between the named areas and the patchwork patterns generated by metric embeddedness pace. The segment models of London and Beijing were respectively indexed and coloured, according to a series of metric embeddedness pace at 400m to 10,000m, with an interval scale of 400m[101]. Red indicates low values, and blue denotes high values. And then those images in the two central districts were respectively superimposed on the artificial boundaries[102] of the named areas, in an attempt to see whether the boundaries of the mathematically created patches visually correspond to the artificial boundaries of those named areas.

[101] The detailed procedure for generating the patchwork pattern regarding metric embeddedness pace was elaborated in Section 4.3.3.
[102] For the introduction of the artificial boundaries of those named areas, see section 5.2, as well as Fig.5.4 aandb.

For example, **Fig. 5.15 and 5.16**, respectively, illustrate the patchwork pattern of London and Beijing, created by the metric embeddedness pace from 1000m to 1400m, as well as the boundaries of the named areas. In London, the City is dominated by red and orange segments, Bloomsbury and Holborn mainly coloured in blue; whilst, in Beijing, Zhonggulou is roughly shaded in orange; Dongdan and Nanluguo roughly coloured in blue. To a large extent, this suggests that those areas are identified at the radius of 1000m to 1400m, but the others are not. In fact, it is clear we cannot mark out all the named areas at the same time at a fixed radius range (**Fig. D1.1a-g and D1.2a-i, Appendix D**). Then, we continued to investigate whether some areas might be identified by certain radius.

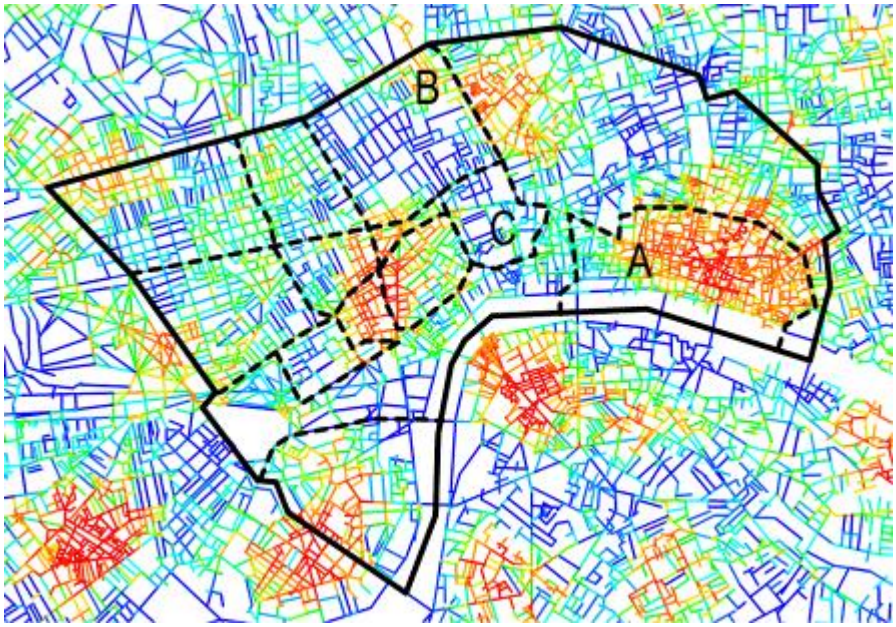

Fig. 5.15 The Patchwork Pattern Generated by Metric Embeddedness pace from 1000m to 1400m and Superimposed by the Artificial Boundaries of the Named Areas of London. Three areas are approximately picked out: A) the City; B) Bloomsbury; C) Holborn.

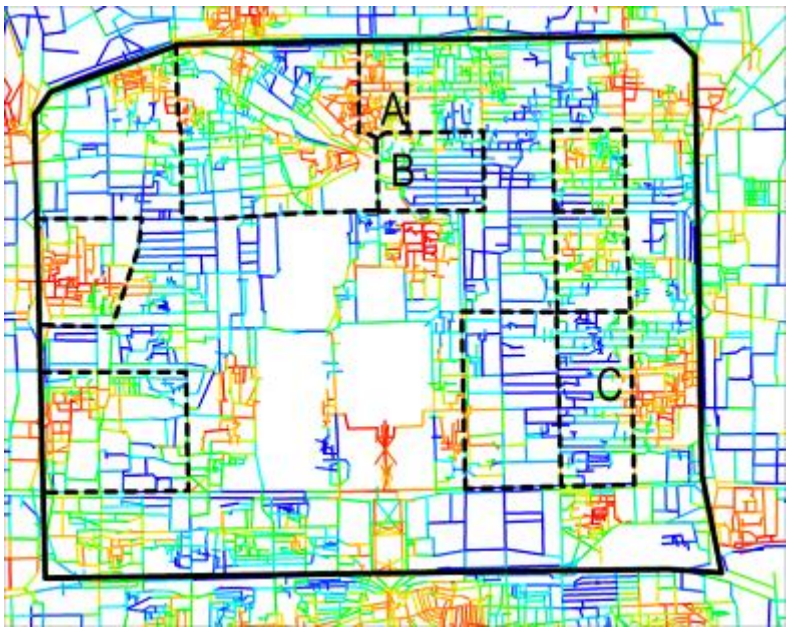

Fig. 5.16 The Patchwork Pattern Generated by Metric Embeddedness pace from 1000m to 1400m and Superimposed by the Artificial Boundaries of the Named Areas of Beijing.

Four areas are approximately picked out: A) Zhonggulou; B) Nanluogu; C) Dongdan.

As **Fig. 5.17** illustrates, several London areas are distinguished at some certain radii. St. James's, Covent Garden and Soho are *roughly* marked out at the radius of 700m to 1100m, although not perfectly; Westminster picked out at the radius of 1900m to 2300m. However, Marylebone and Mayfair are not distinguished at any radius, because several smaller patches constantly remain within, or extend beyond, their boundaries across radii.

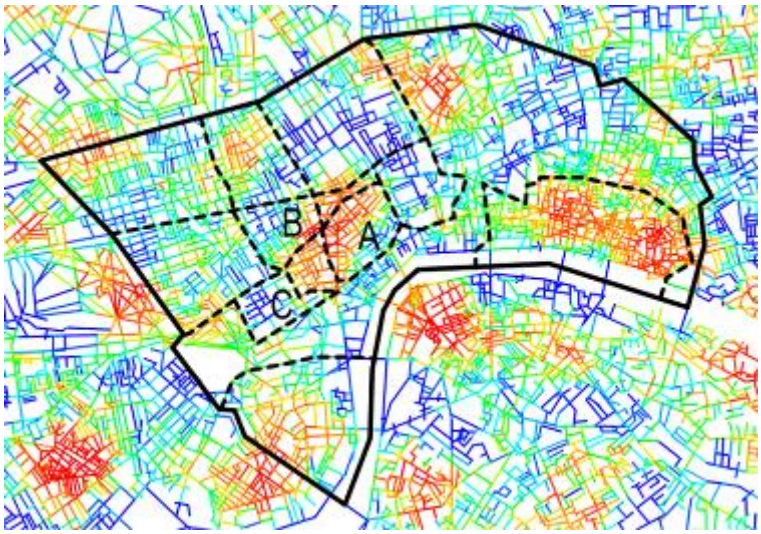

a. Covent Garden (A), Soho (B) and St. James's (C) were *roughly* marked out by metric embeddedness pace from 700m to 1100m.

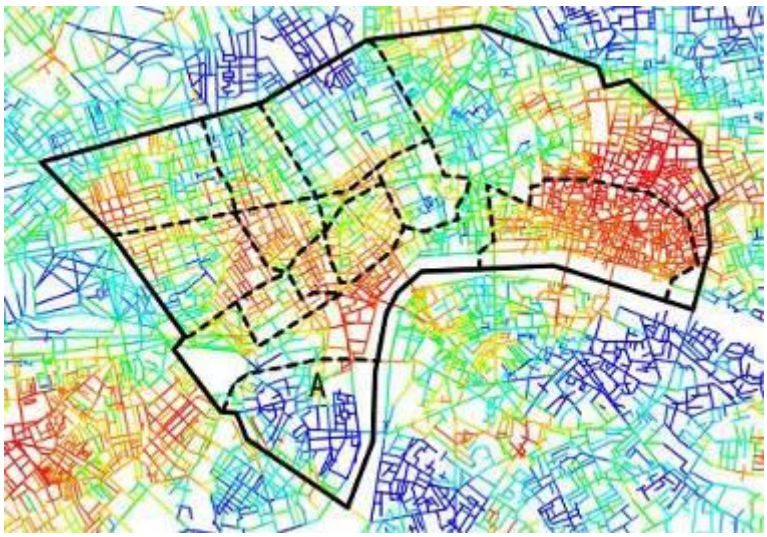

b. Westminster (A) was roughly picked out by metric embeddedness pace from 1900m to 2300m.

Fig. 5.17 Other London Areas Distinguished by Metric Embeddedness pace at Different Radii.

And several Beijing areas also co-incide with the patches produced at some radii (**Fig. 5.18**). Xingtaicang is roughly distinguished at the radius 1400m to 1800m; Dongsi almost picked out at the radius of 2000m to 2400m; Wangfujing approximately identified at the radius of 2100m to 2500m; Fengsheng roughly marked out at the radius of 3600m to 4000m. But there is an outlier of Shichahai.

a. Whitepagoda (A) was roughly picked out by metric embeddedness pace from 800m to 1200m.

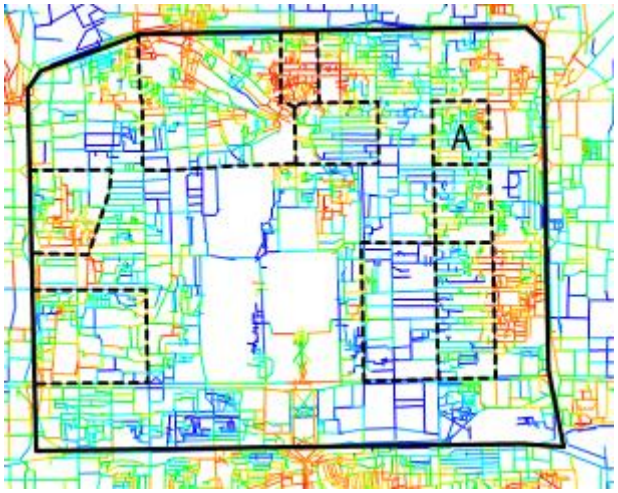

b. Xintaicang (A) was roughly picked out by metric embeddedness pace from 1400m to 1800m.

c. Dongsi (A) was roughly picked out by metric embeddedness pace from 2000m to 2400m.

d. Wangfujing (A) was roughly picked out by metric embeddedness pace from 2100m to 2500m.

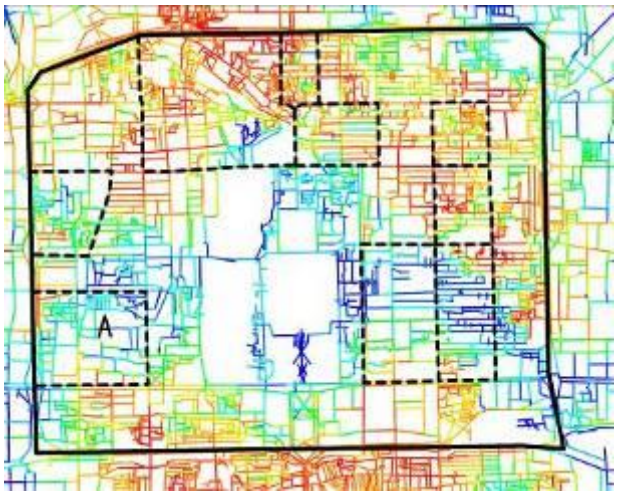

e. Fengsheng (A) was roughly picked out by metric embeddedness pace from 3600m to 4000m.

Fig. 5.18 Other Beijing Areas Distinguished by Metric Embeddedness pace at Different Radii.

The above analysis demonstrates that the London areas (except for Marylebone and Mayfair) and the Beijing areas (except for Shichahai), more or less, have a kind of visual relationship with the patches created by the metric embeddedness pace at certain radii, although not perfectly. It might be suggested that those named areas, roughly associated with the created patches, are not identified at the same scale, but emerge at the different scales.

As for the outliers in those two cases, do the smaller patches found within their boundaries have any meaning? We first present an analysis of the London case. As **section 5.2** indicated, the

area in which Mayfair and Marylebone now occupy was firstly developed between the 17th century and the mid 19th century by various landlords (see **Fig. 5.2**). Marylebone was more or less divided into east and west sections with Marylebone High Street dissecting the two. The west part was mainly constructed by the Portman family, but the east part managed by Howard de Walden. Mayfair, to a large extent, was partitioned into four parts by two north-south streets, New Bond Street and Berkeley Street, and two east-west streets, Mount Street and Bruton Street. The North West part was constructed by the Grosvenor Estate, the north east part built by Conduit Mead and Maddox-Pollen, the south west part developed by the Berkeley Estate, Curzon, Sutton and Audley, and the south east part erected by Burlington[103] (Clout, 1986; GLC, 1969).

The smaller patches generated at the radius of 2600m to 3000m within Marylebone, displayed in **Fig. 5.19a**, demonstrate that Marylebone was roughly divided into east and west parts, which almost corresponded to the historic estate developments whose boundaries are denoted by doted black lines. And the smaller patches produced at the radius of 1000m to 1400m within Mayfair, shown in **Fig. 5.19b**, also approximately suggest the four historical estates developed separately by Grosvenor, Berkeley, Burlington, and Conduit Mead (their boundaries are outlined by dotted lines in **Fig. 5.19b**). This then suggests that Marylebone and Mayfair are spatially divided into the different parts in relation to their surroundings, which in fact has some degree of correspondence to their historic developments initiated by the different estate agencies.

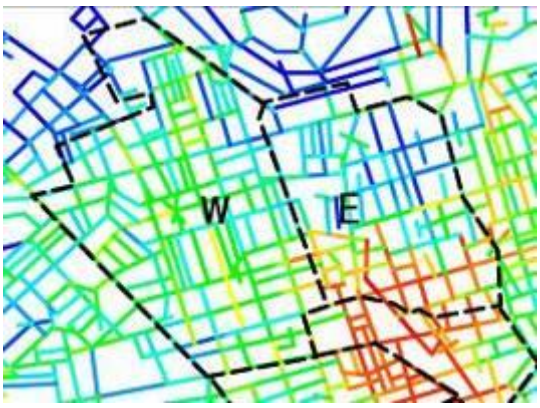

Fig. 5.19a The Patches Generated by Metric Embeddedness pace from 2600m to 3000m in Marylebone of London. The west part of Marylebone is denoted by W; the east part of Marylebone is indicated by E. The black doted lines represent the artificial boundaries of the east and west parts of Marylebone.

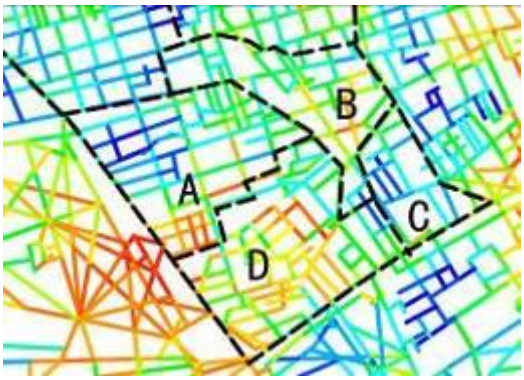

Fig. 5.19b The Patches Produced by Metric Embeddedness pace from 900m to 1300m in Mayfair of London. A, B, C and D denote the four historic estates developed in Mayfair; and the black doted lines represent the artificial boundaries of those historic estates.

In Shichahai, as an outlier of Beijing, there were two gated quarters, called 'Fang' in Chinese, built up within and around this area, according to the grand scheme proposed around 1435[104] (Liu, 1988). Those gated quarters - named Cradle Fang on the bottom, Loyalty of Sun Fang on the top - were marked out by black dotted lines in **Fig. 5.20**. The patches created at the radius of 1600m to 2000m visually correspond to the boundaries of those two gated quarters (**Fig. 5.20**). This also demonstrates that Shichahai is spatially partitioned into two parts regarding

[104] For detail, see Appendix C.

their relations to the surroundings, which reflects the historic gated quarters within the area of Shichahai. It implies that the historic boundaries of those two gated quarters might be investigated by exploring the relationship between the internal and the external at certain radius.

Fig. 5.20 The Patches Produced by Metric Embeddedness pace from 1600m to 2000m in Shichahai of Beijing. A and B denote the historic gated quarters in Shichahai, and the black doted lines represent the artificial boundaries of those gated quarters.

However, the smaller patches representing the historic developments within the three outlier areas are separately merged into their surroundings with an increase radius, but do not form any larger patches co-inciding with those three outliers. This indicates that the technique of metric embeddedness pace can *not* be applied to simulate those three outliers as a whole. However, it implies that the historic estates within Marylebone and Mayfair as well as the historic gated quarters in Shichahai perhaps have a better relationship with the contexts of those three outlier areas, rather than the internal developments within each outlier area. In this sense, this technique still can be used to investigate smaller parts within those outlier areas.

5.4.2 The visual relationship between the named areas and the patches created by metric mean depth (MMD)

Then we move to visually compare those named areas with the patches created by MMD. Following the procedure we followed in the last section, the patchwork patterns were created by

MMD at 400m to 10,000m, respectively, and superimposed on the artificial boundaries of the named areas. As before, red indicates low values, and blue denotes high values.

For example, **Fig. 5.21** shows the patchwork pattern of London created at 1400m, and **Fig. 5.22** displays the patchwork pattern of Beijing generated at 1500m. At first sight, as with metric embeddedness pace, the patches created by MMD at a fixed radius (either 1400m or 1500m) seem not to correspond to the named areas all at once. And the observation of all the other images (**Fig. D1.3a-g and D1.4a-g, Appendix D**) supports this point. However, **Fig. 5.21** shows that the City is mainly coloured in red and orange, Bloomsbury is mostly shaded in dark blue, and Holborn more or less occupied by the cyan segments. **Fig. 5.22** illustrates that Zhonggulou is roughly coloured in red and orange, and almost all of Nanluogu is shaded in blue. This indicates that these two Beijing areas are roughly marked out at 1500m.

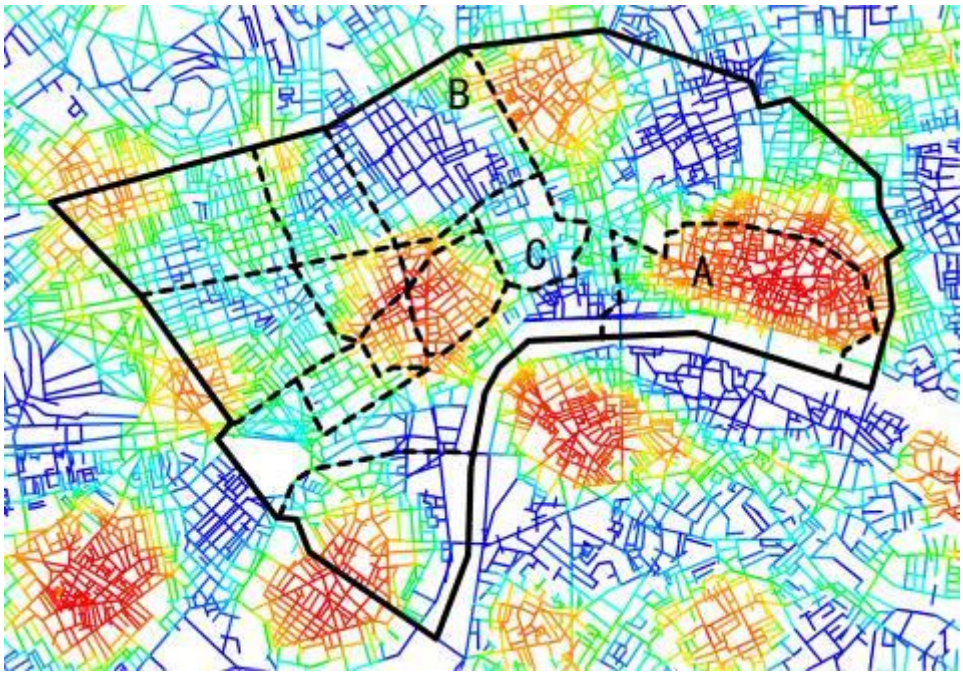

Fig. 5.21 The Patchwork Pattern Generated by MMD R1400 in London and Superimposed by the Artificial Boundaries of the Named Areas of London. Three areas are approximately identified: A) the City; B) Bloomsbury; C) Holborn.

Fig. 5.22 The Patchwork Pattern Generated by MMD R1500 in Beijing and Superimposed by the Artificial Boundaries of the Named Areas of Beijing. Two areas are approximately identified: A) Zhonggulou; B) Nanluogu.

Compared to the study of metric embeddedness pace in the previous section, most of the named areas in the two cases also co-incide with the patches created by MMD at certain radii (see **Fig. 5.23 and 5.24**). In London, St. James's is visually identified at 1400m; Soho and Covent Garden roughly marked out at 1200m; Westminster picked out at 2500m. The outliers still are Marylebone and Mayfair. In Beijing, Whitepagoda and Dongsi are approximately distinguished at 1700m; Xintaicang and Dongdan almost marked out at 1900m; Wangfujing roughly identified at 2500m; Fengsheng more or less picked out at 3700m. Shichahai however is not picked out across radii. The above outlier areas are the same as the outliers found in the previous section.

a. St. James's (A) was roughly picked out by MMD R1000.

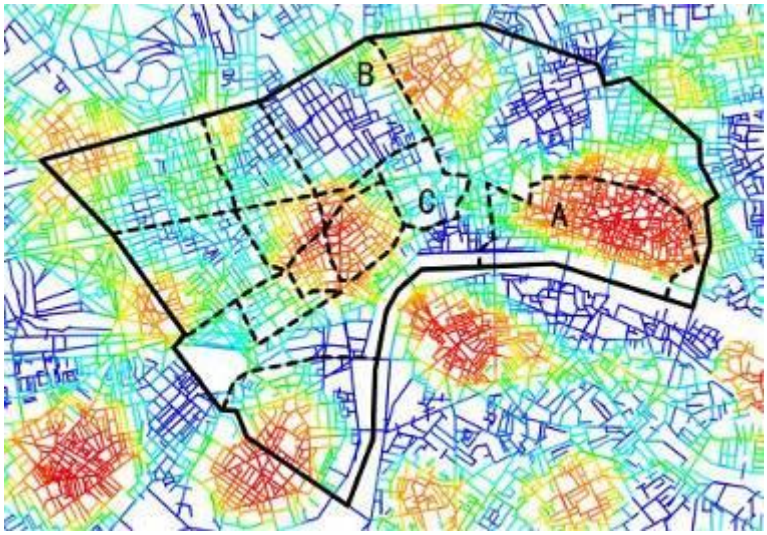

b. The City (A), Bloomsbury (B) and Holborn (C) were roughly picked out by MMD R1400.

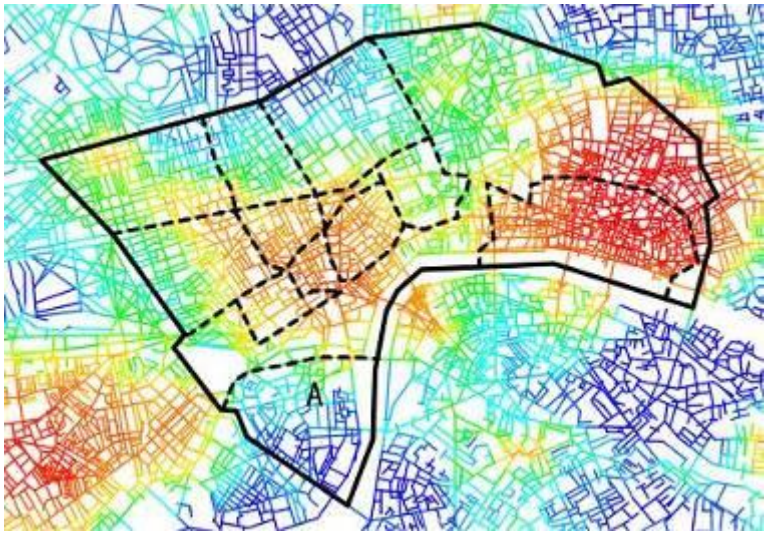

c. Westminster (A) was roughly picked out by MMD R2500.

Fig. 5.23 Other London Areas Distinguished by MMD at Different Radii.

a. Whitepagoda (A) and Dongsi (B) were roughly picked out by MMD R1700.

b. Xintaicang (A) and Dongdan (B) were roughly picked out by MMD R1900.

c. Wangfujing (A) was roughly picked out by MMD R2500.

Fig. 5.24 Other Beijing Areas Distinguished by MMD at Different Radii.

As for the outliers of London, the east and west parts[105] of Marylebone approximately co-incide with the smaller patches created by MMD at 2200m; and those four historical estates[106] of Mayfair roughly correspond to the smaller patches generated at 1200m (**Fig. 5.25a and b**). As for the outlier of Beijing, the two historical gated quarters[107] of Shichahai are almost picked out at 1900m (**Fig. 5.25c**). The historic developments within these outliers also can be differentiated by MMD at certain radii. And meanwhile, these historic developments will be merged into the surroundings of the outlier areas at some larger radii. This also implies that they are more metrically *related to* the contexts of the outlier areas rather than their neighbouring developments.

[105] See the previous comparison between the named areas and metric embeddedness pace at the beginning of Section5.4.1, or see both Section 5.2 and Appendix C.
[106] Ibid.
[107] Ibid.

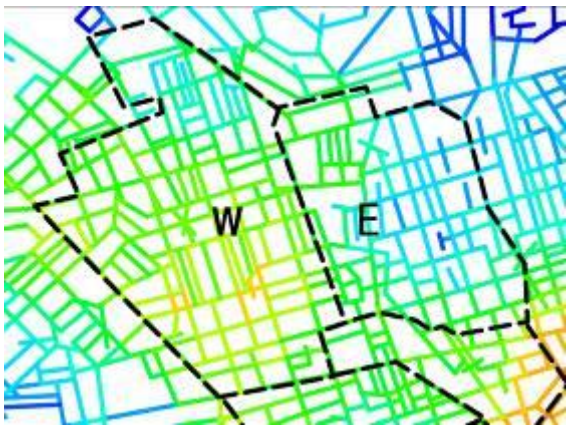

Fig. 5.25a The Patches Generated by MMD R2200 in Marylebone of London. The west part of Marylebone is denoted by W; the east part of Marylebone is indicated by E. The black doted lines (in fact Marylebone High Street) represent the artificial boundaries of the east and west parts of Marylebone.

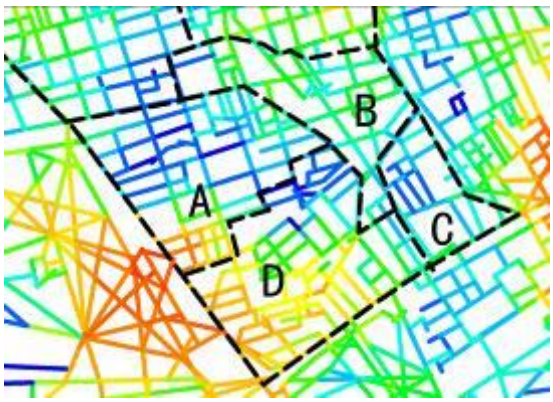

Fig. 5.25b The Patches Produced by MMD R1200 in Mayfair of London. A, B, C and D denote the four historic estates developed in Mayfair; and the black doted lines represent the artificial boundaries of those historic estates.

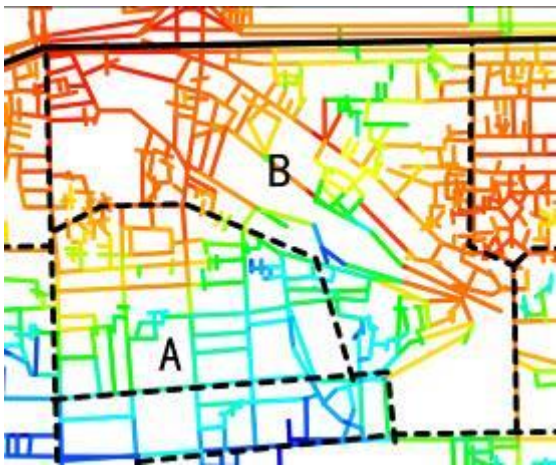

Fig. 5.25c The Patches Produced by MMD R1900 in Shichahai of Beijing. A and B denote the historic gated quarters in Shichahai, and the black doted lines represent the artificial boundaries of those gated quarters.

To a large extent, and with the careful qualifications described, the above analysis suggests that the patchwork patterns created by MMD at different radii also can to some degree be used to distinguish those named areas. It also confirms that the named areas are spatially identified at different radii rather than a fixed radius. This suggests that the way in which they are metrically integrated into the different scaled contexts does relate in some way to the spatial emergence of the named areas (which will be further investigated in next section). In general, it can be argued that the periodic patchwork patterns generated by MMD (as with those produced by metric embeddedness pace) offer a useful spatial framework of investigating the spatial structuring of those named areas.

5.5 What is the spatial mechanism involved in the formation of the named areas?

5.5.1 The peak-trough patterns of the named areas

So next, we sought to investigate how geometric and metric properties of those named areas influence, or even determine, the spatial formation of those areas in the two cities. The previous chapter showed that the periodic patchwork patterns created by MMD can be transformed into the peak-trough patterns by using the technique of the mountain scattergram (plotting MMD at

any fixed radius against MMD at the infinite radius) [108], and this provides a method for investigating the metric integration pattern of any named area at a local radius, in relation to the metric integration pattern of the whole network.

For example, the segments comprising the City of London were selected using DepthMap[109], see points highlighted in yellow (**Fig.5.22a**). We continued to create a series of mountain scattergrams by plotting the MMD Rn, on the x-axis, against the negative of MMD at the radius of k (MMD Rk), from low to high, on the y-axis[110]. At 1600m (on the y-axis), a peak (coloured in yellow) appeared for first time in the window of the scattergram (**Fig.5.26 b**). Then, we coloured the segments of the City (bounded by dotted lines in **Fig. 5.26 c**) in terms of MMD at 1600m; and meanwhile we adjusted the colour range to highlight the location of the most integrated segments within this area (because the summit of the peak denotes the lowest MMD segments, or the most metrically integrated segments). Blue indicates high MMD R1600m and red denotes low values. As **Fig. 5.26 c** show, the MMD R1600m values increase from a small group of metrically integrated segments (more or less located at the geometric centre of the City) to their surroundings, and the City itself is also surrounded by the relatively colder segments. It suggests that the City, by and large, has a metrically integrated centre gradually merged into the less integrated contexts at the radius of 1600m.

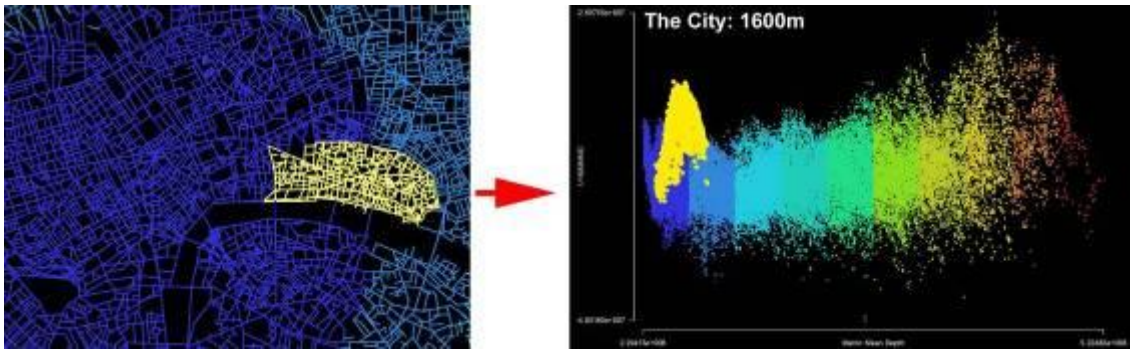

a. to select the City in the segment map

b. to show the mountain scattergram (a peak coloured in yellow)

[108] For technical details, see Section 4.6 of chapter four.
[109] For details, see A Researcher's handbook of DepthMap (Turner, 2004). http://www.vr.ucl.ac.uk/depthmap/handbook.html
[110] The more detailed procedure was elaborated in Section 4.5.

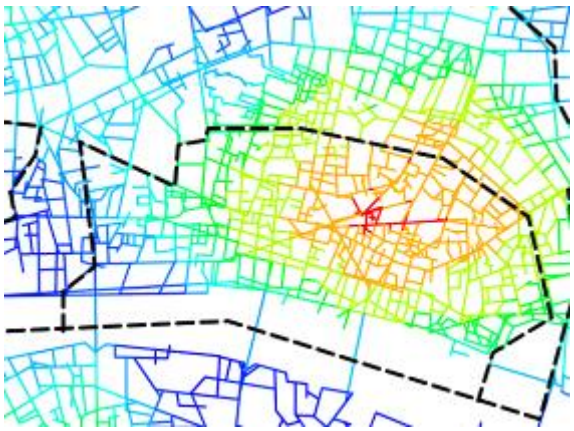

c. the segment map of the City (bounded by the dotted lines) was coloured according MMD R1600. Blue denotes high values, and red indicates low values.

Fig. 5.26 The Mountain Scattergram and the MMD R1600 Pattern of the City.

The above method was then applied to all other areas of London (**Fig. 5.27a - f**). In contrast to the City, Bloomsbury is represented as a trough at 1600m, corresponding to the MMD R1600 pattern where a small group of metrically segregated segments (coloured in blue) located at its geometric centre (**Fig. 5.27a**); and meanwhile, Bloomsbury itself seems to be surrounded by the relatively more metrically integrated segments (coloured in orange, yellow and green). This suggests that Bloomsbury, compared to the City, has no metrically integrated centre, but has more integrated edges. Holborn, Marylebone, Mayfair and Westminster are more or less denoted by troughs at 1800m, 2200m, 1600m and 2200m, respectively (**Fig. 5.27 b, c, d and e**). However, they have different spatial patterns coloured according to the MMD Rk values. In Holborn, the most metrically segregated segments are located near the geometric centre, but other segregated segments focus on its south-east corner; and Holborn itself is surrounded by metrically integrated segments only to the east, north and west. As for Marylebone, the highest MMD R2200m values diminish from the geometric centre of its eastern part (coloured in light blue) to its western part (mainly coloured in yellow) and its surrounding areas. This indicates that the most segregated spaces of Marylebone concentrate on its eastern part rather than its own geometric centre. As for Mayfair, the most segregated segments (coloured in dark blue) are located on the northern edge and the more integrated segments (coloured in yellow) are situated at the south west corner; and Mayfair itself is bounded by more integrated spaces (coloured in orange and yellow) to the east and west. As for Westminster, the most segregated

segments are found at the eastern edge (that is, the edge of Thames River), and the whole area is surrounded by more integrated segments to the other three directions (south, west and north). The above analysis suggests that the most segregated segments of those areas (denoted by the bottom end of those troughs) are not all located at the geometric centre of those areas, but they are surrounded by more integrated segments situated within or outside those areas.

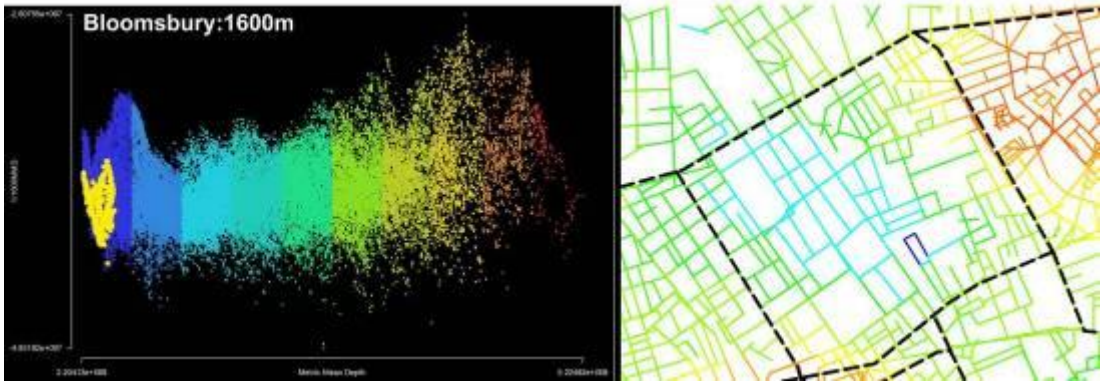

a. Bloomsbury

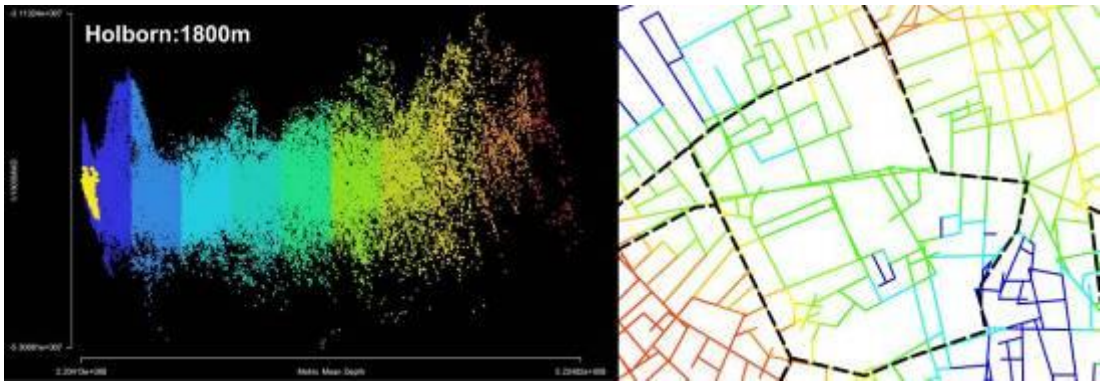

b. Holborn

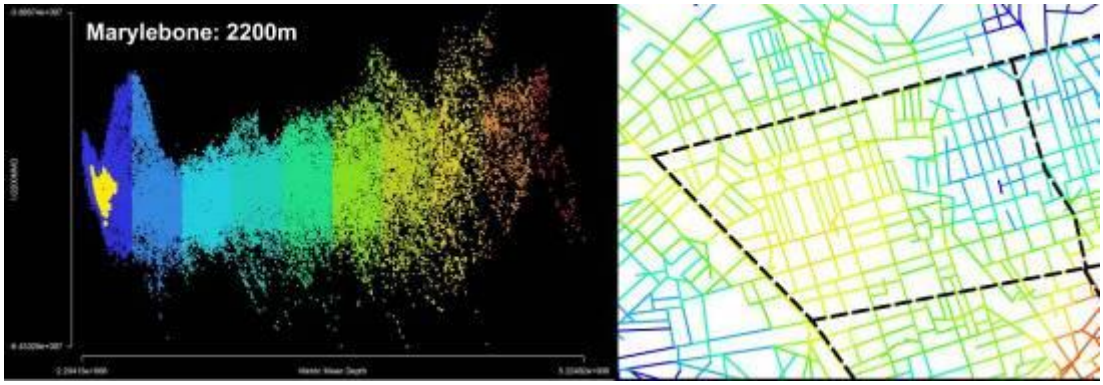

c. Marybelone

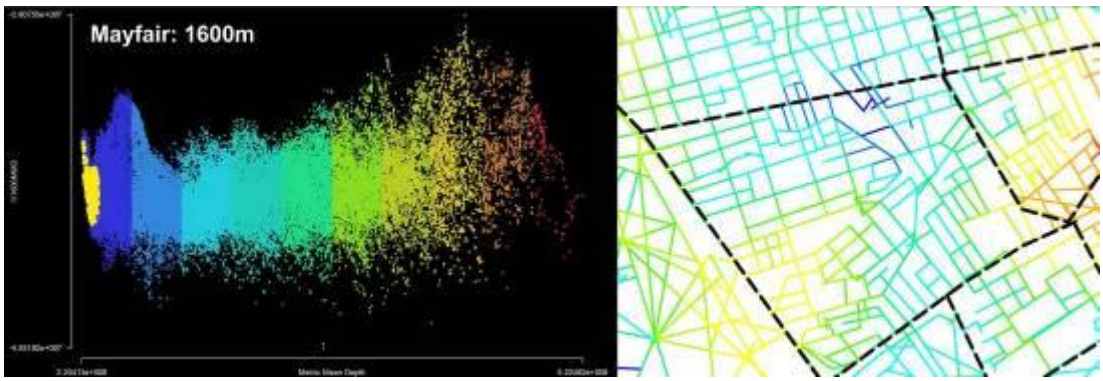

d. Mayfair

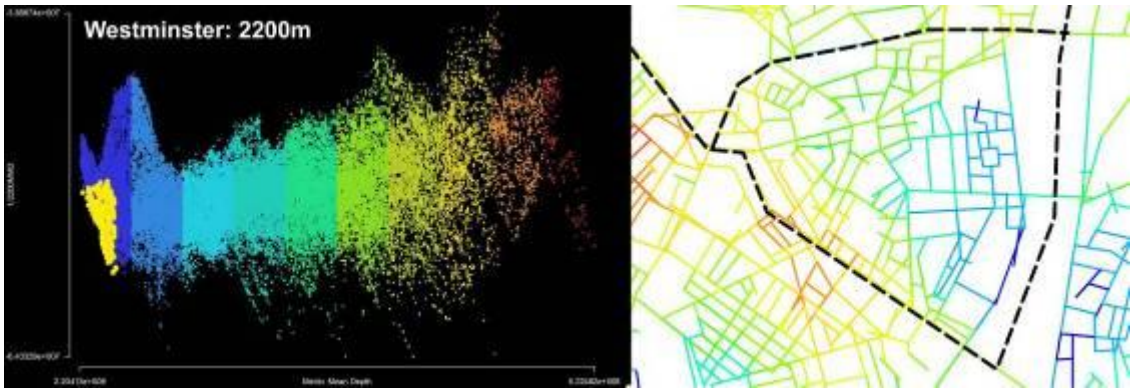

e. Westminster

Left: Yellow indicates the named areas

Right: the segment map coloured according to MMD Rk. Red denotes low value and blue indicates high value

Fig. 5.27 a-e The Mountain Scattergrams (Left) and the MMD Rk Patterns (Right) of Bloomsbury, Holborn, Marylebone, Mayfair and Westminster (Each image to the right has a slightly different colour range in order to clearly show the segments with the highest or the lowest MMD Rk values within each area, because those segments with the extreme values are surrounded by many segments with slightly lower or higher values).

And meanwhile, as with the City, the other three areas, namely Soho, St. James's and Covent Garden, are roughly represented as peaks (**Fig. 5.27 f-h**). However, the most metrically integrated segments (coloured in red or orange) of these three areas, compared to the City, are located at/near the edges. As for Soho, the lowest MMD R1800 values increase from the southern edge to the northern part; as for St. James's, the lowest MMD R1500 values rise up from the north east edge to the south west part; as for Covent Garden, the lowest MMD R1500

values increase from the south west edge to the north east part. This shows that they have more metrically integrated centres located on/near the edge rather than at the geometric centre. By and large, the above analysis suggests that the centres – in terms of metric accessibility from any places to any others – of the named areas are not necessarily arranged at their geometric centres.

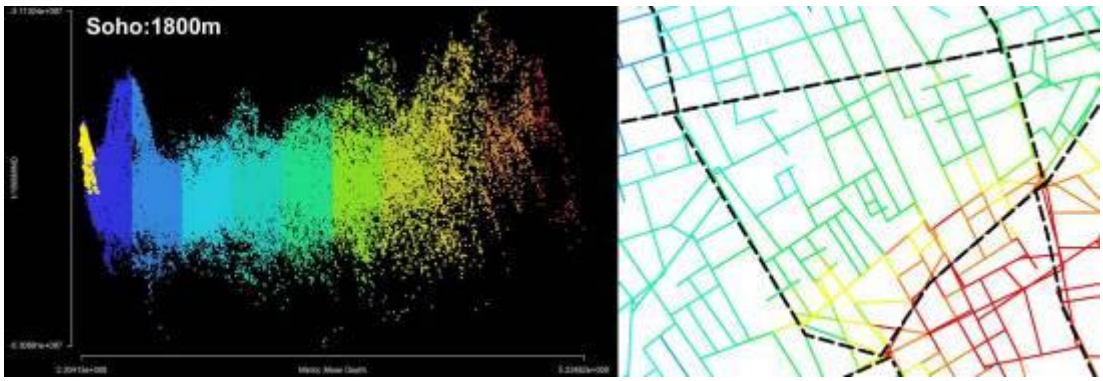

f. Soho

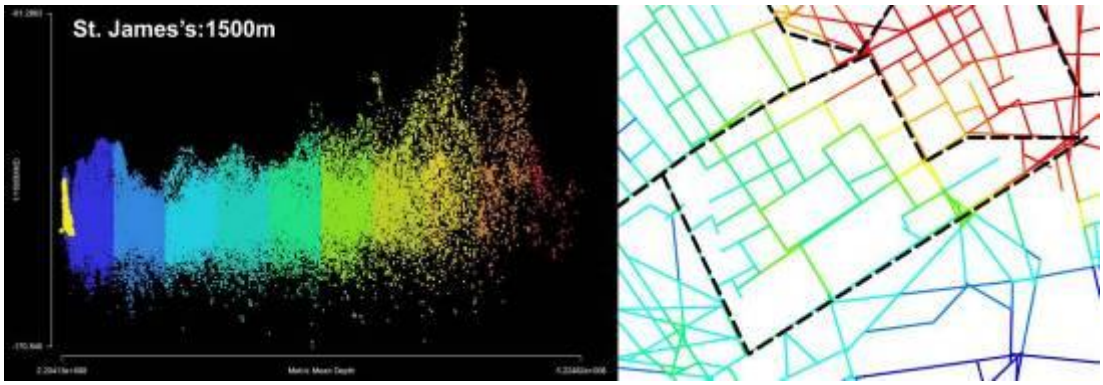

g. St. James's

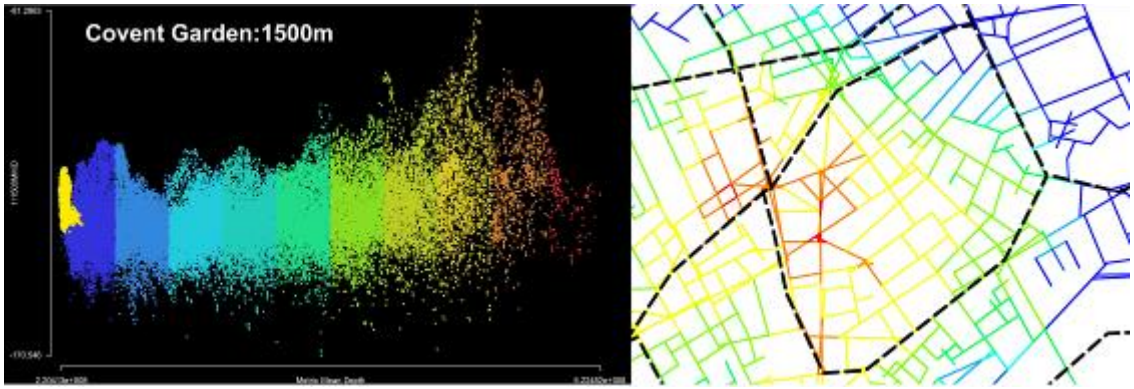

h. Covent Garden

Left: Yellow indicates the named areas

Right: the segment map coloured according to MMD Rk. Red denotes low value and blue indicates high value

Fig. 5.27 f-h The Mountain Scattergrams (Left) and the MMD Rk Patterns (Right) of Soho, St. James's and Covent Garden

We moved to examine the Beijing areas (**Fig. 5.28**). Dongdan and Nanluogu are represented as troughs at 1100m and 1000m, respectively (**Fig. 5.28 a and b**). In Dongdan, the most metrically segregated segments (coloured in blue) are located at its geometric centre; and this area is surrounded by more metrically integrated segments to the east and the south. However, in Nanluogu, the most metrically segregated segments are situated at the south east corner; and this area is bounded by more integrated segments to the south, west and north.

The other Beijing areas are more or less denoted as peaks, but their MMD Rk patterns are not the same (**Fig. 5.28 c-g**). As for Dongxi and Xingtaicang, a small group of the most metrically integrated segments are situated at their geometric centres, and the MMD Rk values increase from the centre to the edge (**Fig. 5.28 c and d**). As for Whitepagoda, the most metrically integrated segments are, however, found near the western edge; and meanwhile this area is surrounded by more metrically segregated segments (**Fig. 5.28 e**). As for Wangfujing, Fengsheng and Zhonggulou, the most metrically integrated are also situated on one of their edges, and the MMD Rk values increase from their metrically integrated centres to the surroundings (**Fig. 5.28 f, g and h**). As for Shichahai, the most metrically integrated segments are located at the geometric centre of its north east part, and its south west part is dominated by the metrically segregated segments (**Fig. 5.28 i**). The above analysis shows the possibility that the metrically integrated centres of those areas, represented as the summit of the peaks, can be located at the different parts of those areas; however the MMD Rk values would always increase from the metrically integrated centres to the surroundings.

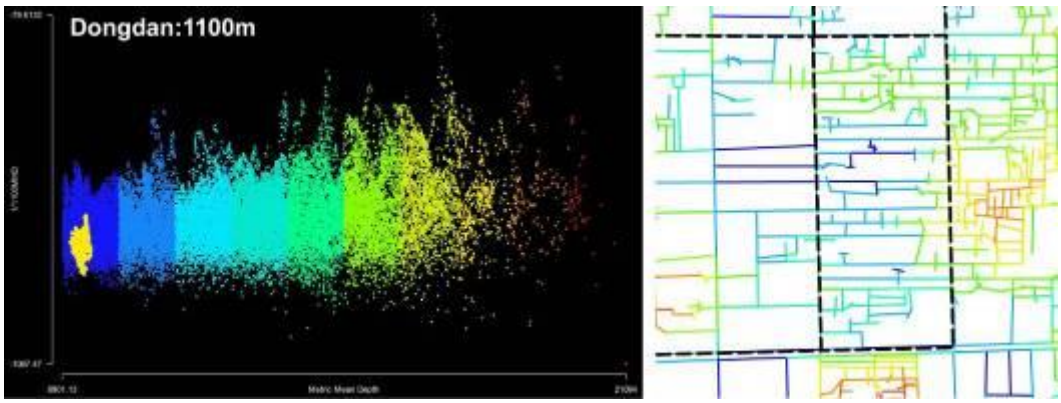

a. Dongdan

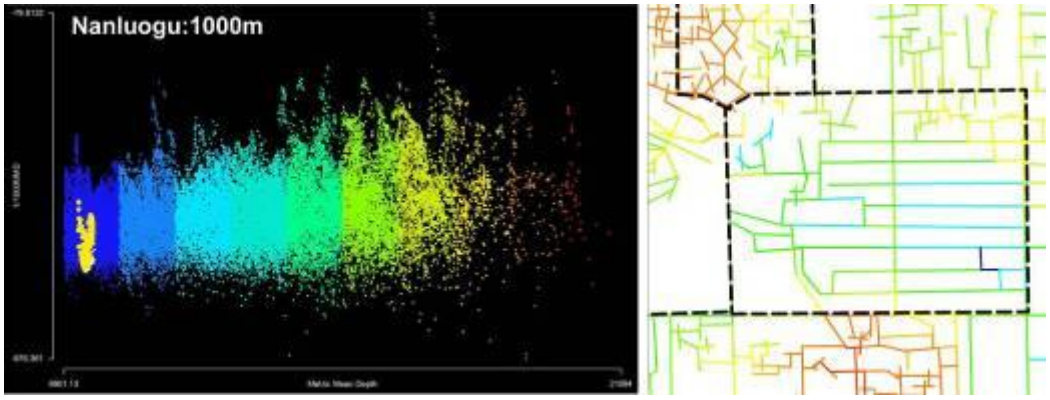

b. Nanluogu

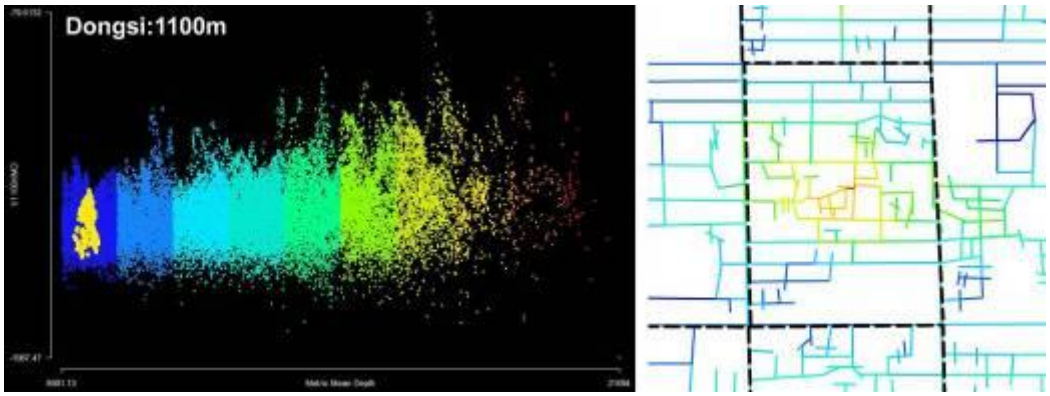

c. Dongsi

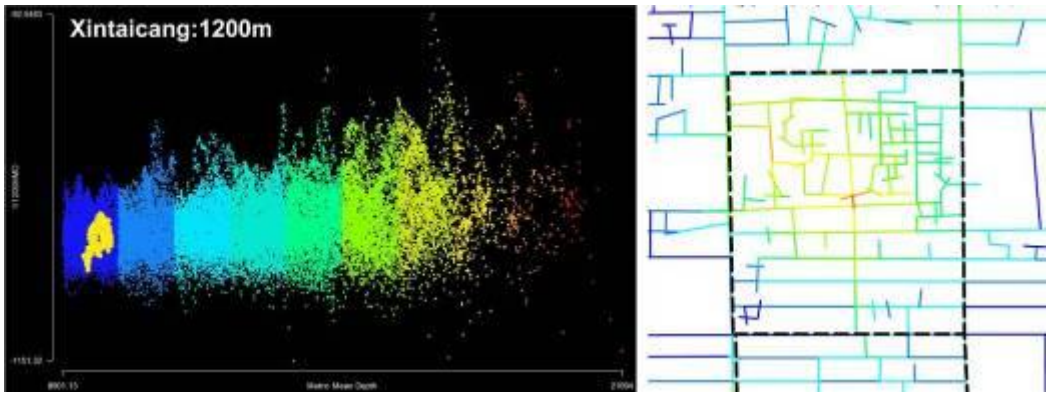

d. Xingtaicang

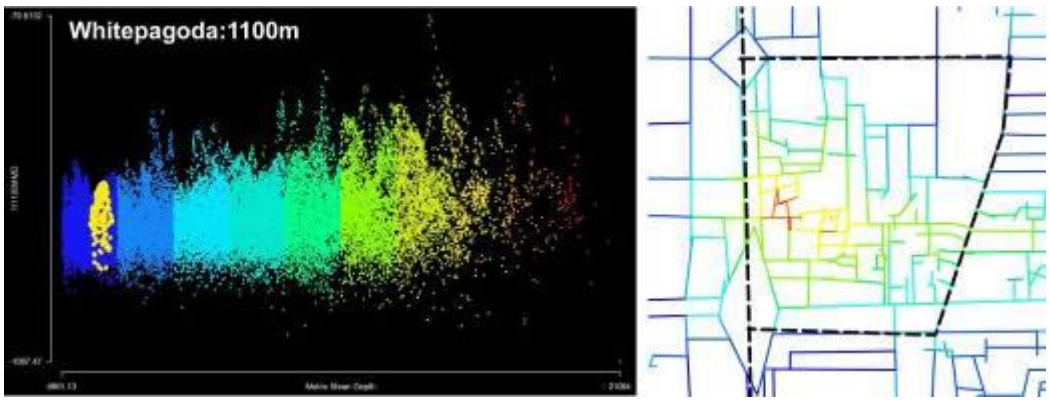

e. Whitepagoda

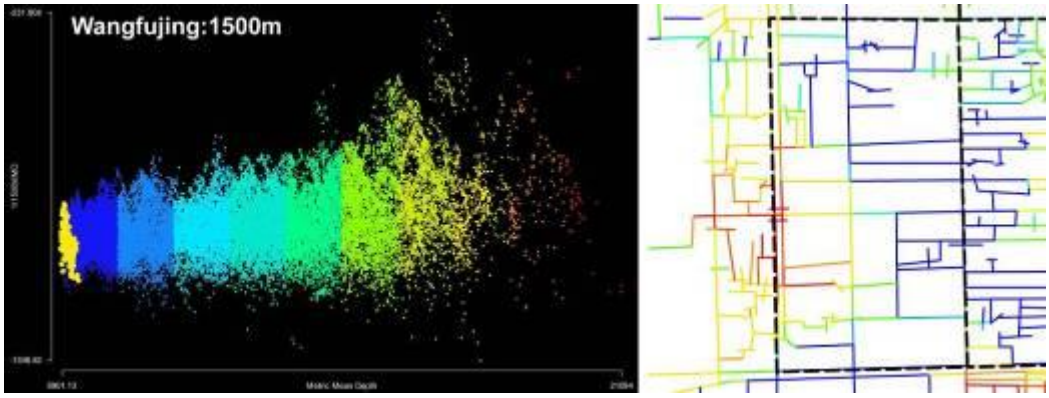

f. Wangfujing

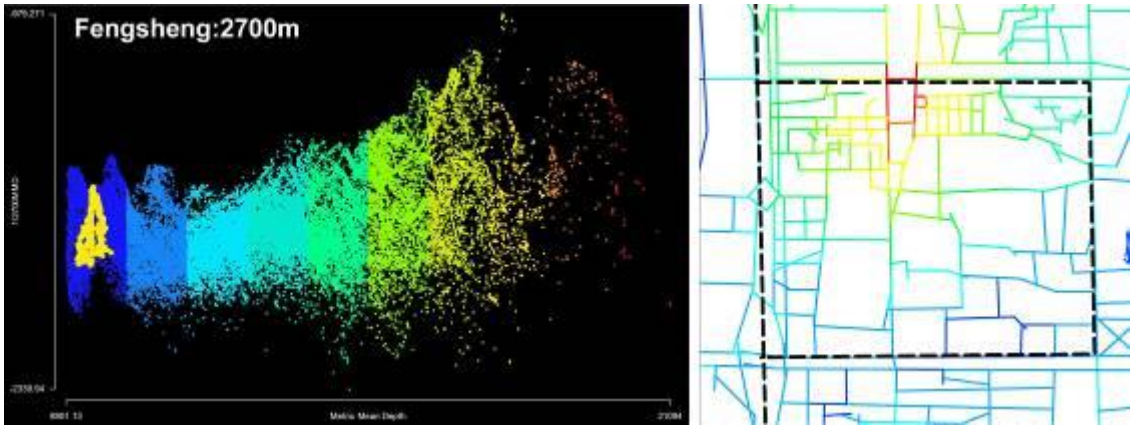

g. Fengsheng

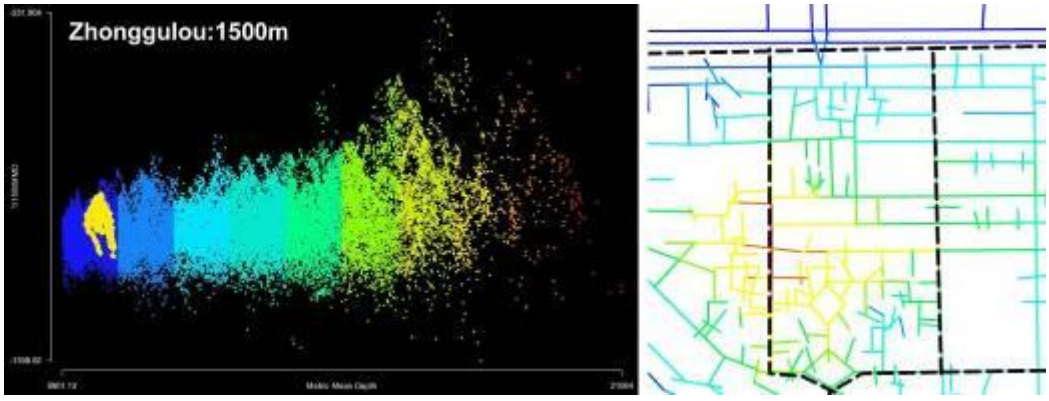

h. Zhonggulou

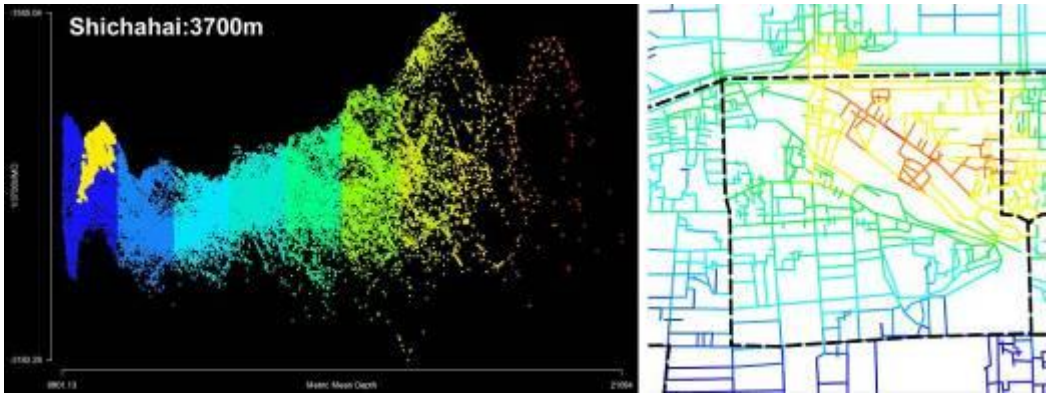

i. Shichahai

Left: Yellow indicates the named areas

Right: the segment map coloured according to MMD Rk. Red denotes low value and blue indicates high value

Fig. 5.28 The Mountain Scattergrams and the MMD Rk Patterns of the Beijing Areas.

In general, it can be demonstrated that *the named areas in London and Beijing can be classified into two types of areas according to their representations in the mountain scattergrams*. Roughly speaking, the peak suggests that the corresponding area has a metrically integrated centre (though not necessarily located at the geometric centre of internal layout); but the trough implies that the corresponding area, without a strong metrically integrated centre, is surrounded by the metrically integrated edge. This might relate to the spatial formation of the named areas. Some named areas, such as the City of London, are formed around a strong geometric centre; but some named areas, such as Bloomsbury, are surrounded by more intensively developed surrounding areas.

5.5.2 The peak-trough patterns of the created patches

So next, we investigated whether each patch created by MMD at a fixed radius, regardless of named areas, would correspond to a peak or a trough produced in the mountain scattergram at the same radius, in order to further explore the geometric and metric mechanism for generating the patches that are associated with the named areas. For example, we created the patchwork

pattern of the central district of London at 1400m (**Fig. 5.29-1**), because this pattern does not seem, intuitively, to generate too small or too large patches. We then selected all the six red patches (from R1 to R6) within the north part of Central London, shown in **Fig. 5.29-1**, and plotted the mountain scattergrams of the MMD R1400 against the MMD Rn. For example, as **Fig. 5.29-2** shows, we selected a red patch (denoted as R1 in **Fig. 5.29-1**) in the segment map (**Fig. 5.29-2 Left**), and then created the mountain scattergram to see how the points denoting R1 are distributed (**Right**). **Fig. 5.29-2-7** respectively demonstrate that six red patches are approximately represented as peaks in the mountain scattergrams. And meanwhile, all the five blue patches within the north part of Central London were also selected to produce the mountain scattergrams respectively (**Fig. 5.30**). These five blue patches are approximately denoted as troughs.

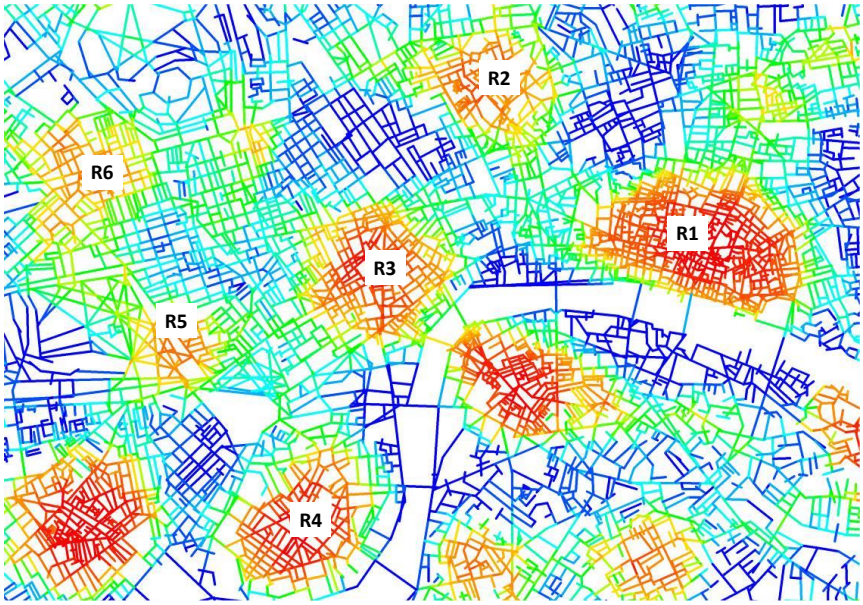

1. The periodic patchwork pattern created by MMD R1400 for London. R1, R2, R3, R4, R5 and R6 denote six red patches that would be investigated.

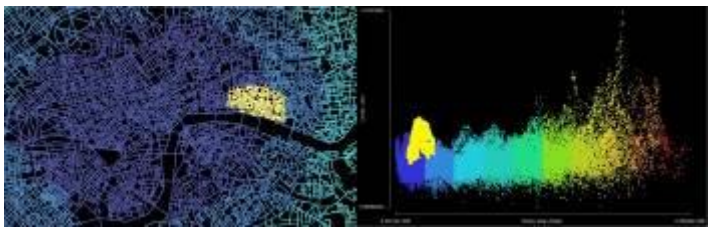

2. **R1** shown as a peak in the mountain scattergram.

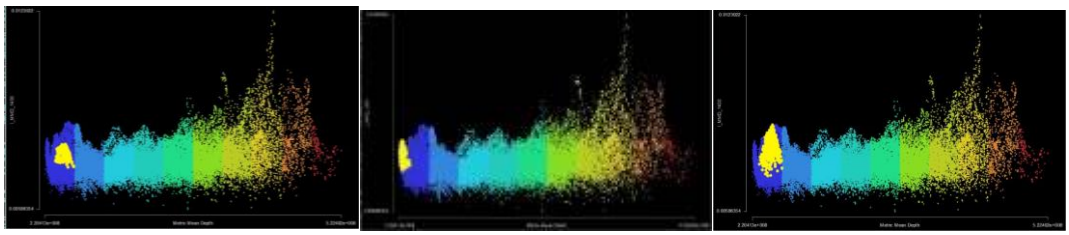

3. **R2** shown as a peak 4. **R3** shown as a peak 5. **R4** shown as a peak

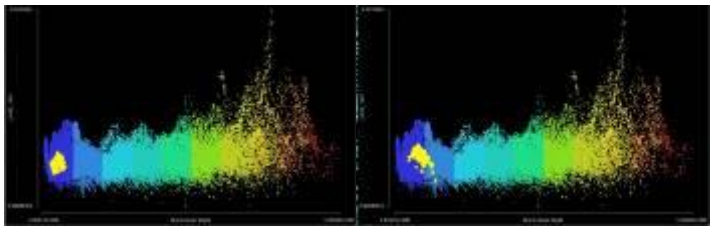

6. **R5** shown as a peak 7. **R6** shown as a peak.

Fig. 5.29 Six Red Patches Displayed as Peaks in the Mountain Scattergram for the London Case. Six red patches were created by the MMD at 1400m and the corresponding mountain scattergrams were produced by plotting the MMD R1400 against the MMD Rn,

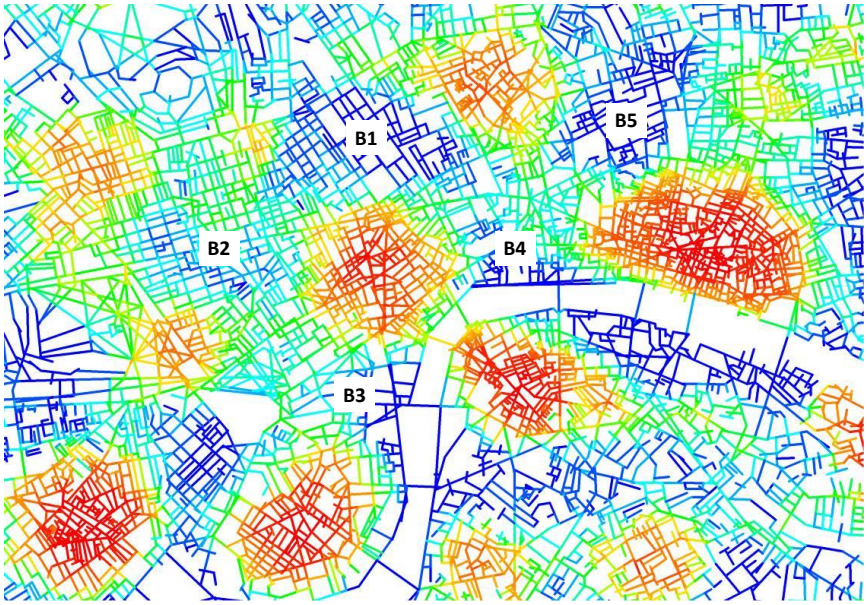

1. The periodic patchwork pattern created by MMD R1400 for London. B1, B2, B3, B4 and B5 denote five blue patches that would be investigated.

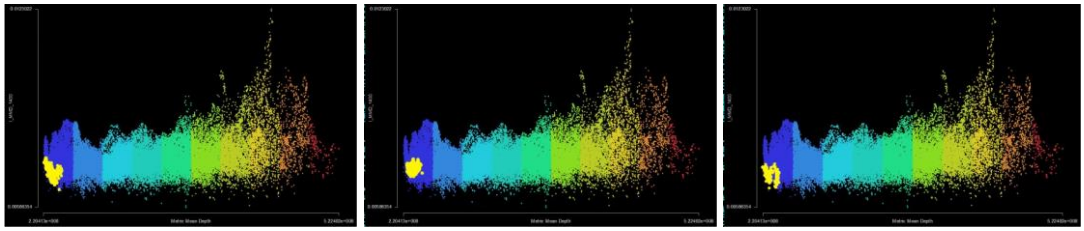

2. **B1** shown as a trough 3. **B2** shown as a trough 4. **B3** shown as a trough

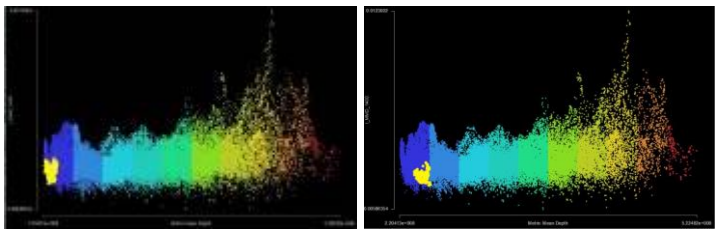

5. **B4** shown as a trough 6. **B5** shown as a trough

Fig. 5.30 Five Blue Patches Displayed as Troughs in the Mountain Scattergram for the London Case. Five blue patches were created by the MMD at 1400m and the corresponding mountain scattergrams were produced by plotting the MMD R1400 against the MMD Rn,

We further examined all the patches within the central district of Beijing. For example, **Fig. 5.31 and 5.32** respectively show that seven red patches produced at 1700m are illustrated as peaks, and six blue patches at 1700m represented as troughs, although not perfectly. In both London and Beijing, all the red patches, with lower MMD values, can be represented as peaks, and all the blue patches, with higher MMD values, denoted as troughs. This demonstrates that the red patches have a more metrically integrated centre surrounded by less integrated spaces, and meanwhile the blue patches have a more metrically segregated part encircled by more integrated spaces.

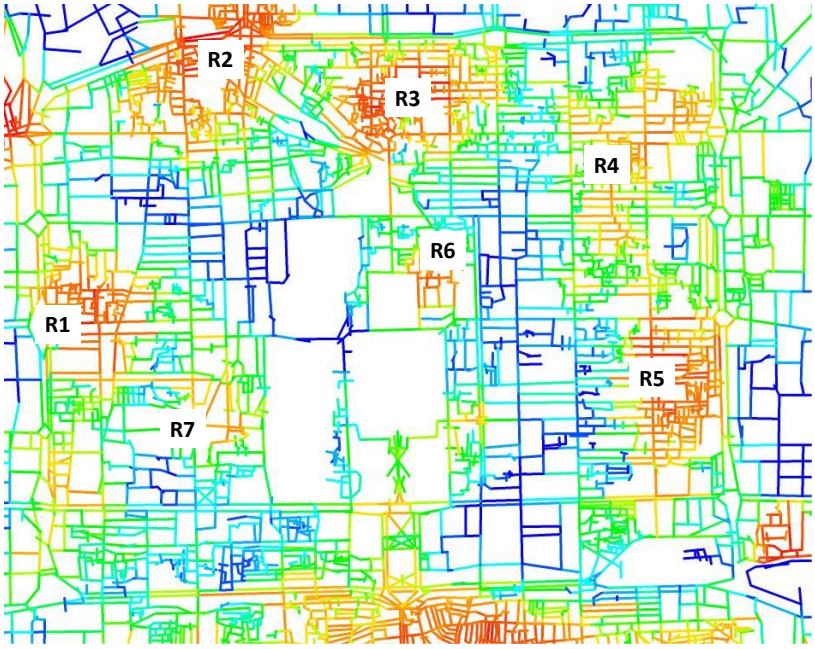

1. The periodic patchwork pattern created by MMD R1700 for Beijing. R1, R2, R3, R4, R5, R6 and R7 denote seven red patches that would be investigated.

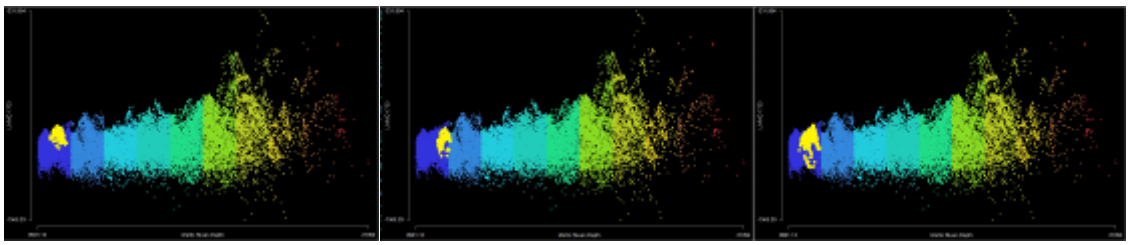

2. **R1** shown as a peak 3. **R2** shown as a peak 4. **R3** shown as a peak

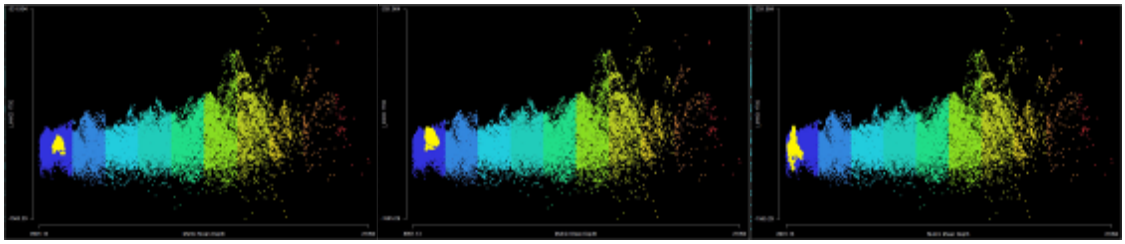

5. **R4** shown as a peak 6. **R5** shown as a peak 7. **R6** shown as a peak

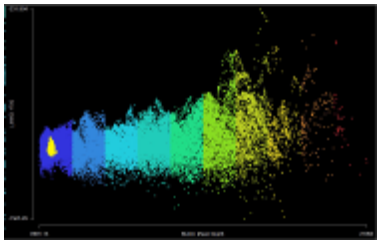

8. **R7** shown as a peak

Fig. 5.31 Seven Red Patches Displayed as Peaks in the Mountain Scattergram for the Beijing Case. Seven red patches were created by the MMD at 1700m and the corresponding mountain scattergrams were produced by plotting the MMD R1700 against the MMD Rn,

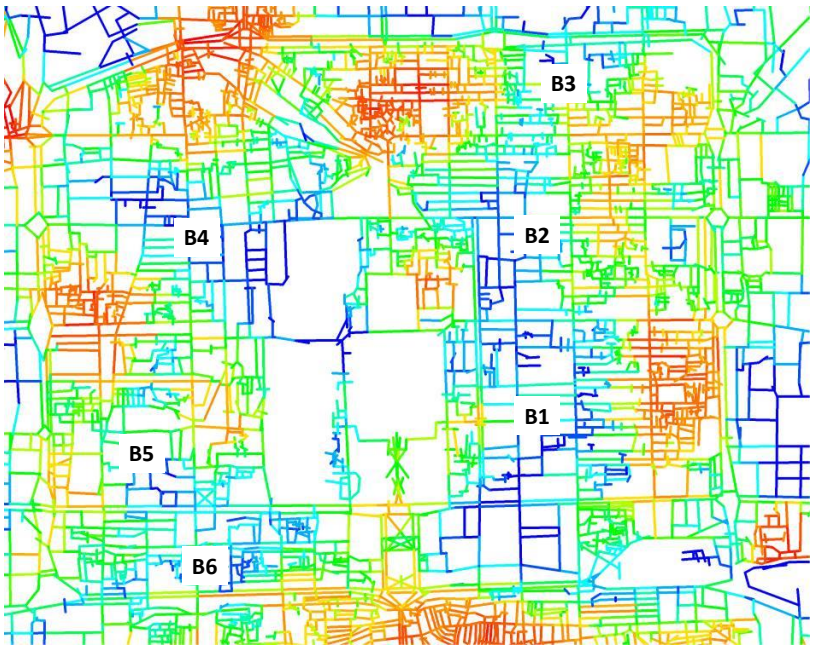

1. The periodic patchwork pattern created by MMD R1700 for Beijing. B1, B2, B3, B4, B5 and B6 denote six blue patches that would be investigated.

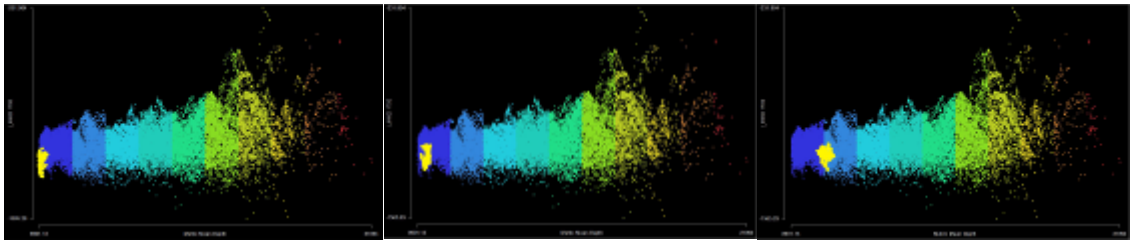

2. **B1** shown as a trough 3. **B2** shown as a trough 4. **B3** shown as a trough

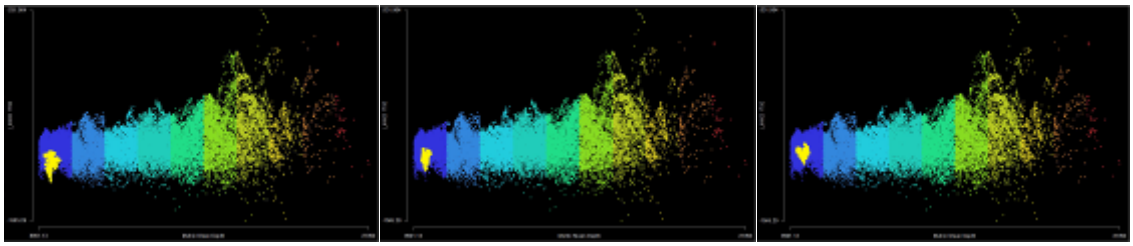

5. **B4** shown as a trough 6. **B5** shown as a trough 7. **B6** shown as a trough

Fig. 5.32 Six Blue Patches Displayed as Troughs in the Mountain Scattergram for the Beijing Case. Six blue patches were created by the MMD at 1700m and the corresponding mountain scattergrams were produced by plotting the MMD R1700 against the MMD Rn,

5.5.3 The Grid Intensification

The interpretation of the peak-trough pattern relates to Hillier's theory of grid intensification[111], which proposes the phenonmenon of city growth leading to a reduction of block size so as to reduce average metric distance from all points to all others in an urban network, as discussed in **Section 4.5**. We then sought to investigate whether the peak-trough patterns generated in the above cases have any empirical relationship with the grid intensification. When an area is occupied by smaller sized blocks, the segment map of the area in general has a larger number of shorter segments; and vice versa. And therefore, we compared the average segment length of the created patches, associated with peaks or troughs, with that of their surrounding segments involved in producing those patches, in order to explore the extent to which the created patches are intensified regarding their surroundings.

An example of a red patch of London (R1 highlighted in **Fig. 5.29-1**) was used to elucidate the method of making the above comparison. As **Fig. 5.33a** shows, we selected the segments making up R1 as the root area, and then highlighted the surrounding segments located up to 1400m away from the selected patch of R1. Since R1 (denoted by black segments in **Fig. 5.33a**) was created at 1400m, the surrounding segments within 1400m (represented by grey segments) contributed to the formation of R1. The average segment length of R1 and that of the surroundings were *visually* and *numerically* compared to achieve a better understanding of the creation of R1.

[111] For detail, see Hillier (1999) *Centrality as a process accounting for attraction inequalities in deformed grids,* Urban Design International, 3/4, 107-127.

a. The red patches (associated with peaks) as well as their surroundings in London

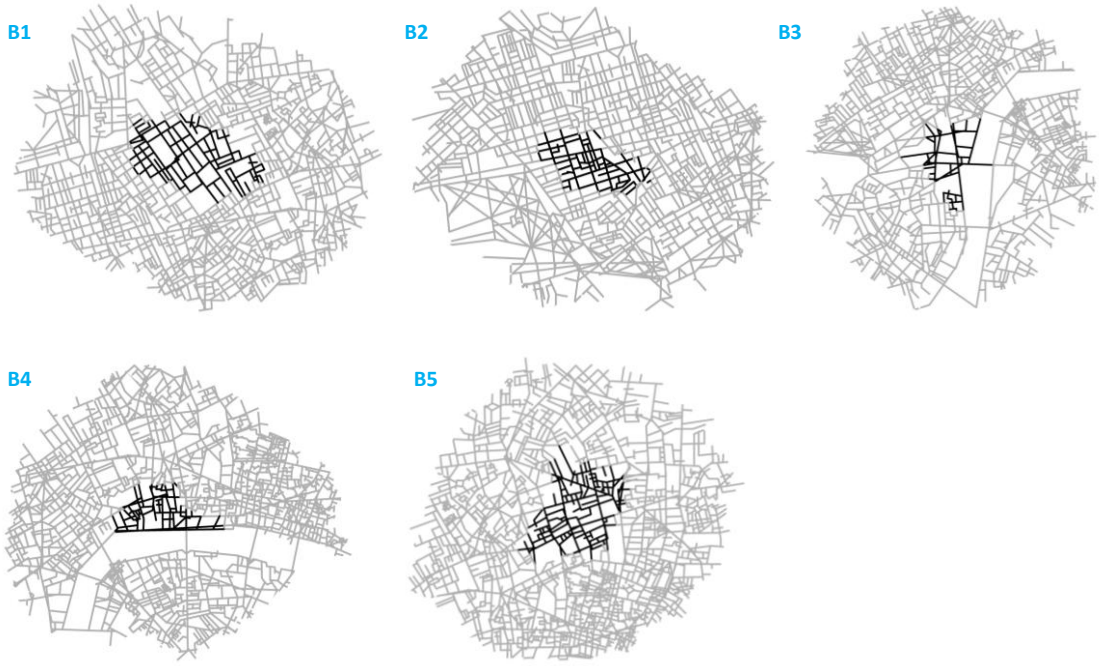

b. The blue patches (associated with troughs) as well as their surroundings in London

Fig. 5.33 The Patches Created at 1400m and Their Surroundings for the London Case. Black denotes the created patches and grey represents their surrounding segments within 1400m.

Fig.5.33 shows the red and blue patches of London (respectively displayed in **Fig.5.29 and 5.30**) as well as their surrounding segments within 1400m. At first sight, it is difficult to tell whether these created patches are more intensified than their surroundings or not, although some red patches, such as R5 and R6, seem more intensified than some parts of their surroundings (eg. parks), and some blue patches, such as B1 and B3, seem less intensified than some parts of their surroundings. However, the quantitative analysis (**Table 5.6**) indicates that all the red patches (associated with peaks) have shorter segments than their surroundings, and all the blue patches (related to troughs) have longer segments than their surroundings.

Compared to the surrounding segments involved in the generation of the patches, the red patches are more intensified but the blue patches less intensified. In particular, both the most intensified patch R1 and the least intensified patch B1 are more geometrically different from their contexts regarding segment length, because R1 has the lowest ratio of 0.674 and B1 has the highest ratio of 1.591.

Table 5.6 A Comparison of the Segment Length of the Created Patches and that of Their Surroundings in the London Case (Ref.: Reference Number; Avg Seg Length: Average Segment Length; Avg R: Average Values of Red Patches; Avg B: Average Values of Blue Patches)

Ref.	Avg Seg Length		
	Patch (Black)m	Surrounding (grey)m	Ratio (Black/Grey)
R1	31.75	47.14	0.674
R2	38.00	51.02	0.745
R3	38.36	48.02	0.799
R4	59.58	61.66	0.966
R5	53.85	56.34	0.956
R6	63.21	66.91	0.945
Avg R	47.46	55.18	0.847
B1	79.74	50.12	1.591
B2	68.31	52.45	1.302
B3	57.80	44.58	1.297
B4	48.28	37.88	1.275
B5	56.00	42.67	1.312
Avg B	62.03	45.54	1.355

Then we moved to investigate the created patches (shown in **Fig. 5.31 and 5.32**) in the Beijing case. **Fig. 5.34a** shows the red patches created at 1700m as well as their surrounding segments within 1700m; and **Fig. 5.34b** displays the blue patches generated at 1700m as well as their surrounding segments within 1700m. The patches are denoted by black segments and

the surroundings are represented by grey segments. At first sight, R3 seems more intensified than its surrounding, and B5 appears sparser than its surroundings. However, it is not easy to draw the conclusion that one patch on average is more or less intensified than its surroundings. For example, R1 is obviously more intensified than the western context, but it seems not more intensified than the eastern and southern contexts. This also suggests that the geometric difference between the created patches and their surroundings in Beijing cannot *easily* distinguished by visual examination.

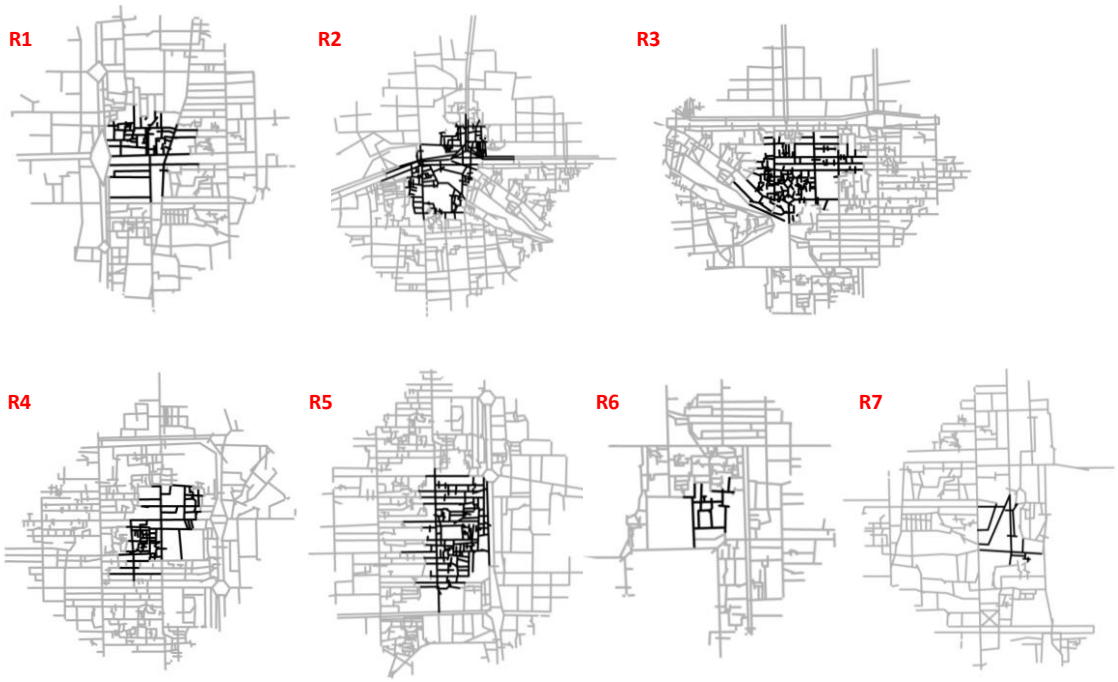

a. The red patches (associated with peaks) as well as their surroundings in Beijing

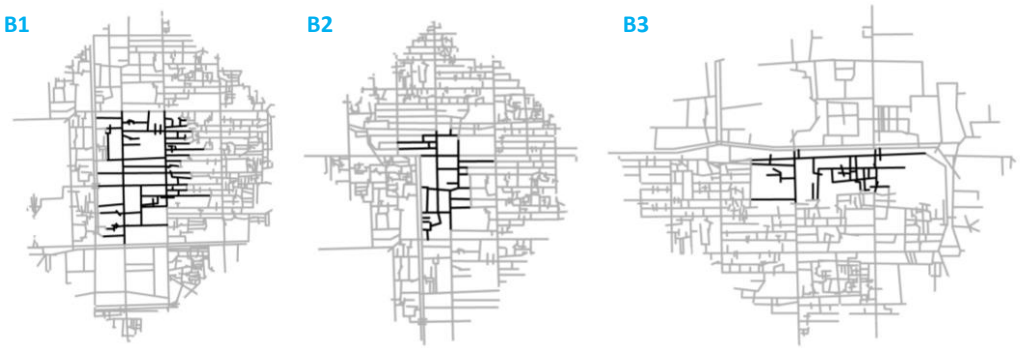

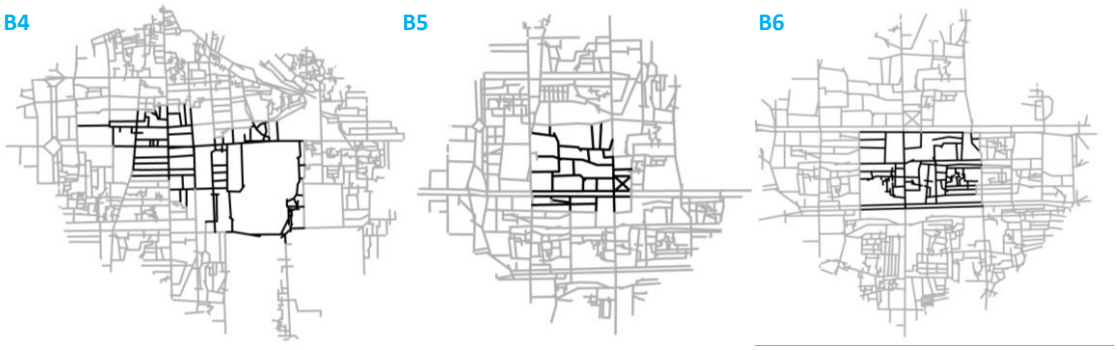

b. The blue patches (associated with troughs) as well as their surroundings in Beijing

Fig. 5.34 The Patches Created at 1700m and Their Surroundings for the Beijing Case. Black denotes the created patches and grey represents their surrounding segments within 1700m.

However, the quantitative analysis of the Beijing case (**Table 5.7**) shows that all the red patches on average have shorter segments than their surrounding areas, and all the blue patches on average have longer segments than their contextual areas. In spite of the fact that the Beijing patches (either the red or the blue patches) on average have longer segments (red: 63.69m; blue: 104.86m) than the London patches (red: 47.46m; blue: 62.03m; shown in **Tables 5.6**), the same relationship between the created patches and their surroundings is also found in the Beijing case. The red patches are more intensified than their surroundings, and the blue patches are less intensified than their contexts.

Table 5.7 A Comparison of the Segment Length of the Created Patches and that of Their Surroundings in the Beijing Case (Ref.: Reference Number; Avg Seg Length: Average Segment Length; Avg R: Average Values of Red Patches; Avg B: Average Values of Blue Patches)

Ref.	Avg Seg Length		
	Patch (Black)m	Surrounding (grey)m	Ratio (Black/Grey)
R1	70.47	87.24	0.808
R2	50.32	72.74	0.692
R3	49.55	68.63	0.722

R4	66.78	82.24	0.812
R5	64.74	82.22	0.787
R6	72.97	77.11	0.946
R7	70.99	80.25	0.885
Avg R	63.69	78.63	0.807
B1	118.70	70.81	1.676
B2	120.26	69.39	1.733
B3	89.53	76.52	1.170
B4	98.51	64.41	1.529
B5	117.42	75.41	1.557
B6	84.72	63.52	1.334
Avg B	104.86	70.01	1.500

As the red and blue patches emerge side by side to form a kind of *periodic structure* (shown in **Fig. 5.29-5.32**), the red patches would act as the surroundings of the blue patches and vice versa. The above analysis therefore implies that more intensified sub-grids are surrounded by, and meanwhile envelope, less intensified sub-grids across the entire historic districts at a constricted radius. The peak-trough pattern in fact captures this kind of *periodicity*. The peak, associated with red patch, denotes a metrically integrated and intensified centre surrounded by less intensified spaces, called *the centre-to-edge motif* in the previous chapter; and meanwhile, the trough, related to the blue patch, represents relatively less intensified central area enclosed by metrically integrated and intensified edges, called *the edge-to-centre motif* in the previous chapter. By and large, it can be proposed that *the periodic patchwork (or peak-trough) pattern might arise from the unevenly intensified grid as a whole system*.

When we investigated the variation between two differently intensified parts, we in fact treated one part as the internal, and another part as the external. The internal can be considered as each root area (or even segment) and the external as the contextual areas (or a group of segments) encountered up to a radius. And meanwhile, radius itself is a tool for defining the contextual areas. Then, *how does the generation of each patch as the internal relate to the*

extension of the contexts as the external, how does the degree of intensification vary with an increase of radius, and how does this account for the formation of the patches?

5.5.4 The change rate of segment density

In order to tackle the above questions, we turned to focus on the idea of *segment density* (as mentioned in **Section 5.3.2**), meaning the number of the segments encountered within a relatively small radius *as a unit*, because the degree of intensification also can be approximately assessed by segment density. Based on the segment maps of London and Beijing, we first visualised the distribution patterns of segment density (approximated by node count at a small radius of k, denoted NC Rk), aiming to make the first step towards investigating whether and how the created patches are influenced by grid intensification.

For example, **Fig. 5.35a and b** illustrate the NC R1400 pattern of London, as well as the NC R1700 pattern of Beijing, as a way of showing the distribution pattern of segment density in the two cities. At first sight, they show two different concentric patterns. In the London case (**Fig. 5.35a**), its geometric centre is most intensified, and segment density roughly decreases from the centre to the edge. In contrast, the geometric centre of Beijing (occupied by the Forbidden City) is less intensified, and enveloped by the most intensified grids within the Second Ring Road; and then segment density diminishes outwards (**Fig. 5.35b**).

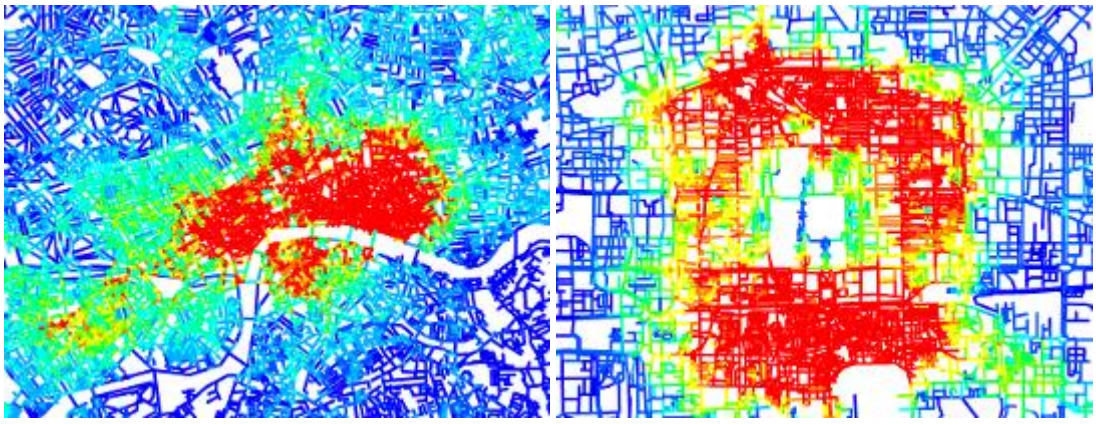

a. The pattern of Central London, produced by NC R1400.

b. The pattern of the Inner City of Beijing, produced by NC R1700.

Fig. 5.35 Two Different Patterns of Segment Density of London and Beijing (approximated by NC at low radius). Red denotes high segment densities and blue indicates low values.

However, both images (**Fig. 5.35a and b**) do not show anything resembling the periodic patchwork patterns, the same as those displayed in **Fig. 5.29-1** and **5.31-1**. In those periodic patchwork patterns, the same coloured patches (either red or blue) emerge across the whole maps of London and Beijing. Thus, the distribution patterns of segment density (**Fig. 5.35a and b**) in fact suggest that the *same* coloured patches have *different* segment densities. In general, the patches located at the central districts of London and Beijing (except for the Forbidden City) are more intensified than those situated at the outside of the central districts. This might be due to a simple fact that the historic central districts in the two cities have been intensively developed. To a large extent, however, it also implies that the variable of segment density *itself* does not account for the patchwork patterns.

Furthermore, when we carefully observed the above two images (**Fig. 5.35a and b**), some orange and yellow clusters can be found within the red parts, and meanwhile, some cyan clusters can be found within the blue parts. Perhaps this demonstrates that segment densities slightly vary within the central districts or the outside. *Does this imply that small variations of segment densities relate to the formation of the patchwork patterns?*

As segment density can be approximated by NC Rk (if k is small), we then focused on how the NC Rk of the individual segments of the same coloured patches varies with respect to the change of radius. For example, in the London patchwork pattern created by MMD R1400, three segments were randomly selected from the different red patches, because there are only three red patches generated at 1400m in the central district of London; and three segments randomly chosen from three different orange patches, and three segments randomly picked out from three different blue patches (**Fig. 5.36a**). In the Beijing patchwork pattern generated at 1700m, nine segments were also randomly selected in the same way we carried out for the London case (**Fig. 5.36b**). The segment reference numbers are displayed in these two images.

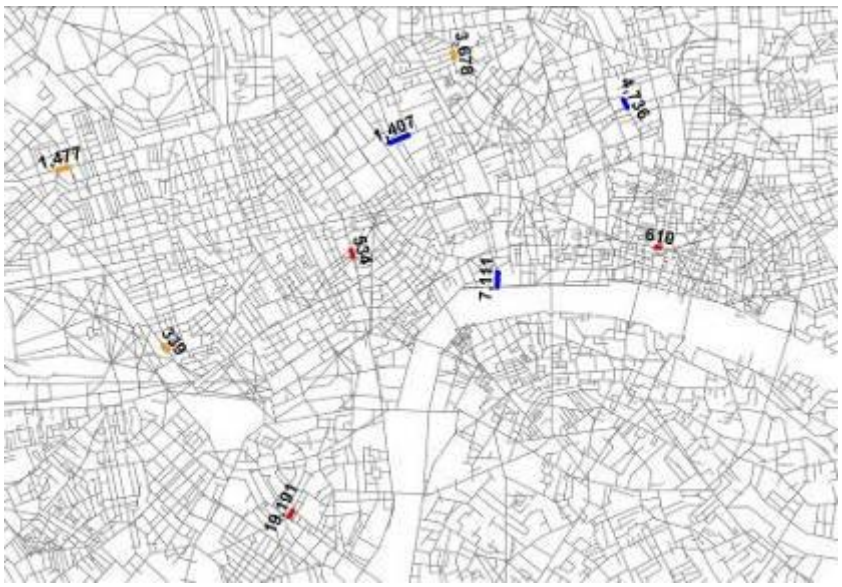

Fig. 5.36a The Individual Segments Selected from the Segment Map of London. Three red segments selected from three different red patches generated at 1400m; three orange segments picked from three different orange patches created at 1400m; and three blue segments chosen from three different blue patches produced at 1400m. The number denotes segment reference number (which corresponds to the reference number in Table 5.8).

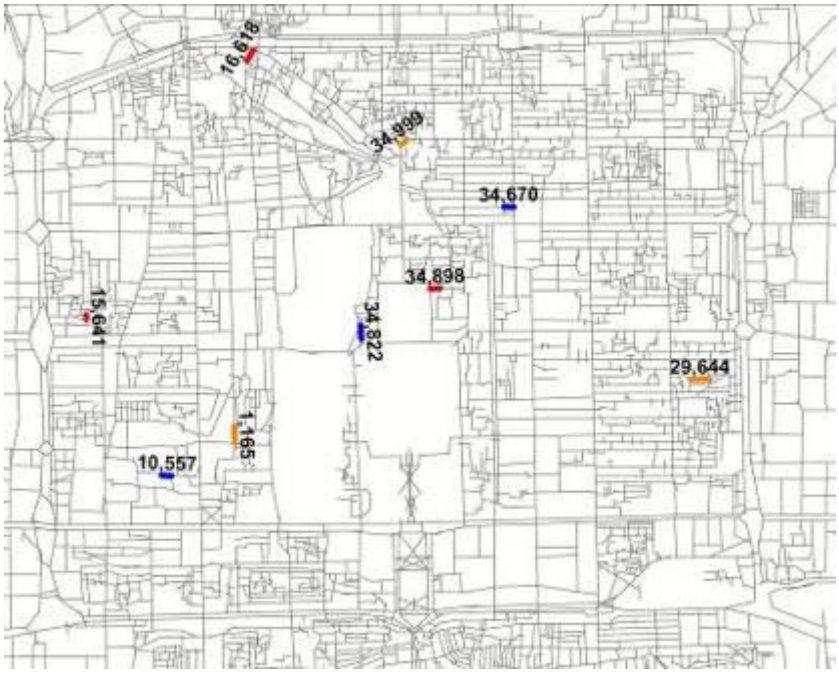

Fig. 5.36b The Individual Segments Selected from the Segment Map of Beijing. Three red segments selected from three different red patches generated at 1700m; three orange segments picked from three different orange patches produced at 1700m; and three blue

segments chosen from three different blue patches created at 1700m. The number denotes segment reference number (which corresponds to the reference number in Table 5.9)

We sought to investigate the variation of segment density - starting from each selected segment – with an increase of radius, and this can be approximated by the metric embeddedness trajectories within the range of 100m to the radius at which the patchwork patterns were generated (1400m for the London case and 1700m for the Beijing case). The metric embeddedness trajectories of all those individual segments were illustrated by plotting NC Rk against Rk. **Fig. 5.37 a and b** illustrate these embeddedness trajectories in London and Beijing respectively (see Appendix for full tables). At first sight, the segments selected from the different coloured patches (in either case) seem to have different shapes of the trajectories; and at least the blue segments have more curved trajectories than the red and orange segments. This possibly suggests that the contexts of the different coloured segments can be intensified in different ways.

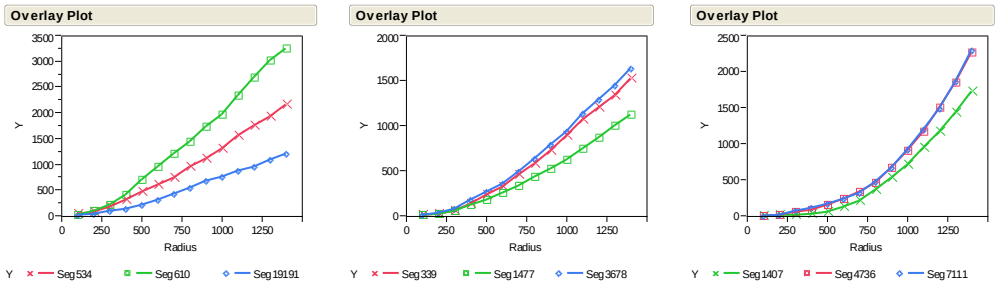

Red segments Orange segments Blue segments

a. The embeddedness trajectories of the nine segments in London.

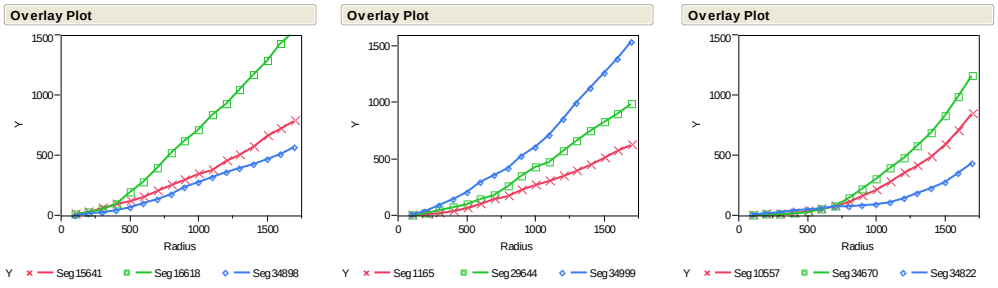

.

Red segments Orange segments Blue segments

b. The embeddedness trajectories of the nine segments in Beijing

Fig. 5.37 The Metric Embeddedness Trajectories of the Individual Segments Selected from the Different Patches in London and Beijing.

The non-linear regression analysis numerically demonstrates that all the above embeddedness trajectories (**Fig.5.35**) are approximately governed by power laws. This suggests that the way in which those segments are metrically embedded into the surroundings is controlled by scale parameter (H) and exponent parameter (α) of the power-law relation between node count and radius (expressed by the equation of $NC_k = H \times k^{\alpha}$ described in **Section 4.3.2**). **Tables 5.8 and 5.9** summarise these two parameters (H and α), together with basic values, such as segment reference numbers (denoted by Depthmap Ref, which corresponds to reference number shown in **Fig. 5.29 and 5.31**), MMD and NC – at certain radius – of each selected segment in London and Beijing respectively.

Table 5.8 The Relationship Among MMD, NC and Power-law Exponents of the Nine Segments Selected from the Different Patches Created by MMD in London.

(MMD_R1400: mean metric depth at 1400m; NC_R1400: node count at 1400m; H: scale parameter of the power-law relation between node count and radius; α: the exponent of the power-law relation between node count and radius.

Variable	Seg 19191	Seg 534	Seg 610	Seg 1477	Seg 339	Seg 3678	Seg 1407	Seg 4736	Seg 7111
Patch Colour	Red	Red	Red	Orange	Orange	Orange	Blue	Blue	Blue
MMD _R1400	818.2	817.7	818.5	863.4	865.7	863.6	1004.4	1004.3	1005.2
NC_ R1400	1208	2159	3248	1125	1523	1638	1728	2268	2294
H	1.71 E-02	3.52 E-02	5.19 E-02	2.73 E-03	3.93 E-03	5.25 E-03	2.82 E-06	5.22 E-06	5.38 E-06
α	1.544	1.523	1.528	1.786	1.779	1.748	2.795	2.745	2.743

Table 5.9 The Relationship Among MMD, NC and Power-law Exponents of the Nine Segments Selected from the Different Patches Created by MMD in Beijing.

(MMD_R1700: mean metric depth at 1700m; NC_R1700: node count at 1700m; H: scale parameter of the power-law relation between node count and radius; α: the exponent of the power-law relation between node count and radius.

Variable	Seg 34898	Seg 15641	Seg 16618	Seg 1165	Seg 29644	Seg 34999	Seg 34822	Seg 10557	Seg 34670
Patch Colour	Red	Red	Red	Orange	Orange	Orange	Blue	Blue	Blue
MMD_R1700	997.4	997.5	999.4	1033.7	1036.2	1035.9	1205.6	1206.8	1206.7
NC_R1700	568	781	1531	618	991	1538	437	842	1159
H	6.06 E-03	7.05 E-03	1.43 E-02	1.81 E-03	2.26 E-03	5.6 E-03	8.44 E-07	2.55 E-06	3.2 E-06
α	1.54	1.561	1.56	1.714	1.75	1.684	2.688	2.635	2.649

As for the London case, we then compared MMD R1400 with NC R1400 (shaded in **Table 5.8**). The same coloured segments (red, orange or blue) have very similar MMD R1400 values, but they do *not* necessarily have similar NC R1400 values. For example, Segment 610 (selected from a red patch co-inciding with the City, see **Fig. 5.29**) has 2.7 times the NC R1400 than Segment 19191 (chosen from another red patch roughly corresponding to Pimlico, see **Fig. 5.29**); but these two segments have almost the same MMD R1400 values (818.5 and 818.2, respectively). Since NC R1400 approximates to segment density, it indicates that the City and Pimlico, both of which are identified as the red patches (**Fig.5.29**), have different segment densities. This demonstrates that the same coloured patches, even located at the central district of London, are differently intensified. When we examined the segments in the Beijing case, we also found that the same coloured segments (shaded in the same colour in **Table 5.9**) have

almost the same MMD R1700, but have significantly different NC R1700. This also indicates that the same coloured patches in the central district of Beijing are differently intensified. The above analysis numerically confirms that the spatial discontinuities within the two central districts are not produced by the variable of segment density itself.

Then, how about the power-law exponents? The segments selected from the same coloured patches (red, orange or blue) in each case have similar values of power-law exponent α (**Tables 5.8 and 5.9**) As discussed in the previous chapter, the power-law exponent mathematically approximates the change rate of node count, and so at relatively small radius, the power-law exponent roughly reflects the change rate of segment density. **Tables 5.8** and **5.9** therefore demonstrate that the same coloured patches in each case have similar rates of change in segment density. This suggests that the patchwork patterns arise from the change rate of segment density, rather than segment density itself.

Or, the above analysis further implies that the transition between the intensified sub-grids and the sparse sub-grids produces the patchwork patterns. For example, the red segments have small exponents, the orange segments have moderate exponents, and the blue segments have high exponents, as **Tables 5.8** and **5.9** show. This numerically demonstrates that the red segments encounter less intensified contexts – with increasing radius – than the blue segments. To some extent, this can support the previous finding that the red patches of the two central districts have more intensified centres, but the blue patches have more intensified edges. This will be theoretically discussed in chapter seven.

In addition, we further *statistically* verified the power law relationship between NC and radius for *all* the individual segments, as well as their relationships between the MMD Rk and the power law exponents, in order to confirm whether the change rate of segment density matters in a more generalised sense. Here we still sought to study the MMD R1400 for London and the MMD R1700 for Beijing. However, we respectively investigated the relationship between NC and radius, within the range of 400m to 1700m for London and within the range of 400m to 2000m for Beijing, with an interval of 100m. As the endpoint of the radius range is larger than the radius at which the MMD Rk values were calculated, this enables us to explore whether the

change rate of segment density beyond the radius of 1400m (for London) and of 1700m (for Beijing), representing the contexts, *empirically* affect the values of MMD Rk, roughly denoting the internal structures.

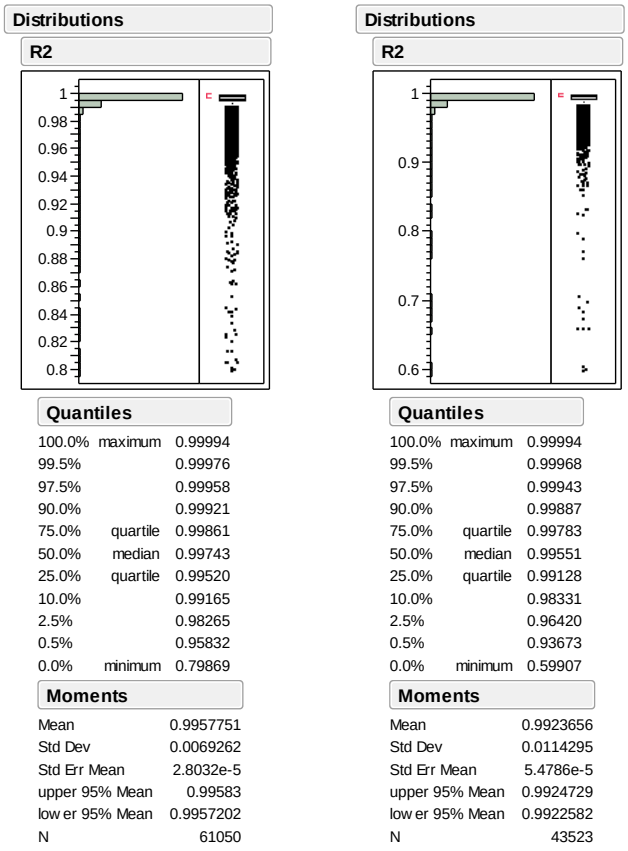

Fig. 5.38 The R-square values of the power-law relationship between NC and radius. Left is the London case; Right is the Beijing case.

Fig. 5.38 shows that 95% segments in the London case have a power law relationship between NC and radius, with the R-square above 0.9, within the range of 400m to 1700m, and 95% segments in Beijing have a power law relationship with the R-square above 0.9 within the range of 400m to 2000m. And **Fig. 5.39** demonstrates that a strong non-linear relationship between the power law exponents and the MMD R1400 values, with the R-square of 0.813, was found in the London case, and a strong non-linear relationship with the R-square of 0.900 identified in the Beijing case. In fact, this suggests that the patchwork patterns generated by the MMD at the radius of k, in these two cases, are *statistically* influenced by the change rates of segment density beyond the radius of k. Morphologically speaking, it can be implied that the density change rate between the internal and the contexts, in the cases of London and Beijing, has

significant impact on the formation of the patchwork patterns. Such change in segment density possibly infers a spatial discontinuity between generated patches in these two urban networks.

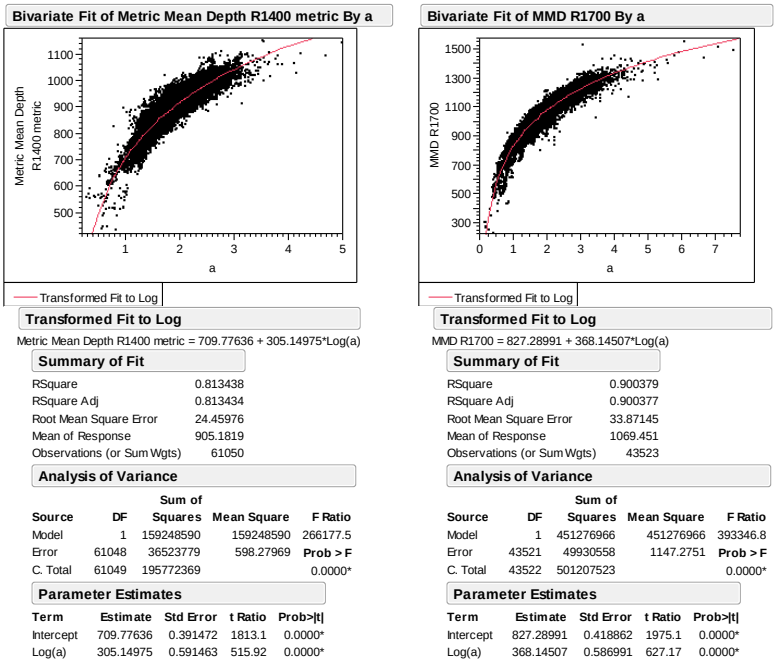

Fig. 5.39 The Correlation between Power Law Exponents and MMD Rk Values. Left is the London case; Right is the Beijing case.

5.6 Discussion

The above comparative study of the historic named areas in the central districts of London and Beijing suggests several discussion points. First, both the descriptive technique for illustrating what a pre-defined area is and the generative techniques for creating the periodic patchwork pattern and the peak-trough pattern have considerable merit as a tool for examining the spatial structures of the named areas in London and Beijing, but it is too complex in their relations to serve simply as a tool for identifying the named areas. For example, Marylebone and Mayfair in London and Shichahai in Beijing *cannot* be identified by the technique for generating patchwork patterns, although their internal historical development parts can be investigated by this technique.

Second, those techniques generating a methodology framework, however, bring to light two much more fundamental structures in the central districts of London and Beijing: the periodic patchworks found at different scales, as well as the patches distinguished as a limited range of pattern types, namely peaks and troughs. Morphologically speaking, those two pattern types with functional implications – associated with named areas in London and Beijing suggest two motifs: the centre-to-edge motif, meaning central blocks are smaller than edge blocks, as well as the edge-to-centre motif, indicating edge block are more intensified than central blocks. To a large extent, this reveals the phenomenon of area structures marked out in the historical districts of London and Beijing, although those two districts in general have been relatively intensified through history.

Third, it can be argued that the area structure found in the two central districts is perhaps associated with small variations – represented by inflexion points along metric embeddedness trajectories – in metric features of the urban networks, so that it is difficult for us to clearly differentiate their boundaries. Those small variations in metric features can be interpreted as the rate of change in segment density *within and outside* each named area. This in fact implies that the spatial discontinuities in the two historic districts empirically arise from the *unevenly* intensified structures. And moreover, the in-depth investigation of the individual segments further suggests that the periodic patchwork patterns are produced by the change rate of segment density, rather than segment density itself. As a result, the rate of change of segment density suggests a kind of syntactic relationship between the internal and the external, rather than local metric conditions of the internal layout, so that it can be argued that the boundaries of the named areas in the two historic districts are *not* determined only by their internal layouts, but also by the way in which they are metrically embedded into the surroundings. How about the new development areas? The next chapter will further investigate the case of London Docklands.

Chapter Six: Spatial Discontinuity in the London Docklands

6.1 Introduction

In contrast to the previous chapter, which investigated historic central districts, this chapter presents an analysis of the London Docklands, a new district developed within a relatively short period of time. This analysis will be used to describe and differentiate the newly developed areas in relation to the London Docklands as a whole, and then explore the spatial mechanism involved in the formation of those areas.

The London Docklands district was selected for two reasons: first, it was the largest development in Europe during the 1980s and 1990s, aiming to transform a derelict and segregated brown field into an urban-like district similar to the West End of London (LDDC, 1998; Hall, 1998); second, various studies (Brownill, 1990; Edwards, 1992, 1993, 1999; Foster, 1999; Gordon, 2001; Carmona, 2009) have pointed out that newly developed areas can remain physically and socially fragmented and self-sustained, without achieving a coherent and integrated district. This chapter focuses attention on investigating the nature of the spatial boundaries of the new areas, from the point of view of spatial configuration. The new areas studied, like many such areas, are usually bounded by arterial roads, water and green areas and seem to be much more easily distinguished than the historic areas discussed in the previous chapter. This chapter aims to obtain an enhanced understanding of the difference and similarity between the Dockland areas and the historic areas with respect to their spatial structuring. However, again it should be mentioned that rather than studying the social and economic dimensions of these new areas, the analysis concentrates on their spatial scope.

6.2 Background

This section briefly introduces the London Docklands and the newly developed areas that we will be analysing, with the aim of providing a background for this case study. The London Docklands development included 22 square kilometres of abandoned new areas, extending 10.8 kilometres along the Thames River within the three Dockland Boroughs of Southwark, Tower Hamlets and Newham. It established a new commercial and business district, incorporating Canary Wharf as its centre with a total floor area of 25.1 million sqms; and built a total of 24,042 new dwellings between 1981 and 1998, forming a new built environment of the Docklands to the east of the City, the historic financial and business centre of London (Brownill, 1990; Edwards, 1992, 1993, 1999; LDDC, 1998) **(Fig. 6.1 and Fig. 6.2)**. In the Urban Design part of the Monographs of the London Dockland Development Cooperation (LDDC), it claimed that '*The LDDC's aim is the creation* of *coherent and diverse yet distinct and identifiable districts similar to those which constitute other metropolitan areas…. it helps orientation, creates a "sense of place" and greatly assists our enjoyment of cities*'.[112] (LDDC, 1998). Part 2 of **Appendix C** gave a brief introduction of the London Docklands development.

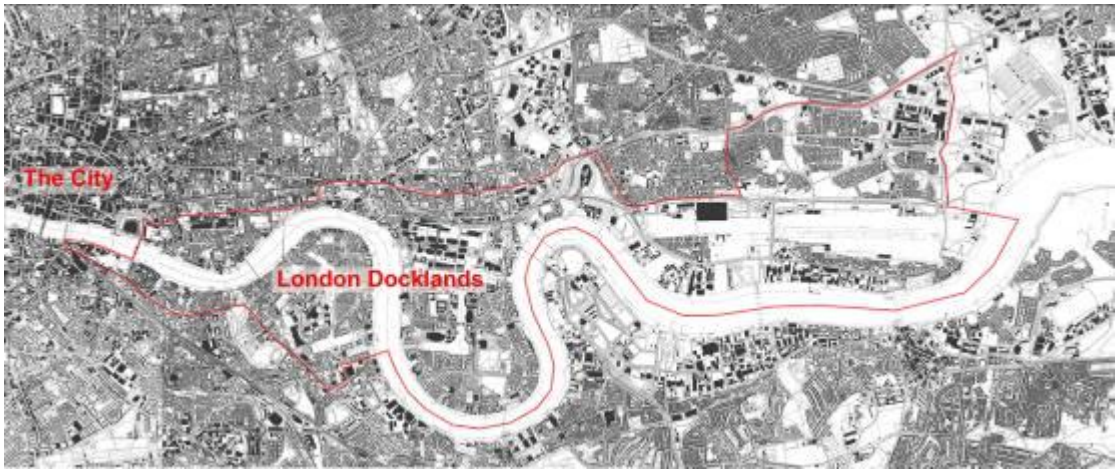

Fig. 6.1 The location of the London Docklands. This district is situated to the east of the City and includes 22 square kilometres abandoned new areas, extending 10.8 kilometres along the Thames River within three Docklands Boroughs of Southwark, Tower Hamlets and Newham. Red denotes its boundary.

[112] http://www.lddc-history.org.uk/planning/index.html#Foreword

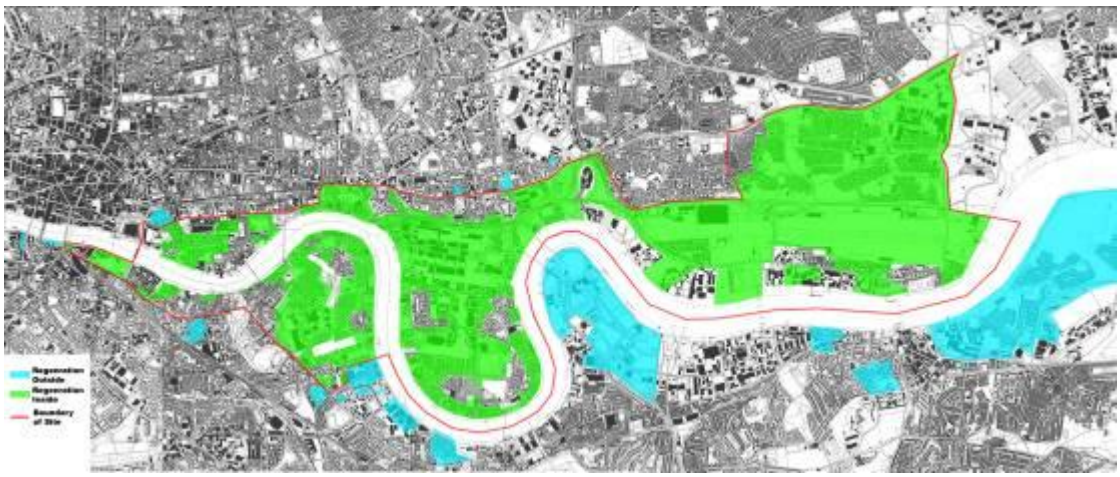

Fig. 6.2 The New Built Environment of the London Docklands. Red denotes the boundaries of the London Docklands; green indicates the newly developed areas within the site boundaries; cyan means the newly developed areas outside the site boundaries.

We focus attention on the spatial formation of the newly developed areas within this district and compare them to the findings about the historic named areas studied in the previous chapter. According to the definition of the larger development areas in the LDDC completion booklets in 1998 (ibid), the London Docklands were divided into seven development areas: Bermondsey, Surrey Docks, Wapping, Limehouse, the Isle of Dogs, Royal Docks and Beckton. However, in the booklet of the Isle of Dogs, this development area was clearly distinguished as two parts, the Isle of Dogs to the south and Poplar to the north, because the two parts were physically separated by the dock walls before the regeneration, and still spatially isolated by Aspen Way (a motorway) after the regeneration (LDDC, 1998). Therefore these two areas will be studied separately.

The case study comprises eight areas, still called *the larger development areas* in this chapter (**Fig. 6.3**): **1) Bermondsey**[113] bounded by King William Street, Duke St Hill, Tooley Street, Jamica Road, Fulford Street and the Thames River, **2) Surrey Dockss** marked out by Fulford Street, Lower Road, Plough Way and the Thames River, **3) Wapping** enclosed by Tower Bridge, East Smithfield, The Hwy, King Edward Memorial Park and the Thames River, **4) Limehouse** bordered by The Hwy, Branch Road, Commercial Road, West India Dock Road,

[113] Bermondsey is also a historic area, but suffered severe damage by bombing during the Second World War and became derelict in the 1960s following the collapse of the river trade. It had been redeveloped under the aegis of the London Docklands Development Cooperation in the 1980s (LDDC, 1998).

Westferry Road and the Thames River, **5) the Isle of Dogs** encircled by West India Dock Road, Aspen Way and the Thames River to the east, west and south, **6) Poplar** confined by West India Dock Road, Aspen Way, Cotton Street and East India Dock Road, **7) Royal Docks** bordered by Victoria Dock Road, Royal Albert Way, Amada Way and the Thames River, **8) Beckton** surrounded by Prince Regent Line, Newham Way, Royal Dock Road, Royal Albert Way and Victoria Dock Road. **Appendix C** also gives a brief introduction of each area.

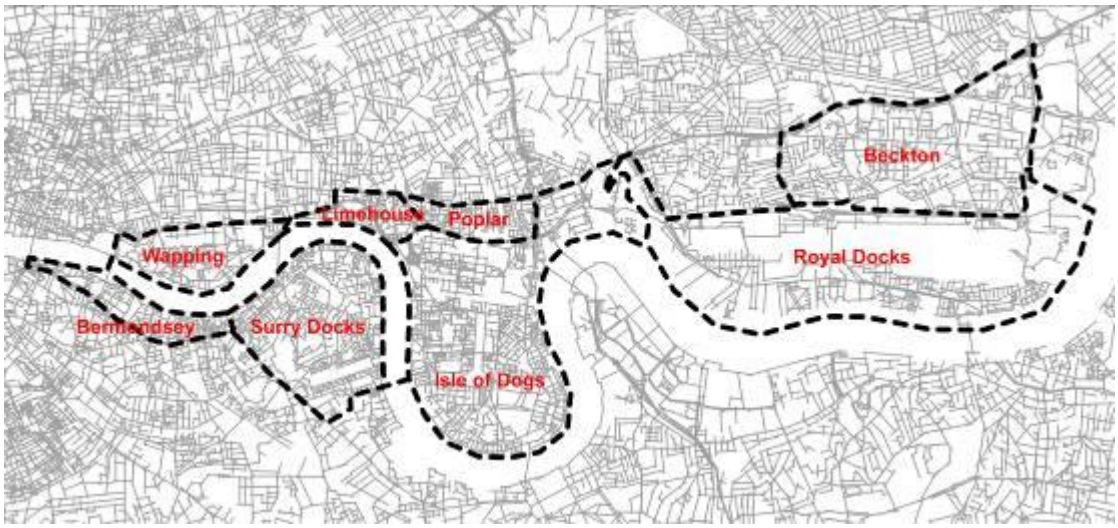

Fig. 6.3 Eight larger development areas including Bermondsey, Wapping, Surry Docks, Limehouse, Poplar, the Isle of Dogs, Royal Docks and Beckton.

These eight larger development areas are much larger than the named areas studied in the previous chapter; and they comprise several smaller yet distinctive parts, according to LDDC's booklets of those larger development areas (LDDC, 1998). In order to understand how the smaller parts of the London Docklands are spatially organised in relation to their surroundings, the sixteen *smaller areas* were further selected according to a combination of the index of household tenure in 2001 and field observation. We adopted the criterion of the index of household tenure, because the London Docklands comprises a mixture of old council housing estates and new luxury housing estates[114], which can be captured by the index of household tenure. And meanwhile, most housing estates, either public or private, can be visually

[114] With the council housing, the physically isolated estates, providing 83% of homes in The London Docklands in 1981, the regeneration has created a better balance of household tenure by constructing 45% of new homes in owner occupation, most of which are the luxury gated communities. For details, see LDDC 1998.

indentified by field observation, because they are often characterised by an inward-looking layout with different architectural styles or colours.

The old council housing and the new luxury housing estates were first investigated according to the 2001 Census Data at the level of the Output Areas[115]. The household tenure was classified into six ranks: Owns Outright, Mortgage, Shared Ownership, Private Letting, ~~to~~ Housing Association and Council House (ONS, 2004). The proportion of Council House in each Output Area was calculated by dividing the number of Council House by the number of all the household tenures, seeking to illustrate the distribution pattern of the council housing estates. The proportion of the sum of Owns Outright, Mortgage and Private Letting was also computed by dividing the sum of those tenures by the total of all the household tenures, in an attempt to approximate the distribution of the luxury housing estates. **Fig. 6.4 and 6.5** respectively illustrate the thematic maps with four grey bands, according to the proportion of Council House, as well as the proportion of the sum of Owns Outright, Mortgage and Private Letting. Dark indicates the proportion over 75%, dark grey denotes the proportion between 50% and 75%, light grey means the proportion between 20% and 50%, and white represents the proportion less than 20%. The proportion of Council House over 50%, to a larger extent, suggests that the area is dominated by social housing estates, and the proportion of the sum of Owns Outright, Mortgage and Private Letting over 50% infers that the area is mainly occupied by luxury housing estates.

[115] '2001 Census Output Areas were built from clusters of adjacent unit postcodes but as they reflected the characteristics of the actual Census data they could not be generated until after data processing. They were designed to have similar population sizes and be as socially homogenous as possible (based on tenure of household and dwelling type) - note though that homogeneity was not used as a factor in Scotland. Urban/rural mixes were avoided where possible (i.e. OAs preferably consisted entirely of urban postcodes or entirely of rural postcodes). They had approximately regular shapes and tended to be constrained by obvious boundaries such as major roads. The OAs were required to have a specified minimum size to ensure the confidentiality of data'. For detail, see http://www.statistics.gov.uk/geography/census_geog.asp, or ONS, 2004.

Fig. 6.4 Thematic Map Coloured by Four Grey Bands according to the Proportion of Council House. Dark indicates the proportion over 75%, dark grey denotes the proportion between 50% and 75%, and light grey means the proportion between 20% and 50% and white represents the proportion less than 20%. The proportion of Council House over 50% suggests that the area is dominated by social housing estates.

Fig. 6.5 Thematic Map Coloured by Four Grey Bands according to the Proportion of the Sum of Owns Outright, Mortgage and Private Letting. Dark indicates the proportion over 75%, dark grey denotes the proportion between 50% and 75%, and light grey means the proportion between 20% and 50%, and white representing the proportion less than 20%. the proportion of the sum of Owns Outright, Mortgage and Private Letting over 50% infers the area dominated by luxury housing estate.

Based on the above thematic images (**Fig. 6.4 and 6.5**), the field observation was carried out in October 2005 to mark out the exact locations of those estates, as well as the newly developed centres, such as Canary Wharf and local commercial centres. In this way, the sixteen *smaller areas* were selected and illustrated in **Fig. 6.6**. The brief descriptions of those smaller areas are listed in **Table 6.1**. The next step is to respectively examine the eight *larger development areas*, as well as the sixteen *smaller areas*, with regard to their contexts. Both types of areas are called *the Dockland areas*, or *the newly developed areas*, in the following text. As the smaller areas were selected from the larger development areas, the comparison between the larger and the smaller areas also enables us to explore the relationship between the sub-grids and the smaller pieces belonging to those sub-grids.

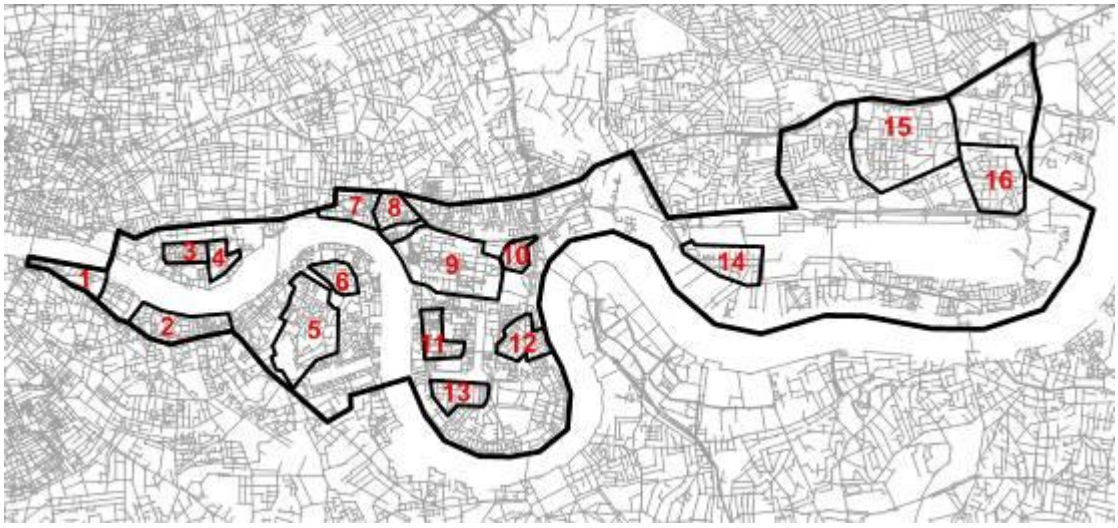

Fig. 6.6 The Locations of Sixteen Smaller Areas. They were selected according to Fig. 6.4a and b as well as field observation. 1,Bermondsey_W; 2,Bermondsey_E; 3,LH_Wapping; 4,SH_Wapping; 5, Centre_SurreyDocks; 6,SH_SurreyDocks; 7,LH_Limehouse; 8, SH_Limehouse; 9, Canary Wharf; 10, Blackwall; 11,SH_NW_IsleofDogs; 12,SH_NE_IsleofDogs; 13, LH_IsleofDogs; 14, LH_RoyalDocks; 15,Beckton_N; 16,Beckton_E.

Table 6.1 A Brief Description of Sixteen Smaller Areas (*: Beckton_E comprises old council houses and several new residential buildings, and so we call it a mixed housing estate; **: Centre_Surrey Docks comprises shopping malls, tube station and houses, so we call it a mixed-use centre area of Surrey Docks)

Smaller Area	Brief description
LH_Wapping	a luxury housing estate bounded by Vaughan Way, Asher Way and Spirit Quay in Wapping
SH_Wapping	a social housing estate bordered by Reardon Street, Green Bank, Prusom Street and Farthing Fields in Wapping
LH_Limehouse	a luxury housing estate delimited by the Thames River, Branch Road, Commercial Road and a canal of the Limehouse basin in Limehouse
SH_Limehouse	a social housing estate surrounded by Commercial Road, a canal of the Limehouse basin, Narrow Street, Limehouse Causeway and West India Dock Road
Blackwall	a luxury housing estate bordered by Trafalgar Way, Fraser Place and Preston's Road in Blackwall
SH_NW_IsleofDogs	a social housing estate surrounded by Byng Street, Westferry Road, Tiller Road, Mellish Street and Alpha Grove in the north west part of the Isle of Dogs
SH_NE_IsleofDogs	a social housing estate delimited by East Ferry Road, Glengall Grove, Manchester Road and Stewart Street in the north east part of the Isle of Dogs
LH_IsleofDogs	a luxury housing estate bounded by Westferry Road, Millwall Outer Dock and Spindrift Ave in the Isle of Dogs
SH_Surrey Docks	a social housing estate surrounded by Salter Road and a green part to the north of Bacon's College in Surrey Docks
LH_RoyalDocks	a luxury housing estate, Silver Town, encircled by Silvertown way, Royal Victoria Dock and Mill Road in Royal Docks

Beckton_E*	a mixed housing estate* bounded by Royal Albert Way, Royal Docks Road, Winsor Terrace, Woolwich Manor Way and East Ham Manor Way in the east part of Beckton
Beckton_N	a luxury housing estate surrounded by Newham Way, Beckton District Park and Woolwich Manor Way in the north part of Beckton
Bermondsey_W	a new office area bounded by the Thames River, King William Street, Duke St Hill, Tooley Street and Tower Bridge Road in the west part of Bermondsey
Bermondsey_E	a mixed residential area enclosed by the Thames River, Mill Street, Jamaica Road and Fulford Street in the east part of Bermondsey
Centre_Surrey Docks**	a mixed-use** central area bordered by Salter Road, Surrey Water, Needleman Street, Surrey Quays Road, Deal Porters Way, Redriff Road, Quebec Way and Timber Pond Road in Surrey Docks
Canary Wharf	a new CBD, bounded by West India Dock Road, Westferry Road and West India Millwall Docks in the Isle of Dogs

6.3 What are the newly developed areas in terms of their contexts?

In the previous chapter, the historic areas in London and Beijing have been characterised and then differentiated in terms of their spatial relations to the surroundings. *Can we also describe and even identify those newly developed areas in the same way?*

6.3.1 The morphological difference between the London Docklands and the historic central districts

Before investigating those new areas, we first made a quantitative comparison between the London Docklands, as the contexts of those new areas, and the two historic central districts of London and Beijing, aiming to provide an informative background for examining the new areas. An axial map of the London Docklands and the surroundings was drawn (**Fig.6.7**) and then

segmented in DepthMap. As **Section 4.2** mentioned, the axial map has the radius-radius[116] of 19; the segment map has the metric system radius[117] of 8,000m. The London Docklands, located at the centre of the segment map, has a minimum buffer distance[118] of 4,500m to minimise edge effect reviewed in Section 3.2.1.

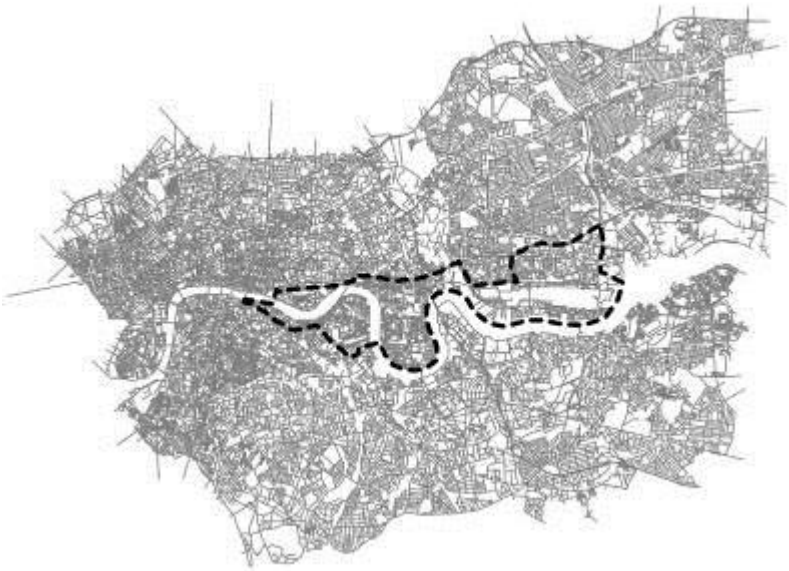

Fig. 6.7 The Unprocessed Axial Maps of the London Docklands and Its Surroundings. The dotted lines denote the boundary of the London Docklands.

Table 6.2 summarises basic geometric and syntactic values – including axial line length, segment length, axial connectivity, segment connectivity, integration Rn and R10[119] and intelligibility – of the London Docklands, as well as of the central districts of London and Beijing. The primary analysis suggests three points. First, the London Docklands has lower degree of *visual continuity* of streets – measured by the length of axial line – than the central districts of London and Beijing, because the London Docklands, on average, has smaller axial line length (140.8m) than the central districts of London (253.4m) and of Beijing (247.4m), respectively. In addition, the axial lines of the Docklands are further broken into shorter segments (41.6m),

[116] Reviewed in Section 3.2.1. The radius-radius is equal to the mean depth of the whole structure from the most integrated line. For detail, Hillier (1996), p163.
[117] See Section 4.2. Metric system radius is defined as the average metric distance from the geometric centre of the segment model to the edge.
[118] See Section 5.3.1. The minimum buffer distance means the minimum metric distance from the edge of the study district to the edge of map.
[119] The radius of 10 is the radius-radius of the axial maps of London and Beijing, so that integration R10 also reflects global syntactic feature of London and Beijing without the edge effect.

compared to those of London (44.4m) and Beijing (69.8m), respectively. Perhaps this might be due to the fact that the London Docklands has a large number of housing estates with very small scale grids. Although those housing estates seem to be extensively intensified (**Fig. 6.6**), their shorter street segments were not aligned to form longer axial lines denoting sightlines. This implies that the street network of the Docklands *might* be visually more fragmented, which will be discussed later.

Table 6.2 The Basic Geometric and Syntactic Values of the London Docklands as well as of the Central Districts of London and Beijing.

(Ax_M_Len: the mean of axial line length; Seg_M_Len: the mean of segment length; Ax_M_Conn.: the mean of axial connectivity; Seg_M_Conn.: the mean of segment connectivity; M_Int.Rn: the mean of integration Rn; M_Int.R10: the mean of integration R10)

District	Ax_M_Len (m)	Seg_M_Len (m)	Ax_M_Conn	Seg_M_Conn.	Seg_M_AConn	M_Int. Rn	M_Int. R10	Intelligibility Rn
Central district of London	253.4	44.4	5.570	4.795	3.221	1.051	1.482	0.200
Central district of Beijing	247.4	69.8	3.537	4.155	2.793	1.002	1.425	0.140
The London Docklands	140.8	41.6	3.551	4.147	2.791	0.487	1.083	0.092

Second, the London Docklands is not well-connected, compared to the central district of London. As **Table 6.2** shows, the Docklands on average has much lower axial connectivity (3.551) than London (5.570), although it has a slightly higher value than Beijing (3.537). And meanwhile, it has a lower segment connectivity (4.147) and segment angular connectivity (2.791) than both London (4.795 and 3.221) and Beijing (4.155 and 2.793). This demonstrates that the relatively shorter segments of the Docklands are less connected to their immediately

neighbouring segments. It can be suggested that the more intensified Dockland areas are less connected to their surroundings regarding visual continuity.

Third, the London Docklands is not only spatially more segregated, but also has the weaker relationship between local and global spatial structures. As **Table 6.2** demonstrates, it has the lowest integration values at the infinite radius (0.487) and at 10 (1.083), compared to the central districts of London (1.051 and 1.482, respectively) and Beijing (1.002 and 1.425, respectively). And it also has the lowest intelligibility (0.092), in contrast to London (0.200) and Beijing (0.140). This implies that the different parts of the Docklands, compared to those of the two central districts, have not been well-combined together to form an integrated structure at a higher scale.

By and large, the above analysis suggests that the spatial structure of the London Docklands, as the context of the newly developed areas, has *not* been transformed into an urban-like structure, comparable to the two historic central districts. Then, *can we still distinguish the Dockland areas regarding their relationships with their contexts? Are the Dockland areas spatially different from the historic named areas investigated in the previous chapter?*

6.3.2 The embeddedness trajectories of the newly developed areas

We then moved to examine the embeddedness trajectories of the eight larger development areas and the sixteen smaller areas by using the descriptive technique of the log-log radius plot (according to the detailed procedure elaborated in **Section 5.3.2**). This allows us to explore how those areas are spatially embedded into their contexts with increasing radius.

The log-log radius plot analysis, based on the axial maps, was conducted within a topological radius range of 1 to 40; and the segment version of the analysis was then carried out within a metric radius range of 400m to 8000m, with an interval of 100m. Compared to the radius-radius (19 topological depths) of the whole axial map or the metric system radius (around 8,000m) of the whole segment map, the endpoints of the whole range (such as 40 topological depths or 8,000m) are large enough to be used to test this descriptive technique.

Topological embeddedness trajectories (based on the axial map)

For topological analysis, **Fig. 6.9** illustrates all the log-log radius plots of the eight larger development areas; whilst, **Fig. 6.10** shows all the plots of the sixteen smaller areas. In contrast to the historic areas studied in the previous chapter (where each plot has three regression lines with different slopes, as **Fig. 5.8 and 5.9** illustrated), some Dockland areas even have four regression lines (denoted by red, green, blue and brown lines respectively). For the eight larger development areas, Surrey Docks (**Fig. 6.9 e**) has four lines; for the sixteen smaller areas, half of them (**Fig. 6.10 c, g, h, k, m, n, o and p**) have four lines. These regression lines still demonstrate that those new areas have a power law relationship between mean node count and topological radius within the constricted topological radius ranges; and the intersections of the consecutive regression lines still represent the discontinuities along the embeddedness trajectories. This therefore suggests that the contexts of the Dockland areas are topologically partitioned into more different levels by those discontinuities. In addition, not all of the Dockland areas have the same number of discontinuities (compared to the historic areas consistently having three topological discontinuities), and thus this implies that the Dockland areas topologically interact with their contexts in a more complex way.

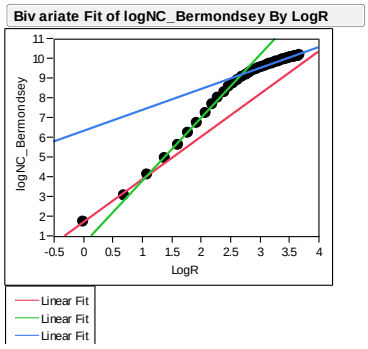

a. Bermondsey

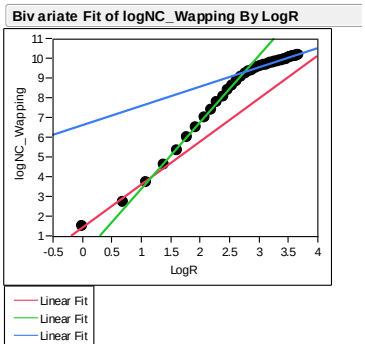

b. Wapping

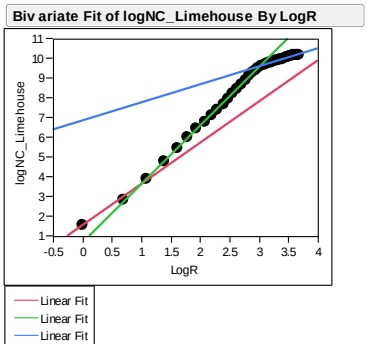

c. Limehouse

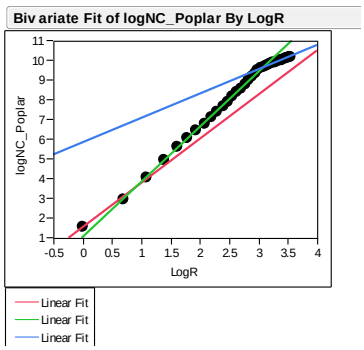

d. Poplar

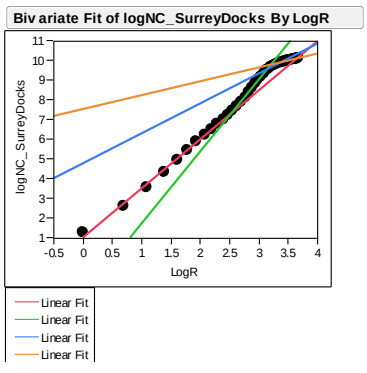

e. Surrey Docks

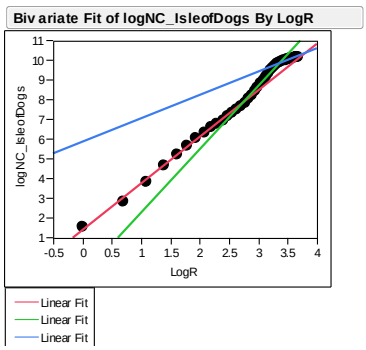

f. The Isle of Dogs

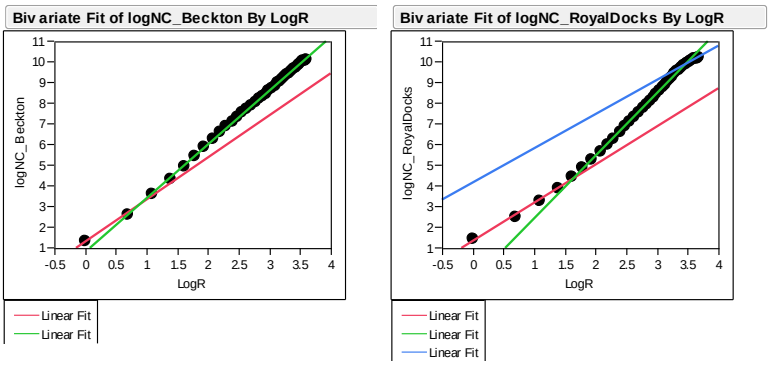

g. Beckton h. Royal Docks

Fig. 6.9 The Topological Embeddedness trajectories of the Eight larger development areas (based on the axial maps). Red, green, blue and brown lines respectively indicate the regression lines generated within the first, second, third and fourth levels of radius ranges (some areas only have two levels of radius ranges, some have three levels and Surrey Docks has four levels).

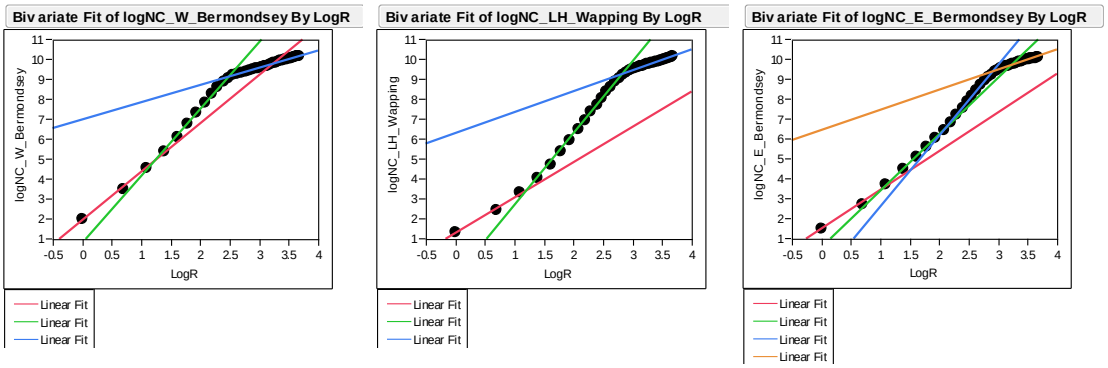

a. W_Bermondsey b. LH_Wapping c. E_Bermondsey

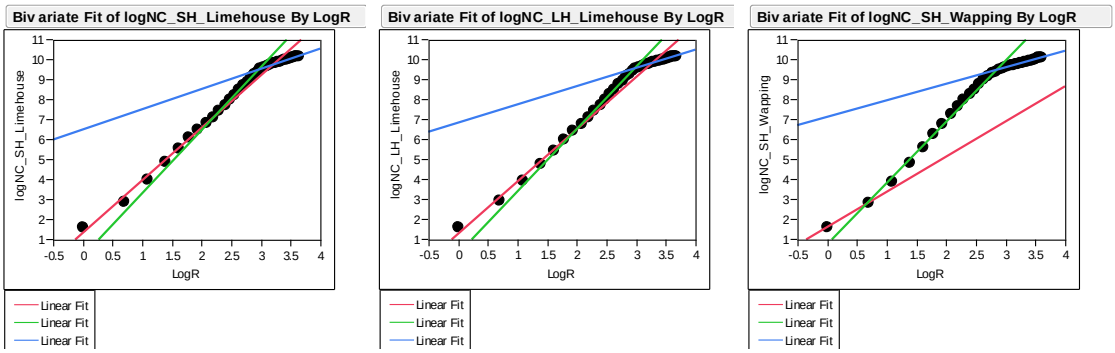

d. SH_Limehouse e. LH_Limehouse f. SH_Wapping

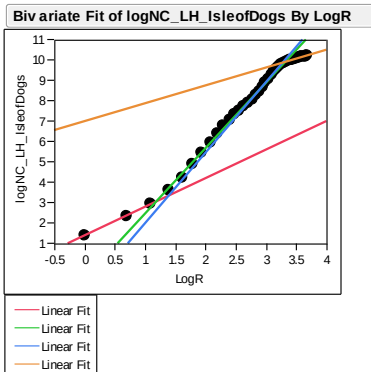

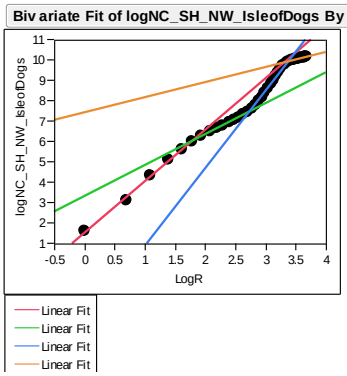

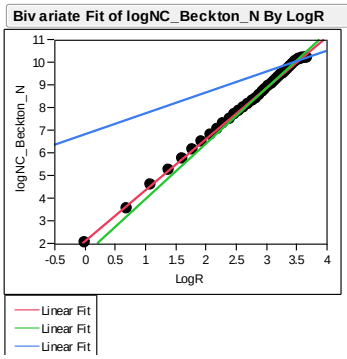

g. LH_IsleofDogs h. SH_NW_IsleofDogs i. Beckton_N

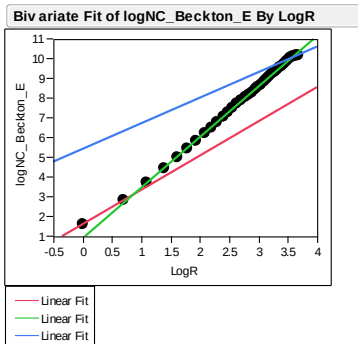

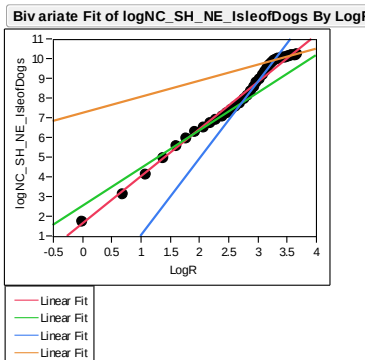

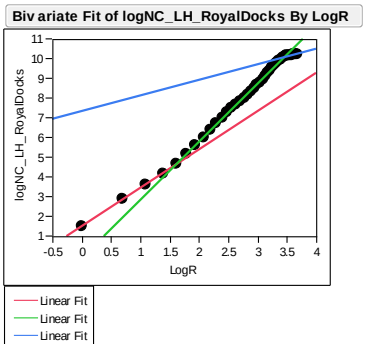

j. Beckton_E k. SH_NE_IsleofDogs l. LH_RoyalDocks

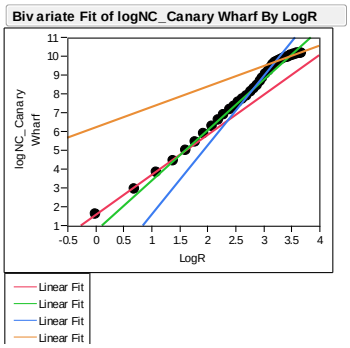

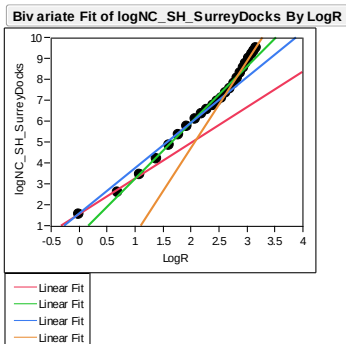

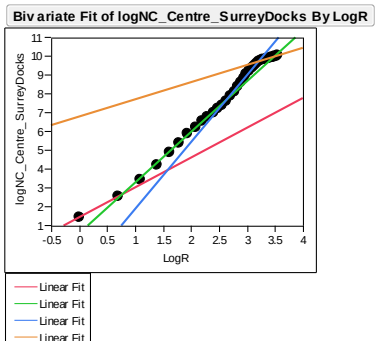

m. Canary Wharf n. SH_Surrey Docks o. Centre_Surrey Docks

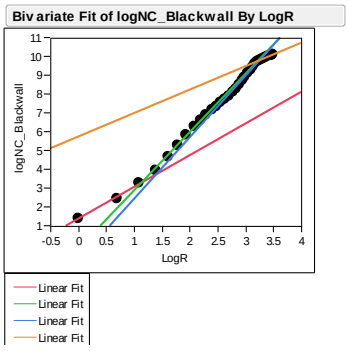

p. Blackwall

Fig. 6.10 The Topological Embeddedness trajectories of the Sixteen Smaller Areas (based on the axial maps). Red, green, blue and brown lines respectively indicate the regression lines generated within the first, second, third and fourth levels of radius ranges

(Beckton_N has two levels of radius ranges, some only have three levels and the others have four levels).

Tables 6.3 and 6.4 summarise power-law exponents, as well as the corresponding small radius ranges, and this numerically illustrates their topological embeddedness trajectories. The endpoint of each radius range denotes the radius at which the discontinuity along the topological trajectory is found (as mentioned earlier). Compared to the London and Beijing historic areas all having the first discontinuities consistently found at 2, both the larger development areas and the smaller areas in the Docklands have the first discontinuities marked out at different radii. This not only demonstrates that the Dockland areas have the different topological relationships with the first level of contexts (at least including their immediate surroundings), but also confirms that the London and Beijing historic areas have the consistent topological relationships with their immediate surroundings in terms of the values of topological depths (as mentioned in **Section 5.3.2**). This supports the argument that the Dockland areas are *not* topologically embedded into their surroundings in a consistent way, as the discontinuities on their topological embeddedness trajectories vary considerably.

Table 6.3 The Power-law Exponents (denoted as α) and the Corresponding Topological Radius Ranges of the Eight larger development areas (based on the axial analysis).

Area	Radius Range 1	α1	Radius Range 2	α2	Radius Range 3	α3	Radius Range 4	α4
Bermondsey	(1,3)	2.164	(3,15)	3.186	(15,40)	1.063		
Wapping	(1,4)	2.174	(4,16)	3.375	(16,40)	0.970		
Limehouse	(1,3)	2.084	(3,21)	2.961	(21,38)	0.915		
Poplar	(1,3)	2.240	(3,19)	2.791	(19,35)	1.236		
Surrey Docks	(1,14)	2.488	(14,24)	3.641	(24,29)	1.516	(29,40)	0.697

Isle of Dogs	(1,11)	2.356	(11,26)	3.211	(26,40)	1.178		
Beckton	(1,3)	2.037	(3,37)	2.601				
Royal Docks	(1,5)	1.845	(5,30)	3.028	(30,40)	1.654		
Mean value	Radius Range 1	2.220	Radius Range 2	3.109	Radius Range 3	1.146	Radius Range 4	0.697

Table 6.4 The Power-law Exponents (denoted as α) and the Corresponding Topological Radius Ranges of the Sixteen Smaller Areas (based on the axial analysis).

Smaller Area	Radius Range 1	α 1	Radius Range 2	α 2	Radius Range 3	α 3	Radius Range 4	α 4
W_Bermondsey	(1,4)	2.42	(4,13)	3.363	(13,40)	0.868		
E_Bermondsey	(1,3)	1.951	(3,9)	2.833	(9,18)	3.565	(18,40)	1.011
LH_Wapping	(1,3)	1.774	(3,16)	3.584	(16,40)	1.05		
SH_Wapping	(1,2)	1.762	(2,21)	3.052	(21,37)	0.832		
SH_Limehouse	(1,10)	2.618	(10,19)	3.144	(19,38)	1.018		
LH_Limehouse	(1,10)	2.614	(10,20)	3.121	(20,40)	0.918		
LH_IsleofDogs	(1,3)	1.407	(3,16)	3.214	(16,28)	3.451	(28,40)	0.871
SH_NW_IsleofDogs	(1,6)	2.523	(6,15)	1.525	(15,31)	3.815	(31,40)	0.739
SH_NE_IsleofDogs	(1,7)	2.4	(7,16)	1.921	(16,27)	3.876	(27,40)	0.813

Canary Wharf	(1,6)	2.123	(6,17)	2.672	(17,25)	3.679	(25,40)	1.089
Blackwall	(1,3)	1.683	(3,11)	3.097	(11,26)	3.261	(26,33)	1.253
Beckton_N	(1,17)	2.254	-17.32	2.452	(32,40)	0.931		
Beckton_E	(1,2)	1.74	(2,34)	2.562	(34,40)	1.291		
SH_Surrey Docks	(1,3)	1.702	(3,8)	2.681	(8,14)	2.175	(14,24)	4.132
Centre_Surrey Docks	(1,2)	1.585	(2,12)	2.693	(12,26)	3.561	(26,35)	0.909
LH_RoyalDocks	(1,5)	1.943	(5,30)	2.956	(30,40)	0.786		
Mean value	Radius Range 1	2.032	Radius Range 2	2.709	Radius Range 3	2.739	Radius Range 4	1.352

Table 6.4 also shows that the smaller areas selected from the same larger development areas, except for W_Bermondsey and E_Bermondsey, have similar power law exponents and the radius ranges in which the power law relationship were verified. This suggests that the smaller areas constituting the larger development areas have similar ways of embedding themselves into their different levels of contexts. However, the outliers of W_Bermondsey and E_Bermondsey demonstrate that the east part of Bermondsey, comparable to the west part, has one more radius range. This implies that the east part is embedded into the contexts in a relatively more fragmented way. Perhaps this might be associated with the situation that Bermondsey is located between the urbanised and the suburbanised districts.

We then further examined the relationship between the first and the second exponents denoting the paces at which those areas are topologically embedded into the first two levels of contexts, with an attempt to understand the embeddedness trajectories of the Dockland areas with less influence of the edge effect. As **Tables 6.3 and 6.4** show, all the endpoints of the first radius ranges are smaller than the radius-radius of 19, and this means that their first discontinuities are not influenced by the system edge. Although most of the larger development areas (except for

Bermondsey and Wapping) and some smaller areas have the second discontinuities found at the radius of larger than 19, the start points of the second ranges, namely the first discontinuities, are not affected by the system edge. This means that their second radius ranges - defined by the first and second discontinuities – is *not fully* affected by the system edge. Therefore, we will focus on the first and second exponents

The larger development areas (**Table 6.3**) and the smaller areas (**Table 6.4**) have smaller means of exponents within the first and second ranges (the mean α1 of 2.220 and the mean α2 of 3.109, and the mean α1 of 2.032 and the mean α2 of 2.709, respectively) than the London historic areas (2.556 and 3.251, see **Table 5.2**) and those of Beijing (2.447 and 3.336, see **Table 5.3**). It can be concluded that the Dockland areas, compared to the London and Beijing historic areas, *on average* are topologically embedded into the first two levels of contexts at a *slower* pace.This suggests that the new areas in the Docklands, *on average*, have a weaker topological relationship with either the immediate surrounding areas or the large-scale contexts.

However, several outliers, namely Bermondsey, Wapping and Surrey Docks selected from the larger development areas and W_Bermondsey, SH_Limehouse and LH_Limehouse from the smaller areas, have similar exponents within the first two ranges as the London and Beijing areas. This might be related to the historical structures of Bermondsey, Wapping, Limehouse and Surrey Docks.

We then investigated the relationship between the first and the second exponents, in order to achieve a better understanding of the discontinuities found between the first two levels of contexts for the Dockland areas. **Fig. 6.11 Left** shows a moderate correlation between the first and the second exponents found for the eight larger development areas, with an R-square of 0.364. As the first exponents of Surrey Docks and the Isle of Dogs (two peninsulas in the London Docklands) measure the embeddedness paces within relatively wider radius ranges, one of which is from 1 to 14 and the other is from 1 to 11 (**Table 6.3**), we excluded these two development areas and then re-conducted a correlation analysis for the rest. **Fig. 6.11 Middle** demonstrates that no correlation was found for the other six larger development areas, with an R-square of 0.022. This indicates that a moderate correlation for the eight larger development

areas is more or less influenced by Surrey Docks and the Isle of Dogs. It demonstrates that the paces at which the eight larger development areas are topologically embedded into the second level of contexts do *not* depend on the paces at which they are topologically embedded into the first level of contexts. Therefore, it suggests that the eight larger development areas have different discontinuities found between the two levels of contexts, and so that they can to some degree be differentiated from each other.

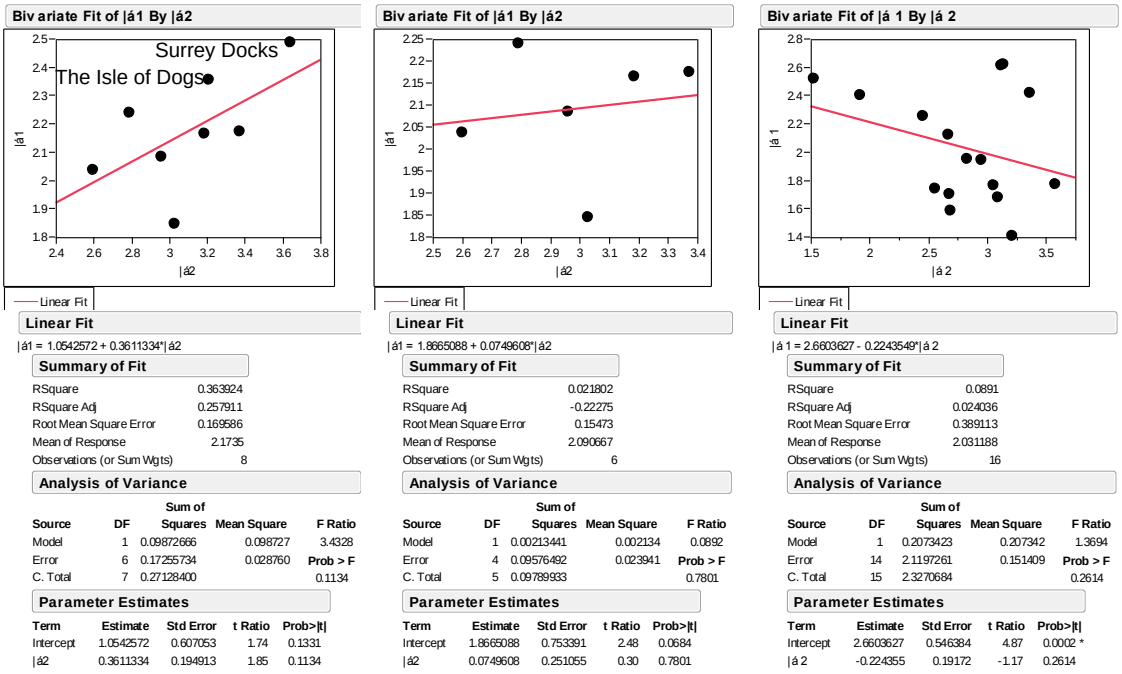

Left: A moderate correlation between the first and the second exponents was found for the eight larger development areas , with an R-square of 0.364 (but this is more or less affected by Surrey Docks and the Isle of Dogs whose first exponents calculated within relatively wide ranges);

Middle: No correlation between the first and the second exponents was found for the six development areas (excluding Surrey Docks and the Isle of Dogs);

Right: No correlation was found for the sixteen smaller areas.

Fig. 6.11 The Correlations between the First and the Second Topological Exponents for The Eight larger development areas and The Sixteen Smaller Areas Respectively (based on the axial map).

In addition, **Fig. 6.11 Right** shows that no correlation between the first and the second exponents was found for the sixteen smaller areas, with an R-square of 0.089. This indicates that the paces at which the smaller areas are topologically embedded into the two levels of contexts are not interdependent. As a result, these sixteen smaller developments also can be distinguished by the ways in which they are topologically embedded into the two levels of contexts.

Metric embeddedness trajectories (based on the segment map)

We continued by examining the metric embeddedness trajectories of the larger development areas and the smaller areas, illustrated in **Fig. 6.12 and 6.13**, respectively. As with the London and Beijing historic areas, the metric embeddedness trajectories of these newly developed areas are much straighter than their topological embeddedness trajectories (**Fig. 6.9 and 6.10**). However, these metric trajectories are also slightly bended, and a stronger power-law relationship between mean node count and metric radius can be identified within smaller radius ranges. **Fig. 6.12 and 6.13** show the regression lines in the log-log radius plots, and the intersections between the consecutive regression lines denote the discontinuities along the metric trajectories. But compared to the London and Beijing cases (**Fig. 5.12 and 5.13**), the angle between the consecutive regression lines in the Docklands, in general, is larger. In other words, the metric embeddedness trajectories of the historic areas in London and Beijing, on average, are straighter than those in the Docklands. This suggests that the newly developed areas are *metrically* added up to the overall structure of the London Docklands in an *inconsistent* way, in contrast to the named areas in the historic districts of London and Beijing.

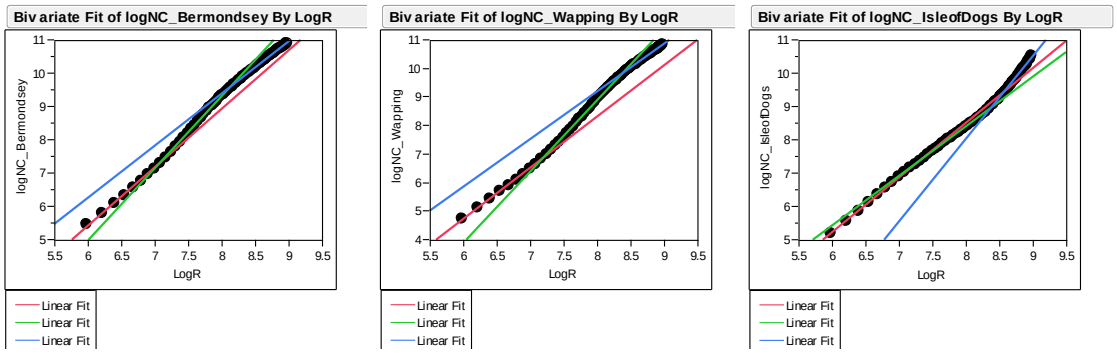

a. Bermondsey b. Wapping c. The Isle of Dogs

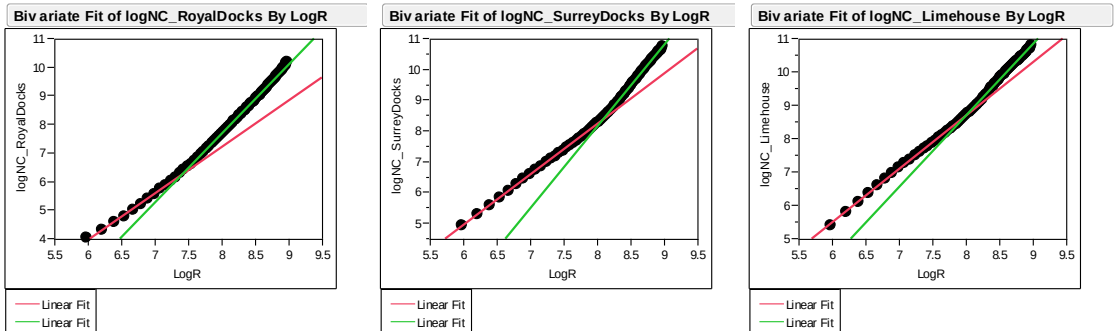

d. Royal Docks e. Surrey Docks f. Limehouse

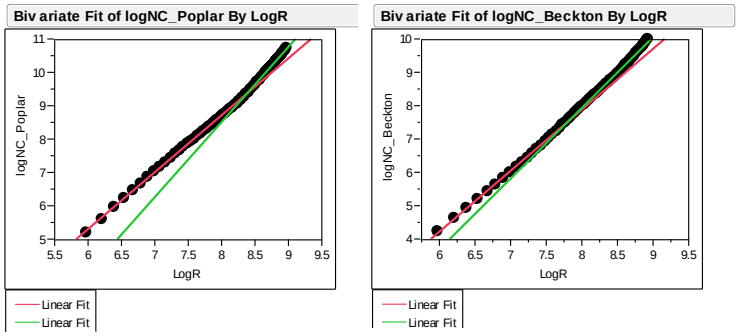

g. Poplar h. Beckton

Fig. 6.12 The Metric Embeddedness trajectories of the Eight larger development areas (based on the segment map). Red, green, blue lines respectively indicate the regression lines generated within the first, second and third levels of radius ranges (some areas only have two levels of radius ranges and the others have three levels).

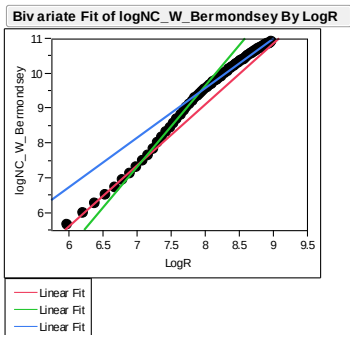

a. W_Bermondsey

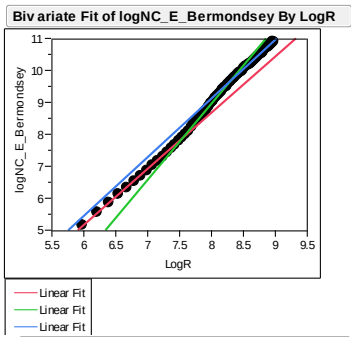

b. E_Bermondsey

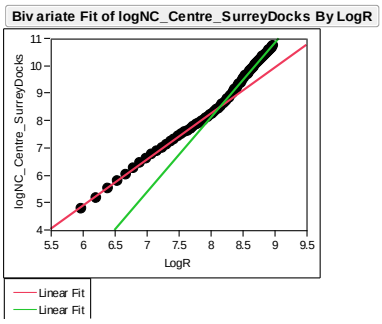

c. Centre_Surrey Docks

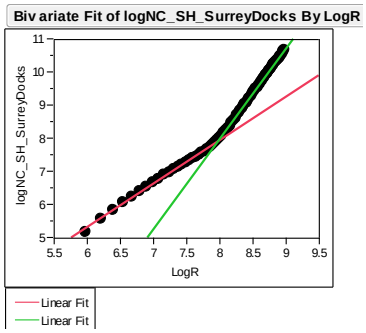

d. SH_Surrey Docks

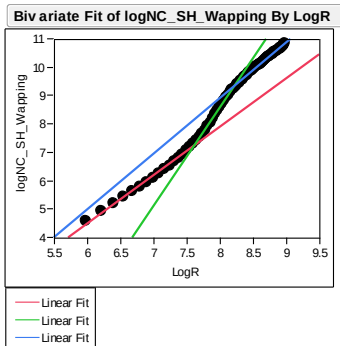

e. SH_Wapping

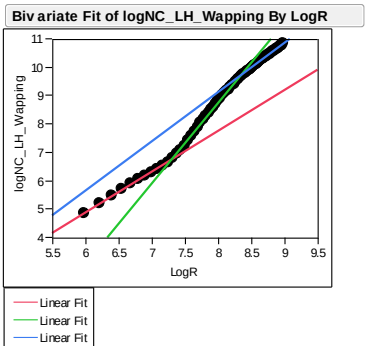

f. LH_Wapping

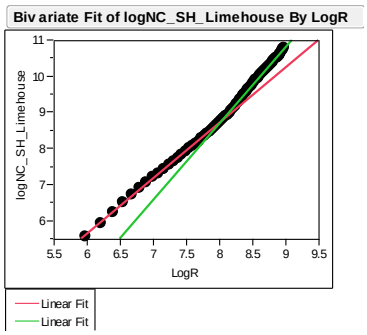

g. SH_Limehouse

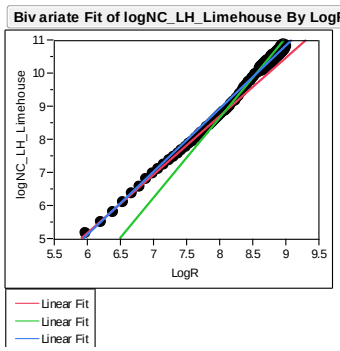

h. LH_Limehouse

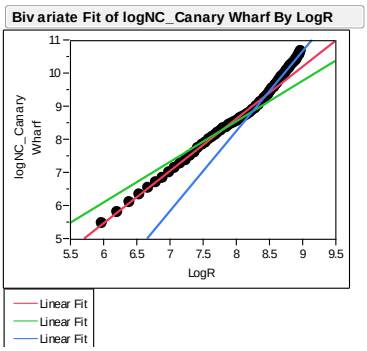

i. Canary Wharf

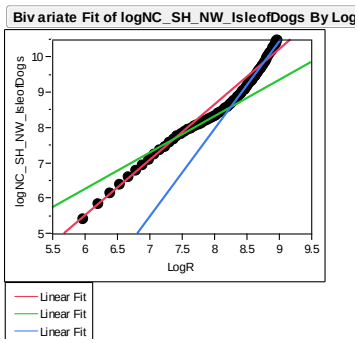

j. SH_NW_IsleofDogs

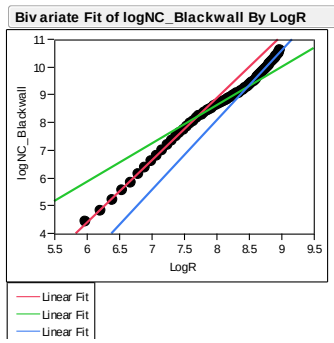

k. Blackwall

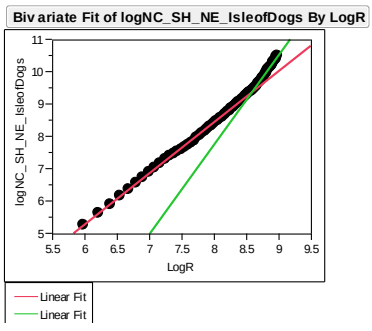

l. SH_NE_IsleofDogs

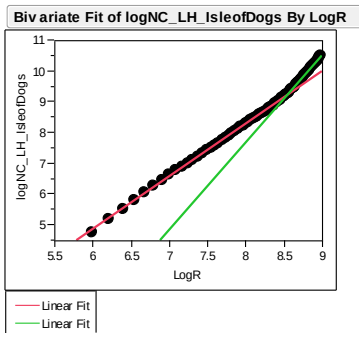

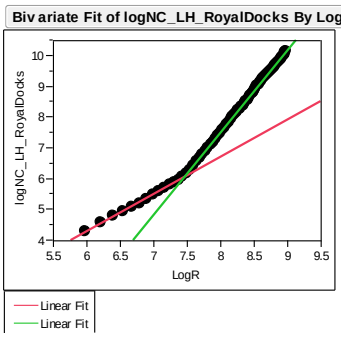

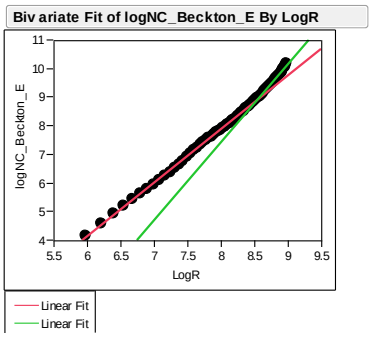

m. LH_IsleofDogs n. LH_RoyalDocks o. Beckton_E

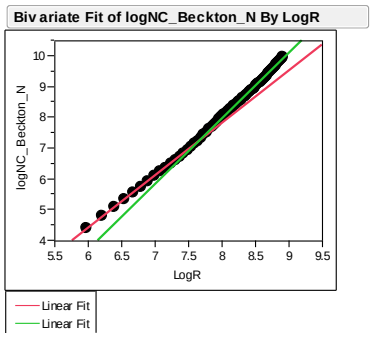

p. Beckton_N

Fig. 6.13 The Metric Embeddedness trajectories of the Sixteen Development Areas (based on the segment map). Red, green, blue lines respectively indicate the regression lines generated within the first, second and third levels of radius ranges (some areas only have two levels of radius ranges and the others have three levels).

Tables 6.5 and 6.6 show their power-law exponents, as well as the corresponding small radius ranges, and this numerically illustrates their metric embeddedness trajectories. Once again, the endpoint of each radius range denotes the radius at which the discontinuities between two neighbouring levels of contexts are marked out, and meanwhile the radius ranges themselves represent the continuous contexts at certain levels. The endpoints of the first ranges are smaller than the system radius of 8000m, and this means that the first discontinuities found between the first two levels of contexts are least affected by the system edge.

Table 6.5 The Power-law Exponents (denoted as α) and the Corresponding Metric Radius Ranges of the Eight larger development areas (based on the segment analysis).

Area	Radius Range 1	α1	Radius Range 2	α2	Radius Range 3	α3
Bermondsey	(400-1500)	1.754	(1500-3400)	2.173	(3400-8000)	1.564
Wapping	(400-1500)	1.793	(1500-4700)	2.511	(4700-8000)	1.671
Isle of Dogs	(400-1800)	1.639	(1800-4300)	1.492	(4300-8000)	2.477
Royal Docks	(400-1500)	1.624	(1500-8000)	2.412		
Surrey Docks	(400-3300)	1.641	(3300-8000)	2.646		
Limehouse	(400-3300)	1.601	(3300-8000)	2.139		
Poplar	(400-5000)	1.707	(5000-8000)	2.248		
Beckton	(400-2400)	1.826	(2400-7700)	2.122		
Mean value	Radius Range 1	1.698	Radius Range 2	2.218	Radius Range 3	1.904

Table 6.6 The Power-law Exponents (denoted as α) and the Corresponding Metric Radius Ranges of the Sixteen Smaller Areas (based on the segment analysis).

Area	Radius Range 1	α1	Radius Range 2	α2	Radius Range 3	α3
W_Bermondsey	400-1500	1.755	1500-2700	2.334	2700-8000	1.422
E_Bermondsey	400-2100	1.762	2100-3900	2.389	3900-8000	1.838
Centre_Surrey Docks	400-3800	1.683	3800-8000	2.719		
SH_Surrey Docks	400-2800	1.317	2800-8000	2.739		
SH_Wapping	400-2200	1.710	2200-3600	3.483	3600-8000	1.961
LH_Wapping	400-1600	1.440	1600-4500	2.836	4500-8000	1.729
SH_Limehouse	400-3500	1.530	3500-8000	2.121		
LH_Limehouse	400-3600	1.770	3600-5600	2.411	5600-8000	1.898
Canary Wharf	400-2600	1.578	2600-3700	1.229	3700-8000	2.419

SH_NW_IsleofDogs	400-1900	1.573	1900-3700	1.035	3700-8000	2.480
Blackwall	400-2300	2.246	2300-4600	1.378	4600-8000	2.517
SH_NE_IsleofDogs	400-5500	1.580	5500-8000	2.776		
LH_IsleofDogs	400-5200	1.712	5200-8000	2.840		
LH_Royal Docks	400-1800	1.213	1800-8000	2.673		
Beckton_E	400-5300	1.881	5300-8000	2.731		
Beckton_N	400-2300	1.704	2300-7500	2.103		
Mean value	Radius Range 1	1.653	Radius Range 2	2.362	Radius Range 3	2.033

At first sight, all the new areas at least have two radius ranges representing two levels of contexts. As **Tables 6.5** shows, Bermondsey, Wapping and Royal Docks have the first discontinuities at 1500m, but their second discontinuities found at different radii; Surrey Docks and Limehouse only have the first discontinuities identified at 3300m; and the other areas have the first discontinuities identified at different radii. As **Tables 6.6** displays, nearly all of smaller areas (except for Blackwall and Beckton_N) have the first discontinuities at different radii, but the second discontinuities of two outlier areas are identified at different radii. Compared to the historic areas in London and Beijing, this not only suggests that the newly developed areas can be more easily distinguished in relation to the discontinuities between the first two levels of contexts, but also confirms that the overall area structure of the London Dockland is inconsistent, compared to the historic districts of London and Beijing.

Then we further investigated the power-law exponents calculated within the first two ranges. This enables us to understand how the newly developed areas are metrically embedded into the first two levels of contexts. We first sought to capture an overall picture by examining the mean values. Compared to the London and Beijing historic areas (with the mean α1 of 1.859 and 1.791, respectively displayed in **Tables 5.4 and 5.5**), the larger development areas (**Table 6.5**) and the smaller areas (**Table 6.6**), *on average*, have smaller first exponents (1.714 and 1.653, respectively). This demonstrates that the new areas in the Docklands, *on average*, are metrically embedded into their first level of contexts, roughly representing the immediate

surroundings, at a slower average pace. This suggests that the Dockland areas, in contrast to the historic areas in London and Beijing, are more metrically separated from their immediate surroundings. For each Dockland area, its surroundings may include other Dockland areas. Perhaps this supports the previous finding (indicated in **Section 6.3.1**) that the Dockland areas are more metrically isolated to each other.

This is further confirmed by investigating the second exponents. The larger development areas and the smaller areas *on average* have larger second exponents (2.218 and 2.362, respectively), than the London and Beijing historic areas (1.699 and 1.868, respectively). This means that the Dockland areas are embedded into the second level of contexts, denoting the further contexts, at a quicker average pace. In other words, perhaps these Dockland areas in general encounter the intensively developed areas (e.g. housing estates with small-scale blocks) at high radii, and therefore their second paces on average become quicker. To a large extent, it can be suggested that the Dockland areas, though extensively intensified, are not well-connected.

However, if examining each individual Dockland area, a complex and informative scenario will be revealed. All of them have lower first exponents and higher second exponents, except for the Isle of Dogs (shaded in light yellow in **Table 6.5**) as well as Canary Wharf, Blackwall(a luxury housing estate) and SH_NW_IsleofDogs (a social housing estate) (coloured in light yellow in **Table 6.6**). The Isle of Dogs has the first exponent (1.639) larger than the second exponent (1.492), although the third exponent (2.477) is the largest. This suggests that the Isle of Dogs, as the focus of the redevelopment initiated by the LDDC (1998) and a peninsula, has a better relationship with the immediately surroundings; but encounters relatively less developed areas between itself and Central London, as the second level of context; and then meets highly intensified areas – comprising the City with very smaller blocks – at a high radius of larger than 4300m, as the third level of contexts. It was confirmed by examining Canary Wharf, Blackwall and SH_NW_IsleofDogs that also have smaller second exponents than the first and third exponents. However, the other smaller areas located in the Isle of Dogs, such as SH_NE_IsleofDogs (a social housing estate) and LH_IsleofDogs (a luxury housing estate), have higher second exponents than the first exponents. This demonstrates that the smaller areas

belonging to the Isle of Dogs are metrically embedded into the different levels of contexts in the different ways. By and large, it can be suggested that the individual smaller areas also aggregate to form the large-scale development areas in an inconsistent way.

In addition, **Fig. 6.14** further demonstrates that no correlation was found between the first and the second exponents for either the eight larger development areas (**Left**) and for the sixteen smaller areas (**Right**). It shows that the paces at which those new areas are metrically embedded into the first level of contexts have no impact on the paces at which they are embedded into the second level of contexts. In this sense, the metric discontinuities found between the two levels of contexts are not interdependent. Therefore, these new areas can be differentiated according to their metric relationships to the different levels of contexts.

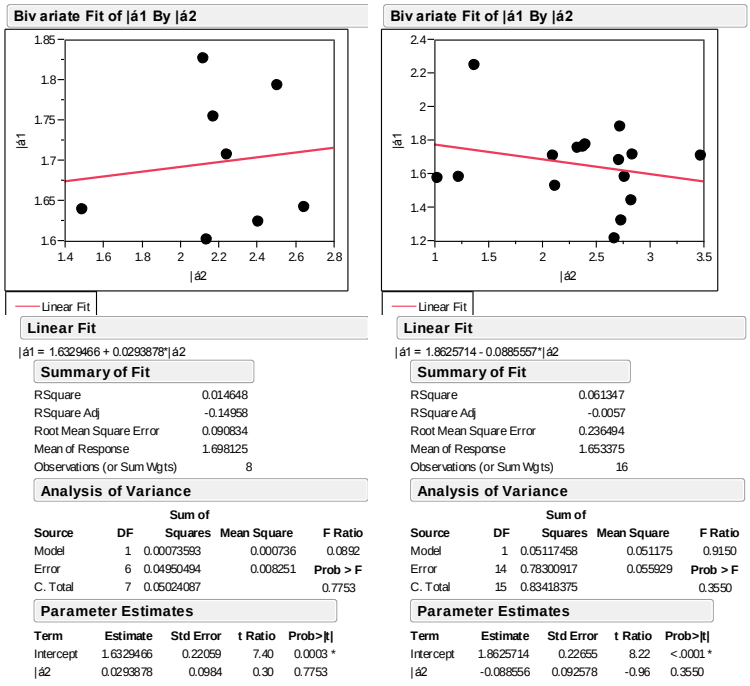

Left: No correlation between the first and the second exponents for the eight larger development areas ;

Right: No correlation between the first and the second exponents for the sixteen smaller areas.

Fig. 6.14 The Correlations between the First and the Second Metric Exponents for The Dockland Areas (based on the segment maps).

Then *can we simulate the newly developed areas regarding their contexts, with an attempt to further elaborate the extent to which these Dockland areas are spatially different from the historic areas in London and Beijing?*

6.4. Do the created patches relate to the newly developed areas?

In **Sections 4.3.3 and 4.4** of chapter four, it showed that the periodic patchwork patterns can be mathematically generated in the London Docklands*. Do the Dockland a*reas, *including the larger development areas and the smaller areas, have any relationship with those patchwork patterns?* This also aims to explore whether the generative technique of creating the patchwork pattern can be applied to the investigation of the newly developed areas. Since a much stronger patchwork pattern of the London Docklands was created by the variables of metric embeddedness pace and metric mean depth (MMD), rather than the topo-embeddedness pace, this section focuses on the patches generated by the first two variables respectively.

6.4.1 The visual relation between the new areas and the patches created by metric embeddedness pace

We first conducted a comparison between the new areas and the patches created by metric embeddedness pace (that more focuses on the contexts, as discussed in chapter four). The segment model of the Docklands was indexed and coloured according to the metric embeddedness paces at the radius of 400m to 10,000m, with an interval scale of 400m. Red indicates low values, and blue denotes high values. The boundaries of the eight larger development areas and of the sixteen smaller areas were, respectively, superimposed on the created patchwork patterns, seeking to investigate whether the boundaries new areas might match the boundaries of those mathematically created patches.

All the larger development areas, except Wapping, are not marked out across radii (**Fig. D3.1 – D3.6, Appendix D**). For example, **Fig. 6.15** illustrates the patchwork pattern created by the metric embeddedness pace from 800m to 1200m, and superimposed by the artificial boundaries of the eight larger development areas. Wapping is roughly distinguished as a red patch. As for

the other development areas, smaller patches appear within or across their boundaries, and this suggests those areas, together with their immediate surroundings, are divided into smaller parts at the radius of 800m to 1200m. For instance, a red patch is located between Limehouse and Popular, which implies a metrically integrated space situated between these two areas. The above analysis indicates that all the larger development areas, except Wapping, *cannot* be roughly distinguished by their pace of metric embeddedness.

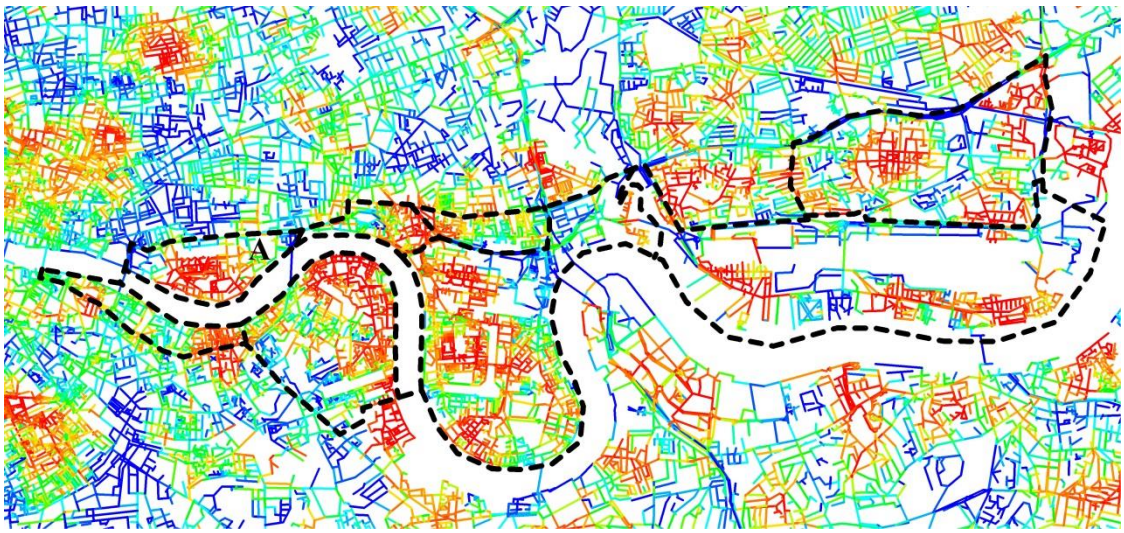

Fig. 6.15 The Patchwork Pattern Generated by Metric Embeddedness pace at the Radius of 800m to 1200m, and Superimposed by the Boundaries of the Eight larger development areas . Wapping (A) is roughly market out.

We then sought to examine whether the created patches visually co-incide with the smaller areas. All the smaller areas, except Bermondsey_E (the east of Bermondsey), Centre_SurreyDocks (a central area in Surrey Docks) and SH_SurreyDocks (a social housing estate in Surrey Docks), are distinguished at certain radius. **Fig. 6.16a**, for example, shows SH_Wapping (a social housing estate in Wapping), SH_NW_IsleofDogs (a social housing estate in the northwest of the Isle of Dogs) and LH_RoyalDocks (a luxury housing estate in Royal Docks) are roughly differentiated at the radius of 400m to 800m, though not perfect; **Fig. 6.17 b** demonstrates that LH_IsleofDogs (a luxury housing estate in the Isle of Dogs), Blackwall (a luxury housing in Blackwall) and LH_RoyalDocks are marked out at the radius of 500m to 900m; **Fig. 6.17 c** illustrates that LH_Limehouse (a luxury housing estate in Limehouse) , Canary Wharf, LH_RoyalDocks and Beckton_N (an area in the north of Beckton) are

differentiated at the radius of 700m to 1100m; **Fig. 6.17 d** demonstrates that Bermondsey_W (the west of Bermondsey) , LH_Wapping (a luxury housing estate in Wapping), SH_Wapping, Blackwall and LH_RoyalDocks are marked out at the radius of 1200m to 1600m. **Fig. 6.17e** shows that SH_Wapping, Blackwall, Beckton_N and Beckton_E (an estate in the east of Beckton) are distinguished at the radius of 1700m to 2100m. **Fig. 6.17 f** illustrates that LH_Limehouse, Blackwall and Beckton_N are marked out at the radius of 2000m to 2400m. **Fig. 6.17 g** displays that Beckton_E is marked out at the radius of 2600m to 3000m. **Fig. 6.17 h** shows that SH_Limehouse, Canary Wharf and SH_NE_IsleofDogs (a social estate in the northeast of the Isle of Dogs) are marked out at the radius of 3600m to 4000m. **Fig. 6.17 i** illustrates that SH_Wapping, SH_NE_IsleofDogs, Beckton_N and Beckton_E are marked out at the radius of 4800m to 5200m. And **Fig. 6.17 j** demonstrates that SH_Wapping, SH_NE_IsleofDogs and Blackwall are marked out at the radius of 8400m to 8800m. The above illustrations indicate that most of the smaller areas, more or less, seem to have a kind of visual corresponding relationship with the patches created at different radii, albeit not perfectly.

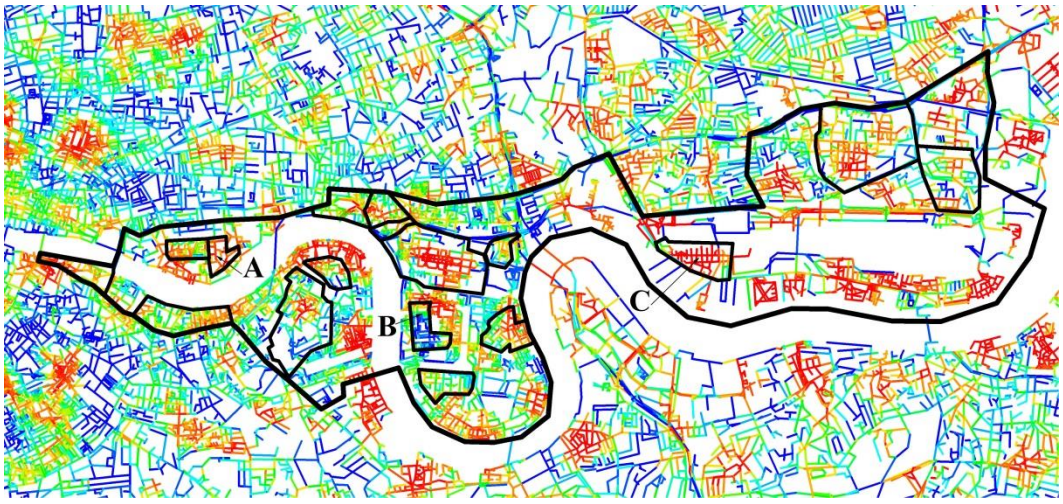

a. SH_Wapping (A), SH_NW_IsleofDogs (B) and LH_RoyalDocks (C) were roughly marked out by metric embeddedness pace at the radius of 400m to800m.

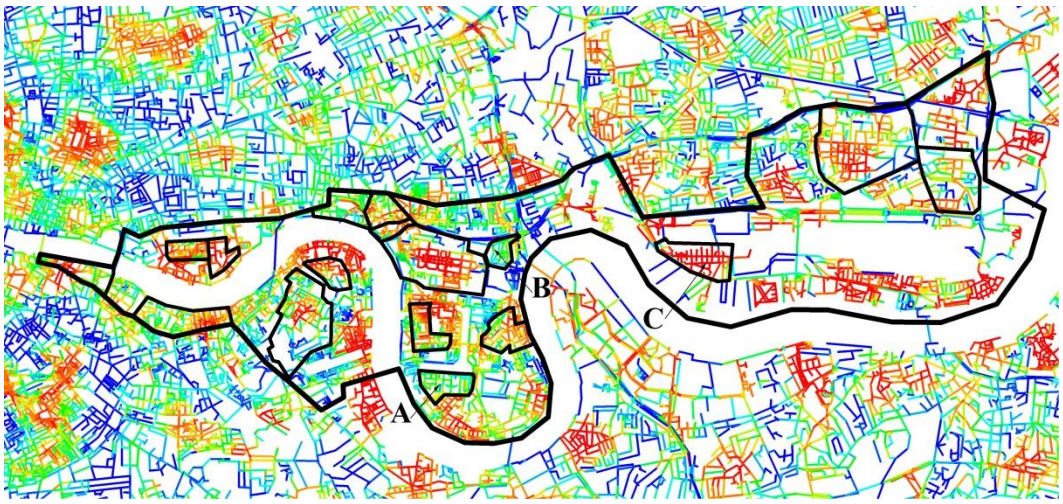

b. LH_IsleofDogs (A), Blackwall (B) and LH_RoyalDocks (C) are roughly marked out by metric embeddedness pace at the radius of 500m to 900m.

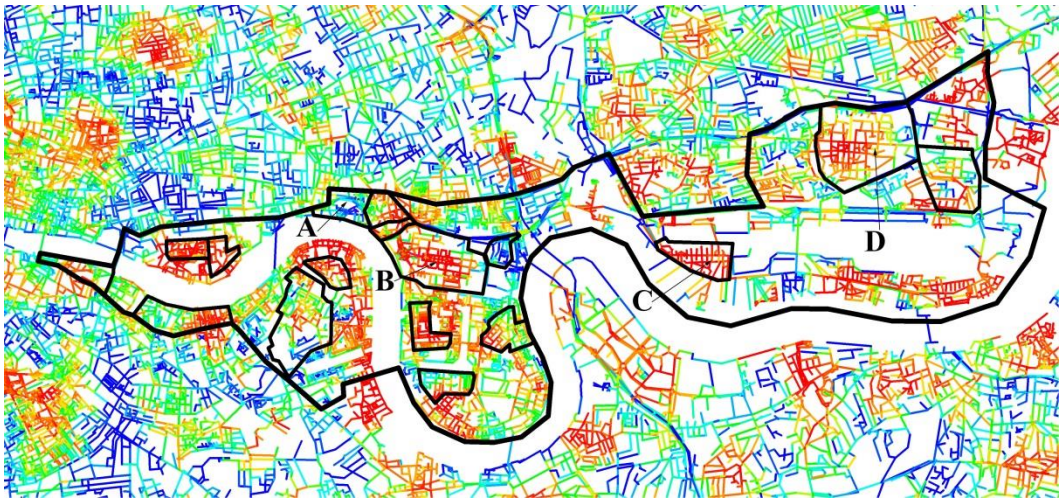

c. LH_Limehouse (A) , Canary Wharf (B), LH_RoyalDocks (C) and Beckton_N (D) are roughly marked out by metric embeddedness pace at the radius of 700m to 1100m.

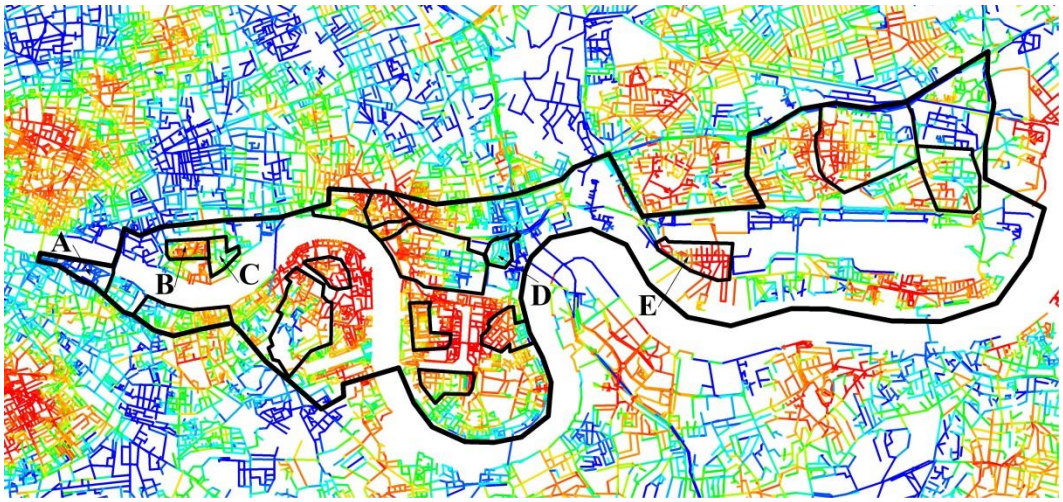

d. Bermondsey_W (A) , LH_Wapping (B), SH_Wapping (C), Blackwall (D) and LH_RoyalDocks (E) are roughly marked out by metric embeddedness pace at the radius of 1200m to 1600m.

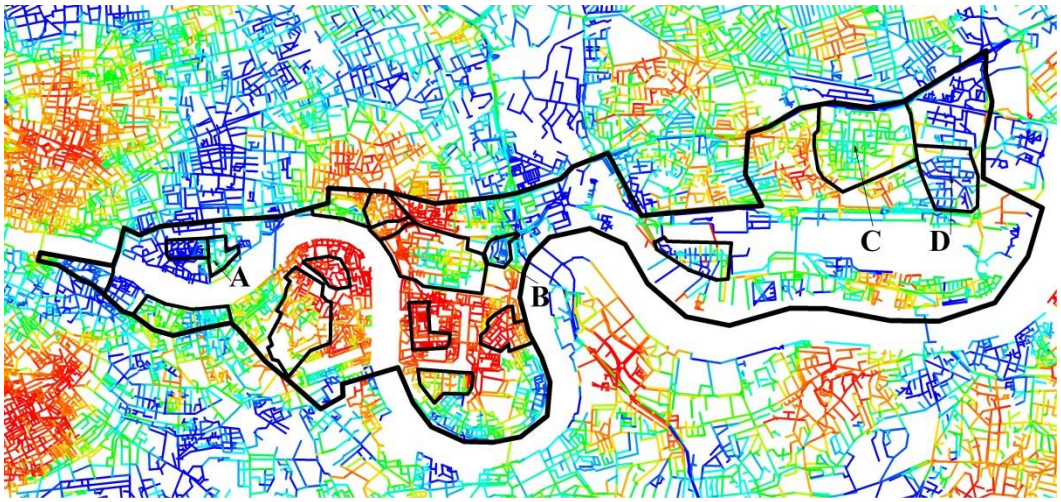

e. SH_Wapping (A), Blackwall (B), Beckton_N (C) and Beckton_E (D) are roughly marked out by metric embeddedness pace at the radius of 1700m to 2100m.

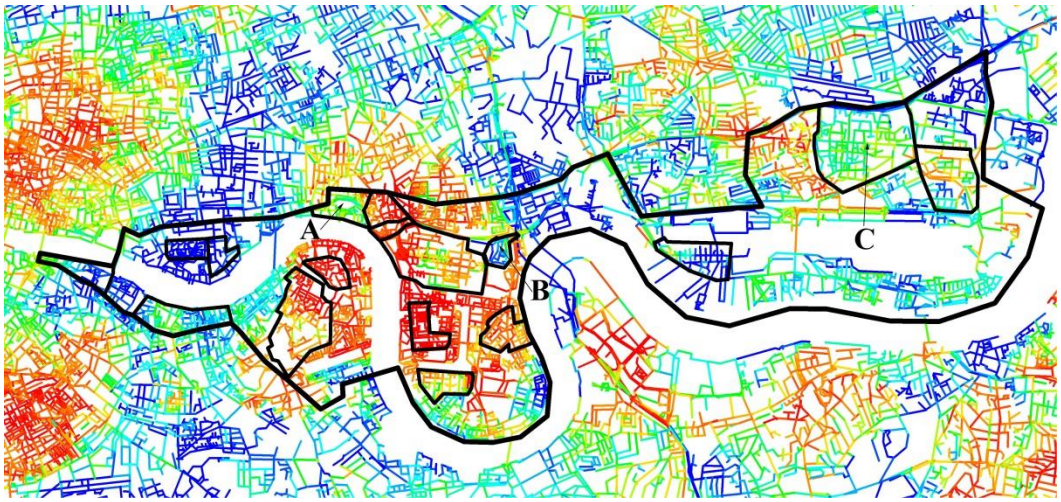

f. LH_Limehouse (A), Blackwall (B) and Beckton_N (C) are roughly marked out by metric embeddedness pace at the radius of 2000m to 2400m.

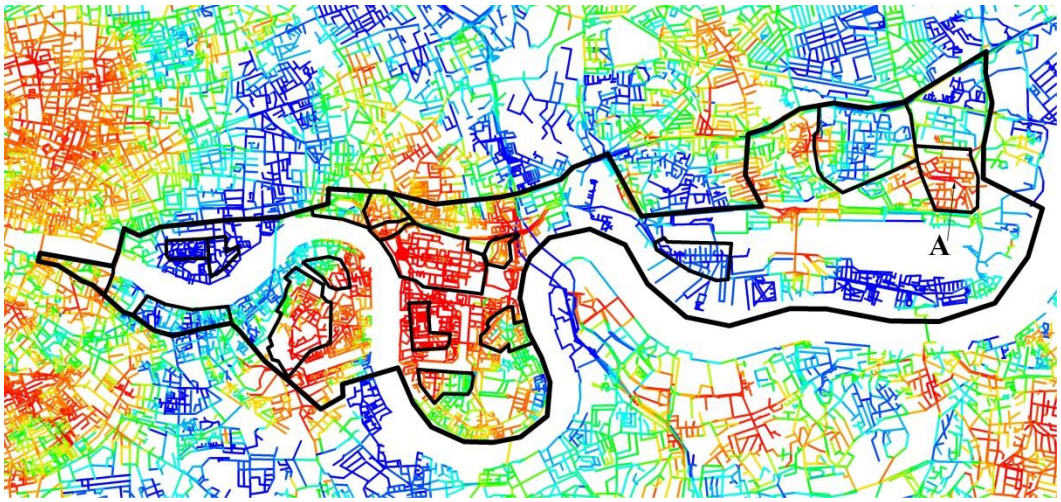

g. Beckton_E (A) is roughly marked out by metric embeddedness pace at the radius of 2600m to3000m.

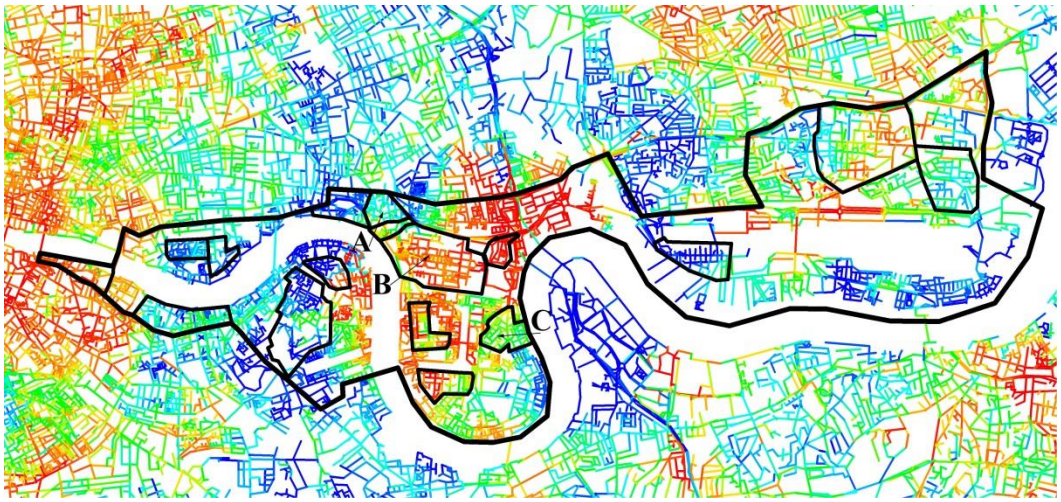

h. SH_Limehouse (A), Canary Wharf (B) and SH_NE_IsleofDogs (C) are roughly marked out by metric embeddedness pace at the radius of 3600m to 4000m.

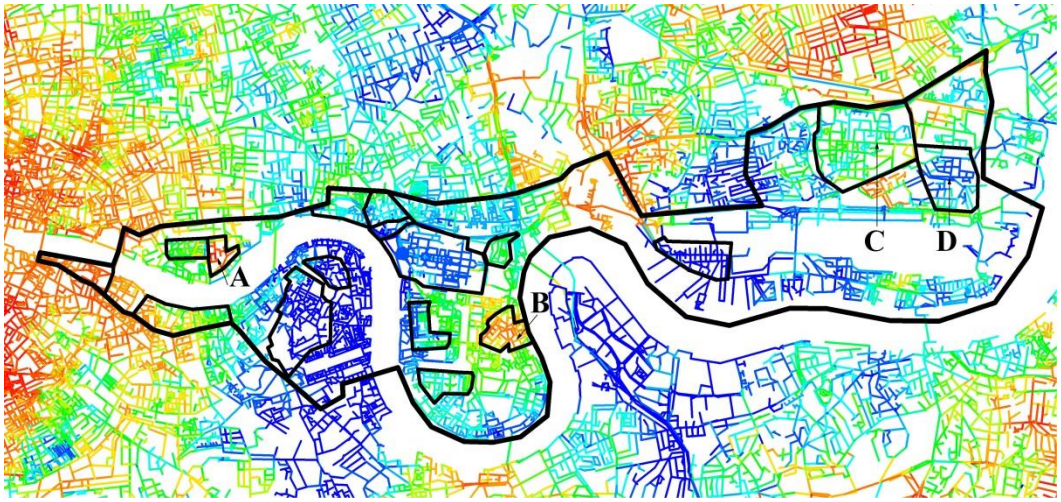

i. SH_Wapping (A), SH_NE_IsleofDogs (B), Beckton_N(C) and Beckton_E (D) are roughly marked out by metric embeddedness pace at the radius of 4800m to 5200m.

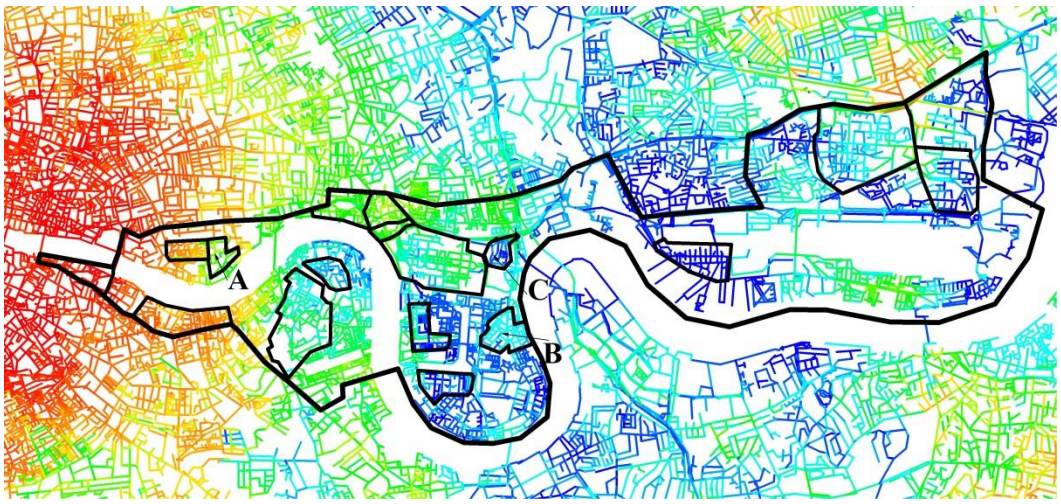

j. SH_Wapping (A), SH_NE_IsleofDogs (B) and Blackwall (C) are roughly marked out by metric embeddedness pace at the radius of 8400m to 8800m.

Fig. 6.16 The Smaller Areas Identified by Metric Embeddedness pace at Different Radii.

Fig. 6.16 also demonstrates that the smaller areas are *not* identified all at once. For example, some smaller areas, such as SH_Wapping, are distinctive when comparing their spatial relations to the immediate surroundings; whilst, other areas, such as Beckton_N, come into sight when comparing themselves with their medium scale contexts. It can therefore be suggested that most of the smaller areas (except three outliers), associated with the created patches, are not spatially structured at the same scale, but were built at the different scales. In this sense, it can be argued that the spatial formation of those smaller areas is mainly influenced by their different scaled contexts, rather than their artificial boundaries.

Compared to the named areas investigated in the previous chapter, some smaller areas are however repeatedly marked out at several different radii, and the patches associated with those smaller areas are reluctant to be merged into the surroundings to form a larger patch at higher radii. For example, LH_RoyalDocks (a luxury housing estate in Royal Docks, namely Silvertown) are marked out at 400m to 800m, 500m to 900m, 700m to 1100m, and 1200m to 1600m, respectively (**Fig. 6.17**). In particular, at the high radius range of 8400m to 8800m, SH_Wapping, SH_NE_IsleofDogs and Blackwall as three relatively small estates, still can be marked out as small created patches (**Fig. 6.16j**). It suggests that the smaller areas have not been spatially integrated with each other to form a larger and coherent entity at a larger scale.

This confirms the previous finding that nearly all the larger development areas *cannot* be marked out, and meanwhile this also supports the argument that the London Docklands are metrically fragmented, meaning that the new areas are not metrically fit into the overall structure in a consistent way (discussed in the previous section).

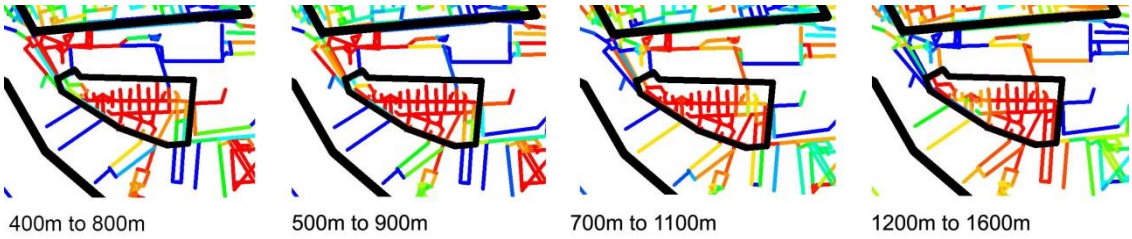

Fig. 6.17 An Example of LH_RoyalDocks (A Luxury Housing Estate in Royal Docks, or Called Silvertown). It is marked out at 500m to 900m, 700m to 1100m, and 1200m to 1600m, respectively.

6.4.2 The visual relationship between the new areas and the patches created by metric mean depth (MMD)

We then continued to make a visual comparison between the new areas and the patches generated by another variable of MMD that gives more weight to internal layouts. Following the procedure we made in the previous section, the segment model of the Docklands was then indexed and coloured according to the MMD values at the radius of 400m to 10,000m, with an interval of 100m. Red indicates low values, and blue denotes high values. Those images were, respectively, superimposed by the boundaries[120] of the eight larger development areas and of the sixteen smaller areas, with an attempt to examine whether the boundaries of the new areas correspond to the boundaries of the created patches.

Fig. 6.18, for example, shows the created patchwork pattern at 1200m, and the dotted lines represent the boundaries of the eight larger development areas. All the development areas, except Wapping, seem *not* to be roughly marked out. For instance, a red patch comes into sight on the boundary between Limehouse and Poplar. We also examined the patchwork patterns

[120] For an introduction of the boundaries of those newly developed areas, see Section 6.2.

generated at other radii. Surrey Docks is approximately distinguished at 2500m (**Fig. 6.19**), but the other larger development areas were not identified across radii (**Fig. D3.13 – D3.18, Appendix D**). For example, **Fig. 6.19** shows that a red patch extends outside the boundary of the Isle of Dogs. This demonstrates that all the larger development areas, except Wapping and Surrey Docks, can *not* be distinguished by the variable of MMD either.

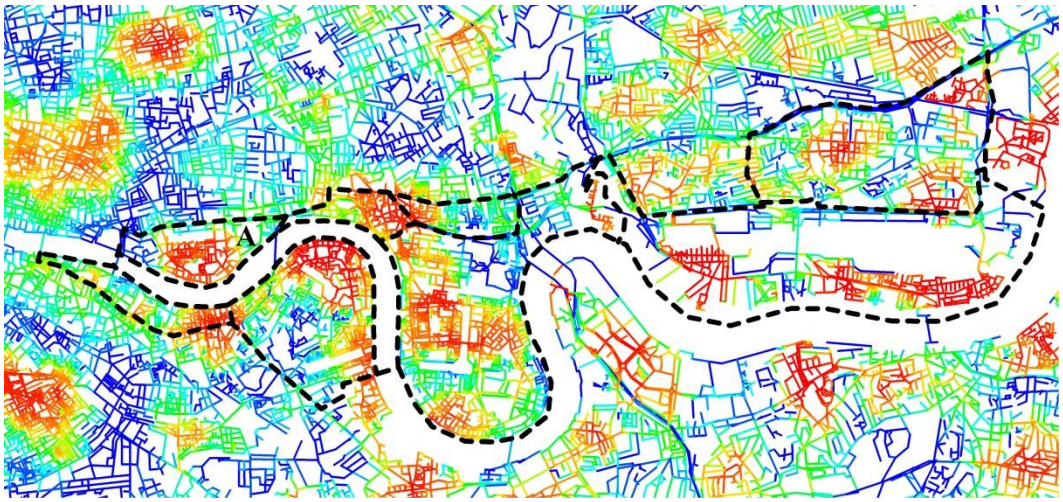

Fig. 6.18 The Patchwork Pattern Generated by MMD at the Radius of 1200m and Superimposed by the Boundaries of the Eight Larger Development Areas. Wapping (A) roughly distinguished at 1200m.

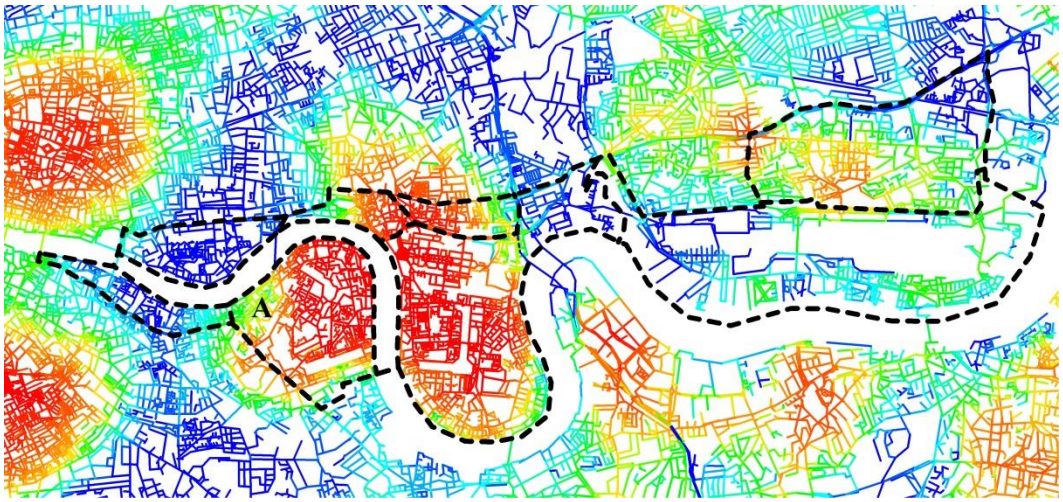

Fig. 6.19 The Patchwork Pattern Generated by MMD at the Radius of 2500m and Superimposed by the Boundaries of the Eight Larger Development Areas. Surrey Docks (A) is roughly distinguished at 2500m.

We continued by presenting an analysis of the smaller areas. All of them, except Bermondsey_E, Canary Wharf and SH_Surrey Docks, are roughly identified at some certain radii, although not perfect again. SH_Wapping, SH_NW_IsleofDogs, Blackwall and LH_RoyalDocks are almost differentiated at 600m (**Fig. 6.20a**); LH_Wapping, SH_Wapping and LH_RoyalDocks marked out at 750m (**Fig. 6.21b**); LH_Limehouse, SH_Limehouse, SH_NE_IsleofDogs and LH_RoyalDocks distinguished at 800m (**Fig. 6.21c**); SH_NW_IsleofDogs, LH_IsleofDogs, SH_NE_IsleofDogs, LH_RoyalDocks and Beckton_N differentiated at 1000m (**Fig. 6.21d**); Centre_SurreyDocks, LH_IsleofDogs, Blackwall and Beckton_N marked out at 1200m (**Fig. 6.21e**); Bermondsey_W, LH_IsleofDogs and Beckton_E marked out at 1400m (**Fig. 6.21f**); LH_Wapping, SH_Wapping and Beckton_E marked out at 1800m (**Fig. 6.21g**). Considering that nearly all the development areas cannot be marked out and those smaller areas were selected from those larger areas, the above analysis also supports the argument that the London Docklands are constituted by a group of smaller new areas without good connections and therefore nearly all the larger development areas - defined by the LDDC (The London Dockland Development Cooperation) – have not been evolved into the urbanised and consolidated areas, the same as the named areas found in the central districts of London and Beijing.

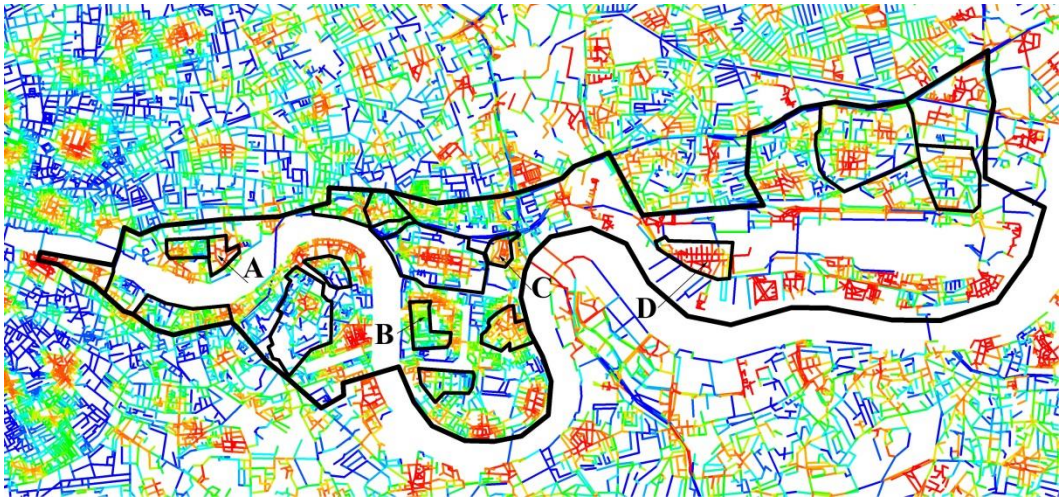

a. SH_Wapping (A), SH_NW_IsleofDogs (B), Blackwall (C) and LH_RoyalDocks (D) are roughly marked out by by MMD at 600m.

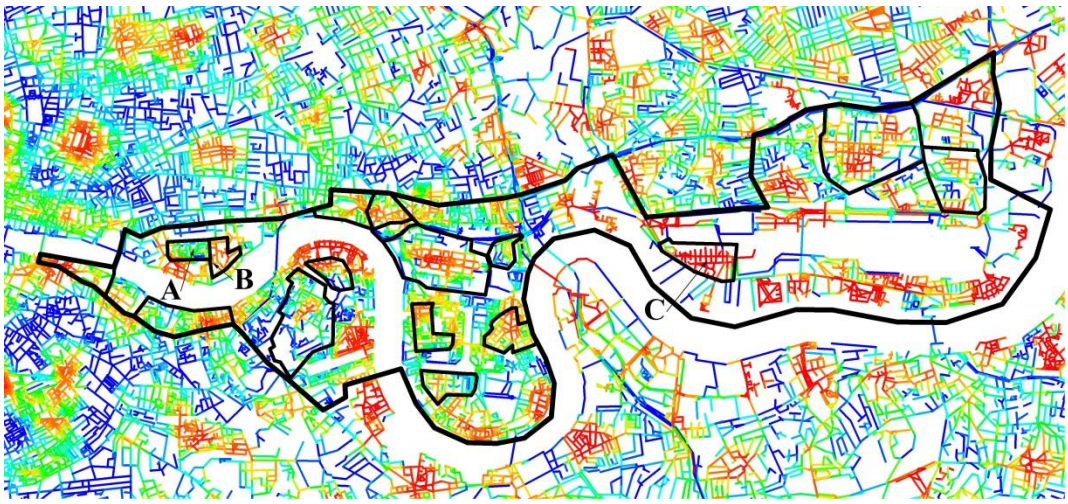

b. LH_Wapping (A), SH_Wapping (B) and LH_RoyalDocks (C) are roughly marked out by MMD at 750m.

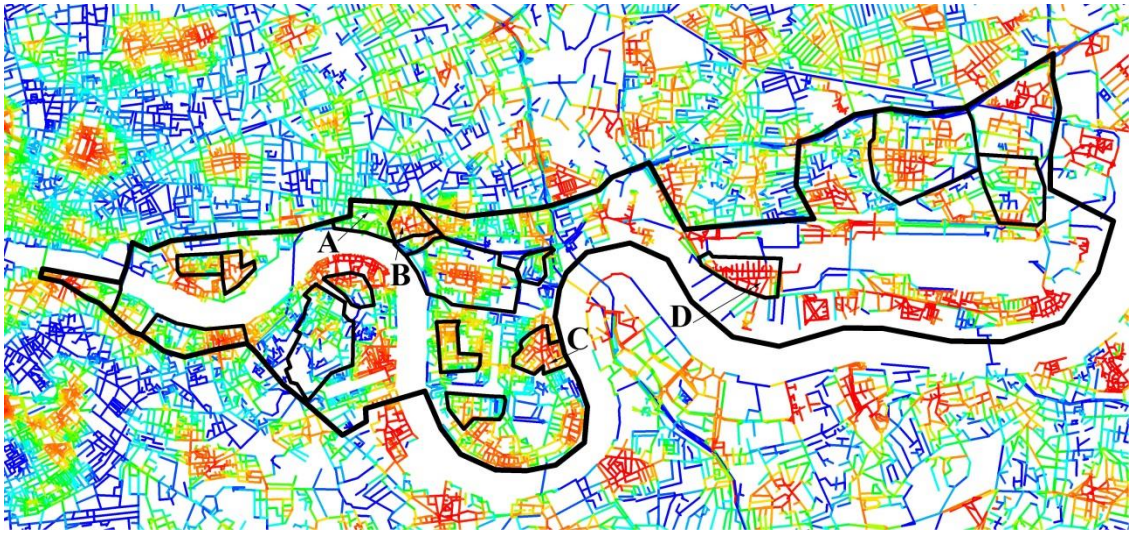

c. LH_Limehouse (A), SH_Limehouse (B), SH_NE_IsleofDogs (C) and LH_RoyalDocks (D) are roughly marked out by MMD at 800m.

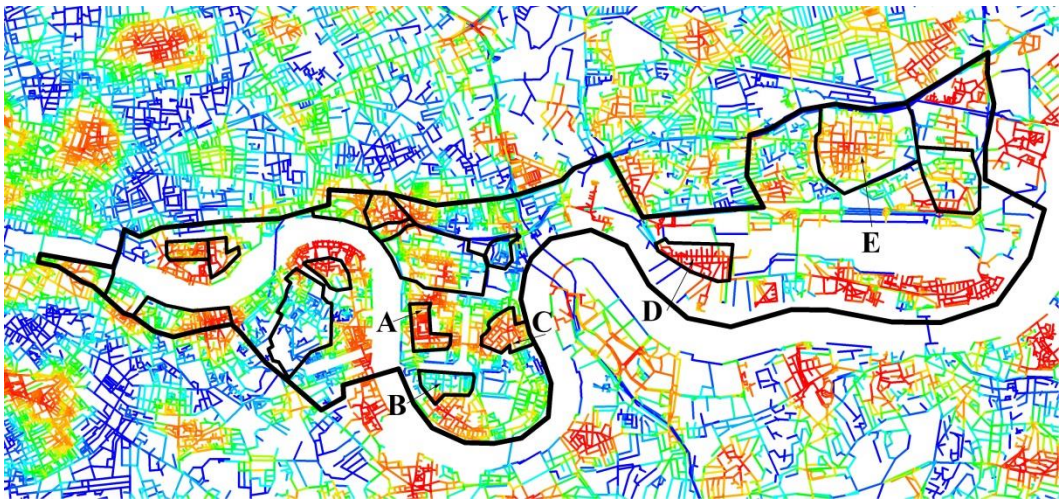

d. SH_NW_IsleofDogs (A), LH_IsleofDogs (B), SH_NE_IsleofDogs (C), LH_RoyalDocks (D) and Beckton_N (E) are roughly marked out by MMD at1000m.

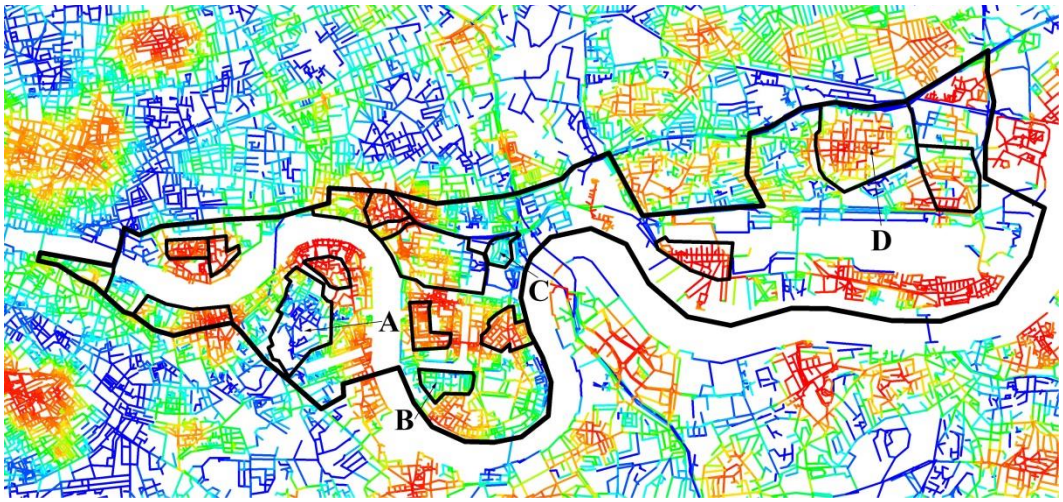

e. Centre_SurreyDocks (A), LH_IsleofDogs (B), Blackwall (C) and Beckton_N(D) are roughly marked out by MMD at 1200m.

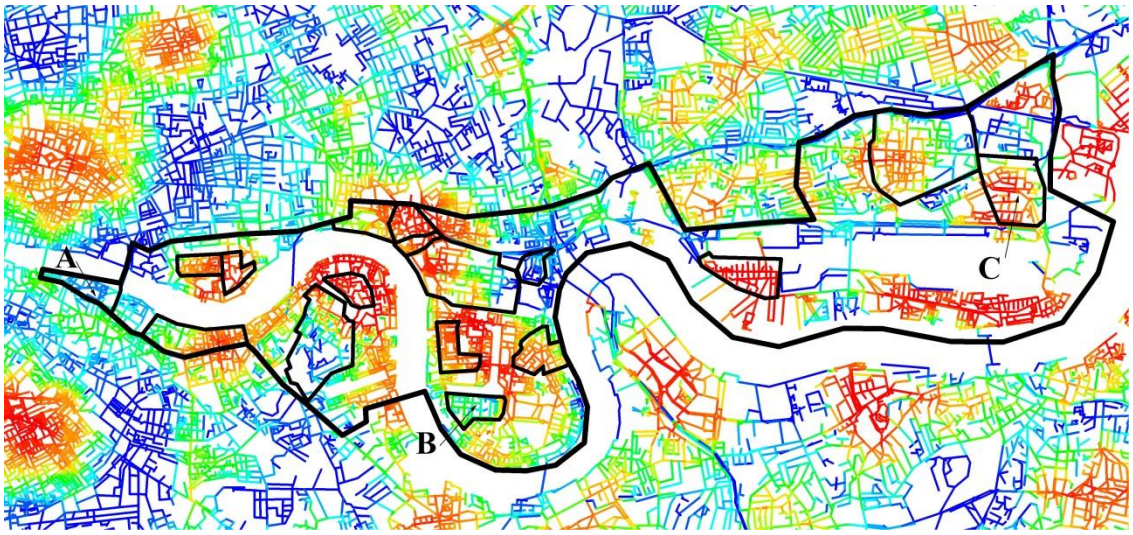

f. Bermondsey_W (A), LH_IsleofDogs (B) and Beckton_E (C) are roughly marked out by MMD at 1400m.

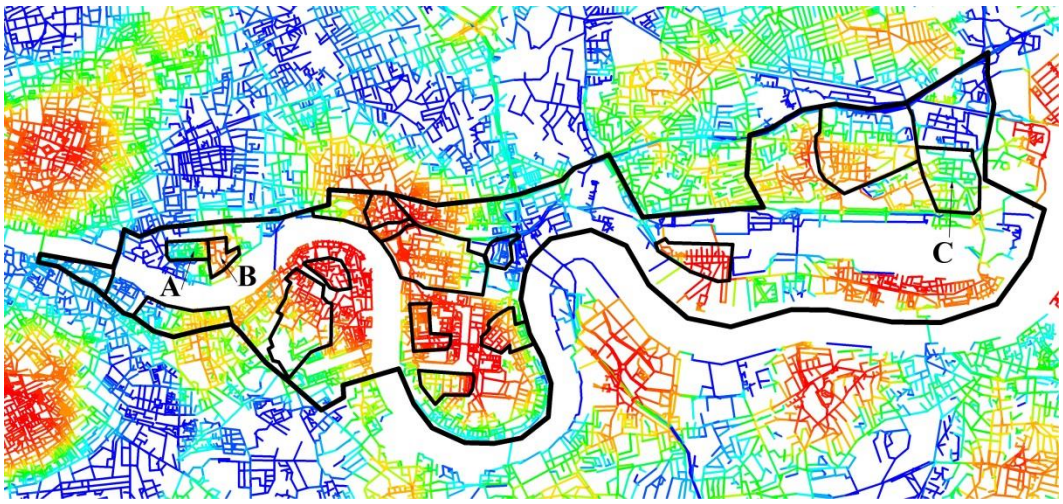

g. LH_Wapping (A), SH_Wapping (B) and Beckton_E (C) are roughly marked out by MMD at 1800m.

Fig. 6.20 The Smaller Areas Identified by MMD at Different Radii.

In general, the above analysis demonstrates that the periodic patchwork patterns generated by MMD (as similar as those produced by metric embeddedness pace) also can be deployed to investigate the spatial structuring of those newly developed areas in the Docklands, although nearly all the larger development areas cannot be identified. It also shows that the large-scaled areas, such as Surrey Docks, are distinguished by larger radii and the small-scaled areas, such as the smaller housing estates, are differentiated by smaller radii. This confirms that the way in which the new areas are metrically integrated into the different scaled contexts does influence the spatial structuring of these areas themselves.

However, some smaller areas like LH_RoyalDocks (called Silvertown) also can be identified at several radii (eg. 600m, 750m, 800m and 1000m displayed in **Fig. 6.20a, b, c andd**). In particular, LH_Wapping and SH_Wapping as the two neighbouring areas can be marketed out at both 750m and 1800m, but they are merged together to form the main part of Wapping at the radius of 1000m to 1400m. This indicates that those two areas are metrically separated to each other according to their immediate surroundings and their further contexts, although they are combined together in relation to their medium-scaled contexts. This also supports the finding (presented in the previous section) that the Dockland areas, compared to the named areas in

the central districts of London and Beijing, are *not* fully merged into the surroundings at larger scale and then *cannot* be represented as larger areas at higher level.

6.5 What is the spatial mechanism involved in the formation of the new areas?

It then raises another question: *by using these generative techniques, can we identify what kind of spatial mechanism is involved in the formation of the newly developed areas?*

6.5.1 The peak-trough patterns of the newly developed areas

We adopted the technique of mountain scattergram, explained in **Sections 4.5 and 5.5.1**, to approach the above questions. This technique allows us to investigate the pattern of metric integration of an area at a local/medium radius against the metric integration pattern of the whole network. For example, Surrey Docks was selected in the segment map window in DepthMap, and the segments constituting this area were simultaneously highlighted in yellow (**Fig.6.21 a**). We continued to create a series of mountain scattergrams by plotting the MMD Rn, on the x-axis, against the negative of MMD at the radius of k (MMD Rk), from low to high, on the y-axis[121]. At 1700m (on the y-axis), a spindle shape combining a peak and a trough (coloured in yellow) appeared for first time in the window of the scattergram (**Fig.6.21 b**). Then, we coloured the segment of Surrey Docks (bounded by dotted lines in **Fig. 6.21 c**) with regard to MMD at 1700m; and meanwhile we adjusted the colour range to attempt to highlight the location of the most metrically integrated (or segregated) segments within this area. Blue indicates the highest values and red denotes the lowest values. This enables us to explore the morphological meaning of the spindle. As **Fig. 6.21 c** shows, the MMD R1700m values increase from a small group of metrically integrated segments (coloured in red and located at the north east of Surrey Docks) to their surroundings; and meanwhile, the MMD R1700m values also decrease from a small group of segregated segments (shaded in blue and located at the south end of Surrey Docks) to their surroundings. This distribution pattern seems to correspond to the spindle shape (shown in **Fig.6.21 b**) whose highest points denote the lowest MMD R1700 values and lowest points represent the highest values. It suggests that Surrey Docks approximately comprises two

[121] The more detailed procedure was elaborated in Section 4.5.

sub-areas, one of which has a metrically integrated centre at 1700m and the other has a metrically segregated place at 1700m.

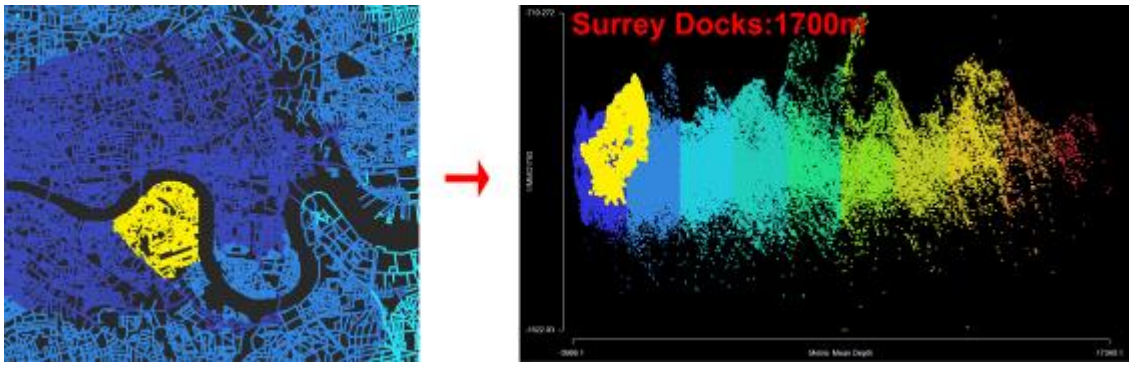

a. to select Surrey Docks in the segment map b. to show the mountain scattergram (a spindle coloured in yellow)

c. the segment map of Surrey Docks (bounded by the dotted lines) was coloured according MMD R1700. Blue denotes high values, and red indicates low values.

Fig. 6.21 The Mountain Scattergram and the MMD R1700 Pattern of Surrey Docks.

We deployed the above technique to investigate the other development areas (**Fig. 6.22a - g**). Poplar and the Isle of Dogs seem to show a peak at 3500m and 2900m, respectively; and the summit of the peak corresponds to a metrically integrated centre coloured in red (**Fig. 6.22a and b**). The centre of Poplar, the single connector to Canary Wharf, is situated on the southern edge; and the Isle of Dogs has a metrically integrated centre located at the north west of the peninsula, the initial development site in the 1980s[122]. However, as with Surrey Docks, Bermondsey, Limehouse and Wapping were more or less represented as spindles at 1200m,

[122] http://www.lddc-history.org.uk/iod/index.html.

1300m and 1000m, respectively(**Fig. 6.22c - e**). This suggests that each area has a metrically integrated centre as well as a metrically segregated space. For example, Bermondsey has an integrated centre at the east and a segregated wharf in the middle; Limehouse has an integrated centre on the eastern edge and a segregated area on the western edge; and Wapping's geometric centre is also metrically integrated but the eastern estate is metrically segregated. By and large, these three areas are roughly divided into two contrasted parts with respect to metric integration. In addition, Beckton seems to have a big peak together with a small peak at 4800m (**Fig. 6.22f**), representing an intersection between Eisenhower Dr and Tollgate Road as well as a western segment on Tollgate Road, respectively. And Royal Docks looks like double peaks at 1700m, and this corresponds to the two metrically integrated centres located at the east and the west (**Fig. 6.22g**). The above analysis suggests that most of the larger development areas are too large to function as one entity with a single integrated centre or a single segregated space. In other words, nearly all the larger development areas, artificially delineated by the LDDC, do *not* arise from the *natural consolidation* of metrically integrated/segregated parts into a larger entity. Perhaps it can be implied that the artificial boundaries of those development areas are least associated with the spatial structuring of those areas and their contexts.

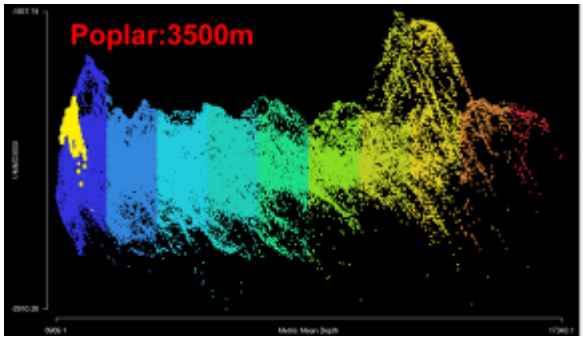

a. Poplar

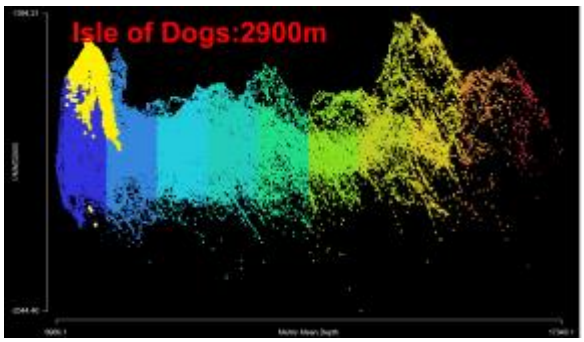

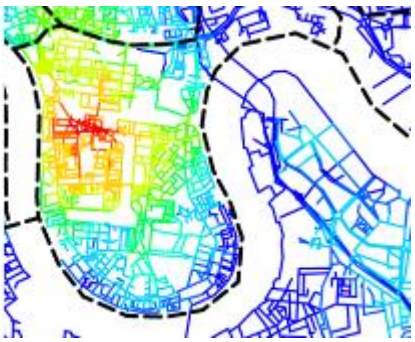

b. the Isle of Dogs

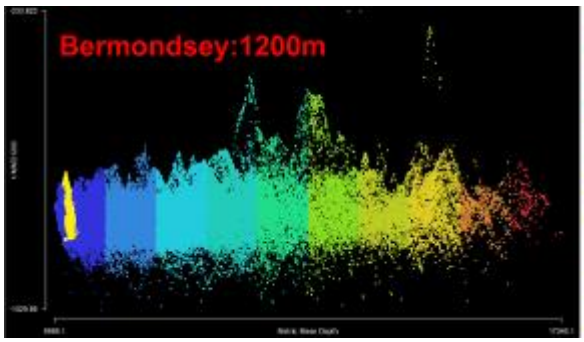

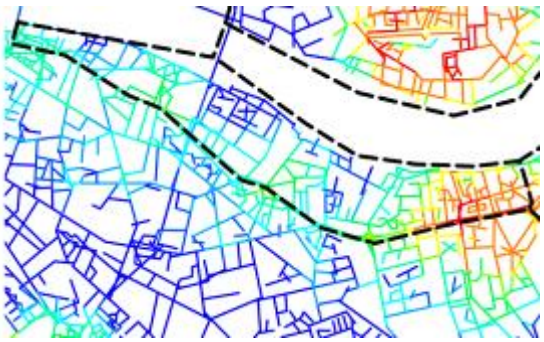

c. Bermondsey

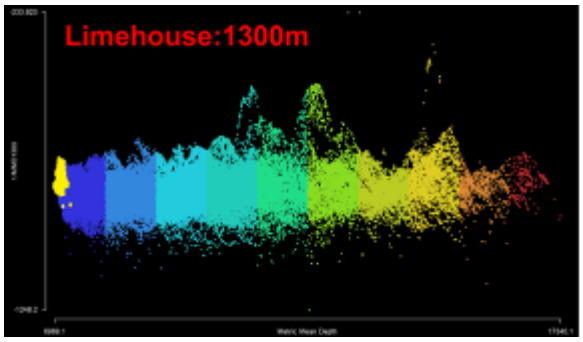

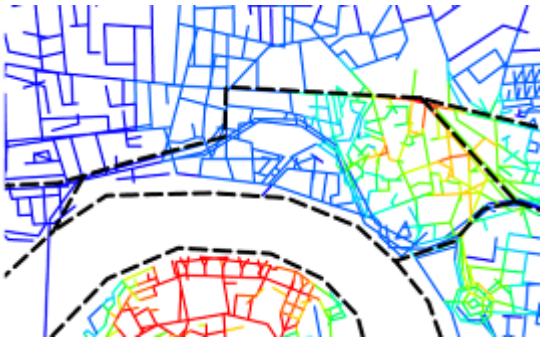

d. Limehouse

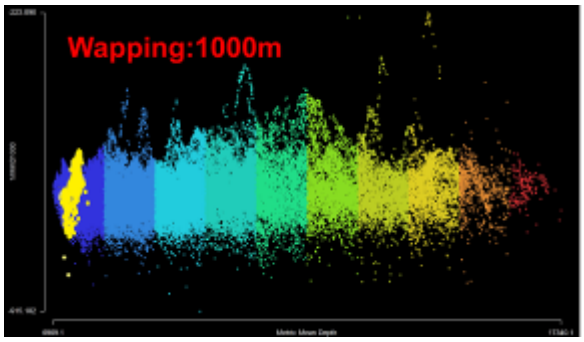

e. Wapping

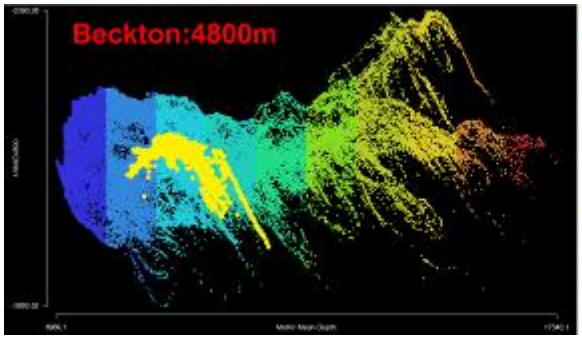

f. Beckton

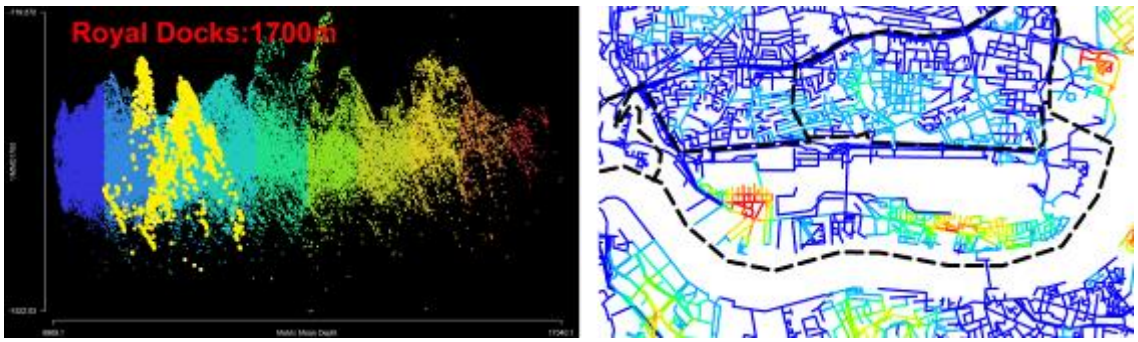

g. Royal Docks

Left: Yellow indicates the named areas

Right: the segment map coloured according to MMD Rk. Red denotes low value and blue indicates high value

Fig. 6.22 The Mountain Scattergrams (Left) and the MMD Rk Patterns (Right) of the Other Development Areas (Each image to the right has a slightly different colour range in order to clearly show the segments with the lowest MMD Rk values within each area).

So next, we further investigated the sixteen smaller areas, aiming to explore metric structures of those smaller areas. Only one smaller area, namely LH_IsleofDogs (a luxury housing estate in the Isle of Dogs), is identified as a trough at 1200m (**Fig. 6.23 Left**); and the most metrically segregated segments (coloured in blue), located near the northern edges, are surrounded by the more integrated segments (**Fig. 6.23 Right**). It indicates that LH_IsleofDogs has no metric centre, but it is enclosed by more integrated contextual spaces.

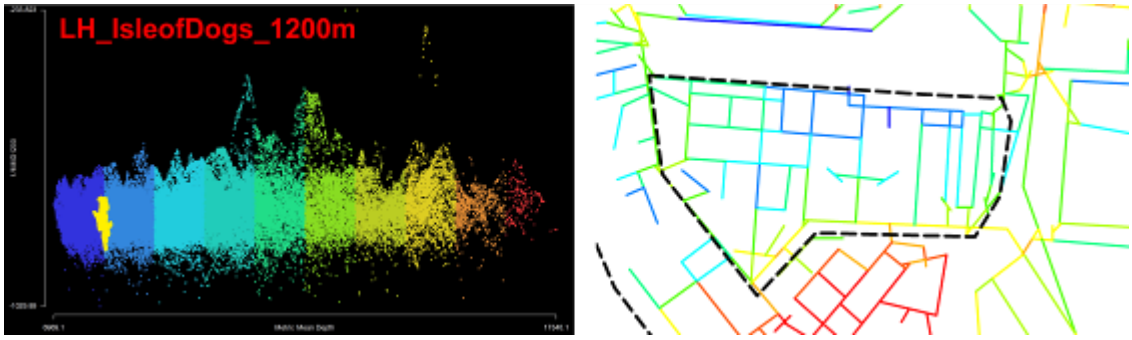

a. LH_IsleofDogs (a luxury housing estate in the Isle of Dogs)

Fig. 6.23 The Mountain Scattergram of LH_IsleofDogs (Left) and The Corresponding Pattern of MMD R1200 (Right)

In contrast, eight other smaller areas are, more or less, denoted as peaks at different radii, but often with strange distortions (**Fig. 6.24a-h**). As for five of them, namely Canary Wharf, Centre-SurreyDocks, SH_NE_IsleofDogs, LH_RoyalDocks and Beckton_N (**Fig. 6.24a-e**), a small group of the most metrically integrated segments, as a metrically integrated centre, is located at the geometric centre of each area, and meanwhile the MMD Rk values increase from the centre to the edge. However, Canary Wharf for example seems to have one smaller peak located below another bigger one (**Fig. 6.24a Left**), and this corresponds to a strong centre to the west and a weak centre to the east (**Fig. 6.24a Right**). Beckton_N has a weak trough below a strong peak, forming a distorted kind of spindle, which suggests a strong metrically integrated centre and a weak segregated area to the east. This indicates that those five areas are represented as the distorted peaks, And it therefore implies that those areas are under the way of being transformed into well-defined areas with strong metrically integrated centres.

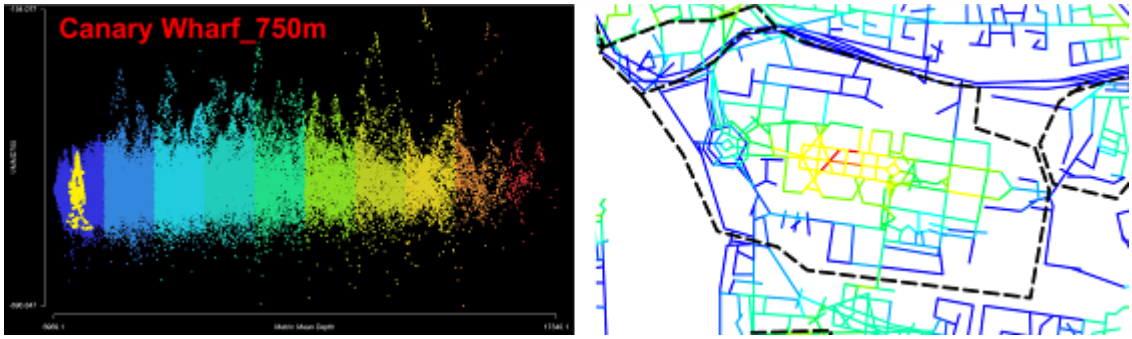

a. Canary Wharf

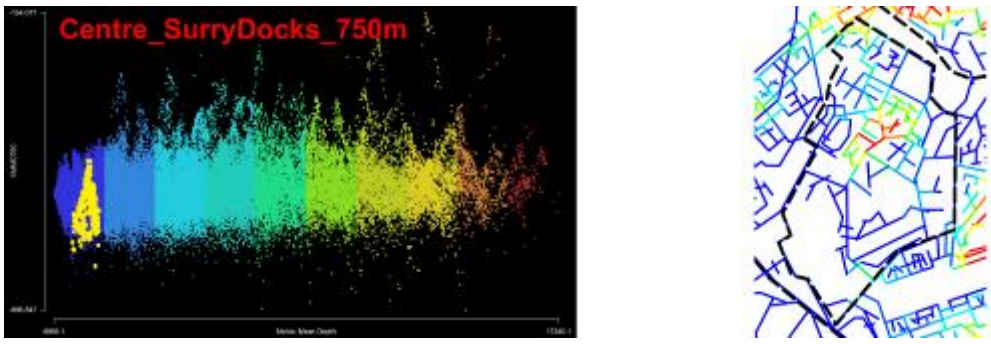

b. Centre_SurreyDocks (Central area of Surrey Docks)

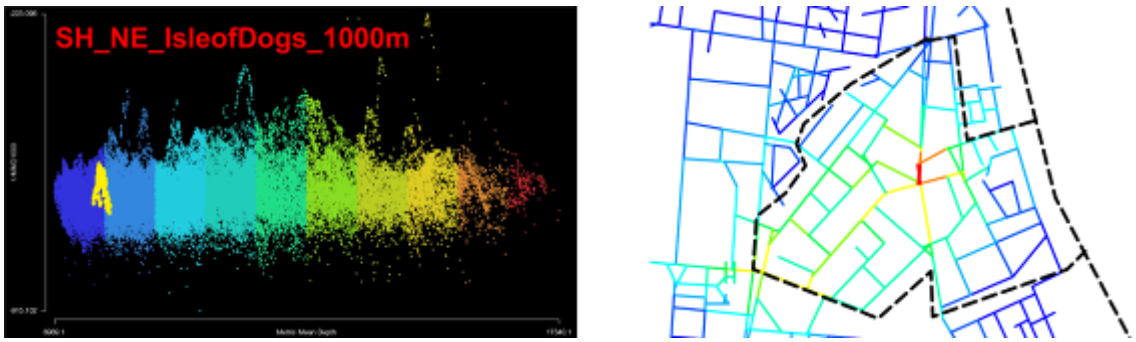

c. SH_NE_IsleofDogs (a social housing estate in the north east of the Isle of Dogs)

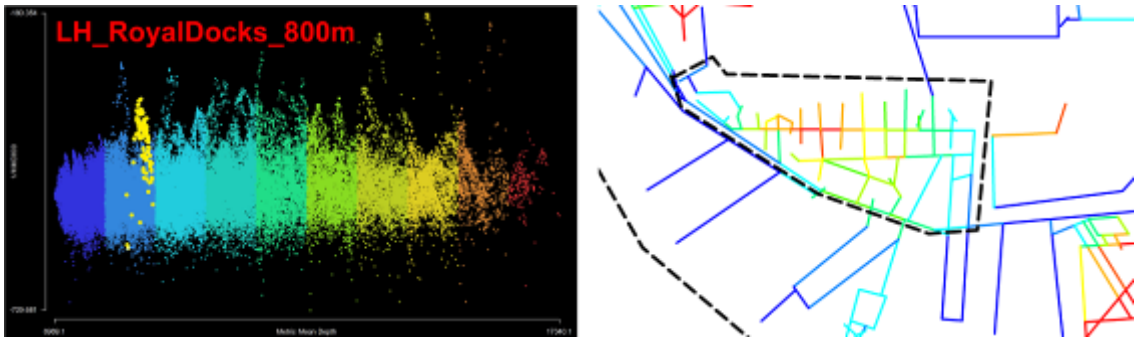

d. LH_RoyalDocks (a luxury housing estate in Royal Docks)

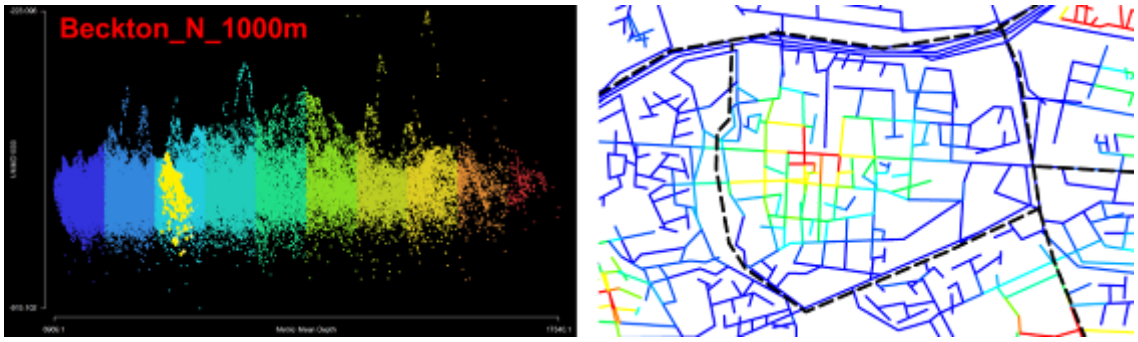

e. Beckton_N (an estate in the north of Beckton)

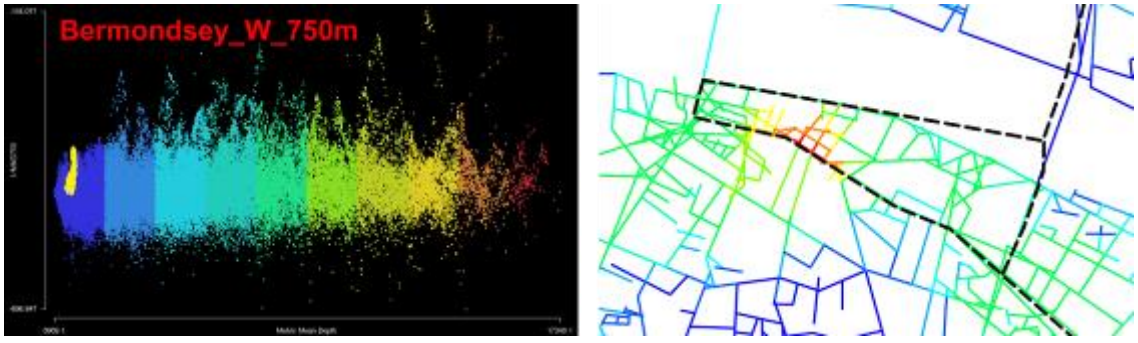

f. Bermondsey_W (the west part of Bermondsey)

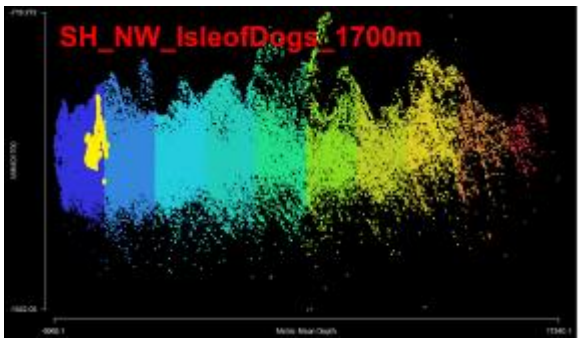

g. SH_NW_IsleofDogs (a social housing estate in the north west of the Isle of Dogs)

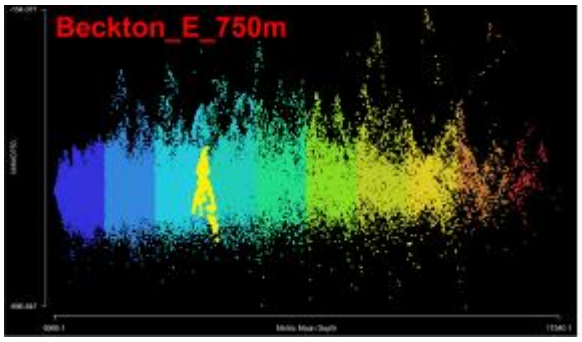

h. Beckton_E (an estate in the east of Beckton)

Fig. 6.24a-h The Mountain Scattergrams (Left) and The Corresponding Patterns of MMD Rk (Right) of Eight Smaller Areas.

The other areas, namely Bermondsey_W, SH_NW_IsleofDogs and Beckton_E (**Fig.6.24f-h**), have more distorted peaks. This corresponds to the similar situation that the most metrically integrated segments are situated at their edges, but meanwhile they are also surrounded by more metrically segregated segments. This demonstrates that the metrically integrated centres are not necessarily detected at the geometric centres of those smaller areas.

However, there are seven outliers (namely LH_Wapping, Bermondsey_E, SH_Limehouse, SH_SurreyDocks, Blackwall, SH_Wapping and LH_Limehouse) that are denoted as the thin spindle shapes (**Fig.6.24 g-m**) with two poles, one of which corresponds to the most integrated segments (coloured in red), and the other indicates the most segregated segments (coloured in blue). The thin shapes suggest relatively smaller number of the segments with moderate values of MMD Rk and this implies a short distance between the most integrated and the most segregated segments as the two poles. Within each of these seven areas, the red segments (with the lowest MMD Rk), surrounded by the orange and yellow segments, are situated opposite to the blue segments (with the highest MMD Rk) enclosed by the cyan and green

segments; and at the same time the warmer coloured segments occupy almost the same area as the colder coloured segments (**Fig.6.24 h-m Right**). Perhaps this suggests that those outlier areas (43.75% of the smaller areas) might be treated as a kind of '*transitional area*' comprising a metrically integrated centre surrounded by less integrated spaces, as well as a metrically segregated area encircled by less segregated spaces, and so that each outlier has not well structured to form a single centre-to-edge (or edge-to-centre) motif (as consistently found in the cases of the central districts of London and Beijing) at certain radius.

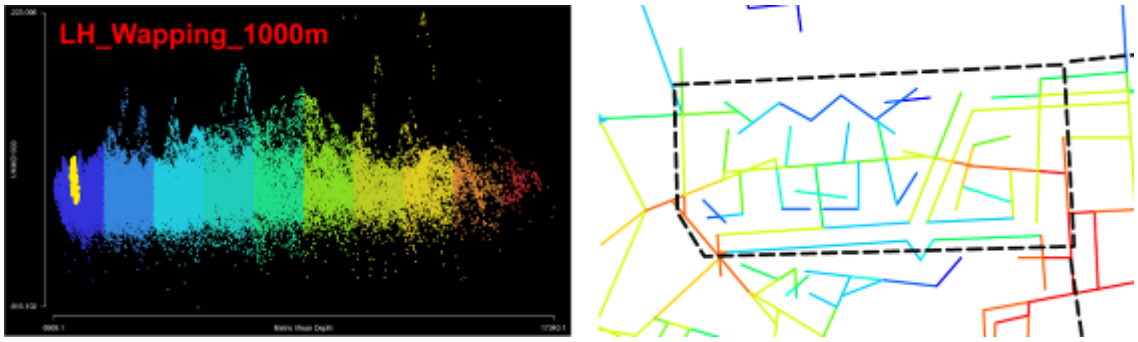

g. LH_Wapping (a luxury housing estate in Wapping)

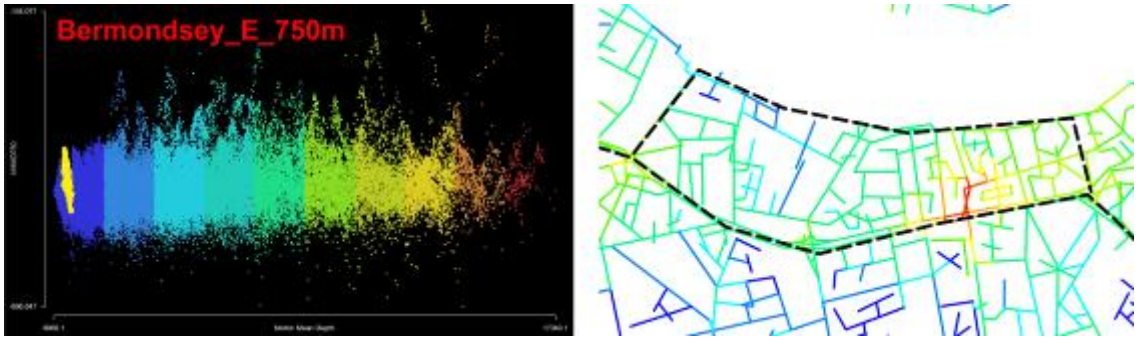

h. Bermondsey_E (the east part of Bermondsey)

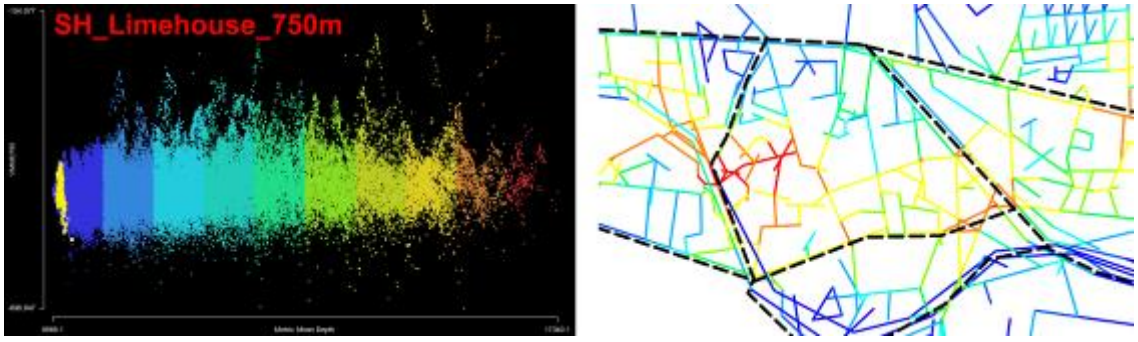

i. SH_Limehouse (a social housing estate in Limehouse)

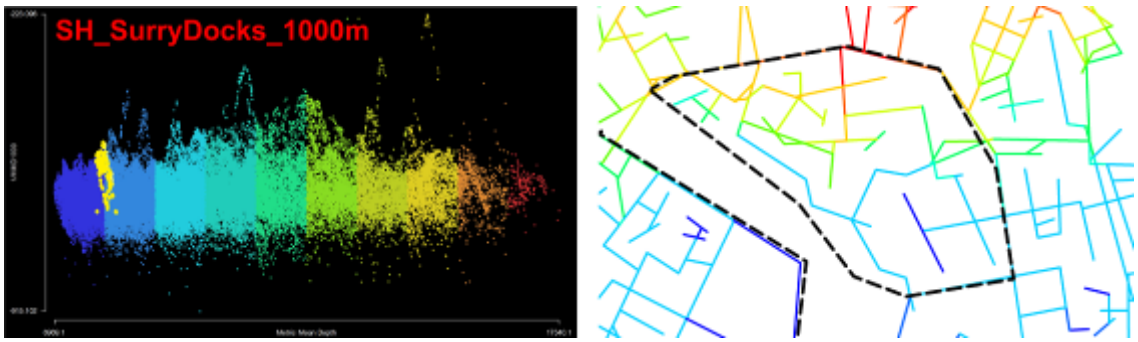

j. SH_SurreyDocks (a social housing estate in Surrey Docks)

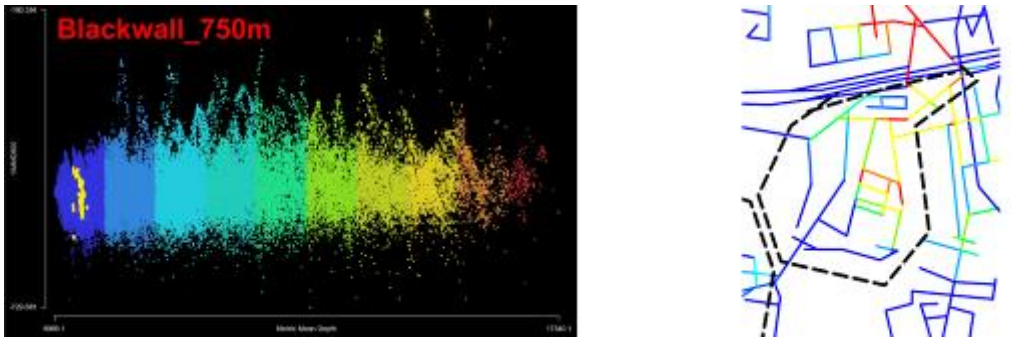

k. Blackwall (an estate in Blackwall)

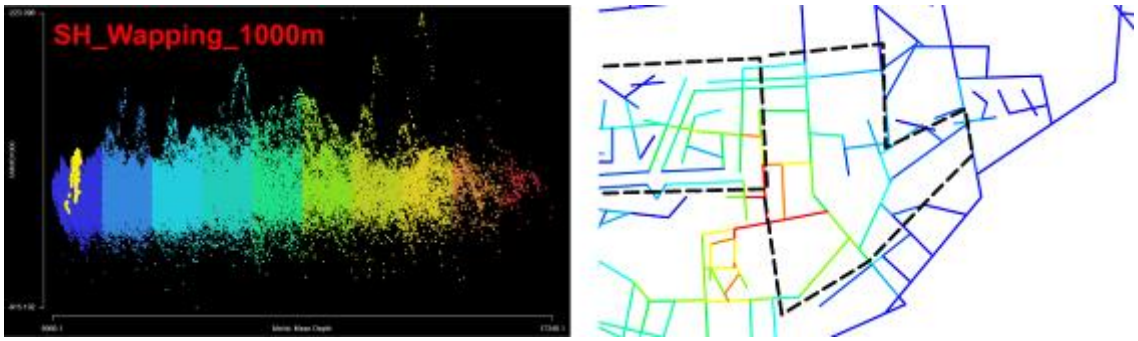

l. SH_Wapping (a social housing estate in Wapping)

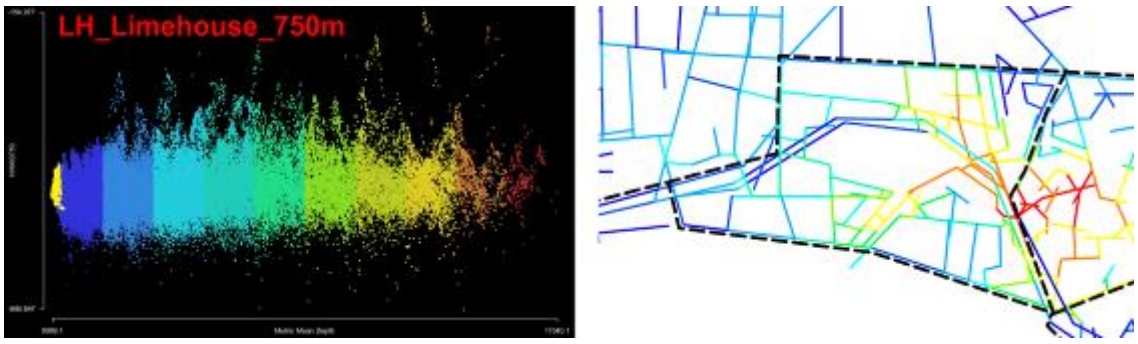

m. LH_Limehouse (a luxury housing estate in Limehouse)

Fig. 6.24g-m The Mountain Scattergrams (Left) and The Corresponding Patterns of MMD Rk (Right) of Seven Smaller Areas.

6.5.2 The peak-trough patterns of the created patches

The above section shows that most of the larger development areas and nearly half of the smaller areas (both of which can be treated as newly developed areas) are not represented as a single peak or trough. We further examined whether and how the mathematically created patches at a fixed radius, regardless of the newly developed areas, correspond to a peak or a trough, with an attempt to understand the geometric and metric mechanism for generating the patchwork patterns in association with the new areas. For example, we observed the patchwork pattern created by the MMD at 1200m (**Fig. 6.25-1**), because these created patches are, intuitively, not too small or too large. We selected each created patch (shaded in red or blue) in the segment map according to the patchwork pattern shown in **Fig. 6.25-1 and 6.26-1**, and then plotted the mountain scarttergram of the MMD R1200 against the MMD Rn. For example, as **Fig. 6.25-2** displays, we selected a red patch (called R1 in **Fig. 6.25-1**) in the segment map (**Fig. 6.25-2 Left**), and then produced the mountain scattergram to see how the points denoting R1 are distributed (**Right**).

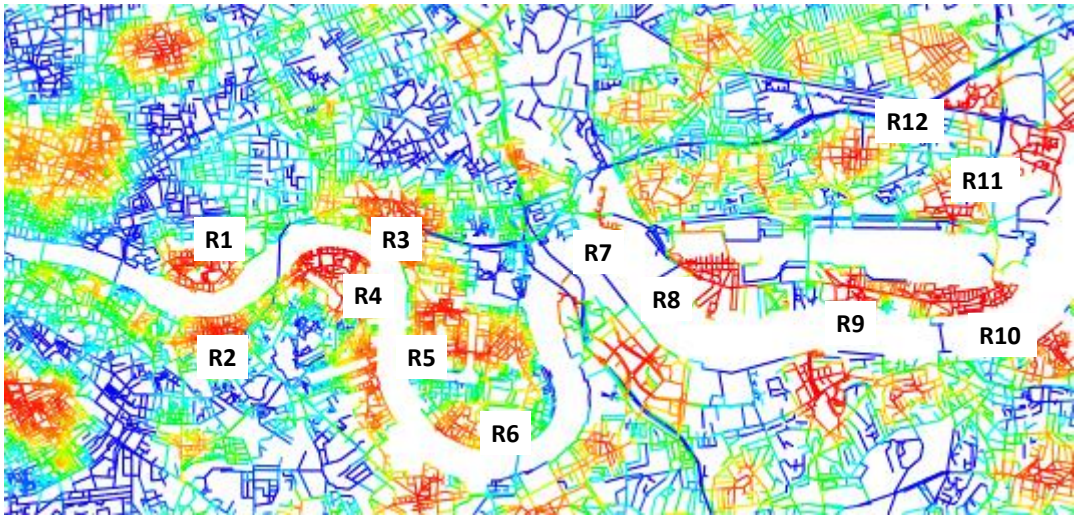

1**.** The patchwork pattern generated by MMD R1200m. R1-R12 refer to twelve red patches that would be investigated.

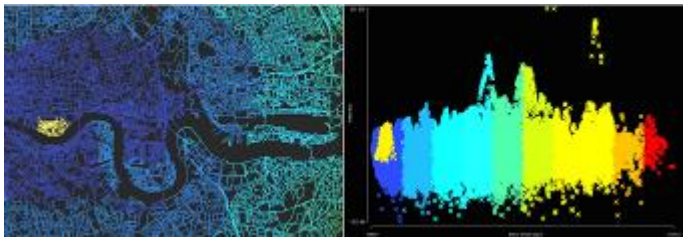

2. **R1** shown as a peak in the mountain scattergram.

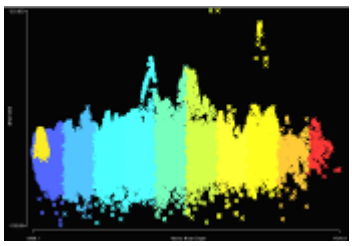
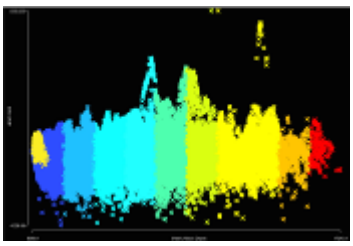
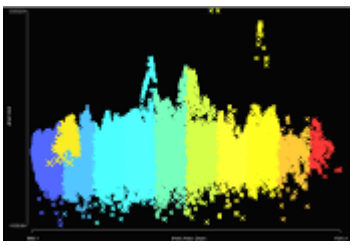

3. **R2** shown as a peak 4. **R3** shown as a peak 5. **R4** shown as a peak

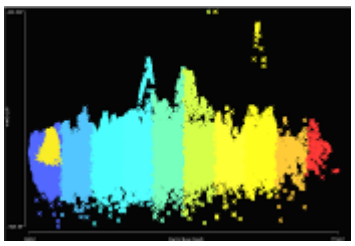
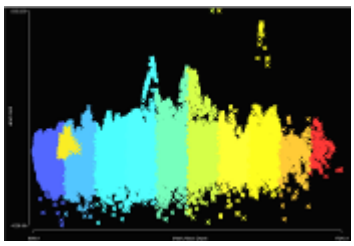
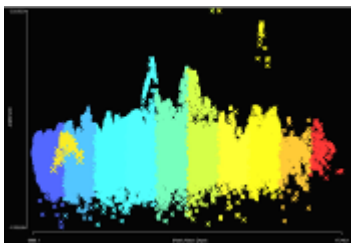

6. **R5** shown as a peak 7. **R6** shown as a peak 8. **R7** shown as a peak

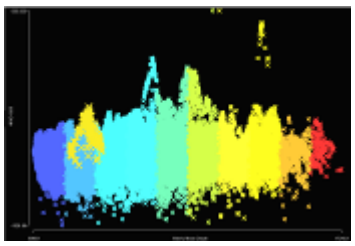
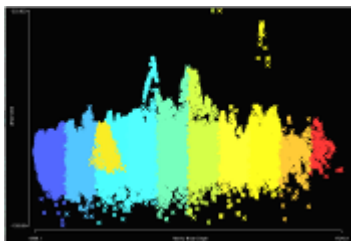
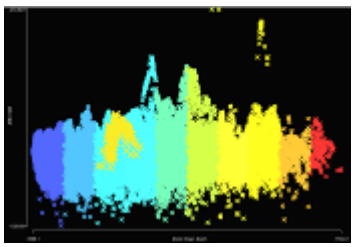

9. **R8** shown as a peak 10. **R9** shown as a peak 11. **R10** shown as a peak

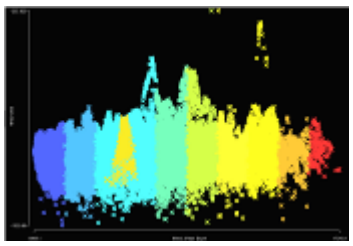
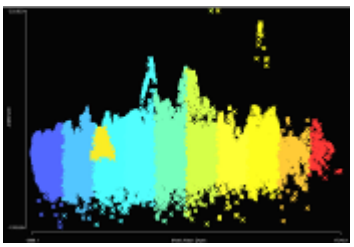

12. **R11** shown as a peak 13. **R12** shown as a peak

Fig. 6.25 Twelve Red Patches Displayed as Peaks in the Mountain Scattergram for the Docklands Case. Twelve red patches were created by the MMD at 1200m and the corresponding mountain scattergrams were produced by plotting the MMD R1200 against the MMD Rn,

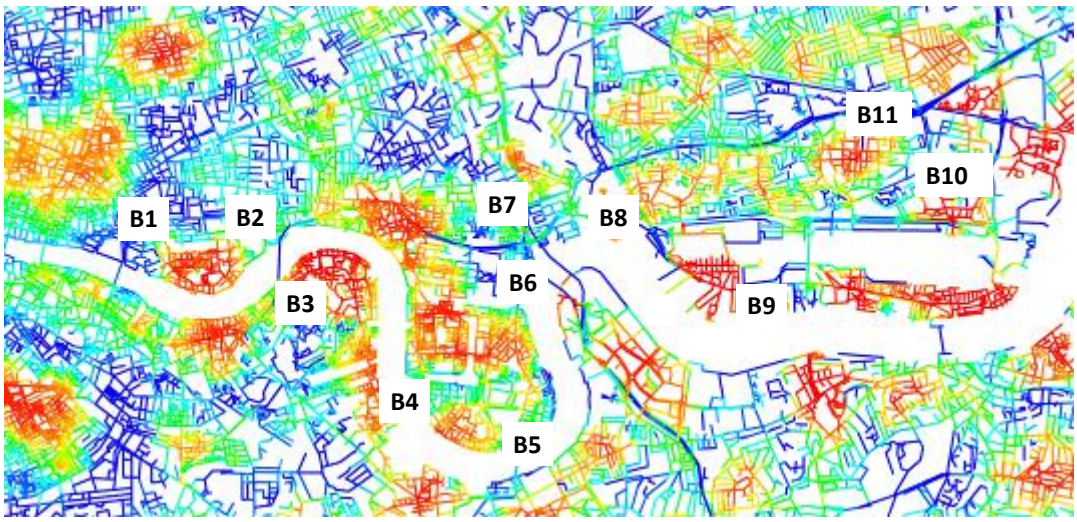

1. The patchwork pattern generated by MMD R1200m. B1-B11 refer to eleven red patches that would be investigated.

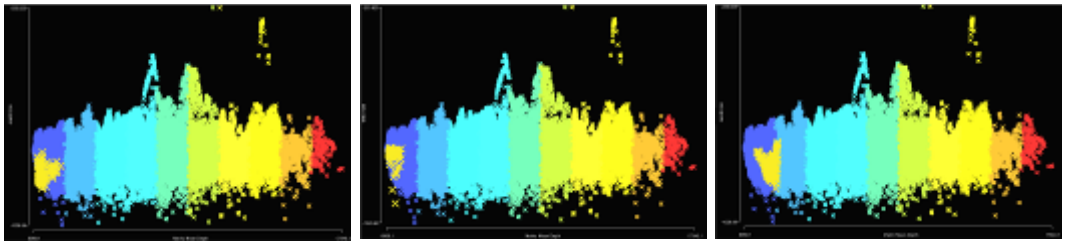

2. **B1** shown as a trough 3. **B2** shown as a trough 4. **B3** shown as a trough

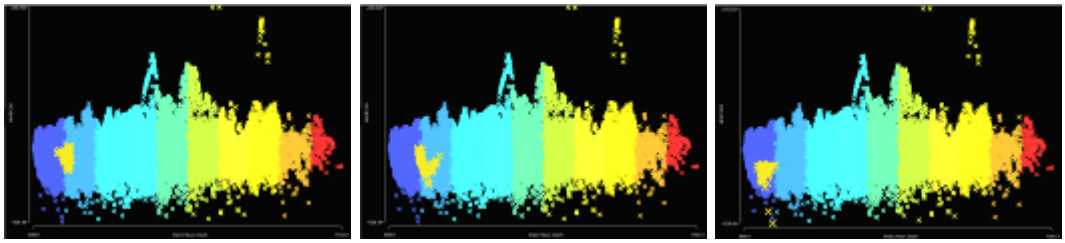

5. **B4** shown as a trough 6. **B5** shown as a trough 7. **B6** shown as a trough

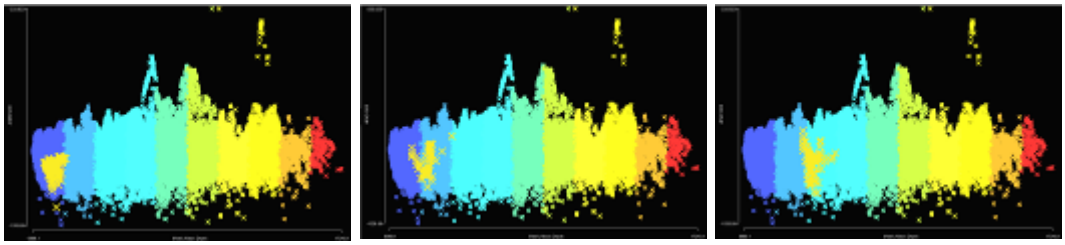

8. **B7** shown as a trough 9. **B8** shown as a trough 10. **B9** shown as a trough

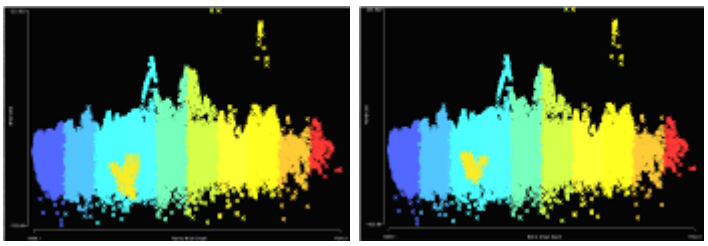

11. **B10** shown as a trough 12. **B11** shown as a trough

Fig. 6.26 Eleven Blue Patches Displayed as Troughs in the Mountain Scattergram for the Docklands Case. Eleven blue patches were created by the MMD at 1200m and the corresponding mountain scattergrams were produced by plotting the MMD R1200 against the MMD Rn,

Fig. 6.26 shows that all the twelve red patches, with lower MMD R1200m values, are more or less represented as peaks; and whilst, **Fig. 6.26** indicates that all the eleven blue patches, with higher MMD R1200m values, are roughly denoted as troughs. This suggests that the patchwork pattern of the London Docklands, as with the patchwork patterns of the central districts of London and Beijing, also can be represented by the peak-trough pattern, and vice versa. The red patches have a more metrically integrated centre (denoted as the summit of each corresponding peak) surrounded by less integrated places; and at the same time, the blue patches have a more metrically segregated part (denoted as the bottom of each trough) encircled by more integrated spaces (as discussed in the previous chapter).

Then we continued by investigating whether the above peaks and troughs have any relationship with grid intensification[123], meaning the reduction of block size to reduce average metric distance from all segments to all others in an urban network. As indicated in the previous chapter, each patch (**Fig. 6.25-1 and 6.26-1**), represented as peak or trough, was selected and coloured in black, and then the surrounding segments within 1200m were highlighted and shaded in grey (**Fig. 6.27**); and a comparison of average segment length between the black and the grey segments was conducted in order to explore whether the created patch, on average, is more intensified than its surrounding segments involved in the production of that patch.

[123] For detail, see Hillier (1999) *Centrality as a process accounting for attraction inequalities in deformed grids*, Urban Design International, 3/4, 107-127.

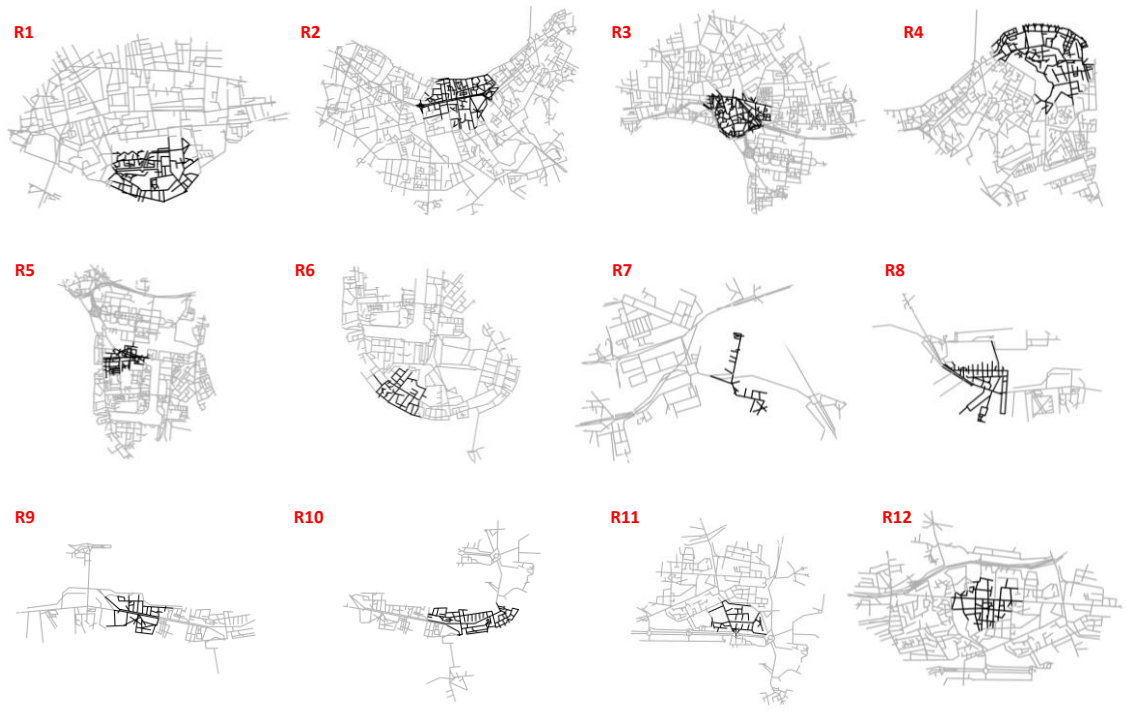

a. The red patches (associated with peaks) as well as their surroundings in London Docklands

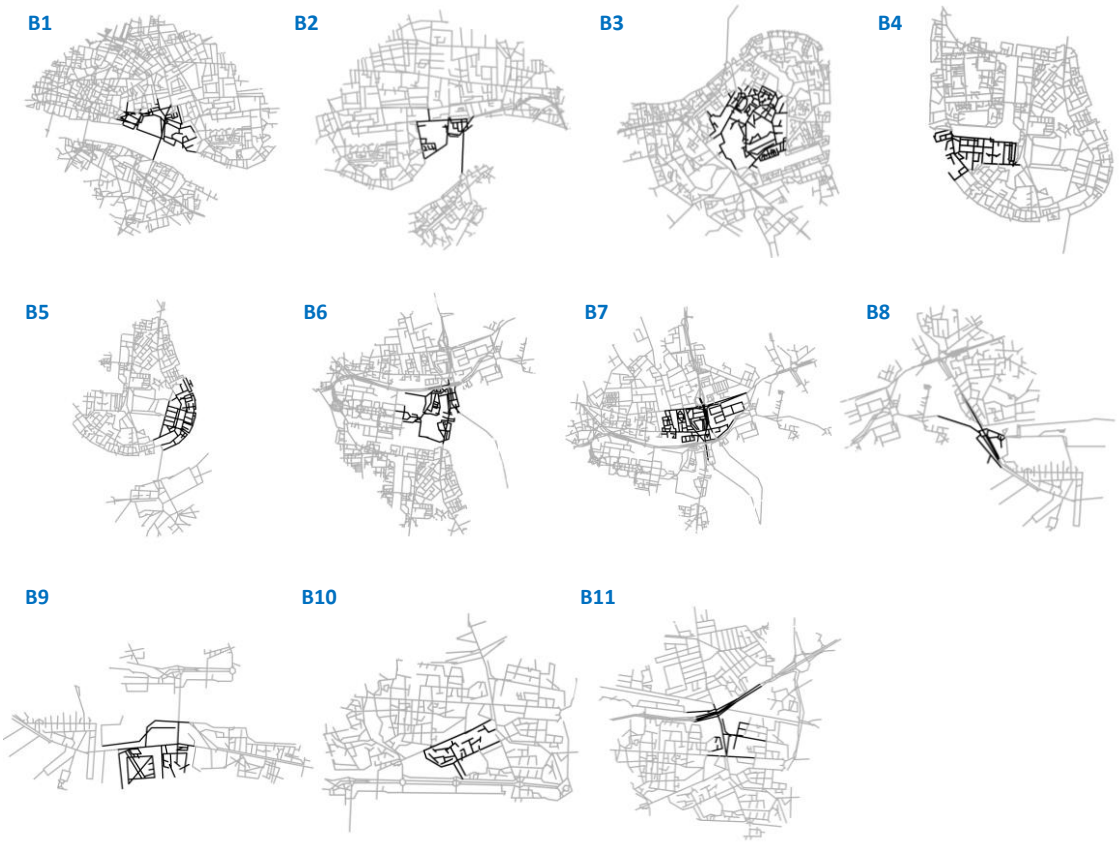

b. The blue patches (associated with troughs) as well as their surroundings in London Docklands

Fig. 6.27 The Patches Created at 1200m and Their Surroundings for the London Docklands Case. Black denotes the created patches and grey represents their surrounding segments within 1200m.

Fig. 6.27a shows the red patches and their surroundings and **Fig. 6.27b** illustrates the blue patches and their surroundings. Compared to the London and Beijing cases (**Fig. 5.33and5.34**), more patches in the London Docklands can be easily differentiated by making a visual comparison between the created patches and their surroundings involved in creating the patches. For example, five red patches (e.g. R1, R2, R7, R8 and R10), shown in **Fig. 6.25a**, look like more intensified than their contexts; and whilst, six blue patches (e.g. B1, B2, B6, B9, B10 and B11), demonstrated in **Fig. 6.26a**, seem less intensified than their surroundings. Furthermore, nearly all the Dockland patches, except for R12 and B11, do not extend in all directions, because those patches are physically constricted by the Thames River, the quays and green areas (that also can be considered as big blocks bounded by relatively longer segments); but nearly all the London and Beijing patches spread out in all directions (**Fig. 5.33and5.34**). This is another reason why more Dockland patches can be visually identified, in contrast to the London and Beijing patches.

And moreover, the numerical comparison of the created patches and their surroundings (**Table 6.7**) demonstrates that each red patch *on average* has shorter segments (41.63m) than its contextual structures (50.50m) within 1200m, and each blue patch *on average* has longer segments (60.76m) than its surrounding areas (44.46m) within 1200m. This indicates that in the case of the London Docklands, the red patches are also more intensified than their surroundings and the blue patches are also less intensified than their contexts. In fact, it can be concluded that the centre-to-edge and the edge-to-centre motifs – the grid with small centre blocks and large edge blocks as well as the grid with large centre blocks and small edge blocks – are consistently found in the London Docklands regardless the artificial boundaries of the newly developed areas. As for this newly developed district, the periodic patchwork pattern also seems to arise from the unevenly intensified grid as the whole of the London Docklands.

Table 6.7 A Comparison of the Segment Length of the Created Patches and that of Their Surroundings in the London Docklands Case (Ref.: Reference Number; Avg Seg Length: Average Segment Length; Avg R: Average Values of Red Patches; Avg B: Average Values of Blue Patches)

Ref.	Avg Seg Length		
	Patch (Black)m	Surrounding (grey)m	Ratio (Black/Grey)
R1	41.93	47.35	0.886
R2	32.57	40.94	0.796
R3	32.05	39.97	0.802
R4	29.93	37.90	0.790
R5	26.13	34.31	0.762
R6	42.75	50.29	0.850
R7	36.58	52.35	0.699
R8	53.96	70.22	0.768
R9	52.95	59.52	0.890
R10	48.49	54.37	0.892
R11	48.32	61.87	0.781
R12	53.87	56.95	0.946
Avg R	41.63	50.50	0.822
B1	37.90	31.93	1.187
B2	57.40	45.10	1.273
B3	45.17	37.51	1.204
B4	47.15	34.49	1.367
B5	50.54	38.06	1.328
B6	47.41	36.08	1.314
B7	55.08	41.35	1.332
B8	82.74	53.08	1.559
B9	74.57	54.77	1.362
B10	63.80	54.48	1.171

B11	106.62	62.26	1.712
Avg B	60.76	44.46	1.346

6.5.3 The change rate of segment density

Then, *how does the degree of intensification of the Dockland patches change with an increase of radius, and how does this relate to the formation of these Dockland patches?* We first investigated whether the segment density (approximated by node count at a given radius) is associated with the generation of patchwork patterns of the London Docklands. At first sight, the periodic patchwork patterns are not created by node count at any radius. For example, the pattern produced by NC R1200, displayed in **Fig.6.28**, illustrates that the segment density, by and large, decreases from west to east in the London Docklands, although the areas in and around Canary Wharf at the geometric centre of this district have relatively higher segment density. This pattern is different from the concentric pattern found in the historic central districts of London and Beijing (**Fig. 5.35 in Section 5.5.4**). However, this also suggests that the patchwork pattern of the London Docklands is not produced by the variable of segment density either, and those same coloured patches created by MMD at 1200m (**Fig.6.19**) have different segment densities.

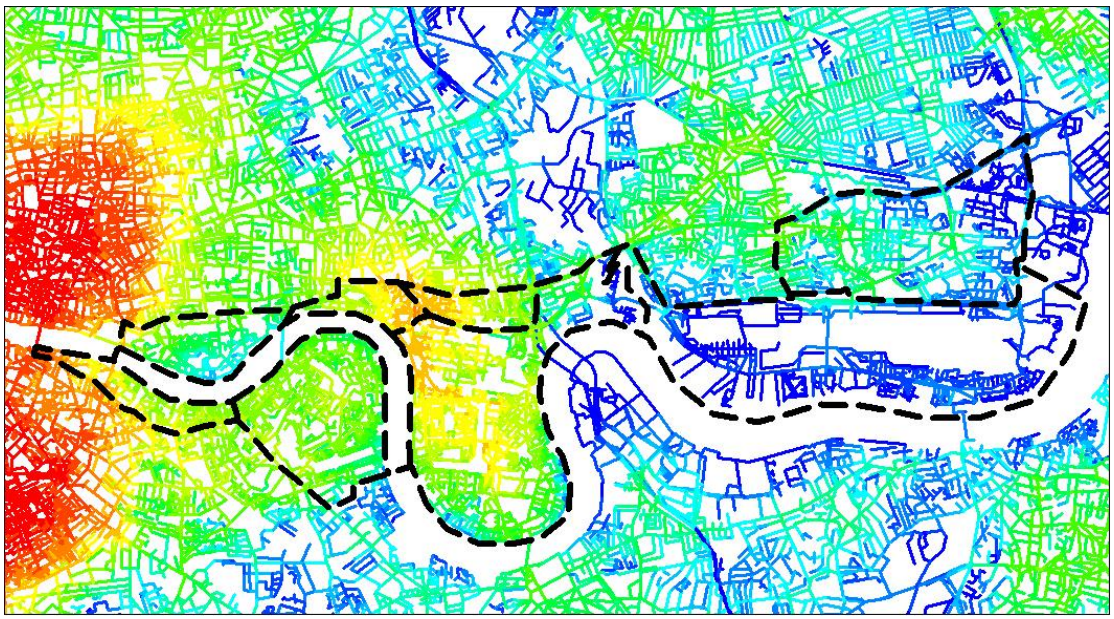

Fig. 6.28 The Pattern Generated by Node Count at 1200m. This aims to approximate segment density. Red denotes high value, and blue mean low value.

As discussed in the previous chapter, each patch (either more intensified or less intensified) can be treated as the internal layout, and its neighbouring patches as the contextual areas. As a result, to investigate the change between the differently intensified parts is to explore how NC Rk (approximating segment density if k is relatively small) varies from the internal to the external. Thus we examined the metric embeddedness trajectories of individual segments selected from the same coloured patches, seeking to approximate the variation of segment density within and around each created patch. For example, in the patchwork pattern created at 1200m, five segments were randomly selected from five different red patches (with similar lower MMD R1200), and then another five segments chosen from five different blue patches (with similar higher MMD R1200). **Fig. 6.29** shows the locations of those segments.

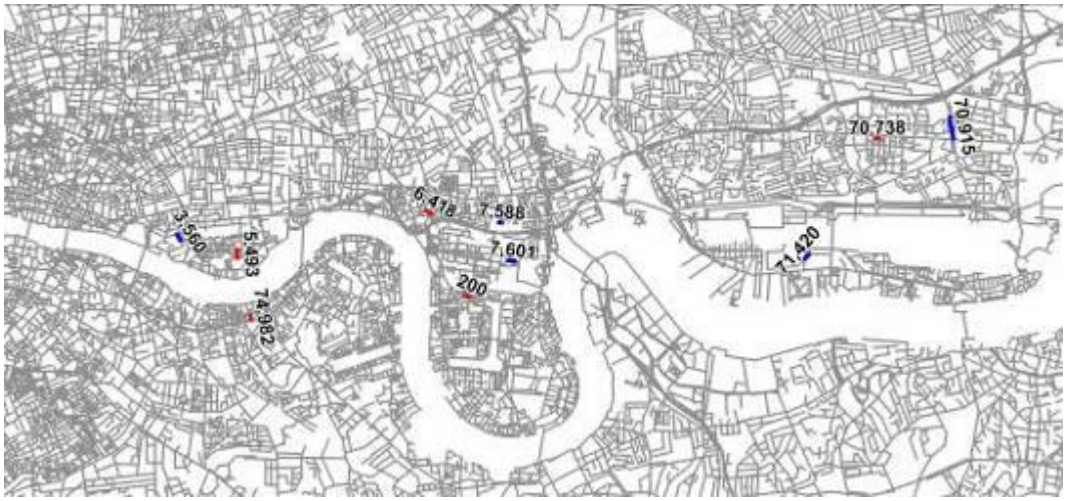

Fig. 6.29 The Locations of the Selected Individual Segments. In the patchwork pattern created at 1200m, five segments were randomly selected from the different red patches (with similar lower MMD R1200), and then another five segments chosen from three different blue patches (with similar higher MMD R1200). The numbers are the reference numbers of individual segments (which was also shown in Table 6.9).

In order to visualise how segment density varies with radius, the metric embeddedness trajectories of those ten segments - within the radius range of 400m to 1200m, with an interval of 100m - were respectively illustrated (**Fig. 6.30**). At first sight, the red segments (**Left**) have straighter trajectories than the blue segments (**Right**). This visually demonstrates that the blue segments have higher change rates of node count at higher radii, because they have relatively sharper slopes at higher radii.

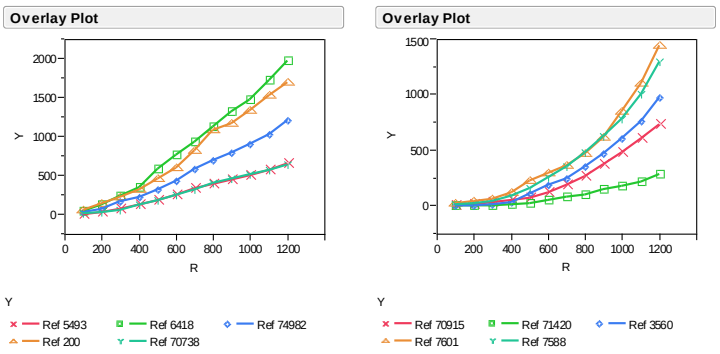

Red segments Blue segments

Fig. 6.30 The Metric Embeddedness trajectories of the Individual Segments Selected from The Red (Left) and Blue (Right) Patches in The London Docklands.

The non-linear regression analysis then demonstrates that their embeddedness trajectories all are approximately governed by power laws, and this suggests that the way in which those segments, either in red or in blue, are embedded into the surroundings is also controlled by the scale parameters (H) and the power-law exponents (α) (see **Equation 4.6** in **Section 4.3.2**). **Table 6.8** displays the values of the two variables, as well as NC R1200 and MMD R1200 of the ten segments. We then sought to explore whether the creation of these patches (produced by MMD R1200) might be influenced by the two parameters of the embeddedness trajectories, and whether this is associated with segment densities (approximated by NC R1200).

Table 6.8 The Relationship Among MMD, NC and Power-law Exponents of Ten Segments.

Five segments, with the similar MMD at 1200m, were chosen from the different red patches, and another five, with the similar MMD at 1200m, selected from the different blue patches. (Ref: reference number of segments, given by the DepthMap; NC1200: node count at 1200m; MMD 1200: metric mean depth at 1200m; H: scale parameter of power law relation found between node count and radius; α: exponent of power law)

Ref	Colour	NC1200	MMD1200	H	α
5493	Red	649	694.2	2.68E-02	1.426
6418		1974	696.1	7.37E-02	1.438
74982		1212	703.5	4.03E-02	1.453
200		1694	694.1	6.70E-02	1.433
70738		642	708.6	2.90E-02	1.415
70915	Blue	733	865.8	1.40E-05	2.508
71420		287	879.0	4.59E-06	2.531
7601		1446	866.1	2.41E-05	2.521
7588		1295	865.7	4.13E-05	2.431
3560		977	874.7	1.30E-05	2.557

We first made a simple comparison between MMD R1200 and NC R1200 (displayed in **Table 6.8**). The segments in the same colour (either red or blue) have similar MMD R1200, but do not necessarily have similar NC R1200. For example, Segment 5493 in Wapping and Segment 6418 in Limehouse have almost the same MMD R1200 values (694.1 and 696.1, respectively), but the former has around 60% of NC R1200 of the latter. Since NC R1200 approximates segment density, this suggests that Wapping is less intensified than Limehouse, although both areas are represented as red patches. It numerically confirms that that the patchwork pattern of the Docklands does not result from segment density itself.

We then continued by investigating the power-law exponents. As **Table 6.8** shows, the five segments selected from the same coloured patches, either red or blue, have similar exponents,

although those segments have the different NC R1200 values. Since the power-law exponent in fact represents the change rate of node count (see **Section 4.3.2**), it indicates that the same coloured segments have the similar change rate of node count. As NC R1200 approximates segment density (as mentioned earlier), this suggests that the same coloured patches, perhaps with the different degrees of intensification, have the similar rate of change in segment density. It therefore supports the argument that the created patches (indicating spatial discontinuity of the London Docklands as a newly developed district) also result from the variations between differently intensified sub-systems (defined by a fixed radius), rather than the intensification of each sub-system.

In addition, we further conducted a statistical analysis for all the individual segments of the London Docklands to explore whether power law relationship between NC and radius might be found within a fixed radius range. Here we still sought to study the MMD R1200. However, we investigated the relationship between NC and radius within the radius range of 400m to 1500m. Since the endpoint of 1500m is larger than 1200m at which MMD Rk values were calculated, this enables us to examine whether the change rate of segment density calculated beyond the radius of 1200m (representing the contexts) *empirically* affect the values of MMD Rk roughly denoting the internal structures.

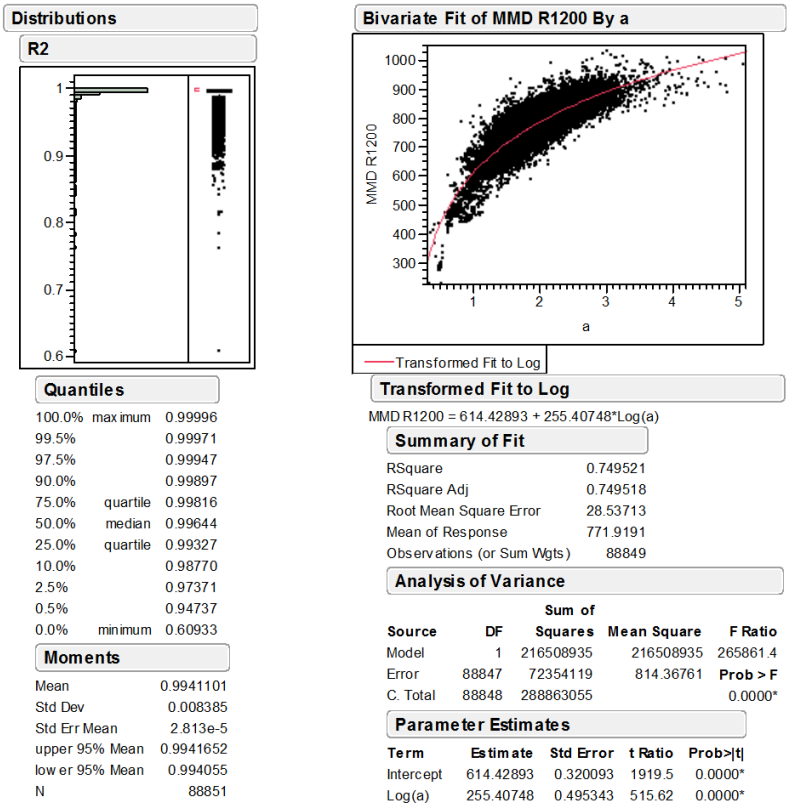

Fig. 6.31 The R-square values of the power-law relationship between NC and radius (Left) and The Correlation between Power Law Exponents and MMD Rk Values (Right) for the London Docklands.

Fig. 6.31 (Left) indicates that 94.7% segments in the London Docklands have a power law relationship between NC and radius, with the R-square above 0.9, within the range of 400m to 1500m. As **Fig. 6.31** (Right) displays, a strong non-linear relationship between the power law exponents – approximating the change rate of segment density – and the MMD R1200 values was found with the R-square of 0.750. It can be concluded that the patchwork patterns generated by the MMD R1200 in the London Docklands are *statistically* affected by the change rates of segment density beyond the radius of 1200m. As a result, this implies that the change rate of segment density between the internal and external of the created patches also plays a morphological role in generating the patches in the London Docklands as the newly developed district.

6. 6 Discussion

The analyses conducted in this chapter suggest three major points. First, the descriptive analysis revealed that the embeddedness trajectories, either topological or metric, of the Dockland areas in general are more bended than those of the central districts of London and Beijing; and it also demonstrates that greater variations in radii at which points of inflexions were found. It can be suggested that the Dockland areas aggregate to form the whole network of the London Docklands in an inconsistent way; and meanwhile, this retrospectively indicates that the historic structure of the London and Beijing have a certain consistency in the way areas add up to the whole network. In this sense, it means that the spatial network of the London Docklands, compared with that of those two historic central districts, is more fragmented, and therefore the *spatial discontinuity* in the London Docklands can be interpreted as a relatively weaker relationship between each pair of the Dockland areas with regards to the ways those areas are (topologically and metrically) embedded into the whole network.

Second, the smaller areas – except a small number of outliers such as Bermondsey_E (the east of Bermondsey) – visually co-incided with the patches created by metric embeddedness paces and MMD at certain radii, but nearly all the larger developments have not such relationship with the created patches. In particular, some smaller areas, such as LH_RoyalDocks (a luxury housing estate in the Royal Docks), are marked out at different radii and they refrain from being merged into their immediate surroundings to form larger areas at higher scale. This confirms that the Docklands as the whole is constituted by a group of spatially segregated smaller areas. Considering the situation that the named areas investigated in the historic districts of London and Beijing are merged into larger areas at higher radii, it can be argued that the inconsistency of the overall structure of the Dockland areas is an important difference between itself and historic urban form.

Third, the technique for generating the peak-trough patterns further demonstrates that the Dockland areas, including the larger development areas and the smaller areas, are *morphologically* structured in a more *complex* way, compared with the historic areas in the central districts of London and Beijing. In the mountain scattergrams, most of the larger development areas (except Poplar, the Isle of Dogs and Beckton) as well as the half of the

smaller areas are *not* represented as a peak or a trough across radii, but all the historic areas in London and Beijing are denoted as a peak or a trough at certain radius. Those Dockland areas are denoted as, for example, two peaks or a kind of spindle shape combining a peak with a trough at certain radius. This suggests that a number of the Dockland areas, as the newly developed areas, do not have one single dominate centre regarding metric integration at certain scale, or one single segregated area surrounded by more integrated spaces at certain scale. It could be argued that they are always divided into two/several parts, each of which has an integrated centre or a segregated place. In this sense, those Dockland areas, compared with the historic areas, *cannot* be morphologically treated as the centre-to-edge or the edge-to-centre motifs at any radius, and therefore they are also fragmented at the level of the areas. To a large extent, it can be argued that the boundaries (though clearly and arbitrarily defined) of the Dockland areas do *not* manifest *a kind of natural process* that the urban network is spatially partitioned into the different parts with respect to the subtle relationship between each space and its contexts, rather than artificial barriers.

Fourth, all the *mathematically* created patches in the London Docklands can still be manifested as either the centre-to-edge or the edge-to-centre motifs. And this means that they also result from the rate of change in segment density, in spite of the fact that nearly all the Dockland patches do *not* extend into the surroundings in all directions (compared to the historic areas in the central districts of London and Beijing) (**Fig. 6.28**). This suggests a kind of spatial discontinuity in the newly developed region. The next chapter will investigate the theoretical nature of spatial discontinuity in the urban grid.

Chapter Seven: Discussion

7.1 Introduction

The two previous chapters, using the descriptive and generative techniques developed in chapter four, identified and investigated the spatial discontinuities - associated with the area structures - in the two historic central districts and a newly constructed region, and those empirical cases helped us to clarify how the concept of spatial discontinuity in urban networks, where spatial configurational values change dramatically with depth, empirically relates to the unevenly intensified grids (although the historic districts and the newly constructed region have different structures of areas). Based on which, this concluding chapter aims to clarify the nature of area boundaries with respect to the concept of spatial discontinuity. It first reviews the key ideas developed in the descriptive analysis, in order to elaborate how small variations in the relationship between internal layout and multi-scale external structures of a pre-defined area impact on the spatial definition of the area boundary across different cases. It then goes through the main findings of the generative analysis, with an attempt to explore the conceptual relationships amongst these findings, and in particular, to achieve a better understanding of the spatial mechanism for generating different periodic patchwork patterns in different cases. This will allow us to make the first step towards the spatial laws causing partitioning of the urban network into different parts. On these grounds, it finally seeks to propose a new heuristic model of area boundary in relation to the change rate of segment density empirically discussed in Chapters Five and Six. This might enable us to contribute to answering the theoretical questions posed in the introductory chapter and discussed through the previous chapters: *what, in terms of space, are urban areas? How do urban areas aggregate into a city as a whole?*

7.2 The role of multi-scale external structures of an area in describing the area boundary

The key theoretical idea of the descriptive analysis was that if we represent the increase in node count with depth from a segment as a graph (called the embeddedness trajectory), as in **Fig.**

5.9 and 5.12, then changes in the rate of growth, would represent discontinuities in the urban fabric – for example, a reduction in the rate of growth should mean a reduction in the density of development, and an increase an increase in the density of development. The points of rate change can then represent some kind of boundary between areas, and the continuous slopes between the points of change can represent homogeneous areas. This would only be the case, however, if points of change and continuous slopes between them could be identified from *all* the segments making up an area rather than just for individual segments, as in the theoretical case.

That this turned out to be the case is a significant discovery, suggesting that important external spatial properties of areas might be identified in this way. But it was not a simple phenomenon. In each case of the London and Beijing historical areas, there was a point of inflexion at low radius, another at mid radius and possibly another at high radius – though the latter was likely to be affected by the overall boundary of the system, so did not offer the same degree of interest as the first two. This suggests that areas are embedded into their contextual areas at two levels at least: the level of the immediate environment and the level of their positioning in the higher level urban system. Both seem relevant to the possibility that external, as well as internal factors, are relevant to the spatial definition of an urban area.

Moreover, the non-correlation between the slopes at the first two levels of contexts further suggests that the discontinuities along the embeddedness trajectories are *not* trivial things, in spite of that nearly all the segments in each case of the London and Beijing areas had a strong power-law relationship between node count and radius (as shown in Chapter Four). As indicated in Chapters Five and Six, the discontinuities of the most areas were found at different radius. This demonstrates that those areas are not only spatially embedded into different levels of contexts, but also possibly embedded into the same level of context at different rates. As a result, the areas are to some degree distinguished in terms of the discontinuity in their relationship to the different scaled contexts. To a large extent, it can be argued that small discontinuities along the embeddedness trajectories reflect a critical feature of area structure of the historic districts.

However, in the London Docklands as a newly developed region, a much less consistent pattern of embedding was found, with much greater variations in the radii at which points of inflexion were found. This suggests that the two historic districts are much more consistent in their overall structure of area than the newly developed region, and in the way areas, while varying in the pace of embedding, are embedded in the whole.

We therefore have two phenomena through which to investigate the spatial nature of areas: the slopes of the phases of continuous growth, which we define as embeddedness pace (alpha) and define as $Emd(k,\sigma) = \alpha(k,\sigma) = \frac{\ln NC_k - \ln NC_{k-\sigma}}{\ln k - \ln(k-\sigma)}$ [124] and can represent continuous areas; and the points of inflexion, or points in the node count growth where there is a significant change in embeddedness pace (alpha), which might represent discontinuities or even boundaries of some kind. Both phenomena are associated with multi-scale contextual structures.

7.3 The spatial mechanism of generating the patchwork structure

7.3.1 A morphological reflection on the periodic patchwork pattern

On this ground, one of the key findings of the generative analysis was that if each segment was assigned by metric embeddedness pace (alpha) values[125] at a fixed non-global radius, a kind of periodic patchwork pattern – meaning that several groups of neighbouring segments acquire the similar alpha values, and so are shaded in the similar colours and surrounded by the discontinuities where the values change significantly – was created in each case of Central London, Central Beijing, the London Docklands, Chicago, Birmingham and Amsterdam, as shown in **Fig. 4.13 and 4.14**. Smaller patches were generated by lower radius, and larger patches produced by higher radius. In particular, the similar periodic patchwork patterns, were

[124] where $Emd(k,\sigma)$ denotes embeddedness pace of a segment at the radius of (k-σ) to k; $\alpha(k,\sigma)$ indicates the slope of the regression line found at the radius of (k-σ) to k in the log-log radius plot; and NC_k means node count of the line (or segment) at the radius of k.

[125] The patchwork patterns generated by metric embeddedness pace (based on segment map) are much stronger than those produced by topo-embeddedness pace (based on axial map). For details, see Section 4.3.3 in Chapter Four.

also generated by another variable of metric mean depth (MMD), meaning average metric distance from all segments to all others. As discussed in Chapter Four (following Park's work[126]), the rank order of metric embeddedness pace mathematically approximated that of MMD, although one of which seemed to focus on the contexts, and the other expressed on the internal layouts. This in fact suggests that both variables might capture the same properties of urban grid. By and large, the periodic patchwork patterns – generated by either variable – at least *mathematically* reveal a regularity of *spatial discontinuity* – where the values of metric embeddedness pace or MMD change significantly – in the urban grid.

By creating the periodic patchwork patterns at different radii (and across different cases) it was possible to represent, observe, measure, compare and even experiment upon the significant regularity of spatial discontinuities in urban grids by manipulating spatial data in a syntactic way. Therefore, it can be argued that the periodic patchwork pattern can be treated as *a created phenomenon*, termed by Hacking (1983), that a noteworthy discernible regularity under definite circumstances is revealed, represented or created by designing and doing experiments.

Moreover, another significant finding of the generative analysis was that the periodic patchwork pattern can be represented as the peak-trough pattern in the mountain scattergram plotting the reversal of MMD at a fixed radius on the vertical axis against MMD at the infinite radius on the horizontal axis. In each case of Central London, Central Beijing and the London Docklands (demonstrated in Chapters Five and Six), red patches corresponded to peaks, and blue patches related to troughs. Since smaller MMD meant higher metric integration, the peak represented a layout in which MMD values increased from a metrically integrated centre (denoted by the summit of the peak) to the surroundings; and meanwhile, the trough denoted a layout in which MMD values decreased from a metrically segregated place (represented by the bottom of the trough) to the surroundings. As a result, those patches generated at the *non-global* radii were *morphologically* categorised into two groups according to their representations in the mountain scattergram. The spatial transition between these two groups of patches might suggest a kind of spatial discontinuity represented by the periodic patchwork patterns. It can be argued that such

[126] See the appendix in Hillier, B. et al (2010) Metric and Topo-geometric Properties of Urban Street Networks: Some Convergences, Divergences and New Results, *The Journal of Space Syntax*, 258-79, p. 258-9.

periodic patchwork patterns, created by metric embeddedness pace or MMD, help to set up a spatial framework of exploring what an area is in term of spatial configuration.

7.3.2 The conceptual relationship among two morphological motifs, the periodic patchwork and the peak-trough pattern

The empirical analysis (conducted in Chapters Five and Six) further suggested two kinds of morphological motifs (respectively associated with two types of created patches): *the centre-to-edge motif*, meaning the sub-grid in which smaller blocks are placed at the centre and bigger blocks at the edge; *the edge-to-centre motif*, indicating the sub-grid in which smaller blocks are situated at the edge and bigger blocks at the centre. For example, in each case of Central London, Central Beijing and the London Docklands, red patches were surrounded by blue patches, and vice versa. By and large, this suggested that these two types of morphological motifs appeared alternatively across the urban network as a whole. It can be therefore inferred that more intensified sub-grids tend to be placed side by side with less intensified sub-grids.

Moreover, red patches produced at a fixed radius *on average* had shorter segments than the surrounding segments involved in creating that red patch; and meanwhile, blue patches *on average* had longer segments than the contextual segments involved in creating that blue patch - although the segment structures of both the red and blue patches in the London Docklands morphologically extended out in several constricted directions rather than all directions, in contrast to the patches in Central London and Central Beijing. Since shorter segments and/or smaller blocks mean more intensified parts, and longer segments and/or larger blocks indicate less intensified parts, the above analysis suggests that the transition between different degrees of intensified parts, expressed by the change rate of segment density, were involved in producing the periodic patchwork patterns in the empirical studies of Central London, Central Beijing and the London Docklands.

However, the patches – either in red or in blue – located at the edge of the whole city were less intensified than the patches situated at the centre, which was empirically demonstrated in Chapter Five. By examining notional examples (**Fig.7.1**), we seek to further clarify the *morphological* mechanism of generating the same coloured patches at both the centre and the

edge of a city as a whole system, and then to explore a theoretical relationship between segment density and radius.

Fig. 7.1 a and **b** display two centre-to-edge sub-grids picked out by the same fixed radius from the root segment (marked by black dot). The former theoretically represents a less intensified sub-grid found *at the edge of a larger system*, and the latter shows a more intensified one located *at the centre of the larger system*. We respectively calculated the change rate of node count (metric embeddedness) and MMD of the root segment. The root segments of these two sub-grids have similar metric embeddedness (1.56 and 1.59, respectively) and MMD (9.03 and 9.07, respectively) at the level of the sub-grid. This suggests that metric embeddedness or MMD at the local scale captures the locally defined feature that the block size of these two sub-grids *reduces*, in a consistent way, from the centre to the edge.

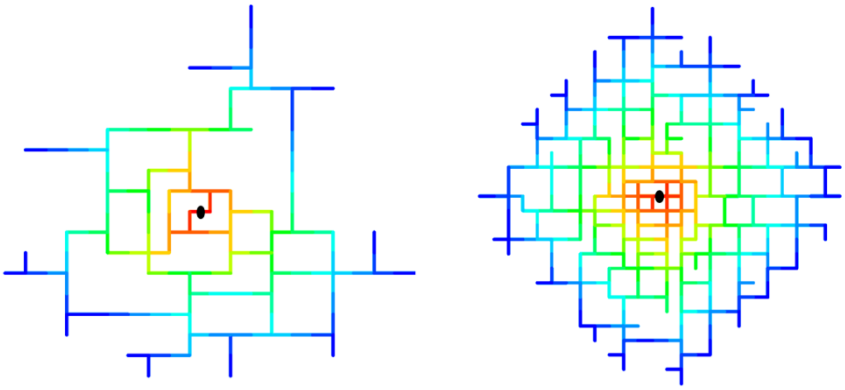

a. A less intensified centre-to-edge sub-grid b. A more intensified centre-to-edge sub-grid

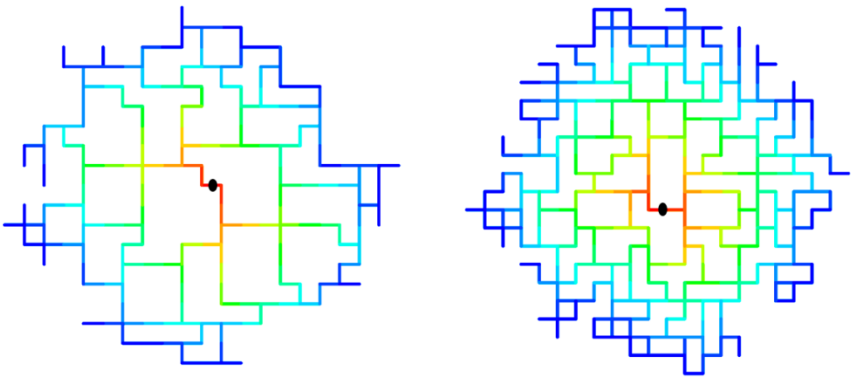

c. A less intensified edge-to-centre sub-grid d. A more intensified edge-to-centre sub-grid

Fig. 7.1 Four Notional Sub-grids Selected From A Larger Grid. Each sub-grid has the same fixed radius of 14 from its root segment (highlighted by black dot) to its edge segment; and each

of them is coloured with regard to the depth from its root segment. (Red denotes the segments closing to the root segment, and blue indicates the segment far from the root segment)

Moreover, **Fig. 7.1 c** and **d** demonstrate two edge-to-centre sub-grids defined by the same fixed radius from the root segment (highlighted by black dot). Again, the former represents a less intensified sub-grid found *at the edge of a larger system*, and the latter shows a more intensified one located *at the centre of the larger system*. The root segments of these two sub-grids have similar metric embeddedness (2.14 and 2.15, respectively) and MMD (10.1 and 10.0, respectively) at the level of the sub-grid. This indicates that metric embeddedness or MMD calculated at the local scale reflects a kind of local property that the block size of these two sub-grids *increases*, in a consistent way, from the centre to the edge, although they have different degrees of intensification.

In general, it can be suggested that the patches (created by metric embeddedness or MMD at a fixed radius) manifest *the geometrical arrangement* that all the blocks of each sub-grid (defined by the local radius) geometrically vary from the centre to the edge. As the whole system is not evenly intensified, the different sub-grids have the different geometrical arrangements of blocks and segments at local scales, which perhaps generate the differently coloured patches. For example, the centre-to-edge sub-grids relate to red patches, and the edge-to-centre sub-grids are associated with blue patches. In this sense, it can be argued that the geometrical arrangement of blocks taking place at local scales result in the periodic patchwork patterns.

More accurately, the idea of geometrical arrangement involves two variables, namely segment density and the change in radius. Segment density basically measures the number of segments encountered within a fixed radius as a unit. And this reflects a *static* geometric feature of grid intensification[127], in which the reduction in block size would reduce MMD from all segments to all others. And as reviewed in Chapter Three, radius can be treated as a tool for selecting a group of segments up to a fixed metric distance away from root segment[128], and this suggests the concept of *catchment area* from the root segment. The change in radius therefore captures the variation of catchment areas, and this indicates *dynamic* view of observing catchment areas.

[127] For a theory of grid intensification, see Hillier (1999, 2007, 2010). This was reviewed in Chapter Four.
[128] For details, see Section 3.23.

Thus, the combination of segment density and the change in radius, to a large extent, suggests *a kind of local geometric dynamics*, meaning the variations of block size and/or segment length in relation to a sequence of different sized catchment areas representing the view fields starting from root segment. To large extent, this implies that the dynamic variations of local geometric features, if we observe from all the segments at a series of local radii, are essentially involved in the creation of the periodic patchwork patterns.

Considering that the original idea of embeddedness trajectory - on which each segment is spatially embedded into the contexts, regarding to its distances to them, with an increase of radius - also shows the variation of catchment areas (shown in Fig. 4.1 in Chapter Four), the local geometrics dynamics seems to relate to the embeddedness trajectory. By numerically examining the log-log relationship between node count and radius for individual sample segments (conducted in Chapters Five and Six), each empirical case study demonstrated that the segments selected from the red patches had similar power-law exponent of smaller than 2, but the segments chosen from the blue patches had similar exponent of larger than 2 (**Tables 5.8, 5.9 and 6.8**). In contrast, any a segment selected from an evenly intensified grid – without taking account of edge effect – theoretically have a power-law relationship, with the approximated exponent of 2, between node count and radius. Since urban grid is theoretically embedded into a two-dimensional surface, the power-law exponent of 2 in fact suggests the way of evenly intensifying the urban grid. As a result, red patches with the exponent of smaller than 2 indicates that these red patches encountered less intensified sub-grids with an increase of radius; and blue patches with the exponent of larger than 2 demonstrates that these blue patches met more intensified sub-grids with an increase of radius. This suggests the kind of *dimensional distortion of urban grid* in which red patch, with the dimensions of smaller than 2, is interpreted as the centre-to-edge motif, and blue patch, with the dimensions of larger than 2, is treated as the edge-to-centre motif. As Chapter Four suggested that power-law exponent is associated with the variable of MMD at a fixed radius, do different dimensions of the sub-grids imply the optimisation of MMD of those sub-grids at local scales? Or, why is urban grid unevenly intensified?

7.3.3 The Multi-scale Grid Intensification

Then, we conducted a notional experiment in order to explore whether a sub-grid –selected from a large grid – seeks to optimise its MMD values at low and medium radii by taking the unevenly intensified form. We started by examining a 700m× 700m regular grid, with each cell constituted by 10 one-metre-segments at each side, called Grid A (**Fig. 7.2**). Then, A 300m×300m sub-grid, located at the centre and highlighted by red lines, was selected to calculate MMD at the radius of 20m to 200m, with an interval of 20m. It is called sub-grid A. As the distance from the edge of this sub-grid to the edge of the grid is 200m, the radius of smaller than 200m - at which the central sub-grid was studied - would help us to avoid the edge effect of the whole grid.

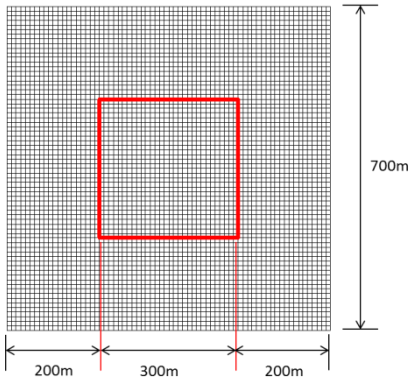

Grid A

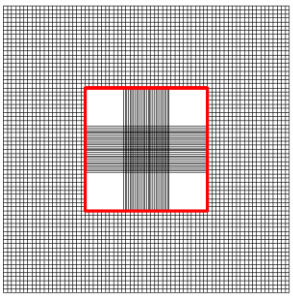

Grid B

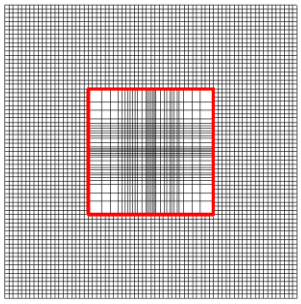

Grid B1

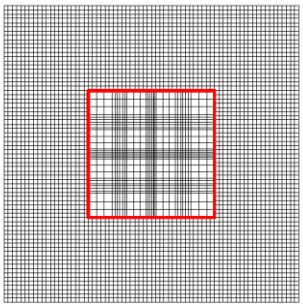

Grid B2

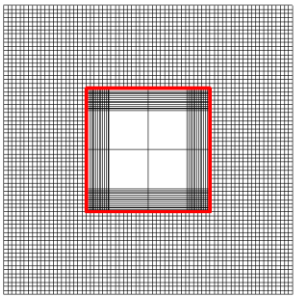

Grid C

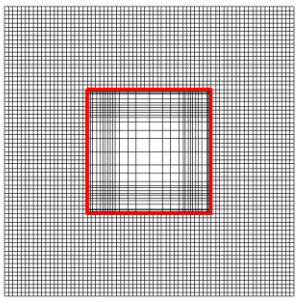

Grid C1

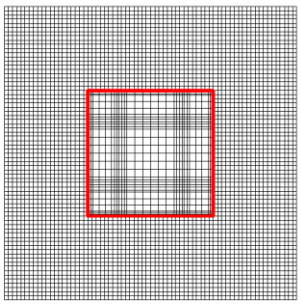

Grid C2

Fig. 7.2 Five Notional Grids with The Central Sub-grids. Grid A is a 700m× 700m regular grid, with each cell constituted by 10 one-metre-segments at each side; Sub-grid A is a 300m×300m sub-grid located at the centre and highlighted by red lines. The 300m×300m sub-grid is transformed into the centre-to-edge subgrids with the different degrees of intensification, and this is represented by Grids B, B1 and B2, respectively. And the 300m×300m sub-grid is also transformed into the edge-to-centre subgrids with the different degrees of intensification, and this is represented by Grids C, C1 and C2.

On one hand, the 300m**×**300m sub-grid was intensified at the *centre* to produce three sub-grids representing the centre-to-edge motif (**Fig. 7.2**). Sub-grid B1 is less intensified at the centre than Sub-grid B, but more intensified at the centre than Sub-grid B2. On the other hand, the 300m**×**300m sub-grid was intensified at the *edge* to generate three sub-grids representing the edge-to-centre motif. Sub-grid C1 is less intensified at the edge than Sub-grid C, but more intensified than Sub-grid C2. The MMD values at the radius of 20m to 200m were calculated for these six sub-grids respectively.

Table 7.1 The Metric Mean Depth (MMD) at Local and Global Radii of The Central Sub-grids.

Light red denotes low values and dark red indicates high values; MMD_R20 means metric mean depth at 20m, and MMD_n indicates metric mean depth at the infinite radius.

	MMD_R20	MMD_R40	MMD_R60	MMD_R80	MMD_R100	MMD_R120	MMD_R140	MMD_R160	MMD_R180	MMD_R200	MMD_n
SGrid A	13.0	26.5	39.8	53.1	66.4	79.7	93.1	106.4	119.7	133.0	372.9
SGrid B	11.8	25.8	41.6	55.9	69.5	82.1	94.2	106.0	117.8	129.6	361.7
SGrid B1	12.8	26.7	40.1	53.4	66.6	79.7	92.7	105.7	118.5	131.4	365.4
SGrid B2	12.8	26.4	39.5	52.9	66.4	79.7	92.8	106.1	119.3	132.4	369.0
SGrid C	11.8	25.6	40.9	54.5	67.6	80.3	92.9	105.5	118.4	131.4	388.0

SGrid C1	12.7	26.5	39.8	52.9	65.9	78.9	92.0	105.1	118.4	131.9	380.4
SGrid C2	12.7	26.3	39.5	52.8	66.2	79.4	92.6	106.0	119.4	132.9	376.9

Table 7.1 shows that Sub-grid A, the evenly intensified sub-grid, is not the most metrically integrated across all the non-global radii, comparable to all the other intensified sub-grids. At the radius of 20m and 40m, Sub-grids C and B, respectively representing the edge-to-centre and the centre-to-edge motifs, are most integrated; at the radius of 60m and 80m, Sub-grids C2 and B2 are most integrated, but Grids B most segregated; at the radius of 100m to 160m, Sub-grid C2, an edge-to-centre motif, is most integrated, but Sub-grid B most segregated (except 160m); at the radius of 180m and 200m, Sub-grid B is most integrated but Sub-grid A most segregated. This suggests two points. First, if a sub-grid selected from an evenly intensified grid was transformed into the sub-grids more intensified at either the centre or the edge, it would become more metrically integrated at relatively lower or medium radii (without the edge effect). Second, the sub-grid taking the form of the centre-to-edge motif is more integrated at higher radii and the lowest radii, but the sub-grid taking the form of the edge-to-centre motif is more integrated at lower and medium radii. It can be suggested that the unevenly intensified sub-grids, located at the centre of the whole grid, are more metrically integrated than the evenly intensified sub-grids across scales.

Table 7.2 The Metric Mean Depth (MMD) at Local and Global Radii of Seven Larger Grids. Light red denotes low values and dark red indicates high values; MMD_R20 means metric mean depth at 20m, and MMD_n indicates metric mean depth at the infinite radius.

	MMD_R20	MMD_R40	MMD_R60	MMD_R80	MMD_R100	MMD_R120	MMD_R140	MMD_R160	MMD_R180	MMD_R200	MMD_n
Grid A	13.0	26.3	39.4	52.4	65.4	78.3	91.0	103.7	116.3	128.8	470.0
Grid B	12.8	26.2	39.7	52.9	65.8	78.5	91.0	103.4	115.7	127.9	467.8

Grid B1	12.9	26.3	39.4	52.4	65.3	78.2	90.9	103.5	116.0	128.5	468.2
Grid B2	13.0	26.3	39.3	52.4	65.3	78.2	91.0	103.6	116.2	128.7	469.1
Grid C	12.8	26.1	39.7	52.8	65.7	78.5	91.2	103.7	116.2	128.6	474.3
Grid C1	12.9	26.3	39.5	52.5	65.4	78.2	90.9	103.5	116.1	128.6	471.9
Grid C2	12.9	26.3	39.4	52.4	65.4	78.2	91.0	103.7	116.3	128.8	471.0

Then, we further examined whether the larger grid in which the central sub-grid is embedded would become more integrated or segregated across radii. As **Fig. 7.2** shows, Grids B and C are more integrated at the radius of 20m and 40m; Grids B2 and C2 seem to become more integrated at the radius of 60m, 80m and 100m; Grids B1 and C1 intend to become more segregated at the radius of 100m to 140m; Grid B is most integrated at the radius of 160m to 200m. Roughly speaking, at the radius of smaller than 140m, the central sub-grid corresponding to either the centre-to-edge motif or the edge-to-centre motif helps to reduce the MMD Rk of the whole system; at the radius of not smaller than 140m, the sub-grid B, associated with the centre-to-edge motif, makes the whole system more integrated. This suggests that the unevenly intensification of the sub-grids also contribute to the optimisation of metric integration of the whole grid into which those sub-grids are embedded. In other words, when a sub-grid is intensified either at the centre or at the edge of the sub-grid, the whole system into which it is embedded will also become more metrically integrated at a series of relatively *local* radii and the global radius.

In theory, a city as a whole seeks to take the form of the centre-to-edge motif, with an attempt to maximise MMD at the level of the whole system, as discussed in Chapter Three. **Fig. 7.2** also demonstrates that even the central sub-grid taking the centre-to-edge motif results in the reduction of MMD at global scale for the whole system. Thus, it can be theoretically argued that urban grid results from a combination of different layers of multi-scaled grid intensification, namely *a single centre-to-edge grid* in which the centre part of urban grid as a whole *on average* is more intensified than the edge part, as well as the *periodic patchwork patterns* in

which *the centre-to-edge motifs* are mixed with *the edge-to-centre motifs* identified at a series of relatively local radii. For the urban grid, some patches at the edge of the whole system, albeit less intensified at the global scale, would have almost the same degrees of local-scale metric integration as those at the centre of the whole system. This aims to optimise, rather than maximise, metric integration of the whole system at those local/medium scales. In this sense, cities seek to *simultaneously* intensify their grids and/or sub-grids at both global and local scales, in order to balance the optimisation of global metric integration with that of local metric integration. We call it the *multi-scale grid intensification*, which might facilitate inter-accessibility between all the streets at the radius ranging from the global to the local.

Then, it can be argued that the periodic patchwork patterns - in which red patches emerge side by side with blue patches at a series of local radii - *roughly* manifest the layers of the grid intensification taking place at *local* scales, rather than the global scale of the whole system, in order to optimise metric mean depth of the whole system at the *non-global* scales.

7.4 The nature of the boundaries of the pre-given areas

However, *not* all the created patches visually related to the pre-given areas investigated in Chapters Five and Six. The majority of the historic areas in London and Beijing and many smaller areas in the London Docklands were visually associated with the patches created by metric embeddedness paces and MMD; but a few of those historic areas – such as Marylebone and Mayfair of London and Shichahai of Beijing – as well as nearly all the larger development areas and some smaller areas – such as the east part of Bermondsey – in the Docklands did not visually co-incide with the patches created at any a radius. The outliers in the historic areas were influenced by their historic development in that the smaller historic clues can be approximately identified by smaller patches created by smaller radii; and the outliers in the Docklands were perhaps affected by both historic structures of those larger development areas and the fragmented structure of the whole Docklands district. This in fact suggests a complex relationship between the pre-given areas and the periodic patchwork patterns generated by the variables of metric embeddedness paces and MMD.

Moreover, each historic area in London and Beijing was identified by one certain radius, if possible; and with an increase of radius, the patches associated with those historic areas would be consolidated into larger patches, and therefore the pattern of the spatial discontinuities was changed. In contrast, a number of the smaller areas in the Docklands were marked out by several radii. For example, a luxury housing estate in Royal Dock called Silvertown was differentiated by the radii of 500m to 900m, 700m to 1100m, and 1200m to 1600m, respectively (**Fig. 6.17**). And the patches related to those smaller areas of the Docklands hesitated to be merged with their surroundings to form larger patches generated at higher radii. It can be suggested that the boundaries of those Dockland areas seem to function as spatial barriers according to the relationship between the internal structures and their contexts, but the boundaries of those historic areas more serve as spatial integrators connecting neighbouring areas. To a large extent, it can be argued that the boundaries of the pre-given areas might be measured by the degrees of spatial discontinuity - between the internal and the external – generated in urban grid.

Finally, the mountain scattergrams of those pre-given areas showed a much more complex but subtle scenario with morphological implications. The London and Beijing areas were either represented as a peak or denoted as a trough at certain radius; and meanwhile, a high proportion of the Dockland areas were not manifested as a single peak or a single trough across radii, but denoted as two peaks or a combination of one peak and one trough (like a spindle shape). This demonstrated that each of those Dockland areas, compared to the historic areas in London and Beijing, was not structured into a single motif, either the centre-to-edge motif or the edge-to-centre motif, at any radius; but divided into at least two morphological parts. In this sense, it can be suggested that those Dockland areas, as the newly developed areas, do not function as a single morphological entity that was naturally developed at certain radius. As a result, it can be implied that the relatively clear boundaries of the newly developed areas have less degree of correspondence to the spatial discontinuities in the London Docklands as a whole.

7.5 Synthesis: fuzzy boundaries

Based on the discussions conducted in the previous sections, a theoretical concept that area discontinuities arise from the spatial discontinuities in urban grid is proposed, and this casts new light on the spatial definition of urban areas. In contrast to the conventional idea – reviewed in Chapter Two – that a city as a whole is considered as a collection of territorially bounded units with *either clear or soft boundaries*, analogous to cell walls, supporting socio-economic, cultural and functional activities within each unit, this thesis argues that urban areas *emerge* from the way in which individual spaces are structured internally and how this relates to the spatial structuring in the contexts found at different scales. As a result, the area boundaries, in general, are *fuzzy* in the sense that they are the manifestations of the spatial discontinuities (where the configurational relationships change significantly) varying at different scales, but do not depend on the area being either self-contained, geometrically differentiated, or having clear spatial limits.

On this ground, *a conceptual model* can be proposed to explain the spatial mechanism of generating area structures represented by the periodic patchwork patterns produced at different radii. It comprises two parts. First, a city is unevenly intensified at both global and local scales, usually shown by *the centre-to-edge grid at global scale*, as well as *the centre-to-edge and edge-to-centre motifs alternatively found at a series of non-global or local radii*, in order to optimise metric integration at both global and local scales, rather than maximise metric integration at a fixed scale. Perhaps this might result from small-scale economic activity process (Hillier, 1999) that aims to maximise interaccessibility from all places to all the others at both global and local scales, in that people need to reduce travel distance across different levels of areas, ranging from street to quarter, neighbourhood, district, city and even region. In this sense, it might be the multi-scale microeconomic process that serves as an essential tool of spatially aggregating urban parts into a whole.

Second, the different parts of the urban grid then obtain the different rates of change in street density (approximated by segment density), as the urban grid has been unevenly intensified. At non-global scale, each of the streets making up an area is also spatially embedded into the multi-scale contextual structures at different rates. This can be numerically described by the

embeddedness trajectories with the discontinuities where the embeddedness rates change dramatically. The fuzzy boundaries of urban areas then arise from, and vary with, their relations with the multi-scale external structures involved in generating those areas at different radii.

It can be suggested that this conceptual model provides a new way of defining urban areas with regard to spatial configuration. The fuzzy boundaries of urban areas, it has been argued, are at least as much more influenced by the contexts as by the internal structure itself, in that the previous three chapters empirically and theoretically showed a kind of *remote effect* through which the spatial structuring in the larger – even much larger- context interacts with the local – and even the non-local – spatial properties of an area, and creates the fuzzy boundary effect, which becomes a main factor in the definition of the areas represented at the non-global level.

This thesis has suggested that urban areas pre-defined in terms of other socio-economic variables, such as named areas and the newly developed areas, can be characterised and differentiated according to the way they are spatially embedded into the surroundings. However, it just made an initial step towards investigating functional meaning of the created patches, and focused on the spatial rather than the socio-economic. The latest space syntax researches suggested that *the street itself was a place for community interaction, with varying degrees of mixing across social groupings* (Vaughan, 2018: 215). The empirical studies also implied that urban spatial configuration might play a key role in socio-economic differentiation (Omer, Goldblatt, 2012; Law, 2017; Major, 2018). It might be conjectured that the created patches, arising from the spatial interaction between the internal and the external, might sustain social differentiations and/or groupings. Movements along the streets between the patches and the contexts play a fundamental role in generating those patches. A more systematical, detailed and in-depth comparison between socio-economic data and created patches is required to help understand the social or economic significance of the periodic patchwork patterns.

Appendix A: The Mathematical Relation between Metric Embeddedness and Metric Mean Depth (MMD)

In the light of the idea of embeddedness trajectory as discussed in **section 4.2** (**Fig. 4.5 Bottom Right**), we first propose a method of calculating MMD (based on segment representation) by plotting node count, that is, the sum of segments encountered up to a fixed radius, on the x-axis, against metric radius, on the y-axis (Yang and Hillier, 2012). The variable of node count can be expressed as a function of metric radius shown as follow:

$$NC_k = f(k) \qquad (4.7)$$

where k indicates radius, and NC_k denotes node count at k.

Fig. B.1, for example, illustrates the scattergram of such function of radius. As radius goes up, node count of any a root segment always increases until the root encounters all other segments within the system. Thus, the slope of the curve of $f(k)$ is not below zero. In the meanwhile, total metric depth of the root at k, meaning the sum of metric distance from the root to all other segments up to k, can be expressed as follow:

$$TMD_k = \int k \times df(k) \qquad (4.8)$$

where k means the radius, TMD_k denotes total metric depth at k, and $df(k)$ indicates the derivative of NC_k, equal to the slope of the curve of $f(k)$ ($df(k) \geq 0$).

Thus, metric mean depth is defined as follow:

$$MMD_k = \frac{TMD_k}{NC_k} = \frac{\int k \times df(k)}{f(k)} \qquad (4.9)$$

where MMD_k denotes metric mean depth at k, TMD_k means total metric depth at k, and NC_k indicating node count at k.

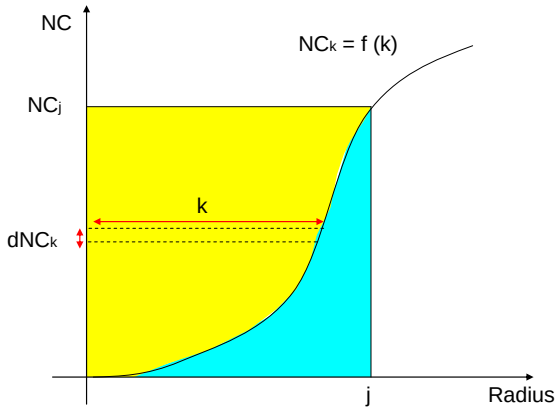

Fig. B.1 Node count (NC_k) can be expressed as a function of radius (k): $NC_k = f(k)$.

Total metric depth (TMD_k), defined as $TMD_k = \int k \times df(k)$, is equal to the area of the yellow shape.

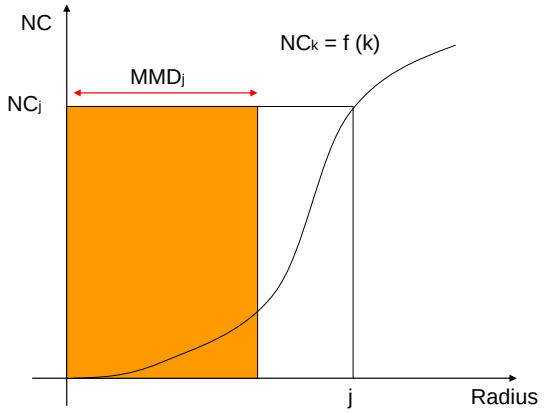

Fig. B.2 The yellow shape showed in ***Fig. B.1*** can be transformed into a rectangle coloured in orange. The width of this orange rectangle is equal to metric mean depth at a fixed radius of j (MMD_j), expressed as follow $MMD_k = \frac{TMD_k}{NC_k} = \frac{\int k \times df(k)}{f(k)}$.

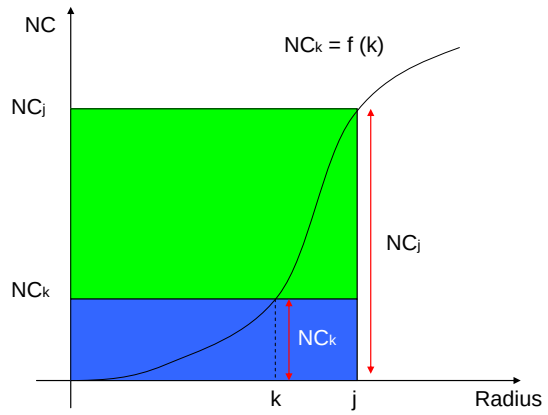

Fig. B.3 The yellow shape showed in ***Fig. B.1*** also can be transformed into a green rectangle; whilst the cyan shaped illustrated in ***B1.1*** can be converted into a blue rectangle. Metric mean depth at a fixed radius of j (MMD_j) also can be expressed as follow: $MMD_j = j \times (1 - \frac{NC_k}{NC_j})$

As **Fig. B.1** shows, a rectangle whose width is j and length is NC_j can be divided into two parts, the top right coloured in yellow and the bottom left coloured in cyan. The derivative of NC_k can be expressed as the smallest interval at NC_k (denoted as dNC_k) on the vertical side of the yellow shape, and k can be expressed as the length of the horizontal section of the yellow shape at NC_k. The value of dNC_k approximates the number of the segments encountered at k. Thus, total metric depth at a specified radius of j (denoted as TMD_j) is expressed by $\int k \times dNC_k$, according to **equation 4.8**. And meanwhile, the total area of the yellow shape is in fact equal to the value of $\int k \times dNC_k$, so that the total metric depth at j is represented by the total area of the yellow shape.

Then, we can calculate MMD at the radius of j (denoted as MMD_j) in two different ways. On the one hand, the yellow shape (**Fig. B.1**), representing TMD_j, can be transformed into an orange rectangle with the same area, as shown in **Fig. B.2**, and the length of its vertical side is equal to the node count at j (denoted as NC_j). Thus, the horizontal side of this orange rectangle

should be equal to MMD_j (**Fig. 4.18)**, according to **equation 4.9**. Then MMD_j can be interpreted as the average metric distance from the root segment to all other segments up to the radius of j.

On the other hand, the yellow shape (**Fig. B.1**), representing TMD_j, also can be transformed into a green rectangle with the same area (**Fig. B.3**); and meanwhile, the cyan shape, also showed in **Fig. B.1**, can be transformed into a blue rectangle with the same area (**Fig. B.3**). The green rectangle has a width of j and a length of ($NC_j - NC_k$) and the blue rectangle has a width of j and a length of NC_k. The sum of the areas of the green and blue rectangles, illustrated in **Fig. B.3**, is equal to the area of the rectangle whose width is j and length is NC_j, showed in **Fig. B.1**. Thus, the area of the green rectangle, representing TMD_j, is equal to the value of ($j \times NC_j - j \times NC_k$), and so MMD_j can be expressed as follow:

$$MMD_j = j \times (1 - \frac{NC_k}{NC_j}) \qquad (4.10)$$

where MMD_j denotes metric mean depth at a certain radius of j, j indicates a certain radius of j, NC_k means node count at k and NC_j means node count at j.

According to **equation 4.6 in chapter four**, metric embeddedness can be expressed as follow:

$$Emd(j, j-k) \sim \frac{NC_j}{NC_k} \qquad (4.11)$$

where $Emd(j, j-k)$ denotes the metric embeddedness of a segment at the radius j, meaning the change rate of node count of the segment at the metric radius of (j-k) to j, and NC_j means node count at the radius of j.

The above **equation 4.11** shows that metric embbeddedness at the radius of j can be approximated by NC_j divided by NC_k. According to **equation 4.10**, MMD at the radius of j has a positive linear relation with the value of NC_j divided by NC_k. Thus, MMD at j also has a positive linear relation with metric embeddendness at j. This suggests that *MMD at a fixed radius also can be interpreted as a function of the change rate of node count between the two specific metric radii*.

In this sense, the variable of MMD can be used to capture the discontinuity along the embedded trajectory. Mathematically speaking, MMD at a fixed radius and metric embeddedness within a constricted radius range will generate the same periodic patchwork patterns, if we choose an appropriate radius range for calculating metric embeddedness.

Appendix B: A Brief Introduction of the Central Districts of London and Beijing

Although both Central London and the Inner City of Beijing are the historic districts which have evolved over several centuries, they were constructed in different ways associated with the formation of the distinctive named areas in history. The following section will briefly review how the named areas were generated during the process of spatial transformation taking place in the two cities, in order to provide an informative background for investigating the named areas in the two contrasting cases of London and Beijing.

D.1 The north part of Central London

As many writers (Clout and Wood, 1986; Hall, 1989; Morris, 1994; Kostof, 1999; Hebbert, 2001) pointed out, Central London always resisted the grand overall design, and evolved in a rather more piecemeal fashion throughout history. It originated from the Roman city of Londinium established as a trade port around 50AD. The boundary of the Roman city was almost the same as the boundary of the City of London which exists today. The Romans built London Wall around the landward side of the City around 190 to 225AD. After the Romans withdrew from Britain in 410 AD, the settlement of Londinium declined and was eventually abandoned. Later, a Saxon village[129] called Lundenwic – meaning London trading town - was built about one mile west from the original Londinium, and covered the area stretching from today's National Gallery site to Aldwych. Another new settlement named Ealdwic was also established within the old Roman walls in the later 9th century and became an important trading centre in the early 10th century. In 1097, Westminster Hall was constructed to and formed the foundation of the Palace of Westminster, the royal residence. Around 1200, the royal government moved to Westminster. As a result, the smaller town of Westminster became the Royal capital and central government, but spatially separated from the City of London as a commercial town. The sections between

[129] For Saxon village, see Biddle, M. (1976) Towns, in Wilson (ed) The Archaeology of Anglo-Saxon England, and Ross, C. and Clark, J. (2008) London: The Illustrated History, Pengiun Group: P54-55.

these areas were still rural in the late 16th century. For example, Covent Garden was a garden market and Bloomsbury was the location for hospitals and convalescent homes (Sheppard, 1998; Ross and Clark, 2008).

From the 1660s onwards, the spatial expansion of London increased enormously and London was transformed from a medieval town of wooden buildings within the City into a modern metropolis of brick and stone stretching out beyond the city wall (McKellar, 1999). In the early 17th century, mansions were progressively built along the old road of the Strand, from the City to Westminster, and several clusters of new houses were also constructed to the west of the City. For example, Lincoln's Inn Fields was built in about 1629, and houses were constructed at Covent Garden, on the Strand and at Long Acre shortly afterwards (Sheppard, 1998; Ross and Clark, 2008).

The old City of London and its immediate surroundings was entirely transformed by the Great Fire of London, which began in a baker's house on Pudding Lane at around 1 am on the 2nd September 1666[130]. In just four days, it destroyed most of the walled area including 86 churches and around 11000 dwellings, together with the old St Paul's Cathedral and the old Royal Exchange (Clout and Wood, 1986). The King, his Privy Council and the Parliament were active in formulating rebuilding regulation and a new design code. At the same time radical reconstruction schemes, encouraged by the King, were proposed by Christopher Wren, John Evelyn and Robert Hooke[131]. However, the reconstruction carried out over a full decade conformed roughly to the old street plan, rather than to follow an entirely new plan along the line of Wren's. The reconstructed City was adjusted on the grounds of hygiene and fire safety and included wider streets, a steady line of frontage and houses built of brick and stone rather than wood. Such incremental transformation of the urban form through the decade's adjustment to the old fabric was caused by the balance between the King, the public authority, and the owners and users of private properties (Kostof, 1999: 250). Many aristocratic residents never returned

[130] As for the detailed discussion about the impact of the Great Fire of London on urban transformation, see Morris, A.E.J. (1994) History of Urban Form: Before the Industrial Revolution, Pearson Education Limited: P255; Kostof, S. (1999) The City Assembled: The Elements of Urban Form Through History, Thames and Hudson Ltd: 245-50.

[131] For the plans proposed by Christopher Wren, John Evelyn and Robert Hooke, see Morris, A.E.J. (1994) History of Urban Form: Before the Industrial Revolution, Pearson Education Limited: P256-59.

after the great fire however, which encouraged more piecemeal development to the west of the City, such as St. James's (Clout, 1986; Sheppard, 1998).

In the late 17th century, the City expanded beyond its traditional boundaries into the West End. Elegant houses in squares and broad straight streets in St. James's were completed in 1680; whilst, Soho, Leicester and Golden Squares also became built up within a few years on either side. Fashionable houses started to be built at Bloomsbury and on the road to the village of Knightsbridge. In the 18th century, London spread out at an accelerating pace and swallowed more surrounding rural villages. For example, Mayfair, with its speculative property development, was built for the rich. The built up areas had combined the mediaeval City together with Westminster to form a single city. **Fig. D.1** shows urban extension from medieval to Georgian times (Clout and Wood, 1986).

London continued to grow and expand rapidly during the 19th century, accelerated by the advent of the railway. The city spread into the areas of Holborn, Paddington, Belgravia, Islington, Finsbury, Shoreditch, Southwark, Lambeth, Kensal Green, Hammersmith, Highgate, Clapton, Hackney, and so on, and absorbed nearly all outlying villages and hamlets. It was transformed into the world's biggest city as well as the global political, financial and trading capital (Clout and Wood, 1986; Sheppard, 1998). A series of the old London Map in 1572, 1680 1765 and 1824, illustrated in **Fig. D.2 a through to d**, demonstrates the incremental expansion of Central London from the 16th century to the early 19th century.

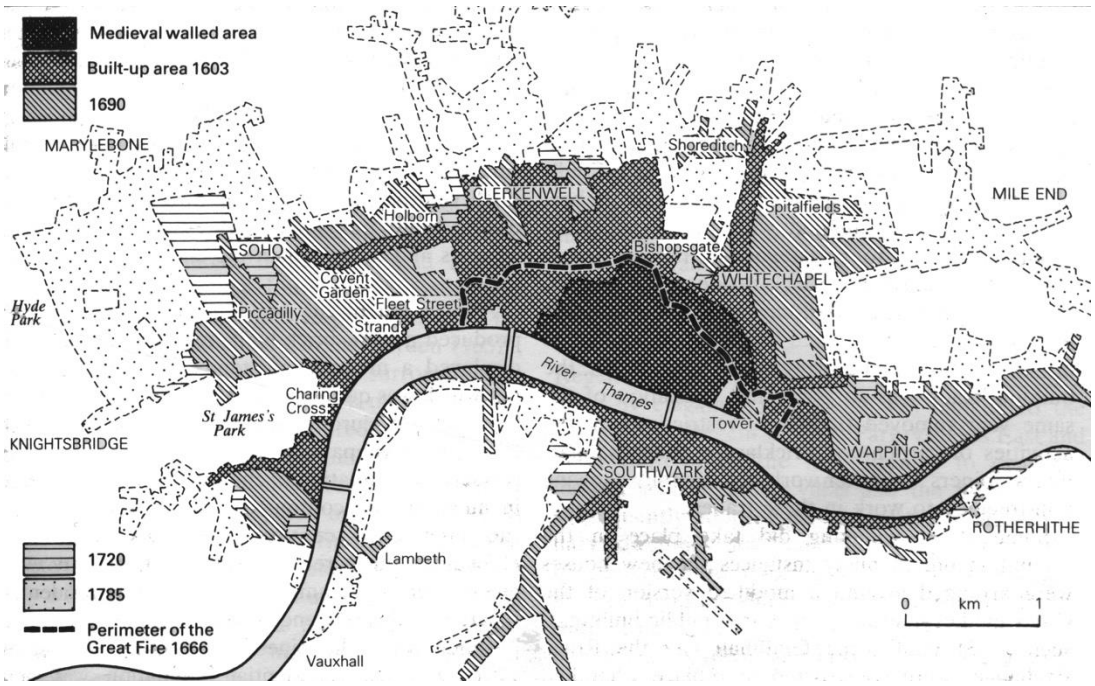

Fig.D.1 Urban transition of London from medieval to Georgian times (source: Clout H. and Wood P. (1986) ed. London: Problems of Chang, Longman Group Limited, P25)

Fig. D.2a London Map in 1572, Londinum Feracissimi Angliae Regni Metropolis (source: Foxell, S. (2007) Mapping London – Making Sense of the City, Black Dog Publishing Limited, P18-19)

Fig. D.2b London Map in 1680, A Map of the City of London and Westminster and Borough of Southwark with their Suburbs as it is now rebuilt since the late dreadful Fire in 1666(source: Foxell, S. (2007) Mapping London – Making Sense of the City, Black Dog Publishing Limited, P29)

Fig. D.2c London Map in 1765, Londres avec le Bourg de Southwark(source: Foxell, S. (2007) Mapping London – Making Sense of the City, Black Dog Publishing Limited, P217)

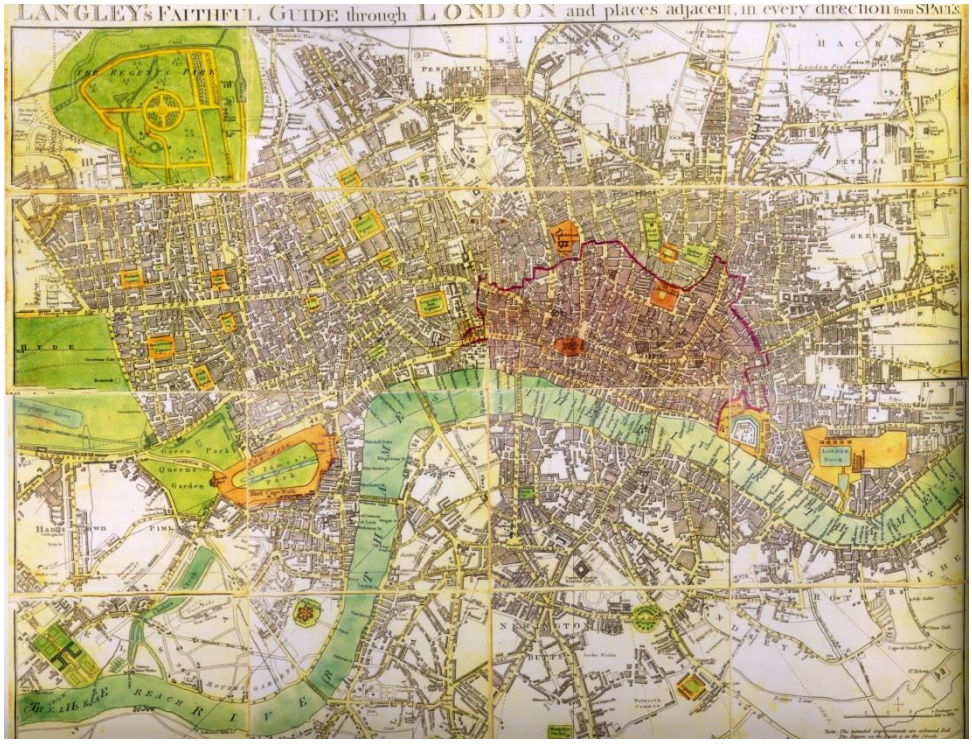

Fig. D.2d London Map in 1824, Langley's Map of London/Langley's Faithful Guide through London and Places adjacent in every direction from St Paul's (source: Foxell, S. (2007) Mapping London – Making Sense of the City, Black Dog Publishing Limited, P39)

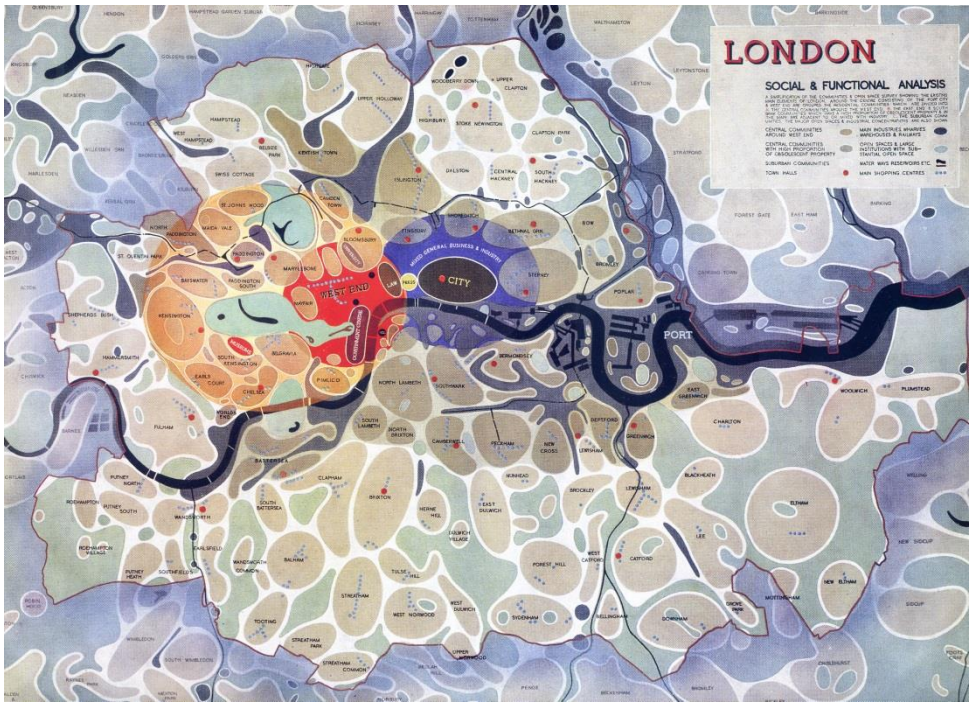

Fig. D.3 The survey map of the natural community structure of London drawn by Abercrombie for his London Plan (source: Forshaw J. H. and Abercrombie P. (1943) County of London Plan, Macmillan and Co. Limited, P20)

In the 20th century, Central London was expected to be transformed into a radically new urban form with pedestrians and an increased number of vehicles moving on different layers or channels without any obstruction (Tripp, 1942; Forshaw and Abercrombie, 1944; Buchanan 1963). Blitz damage around Central London during the Second World War provided an opportunity to test such grand design ideas (Forshaw and Abercrombie, 1944; Hebbert, 2001). For example, the Abercrombie's London Plan proposed the idea of fast motor-ring, tunneled arteries and flyover intersections for reconstructing Central London, in which arteries simultaneously solved the traffic problem and defined the urban areas, thus producing a cellular and organic structure (Forshaw and Abercrombie 1943: 3-10). The Buchanan report further suggested a multi-lane decked motorway along a commercial street, Tottenham Court Road, as well as a four layer intersection between the Euston Road and Tottenham Court Road (Buchanan 1963). Radical Schemes blossomed at Victoria, Piccadilly Circus, Covent Garden and the City. Vertically segregated decks and walkways were proposed to replace the conventional streets all over Central London in the 1960s and 1970s. However, many such grand plans never left the drawing board (Herbert, 2001). For example, Abercrombie's key road proposals, including the 'B' ring road[132] around Central London, were abandoned in 1950 (Collins, 1994); the Ringway network scheme proposed by the Great London Council in 1965 was dropped in 1973 (Hall, 1989); the comprehensive redevelopment of Convent Garden was halted in 1974. 'For the rest of that decade, no one had a word to say in favour of rebuilding, or comprehensive redevelopment, or motorways.' (Hall, 1989: 154) As a result, Central London continued to remain with an irregular structure and experienced incremental adjustments in this century. As Herbert (2001) indentified, the A-Z London in 1996 by and large was the same as the first edition in 1936.

Meanwhile, most of the villages and places swallowed up during the rapid expansion of London from the 17 century to the early 20 century still survive, which has characterized London as a

[132] The 'B' ring road was expected to serve as a by-pass to central London, warding off the through traffic. See Forshaw and Abercrombie 1943: 53-56.

collection of villages or distinct areas (Herbert, 2001). Even in denser Central London, various places with their own distinctive characters, but without official boundaries, are often described in a set of place names[133], such as Bloomsbury, Mayfair, the City and Covent Garden, which were coined by the collective through the daily life and tradition over hundreds years in terms of their situation, ownership, land use, administration, appearance, topography or any other association (Mill, 2001). Such area structure of London was also identified in Abercrombie's London Plan and illustrated in his survey map on communities **(Fig. D.3)**, which represented a starting point for reconstructing post-war London (Forshaw and Abercrombie, 1944; LCC, 1951). Although Abercrombie's proposal was to increase the degree of segregation for the existing sub-areas by arranging the main traffic roads along the boundaries between those sub-areas, Central London still went through the incremental adjustments and each named areas were merged together without the loss of the sense of wholeness. As a result, the subsequent London Plans always addressed the fact that London is unique in its tremendous collection of distinctive areas surprisingly compact within its urban expansion (LPAC, 1995; Hall, 1989; London Plan, 2008).

D.2 The Inner City of Beijing

By contrast, many researchers (Liang, 1952; Hou, 1998; Fu, 1998; Liang 2005) addressed that the Inner City of Beijing was originally planned and constructed according to a grand scheme[134] and the current named areas are closely associated with that original plan, although it has experienced internal reconstruction, adjustment and modification through its long history. Today, the Inner City, about 38 sq km, is bounded by the Second Ring Road to the north, west and east, as well as Chang'an Avenue, the ten-lane road bypassing Tian'an Men Square, to the south. Both the Second Ring Road and Chang'an Avenue were built along the former city wall of the Inner City after the 1960s. Like the north part of Central London, this district is also the

[133] For the evolvement of named areas of London, see Mills, A. D. (2010) A Dictionary of London Place-Names, Oxford University Press, Pxi-xxii.

[134] A conceptual plan of capital city, elaborated in the Confucian etiquette framework in the Zhou Dynasty (1027 - 256 BC), was used to guide the construction of the Inner City of Beijing, which will be discussed in the later part of this section. Or, see Liu Dun Zhen (1980) Chinese Architecture History, China Architecture and Building Press (in Chinese).

historic core of the capital city, and is comprised of the current political, cultural, commercial and financial centres.

Although the city of Beijing was constructed as the city state of Ji located in the southwest of present-day Beijing around 770 BC, and being the capital of the Kingdom of Yan[135], the provincial city of the subsequent Qin, Han, Tang, Song and Jin dynasties, as well as the capital of the late Jin dynasty in 1153, the majority of the current structure of the Inner City of Beijing is in fact inherited from the layout of the old Beijing constructed in the Yuan Dynasty (1271 - 1368) and modified and extended in the Ming (1368 -1644) and Qing (1644 – 1912) Dynasties (Liu, 1980; Hou, 1998; Fu, 1998; Liang, 2005). This is due to the reason that the old towns or cities, respectively named Jicheng, Yandu, Guangyang, Youzhou, Nanjing, Yanjing, Zhongdu etc., built on the site of the current Beijing in the different periods before the Yuan Dynasty, were destroyed by the wars during the dynasty transitions (Fu, 1998). As a consequence, the current Inner City in fact originated from Dadu[136], the capital city of the Yuan Dynasty.

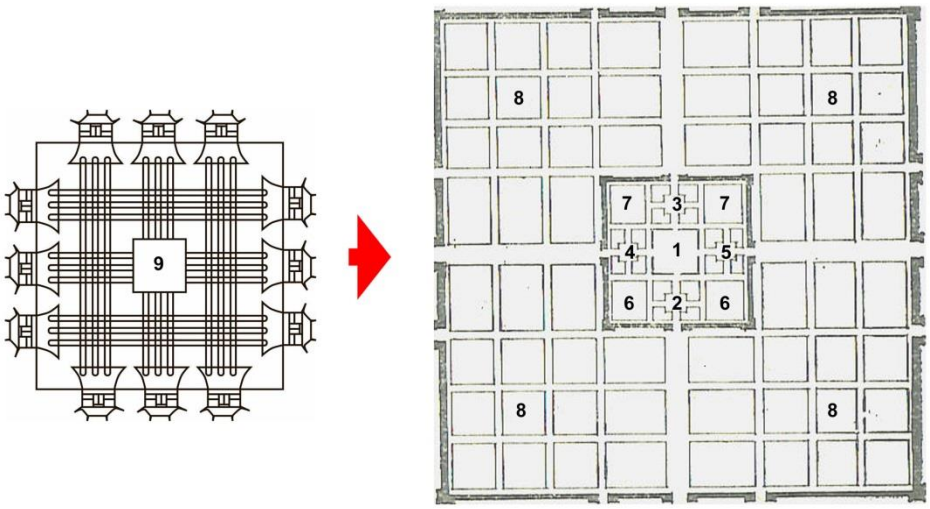

Fig. D.4 A conceptual capital city proposed in the 'Artificers' (source: Liu Dun Zhen (1980) Chinese Architecture History, China Architecture and Building Press)

[135] For the planning of the Kingdom of Yan and the city state of Ji, as well as their geographic relation to the current city of Beijing, See Liang (2005), Chinese Architecture History, Baihua Publisher, p67.
[136] The city of Beijing was called Duda – meaning great capital - in the Yuan Dynasty founded by the Mongol leader Kublai Khan.

1. The Palace City; 2. The government court; 3 The market; 4. The altar for sacrifices to the God of Land; 5.The royal ancestral temple; 6.The administrative offices; 7. The warehouses; 8. The gated residential quarters; 9. The Imperial City

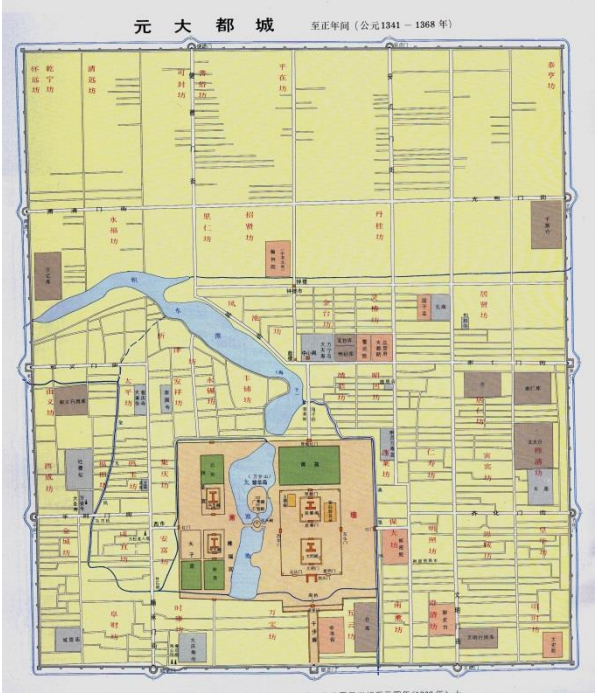

Fig. D.5a The Dadu (Beijing) Map between 1341 and 1368. It was built according to the conceptual plan of capital city proposed in the 'Artificers', and divided into 50 gated quarters. (source: Hou Ren Zhi (1988) A Collection of the Historic Beijing Maps, Beijing Publisher)

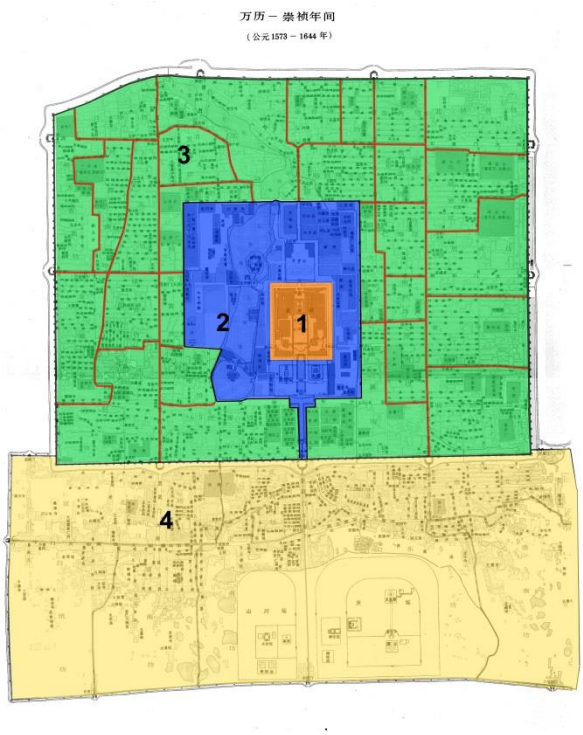

Fig. D.5b The Beijing Map between 1573 and 1644 (source: Hou Ren Zhi (1988) A Collection of the Historic Beijing Maps, Beijing Publisher)

1. The Palace City; 2. The Imperial City; 3; The Inner City; 4. The Outer City

The red lines indicate the boundaries of the gated residential quarters, called Fangs, in the Inner City.

Fig. D.6 The transition of Beijing from the Jin Dynasty (1153 -1271) coloured in cyan through the Yuan Dynasty (1271-1368) coloured in green to the Ming Dynasty (1368-1644) and the Qing Dynasty (1644-1912). The most part of the Inner City was constructed in the Yuan Dynasty and the Imperial City was reconstructed in the Ming Dynasty. The physical structure of the whole old Beijing was seldom changed from the late Ming Dynasty to the Qing Dynasty. (Source: Liu Dun Zhen (1980) Chinese Architecture History, China Architecture and Building Press).

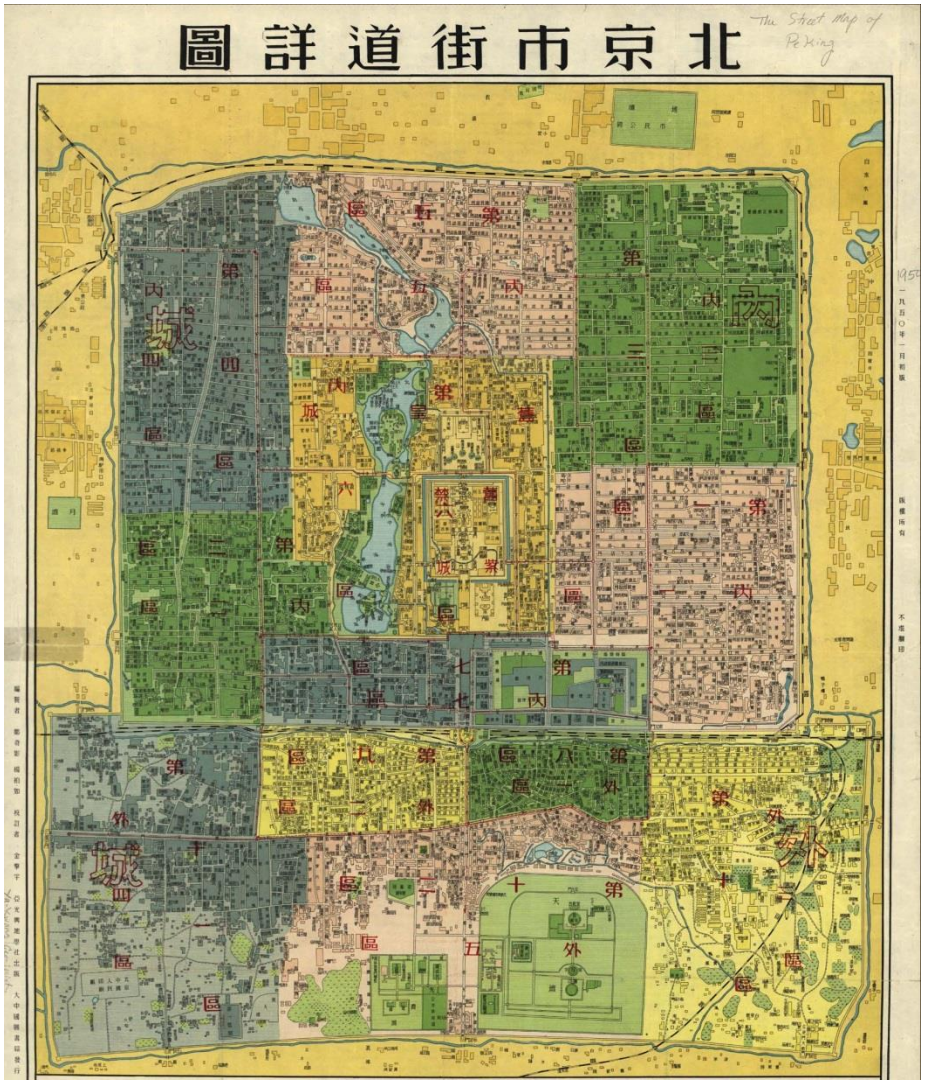

Fig. D.7 The old Beijing map in 1950 (source: Hou Ren Zhi (1988) A Collection of the Historic Beijing Maps, Beijing Publisher)

The whole old Beijing –including the Inner City and the Outer City - in 1950 had not extended outward beyond the city wall since it was completely constructed in 1553.

The city of Dadu, about 50.9 sqkm, began to be constructed in 1267, with the aim of building a capital city for preparing and establishing the Yuan Dynasty. It was deliberately planned and built as an orthogonal grid, according to the chapter of 'Kao Gong Ji' or 'Artificers'[137] on architectural design, city planning and building construction in the ancient Confucian etiquette framework called Zhouli[138]. **Fig. D.4** illustrates a conceptual plan of capital city proposed in the 'Artificers'. For example, a 9 by 9 li (equal to half kilometer) square is selected for constructing a capital city; each side has three gates; within the capital city are nine north-south roads and nine east-west avenues; the roads and avenues are nine carriage tracks in width (around 18m wide); the Imperial City for the emperor, the royal family and governmental officials was located at the centre of the 9 by 9 grid; the royal ancestral temple was located on the left while the altar for sacrifices to the God of Land on the right; the government court in the front and the market in the rear (Liu, 1980; Fu, 1998; Dai, 2003). It combined two kinds of morphologic patterns: the orthogonal grid, as well as the nested structure in which the palace located at the centre is encircled by the administrative offices and the royal temples and altar to form the Imperial City, and then the Imperial City is further enveloped by the ring of residential quarters to generate the capital city (Zhu, 1993).

To a large extent, the city of Dadu, illustrated in **Fig. D.5a**, was built according to an entirely new ground plan along the lines of what the book of 'Artificers' noted (Liu, 1980; Hou, 1998; Fu, 1998). It was planned and supervised by Bingzhong Liu, a Confucianist and governmental officer, and designed by Yeheidie'erding, a Muslim architect who studied Han[139] architecture. Obviously, it had a regular grid pattern
divided by the roads 25m in width and the narrower alleyways, called Hutongs[140], around 7m in width; it has 3 gates on the city wall to the south, west and east, as well as 2 gates on the city

[137] 'Kao Gong Ji' or 'Artificers' , written around 500BC, discussed about the techniques of building construction and the conceptual codes of city planning and design according to the Confucian philosophy. See Dai Wu San (2003) ed. Kao Gong Ji, Shangdong Pictorial Publish: P80.
[138] Zhouli is a classic Confucian book about the secular ceremonial behaviour and the propriety or politeness which colors everyday life in Zhou Dynasty (1027 - 256 BC). The etiquette and politeness were codified and treated as a compressive system of norms to understand each person's place in a society. For example, it allowed people to know who is older and who is younger, who is guest and who is host and so on, and then enabled people to behave in a polite and respectful way. It includes six parts and the last part includes the chapter of 'Kong Gong Ji' or 'Artificers'. For details, see Nylan, M. (2001) The Five 'Confucian' Classics, Yale University Press. P168-202.
[139] Han is a largest ethnic group in China.
[140] Hutong originally means water well, and appeared first during the Yuan Dynasty. It is believed to a word of Mongol language origin.

wall to north; the Palace City encircled by the Imperial City, built on the southern end of the north-south axis, create the form of the nested city; and the rest of the city was divided into 50 gated quarters - called Fangs – physically defined by the main roads and the archway called Paifang, but those gated quarters had not been bounded by walls and their gates or archways were opened to the public, which was in striking contrast to the walled quarters[141] built in the capital of Chang'an of the Tang Dynasty (618-907). Although the quarters or Fangs in Dadu were opened to everyone at anytime, the gates or Paifangs also implied the spatial definition of the quarters (Zhu, 1993) and the gated quarters (Fangs) more or less shaped the morphology of the current named areas of Beijing (Hou, 1998; Fu, 1998; Liang 2005). In addition, the whole city of Dadu, the most part of the today's Inner City of Beijing, was completed in a relative short period of nearly 18 years (Hou, 1998; Fu, 1998).

Although the Imperial City of Dadu was razed and the city name of Dadu was changed to Beiping (and later renamed as Beijing in 1403) at the time when the Ming Dynasty was founded (in 1368), the city of Beijing in the Ming Dynasty in fact inherited the main spatial structure of Dadu, with several adjustments and reconstructions. In 1406, a main reconstruction programme was initiated in preparation of converting the city of Beiping into the capital of the Ming Dynasty (Hou, 1998). **Fig. D.5b** shows the old Beijing map between 1573 and 1644 in the Ming Dynasty and **Fig. D.6** illustrates the reconstruction and adjustment of the city of Beijing in the Ming Dynasty based on Dadu of the Yuan Dynasty, as well as its relationship to the old Beijing in the Later Jin Dynasty (936-947)[142]. The north city wall of Dadu was moved 2.8km south and the northern part of old Dadu outside the new city wall was abandoned. The 0.72 sqkm Palace City, namely the Forbidden City (or Today's Gugong Museum), the 6.87 sqkm Imperial City surrounding the Palace City[143], as well as the Temple of Heaven[144] to the

south of the city of Beijing, were built in 1421. As the new Imperial City was moved to the south, the southern wall of the entire city was also moved 0.8 km to the south as well. As that stage,

[141] Those walled quarters in the Tang Dynasty were expected to be accessed only by the residents of the quarters, and being closed in the evening and opened in the morning, at fixed hours. See Fu (1998).
[142] For details, see Liang (2005), P95.
[143] The Palace City only includes offices, houses and other buildings for the emperor and the royal family, but the Imperial City also comprises the offices for the governmental officials.
[144] The Temple of Heaven was built for the emperor and the senior governmental officers to hold annual ceremony of prayer to Heaven for good harvest.

the current Inner City of Beijing was fully completed and the size of the city was reduced to 35.57 sq km. The old eastern and western city walls, four gates on the two pieces of the city walls, as well as the whole street structure of Dadu in Yuan Dynasty survived, but two gates on the northern end of the old eastern and western city walls were abandoned. Thus, the number of the gates on the city wall was reduced to 9 in total. The ring-like residential district between the city walls and the boundaries of the Imperial City was divided into 28 gated quarters, still called Fangs, which were not bounded by the walls and kept the gates open. The red lines in **Fig. D.5b** illustrate the boundaries of the Fangs[145]. In practice, some gates of the quarters or Hutongs in Beijing were closed by the wood fences at night as a way to prevent burglary, but on average many Fangs were accessible for everyone at anytime (Deng and Mao, 2003).

In 1553, the rural area to the south of the city was built into the walled city, called the Outer City, and thus the Imperial city was renamed as the Inner City **(Fig. D.5b)**. Both the Outer City and the Inner City constituted the city of Beijing in the late Ming Dynasty (Hou, 1998). When the Qing Dynasty (1644 – 1912), founded by the Manchu[146], took the city of Beijing as its capital, the physical structure within the city wall was seldom changed except for some minor amendments (Fu, 1998; Liang, 2005).

The physical structure of the Inner City was improved after the Republic of China was set up in 1912 (Fu, 1998). For example, streets were paved, widened and expanded; city walls and gates were amended in order to enhance traffic efficiency, the railway was extended to the Zhengyang Gate on the southern city wall and the royal gardens were opened to citizens. But to a large extent, the street grid was not changed (Fu, 1998; Deng and Mao, 2003).

The massive building programs within the Inner City were carried out after the People's Republic of China was established in 1949 (Fu, 1998; Wu, 1994, 1998; Deng and Mao, 2004). For example, the city walls were demolished and replaced by a 6-lane Second Ring Road and the 10-lane Chang'an Road; more streets were further widened and expanded to accommodate

[145] For details, see Deng Yi and Mao Qizhi (2003) Quantification Analysis of The Formation of the Community Pattern in the Old City of Beijing: Based on Qianlong Map, Urban Planning Review, Vol. 28, No.5, 61-7 (in Chinese).
[146] The Mangchu people, one minor ethnic group of China, originated in Manchuria, namely today's northeastern China. In the 17th century, they took the power of China and founded the Qing Dynasty.

increasing traffic, and meanwhile, many median or high rise offices and hotels were developed along those main streets; a large number of the traditional quarters were demolished and replaced by the modern housing estates in the 1980s to 2000s. This also implies that a huge number of the traditional Hutongs – alleyways- disappeared during the large-scale constructions within the Inner City. However, the orthogonal grid of the Inner City, by and large, has been retained, partly because the preservation of such grid had been addressed in each around of the city planning since the 1950s (Deng and Mao, 2003). Meanwhile, many area names evolving from the Yuan Dynasty to the Qing Dynasty still survive and the recent Beijing Plan 2004-2020 proposed to preserve area names as cultural inheritance (BMPC, 2004).

In contrast to the north part of Central London, the irregular grid generated by the incremental construction and expansion over several centuries and completed in the early 19th century, the Inner City of Beijing, as a regular structure, was mainly created from 1267 to 1285, according to a grand scheme for the old Chinese capital city originally proposed in the book of 'Kao Gong Ji' or 'Artificers', and then was extended 0.8 km to the south from 1416 to 1421, with regard to the same grand scheme elaborated in the 'Artificers'. But since it was completely built up, the internal structure of the Inner City of Beijing has continued to be modified, reconstructed and changed through a long history. To a large extent, it had not expanded beyond the city walls until the 1950s, and was illustrated by the Beiping (Beijing) map in 1950 **(Fig. D.7)**. It can be suggested that the Inner City was under the various internal transformations over several centuries, though its main structure was originally planned and then completed within a relatively short period of time. In this sense, the Inner City can also be considered as an organic city. The named areas of the Inner City of Beijing, originated from the gated quarters called Fangs in the Yuan and Ming Dynasty and were largely bounded by the main streets, the gates, the Paifangs (archways) or the historic wooden fences. Their boundaries were not officially defined and became blurred after the fall of the Qing Dynasty in 1912.

Appendix C: A brief introduction of the London Docklands

London Docklands development was the largest regeneration project in the West from the 1980s to 1990s. It included 22 square kilometres abandoned dock areas, extending 10.8 kilometres along the Thames River within three Docklands Boroughs of Southwark, Tower Hamlets and Newham. It established a new commercial and business district, incorporating Canary Wharf as its centre with a total floor area of 25.1 million square meters, and built new dwellings of 24,042 from 1981 to 1998, forming new built environment of London Docklands to the east of the City, the historic financial and business centre of London. As a result, the population doubled from 39,400 in 1981 to 83,000 in 1998, and the unemployment rates dropped down from 17.8% in 1998 to 7.2% in December 1997 (LDDC, 1997).

Under the Thatcher's paradox of free market economy, privatisation and centralised governance, the London Dockland Development Cooperation (LDDC) was established in 1981, with aims of initiating the development through the market power, taking over the urban planning power from three Docklands Boroughs, and securing the regeneration of London Docklands through a focused agency at a larger scale (Brownnill, 1990). The LDDC adopted deregulation planning policy to promote the opportunities to investors and developers. This means that the LDDC freed any planning restrictions on the Docklands with minor exceptions and bypassed the local boroughs to create a market, encouraging any new investments, bringing land and buildings into effective use and attracting more people live and work in the area, in contrast to the traditional land use planning.

In April 1982, the Isle of Dogs, the centre of the Docklands, was designated as the Enterprise Zone, a specific geographic area targeted for economic growth and investment in the distressed areas by scrapping planning controls and offering tax advantages and incentives to businesses locating within the zone boundaries (Edwards, 1992; LDDC, 1997). Although most individual development sites had their own design codes and guidelines set up by special agents and developers, there was not an overall spatial strategy planning for London Docklands (Edwards, 1992; Carmona, 2009).

The LDDC considered this flexible and project-orientated planning as an important approach to cope with such large-scale regeneration within at least two decades. It also believed that the surrounding poor areas in East London can be improved by the trickle-down effect, meaning that the benefits given by the new regenerations can be dribbled down to the neighbouring areas, in spite of that many criticisms (Brownill, 1990; Edwards, 1992; Fainstein, 1994) focused on the ignorance of indigenous residents and local boroughs during the process of the regeneration.

And meanwhile, the local councils and the developers, such as Olympia and York who were involved in the development of Canary Wharf in the late 1980s and the early 1990s, in fact had not taken any a strategic planning approach seriously at any stage, but actually had the separated masterplans on the specific sites to attract investment and respond to market shifts (Carmona, 2009). Thus, London Docklands can be a typical case to study how urban spatial structure is gradually generated and enhanced without a top-down physical planning intervention or a coherent and overall design vision in a relative short period of time, if considering the fact that the two decades of regeneration are just one moment in the long history of urban transformation for London.

The LDDC also raised the question of how the new areas can be developed to the urban areas with the specific characters during a large-scale regeneration process (LDDC, 1997). It prepared the separated development frameworks for each of the principle development areas within London Docklands, after identifying that London Docklands was covered by a series of distinct and diverse areas from the fine urban fabric based on the medieval development, such as London Bridge City, Bermondsey Riverside and Wapping, to the vast areas of vacant land and water which make up the Royal Docks. Its aim was to create '*coherent and diverse yet distinct and identifiable districts similar to those which constitute other metropolitan areas…. it helps orientation, creates a "sense of place" and greatly assists our enjoyment of cities'* (LDDC, 1997).

These area development frameworks, however, were much more flexible than the traditional land use planning, as they only set up a list of objectives as development proceeds and priorities which developers can use to assess the opportunities and local people can use to

check whether their concerns had been taken into account. According to the LDDC monograph (LDDC, 1997), there are seven main development areas, Bermondsey Riverside, Surry Docks, Wapping, Limehouse, Isle of Dogs, Royal Docks and Beckton.

Those seven areas formed different ethos, whether urban or suburban, after the 20-year regeneration (LDDC, 1997). Bermondsey Riverside, stretching from London Bridge through the Butlers Wharf and Mill Street Developments to Rotherhithe, conserved its distinctive historic urban character and formed the unequalled mix of day and night-time culture that has attracted a large number of tourists. The regeneration of the area mainly involved site clearance, archaeological excavation, recycling vacant land and buildings and office redevelopment, respecting existed street patterns and built forms. A new office area has been redeveloped between London Bridge and Tower Bridge, the mixed use development has been encouraged in the Butlers Wharf area, and mainly residential environment has been improved and expanded to the east of St. Saviours Dock.

Surry Docks, lying on the peninsula, has been transformed from an isolated and abandoned area into a nice community with some of London's most attractive luxury housing and the largest landscape infrastructure in the Docklands. It also has big shopping centre, business parks, London's largest working marina and other leisure facilities, clustering around the interchange of the Jubilee Line Extension and the East London Line.

Wapping, located between the Highway and the River Thames, was regenerated to improve internal distributor roads and canal system together with the docks so that people can easily enter into this area from the outside and access to the waterfront and the parks, which happened mainly in the 1980s. Besides the riverside warehouses converted to attractive residences and the places of work and the council houses refurbished, new housing was built at the Western Dock and around Shadwell Basin and Hermitage Basin, which formed a mixed community whose ethos was not suburban. There are few big commercial facilities except a Safeway supermarket in Thornas More Street and a failed shopping mall at Tobacco Dock.

Limehouse, a small area between Commercial Road to the north and the River Thames to the south, was mainly a story of the 1990s. The original urban fabric has been preserved and traffic

pressure in this area has been relieved as the 1.8 km Limehouse Link tunnel opened in 1993. Ropemakers's Fields was upgraded and extended as a green park at the centre of Limehouse, almost separating the refurbished the Council houses in the east and the luxury housing around the Limehouse Basin in the west.

The Isle of Dogs, a peninsula on the north of the Thames, has undergone a dramatically transformation to become London's commercial and business district. Canary Wharf has been regenerated as a sheer size of business centre comprising many high-rise office towers in the north, which even changed the image of the East London. The transport revolution, such as Dockland Light Railway (DLR), the Jubilee Line Extension, the Limehouse Link, Docklands Highways and the first River-Bus service, took place at this area that updated its relation to the rest of London. A large number of new luxury houses were built along the Thames and the Docks, as well as the original council houses refurbished to form a mix community.

With Isle of Dogs to its west, Royal Docks is the furthest away from the City. It is the largest development site, comprising about a quarter of the Docklands and covering the largest water area of 94 hectare and open spaces. The second largest infrastructure regeneration in the UK has been implemented including a network of new and improved roads linking the A13/A406 in the east and Aspen Way/Limehouse Link in the west, the extension of DLR, and a comprehensive drainage system. Further, a series of large-scale projects have been scattered in the area, such as London City Airport, EXCel that is an international exhibition centre, the UK's first new urban village at West Silvertown, the Royals Business Park, London Docklands Campus of the University of East London, Bow Creek Ecology Park and the East Indian Dock Bird Sanctuary, but which demonstrated the character of suburban.

Beckton is to the north of Royal Docks, forming a self contained area. Many well established and self contained communities have been developed with all advantages of good facilities and natural environment, which resulted in owner occupation increasing from 20% to 55%, the largest figure at the first ten years regeneration in the Docklands. At the north-east corner of this area, a range of industry and commercial facilities have been improved through the development of the London Industry Park, BandQ, Sainsbury's Savacentre, Asda Supermarket and so on.

In general, it seemed that Bermondsey Riverside, Wapping and Limehouse created more urban like environment, Surry Docks, Royal Docks and Beckton formed more suburban like place, and Isle of Dogs generated a mixture of urban and suburban area (LDDC, 1997). This provides an informative background for investigating the newly developed areas in London Docklands, with regards to spatial configuration.

Appendix D: The Calculation of MMD for Several Ideal Grids

D.1 The calculation of metric mean depth Rk of point A on a two-dimensional surface extending infinitely

The points encountered by A up to the radius of k aggregate to form a circle with radius of k (**Fig. AD.1**). Total depth of A is the sum of distances from A to all points within the circle with radius k; and node count of A is equal to the area of the circle with radius k.

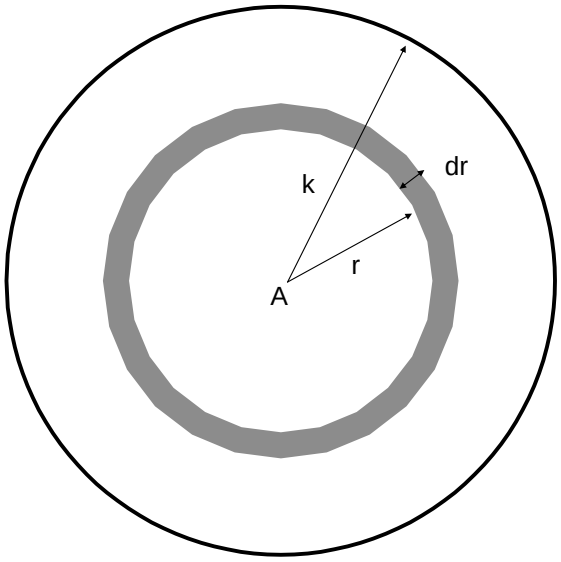

Fig. AD.1 The points encountered by A up to the radius of k (the grey annulus denotes the increase of the area from radius r to radius r+dr, and dr is infinitely small)

We first calculate total depth of A. The sum of points whose distance from A is r, denoted as N_r, is equal to the area of an extreme thin annulus, represented by the grey in **Fig. AD.1**. Thus, N_r is calculated as the below:

$$N\_r = 2\pi r dr \tag{1}$$

where, r is distance from those points to A, and dr is an infinitely small increase of radius.

The sum of metric distance from those points to A (denoted as dTD) is calculated by:

$$dTD = N\_r \times r = 2\pi r^2 dr \tag{2}$$

Thus, total depth of A (denoted as TD_k) is the integral of dTD:

$$TD\_k = \int dTD = \int_0^k 2\pi r^2 dr = \frac{2\pi k^3}{3} \tag{3}$$

Then, we compute node count of A at radius k, denoted as NC_k:

$$NC\_k = \pi k^2 \tag{4}$$

Thus, metric mean depth at radius k, denoted as MMD_k, is calculated by dividing TD_k by NC_k:

$$MMD\_k = \frac{TD\_k}{NC\_k} = \frac{2}{3}k \tag{5}$$

D.2 The calculation of metric mean depth Rk of centre point O of a circular sector OAB with a central angle of θ in radians and a radius of k

Total depth of O is the sum of distances from O to all points within the circular sector, and node count of O equal to the area of the circular sector.

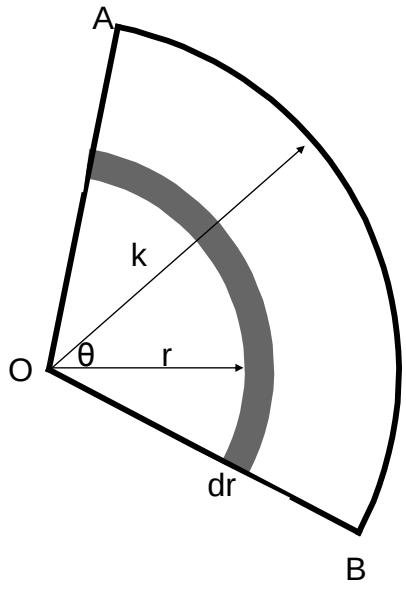

Fig. AD.2 OAB is a circular sector with a central angle of θ in radians and a radius of k (the grey arc denotes the increase of the area from radius r to radius r+dr, and dr is infinitely small)

The sum of points whose distance from O is r, denoted as N_r, is equal to the area of an extreme thin arc, represented by the grey in **Fig. AD.2**. Thus, N_r is calculated as the below:

$$N\_r = \theta r dr \tag{6}$$

where, r is distance from those points to O, θ is central angle in radians, and dr is an infinitely small increase of radius.

The sum of metric distance from those points to O (denoted as dTD) is calculated by:

$$dTD = N\_r \times r = \theta r^2 dr \tag{7}$$

Thus, total depth of O (denoted as TD_k) is the integral of dTD:

$$TD\_k = \int dTD = \int_0^k \theta r^2 dr = \frac{\theta k^3}{3} \tag{8}$$

Then, we compute node count of A at radius k, denoted as NC_k:

$$NC\_k = \frac{\theta k^2}{2} \tag{9}$$

Thus, metric mean depth at radius k, denoted as MMD_k, is calculated by dividing TD_k by NC_k:

$$MMD\_k = \frac{TD\_k}{NC\_k} = \frac{2}{3}k \tag{10}$$

D.3 The calculation of metric mean depth Rn of point at one corner of a square.

Total depth of O is the sum of distances from O to all points within a square OACB, with side length of L, and node count of O equal to the area of the square.

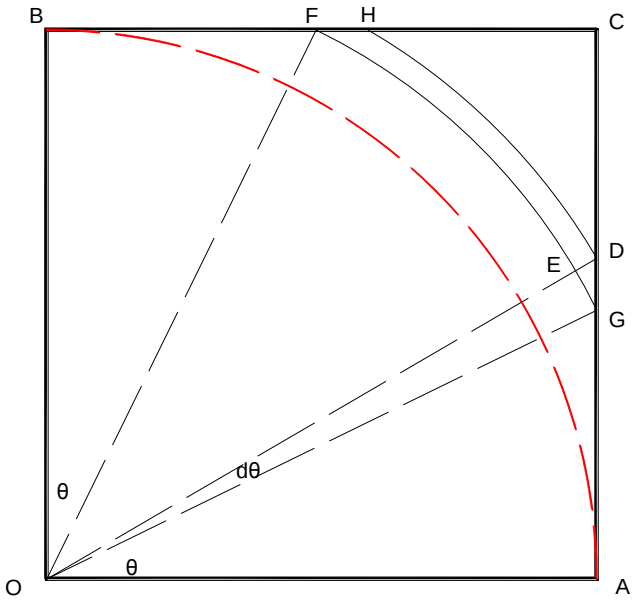

Fig. AD.3 OACB is a square with side length L; OAB is a quarter circle; ABC is the shape bounded by arc AB, side AC and BC.

We first calculate the total depth from O to all the points in quarter circle OAB (denoted as TDOAB), as well as the total depth from O to all the points in ABC(denoted as TDABC), respectively.

For the quarter circle OAB

According to the previous section, TDOAB is calculated as below:

$$TD_{OAB} = \int_0^L \left(\frac{\pi}{2} k \times k \right) dk = \frac{\pi}{6} L^3 = 0.523599 L^3 \tag{11}$$

where, L is side length of the square.

For ABC

$$OG = \frac{OA}{\cos\theta} = \frac{L}{\cos\theta} \tag{12}$$

∠ GOD, denoted by dθ, is an infinite small increase of ∠ AOC (equal to θ), so that the area DGFH is a thinnest arc whose distance to O is OG.

And since dθ is infinite small, ∠ OGA = ∠ ODA; and ∠ GED = π/2.

So, ∠ DGE =θ, and $DE = EG \times \tan\theta$

$$EG = OG \times d\theta \tag{13}$$

According to (12)

$$EG = \frac{L \times d\theta}{\cos\theta} \tag{14}$$

Thus, $$DE = \frac{L \tan\theta \times d\theta}{\cos\theta} \tag{15}$$

Arc FG is the circumference of a circular sector OFG

$$FG = \frac{L}{\cos\theta}\left(\frac{\pi}{2} - 2\theta\right) \tag{16}$$

Thus, the area of thinnest arc shape DGFH is calculated as below:

$$DGFH = FG \times DE = \frac{L \tan^2\theta}{\cos^2\theta}\left(\frac{\pi}{2} - 2\theta\right)d\theta \tag{17}$$

Since DGFH is infinite thin, the distance from all the points of DGFH to O is equal to L.

Thus, the total depth of those points of DGFH is calculated as below:

$$TD_{DGFH} = \frac{L^2 \tan^2\theta}{\cos^2\theta}\left(\frac{\pi}{2} - 2\theta\right)d\theta \tag{18}$$

The shape ABC is the accumulation of DGFH, when θ increases from zero to $\frac{\pi}{4}$

Thus, the total depth from O to all the points in ABC (denoted as TDABC) is calculated:

$$TD_{ABC} = \int_0^{\frac{\pi}{4}} \frac{L^2 \tan^2\theta}{\cos^2\theta}\left(\frac{\pi}{2} - 2\theta\right)d\theta \tag{19}$$

$$TD_{ABC}=\left[\frac{\pi L^3}{6\cos^3\theta}-\frac{L^3}{12\cos^3\theta}\left(\begin{array}{l}8\theta+3\cos\theta\left(\log\left(\cos\frac{\theta}{2}-\sin\frac{\theta}{2}\right)-\log\left(\cos\frac{\theta}{2}+\sin\frac{\theta}{2}\right)\right)\\+\cos^3\theta\left(\log\left(\cos\frac{\theta}{2}-\sin\frac{\theta}{2}\right)-\log\left(\cos\frac{\theta}{2}+\sin\frac{\theta}{2}\right)\right)-2\sin 2\theta\end{array}\right)\right]_0^{\frac{\pi}{4}}$$

(20)

$$TD_{ABC}=0.241596L^3 \tag{21}$$

Thus, the total depth from O to all the points within OACB (denoted as TDOACB) is calculated:

$$TD_{OACB}=TD_{OAB}+TD_{ABC}=0.765195L^3 \tag{22}$$

Since node count of O is equal to the area of the square OACB, that is,

$$NC_{OACB}=L^2 \tag{23}$$

Thus, metric mean depth of O is calculated

$$MMD_{OACB}=\frac{TD_{OACB}}{NC_{OACB}}=0.765195L \tag{24}$$

D.4 The calculation of metric mean depth Rn of the centre point O of a square.

O is the centre point of square ZVXC, with side length of L.

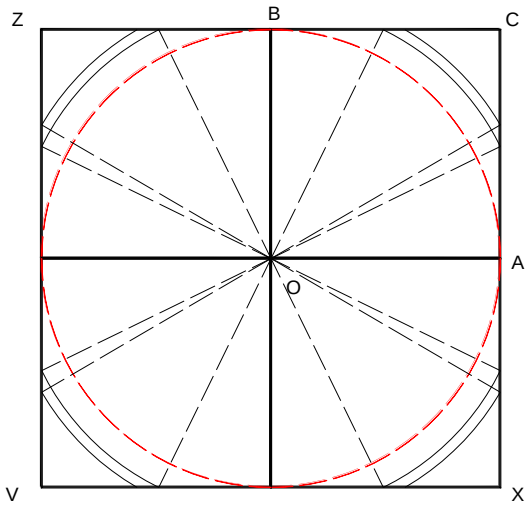

Fig. AD.4 ZVXC is a square with side length L; O is the centre point.

When this square is divided into four smaller squares, shown in **Fig.AD.4**, the centre point O of square ZVXC becomes the corner point of each smaller square, such as OACB. Thus, MMD of O is equal to the average distance from O to all points within OACB.

According to the way we calculate MMD of the corner point of a square, elaborated in the previous section, the point O has the value of MMD_n.

$$MMD_O = \frac{TD_O}{NC_O} = \frac{0.765195L}{2} = 0.382598L \tag{25}$$

where, L is side length of ZVXC.

D.5 The calculation of metric mean depth Rk of any a point O on an extremely thin frame with side length L (k <= L/2).

ABCD is an extremely thin frame with side length L. For any a point O, total depth at radius k (k <= L/2) is the sum of distances from O to all points on the frame within the radius of k, and node count of O at k is equal to the double of the radius (2k).

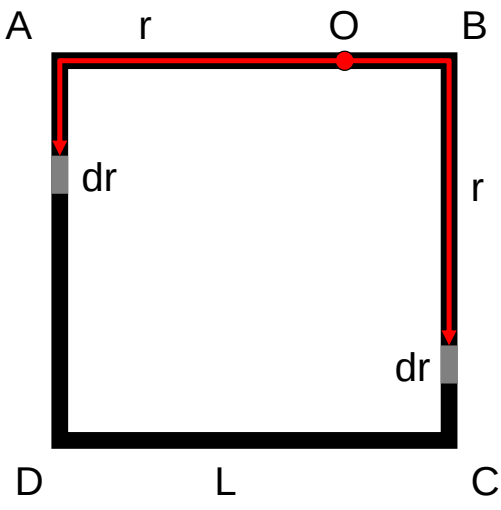

Fig. AD.5 ABCD is a frame with side length L; O is a point on the frame; r denotes any a radius smaller than k; dr is an infinitely small increase of the radius r.

We then calculate total depth of O at k. **Fig. AD.5** shows two points, coloured in grey, whose distance from O is r (r < k), and they can be seen as an infinitely small increase of the radius of r. Thus, their distance from O (denoted by dTDr) can be expressed by:

$$dTD_r = 2rdr$$

The total depth of O at k is equal to the sum of dTDr from 0 to k:

$$TD_o = \int_0^k dTD_r = \int_0^k 2rdr = k^2$$

Since node count of O at k (denoted by NCo) is 2k, metric mean depth of O at k (denoted by MMDo) is calculated by:

$$MMD_o = \frac{TD_o}{NC_o} = \frac{k}{2}$$

Table AD.1 node count Rk of three segments

(End Seg 9 denotes the segment at the end of the side of centre cell of the 50*50 grid, with 9*9 unit cell; Cen Seg 9 indicates the segment at the centre of the side of centre cell of the 50*50 grid, with 9*9 unit cell; Seg 1 means the segment of the side of centre cell of the 300*300 grid, with 1*1 unit cell)

Radius	End Seg 9	Cen Seg 9	Seg 1
1	1	1	1
2	5	3	7
3	9	5	23
4	13	7	47

5	17	9	79
6	21	15	119
7	25	21	167
8	29	27	223
9	33	33	287
10	39	39	359
11	51	45	439
12	63	51	527
13	75	57	623
14	87	63	727
15	99	81	839
16	111	99	959
17	123	117	1087
18	135	135	1223
19	151	151	1367
20	171	165	1519
21	191	179	1679
22	211	193	1847
23	231	207	2023
24	251	233	2207
25	271	259	2399
26	291	285	2599
27	311	311	2807
28	335	335	3023
29	363	357	3247
30	391	379	3479
31	419	401	3719
32	447	423	3967
33	475	457	4223
34	503	491	4487
35	531	525	4759

36	559	559	5039
37	591	591	5327
38	627	621	5623
39	663	651	5927
40	699	681	6239

Bibliography

Abramson, D. B., 1998. Neighborhood Redevelopment as A Cultural Problem: A Western Perspective on Current Plans for the Old City of Beijing, Architecture Journal, 1998, p.47-49.

Aldous, T.,1992. Urban Villages: A Concept for Creating Mixed-use Urban Developments on a Sustainable Scale. London: Urban Villages Group.

Alexander, C., 1965. A city is not a tree. In *Design*, 206, 46-55.

Alexander, C., 2002. The Nature of Order. Berkeley, Calif.

Alexander, C., Ishikawa, S., and Silverstein, M., 1977. A Pattern Language: Towns, Buildings, Construction. Oxford University Press.

Altshler, A. and Luberoff, D., 2003. Mega-projects: The Changing Politics of Urban Public Investment. Washington, DC: Brookings Institution Press.

Barnes, J., 1990. Urban development corporations—the lessons from London Docklands. In J. Montgomery and A. Thornley (eds) *Radical Planning Initiatives*, pp. 59–74. Aldershot: Gower.

BCAB and BSMI, 2005. Beijing Administrative Map Collections. Hunan Map Press.

Biddulph, M., Franklin, B., Malcolm, T., 2003. From concept to completion A critical analysis of the urban village. *Town Planning Review*, 74 (2), 165-93.

Birmingham City Council., 1994. Convention Centre Quarter: Planning and Urban Design Framework.

Boffi, M. & Colleoni, M. 2014. Human behaviour and GIS, Methodologies for analysing urban mobility in a GIS environment. Networks and Communication Studies, 28-1/2: 131-144.

Brownill, S., 1990. Developing London Docklands. Another Great Planning Disaster? London: Paul Chapman Publishing.

Buchanan, C. and Partners, 1963. Traffic in Twons, London: HMSO.

Calthorpe,P. and Fulton, W., 2001. The Regional City. Island Press.

Carmona, M., 2009. The Isle of Dogs: Four development waves, five planning models, twelve plans, thirty-five years, and a renaissance. . . of sorts. *Progress in Planning* 71, p87–151.

Chatwin, J., 1999. The Brindleyplace Masterplan. In: Latham, I, Swenarton, M. (ed.),*Brindleypalce: A Model for Urban Regeneration.* Right Angle Publishing Ltd., London.

Clout, H. and Wood, P., eds. 1986. London: Problems of Change, Harlow.

Collins, M.,1994. Land-use Planning since 1947. In Simmie, J.,(ed.) *Planning London.* UCL Press.

Conzen, MRG, 1988. Morphogenesis, morphological regions and secular human agency in the historic townscape, as exemplified by Ludlow. In: Denecke D, Shaw G (eds) Urban historical geography: recent progress in Britain and Germany. Cambridge University Press, Cambridge,pp 253–272.

Dai W. S., eds. 2003. Kao Gong Ji. Shangdong Pictorial Publish. (in Chinese)

Dalton, N. S. C., 2006. Configuration and Neighbourhood/ Is Place Measurable? Space Syntax and Spatial Cognition Workshop Proceedings, Spatial Cognition 06.

Dalton, N. S., 2005. New Measures for Local Fractional Angular Integration or Towards General Relitivisation in Space Syntax. In: Proceedings of the 5th Space Syntax Symposium, 103-115.

Dalton, N. S., 2007. Is Neighbourhood Measurable? In: Proceedings of the 6th International Space Syntax Symposium, 088-01-12.

Dalton, N., 2001. Fractional Configurational Analysis and A Solution to the Manhattan Problem. In: Proceedings of 3rd International Space Syntax Symposium Atlant 2001, 26.01-26.13.

Dalton, S.C.N. 2010. Synergy, Intelligibility and Revelationin Neighbourhood Places. UCL PhD Thesis.

Dalton, NS and Peponis, J and Conroy-Dalton, R., 2003. To Tame a TIGER One Has to Know its Nature: extending weighted angular integration analysis to the descriptionof GIS road-centerline data for large-scale urban analysis. In: (Proceedings) 4th International Space Syntax Symposium. : London, UK.

Deng, Y., and Mao, Q. Z., 2003. Quantification Analysis of The Formation of the Community Pattern in the Old City of Beijing: Based on Qianlong Map, Urban Planning Review, Vol. 28, No.5, 61-7. (in Chinese)

Dong G.Q., 1998. Strategic concept of Beijing Urban Planning, Beijing Industry Architecture Press. (in Chinese)

DPZ.,1999. The Lexicon of the New Urbanism. Miami: Duany Plater-Zyberk and Company.

DPZ.,2002. The Lexicon of the New Urbanism. Miami: Duany Plater-Zyberk and Company.

Duany, A., and Emily, T., 2002. “Transect Planning, *Journal American Planning Association*,: 245-266.

Duany, A., Plater-Zyberk, E., and Alminana, R., 2003. The New Civic Art: Elements of Town Planning. New York: Rizzoli International Publications.

Duany, A., 1991. Towns and Town-Making Principles. Rizzoli.

Duany, A., Plater-Zyberk, E., Speck, J., 2000. Suburban Nation: The Rise of Sprawl and the Decline of the American Dream. New York: North Point Press.

Duany, A., Plater-Zyberk, E., Speck, J., 2005. Smart Growth Manual, New Urbanism in American Communities. Mcgraw Hill Book Co.

Edwards, B., 1992. London Dockland: Urban Design in an Age of Deregulation. Butterworth Architecture, Oxford.

Edwards, B., 1993. Deconstructing the city: The experience of London Docklands. *The Planner*, 79(2), 16–18.

Edwards, B., 1999. Deconstructing the city: London Docklands. *Urban Design Quarterly*, January, 69, 22–24.

Fainstein, S., 1994. The City Builders: Property, Politics, and Planning in London and New York. Blackwell Publishers, USA, UK.

Fainstein, S., 2001. The City Builders: Property Development in New York and London, 1980-2000. University Press of Kansas, USA.

Florio, S., and Brownill, S., 2000. Whatever happened to criticism? Interpreting the London Docklands Development Corporation’s Obituary. *CITY*, VOL. 4, NO. 1, 2000, pp53-64.

Forshaw, J. H. and Abercrombie P., 1943. County of London Plan, Macmillan and Co. Limited.

Forshaw,J.H., 1944. County of London plan / prepared for the London County Council by J. H. Forshaw and Patrick Abercrombie. London: Macmillan.

Foster, J.,1992. Living with the Docklands Redevelopment: Community view fromthe Isle of Dogs. *London Journal*, 17(2), 179–182.

Foster,J., 1999, Docklands: Cultures in Conflict, Worlds in Collision, UCL press, London.

Foxell, S., 2007. Mapping London – Making Sense of the City, Black Dog Publishing Limited.

Franklin,B. , Tait, T., 2002. Constructing an Image: The Urban Village Concept in the UK. *Planning Theory*, 1; 250-72.

Fu, X. N.,1998. Collection of Architecture History Essays by Fu Xinian, Cultural Relic Publish. (in Chinese)

Galster,G., 2001. On the Nature of Neighbourhood. *Urban Studies*, Vol. 38, No. 12, 2111–2124.

Gao. Y. C., 2000. Hu Tong Scale in the Old City of Beijing, 4/2000, *Beijing City Planning and Construction Review*, p.14-16. (in Chinese)

Giddens, A., 1991. Modernity and Self-Identity: Self and Society in the Late Modern Age. Cambridge, Polity Press.

Gil, J. 2016. Street network analysis “edge effects”: Examining the sensitivity of centrality measures to boundary conditions. Environment and Planning B: Urban Analytics and City Science. 44(5), pp. 819–836.

GLC, 1968. Greater London Development Plan: Report of Studies. Greater London Council.

Gold, J. R., 1998. Creating the Charter of Athens: CIAM and the Functional City, 1933-43. *The Town Planning Review*, Vol. 69, No. 3 (Jul., 1998), pp. 225-247.

Gordon, D L. A., 2001. The Resurrection of Canary Wharf. *Planning Theory and Practice*, Vol. 2,No.2, 149-168.

Gratz, R. B., 1994. The Living City: How America’s Cities Are Being Revitalized By Thinking Small in A Big Way. John Wiley and Sons.

Hacking, I., 1983. Rrepresenting and Intervening - Introductory Topics in The Philosophy of Natural Science. Cambridge University Press.

Hall, P. and Hardy, D. and Howard, E. and Ward, C., 2003. To-morrow: A Peaceful Path to Real Reform. Routledge: Abingdon, UK.

Hall, P., 1989. London 2001. Unwin Hyman, London.

Hall, P., 1998. Cities of Tomorrow. Basil Blackwell, London.

Hall, P., Pain, K., 2006., The Polycentric Metropolis: Learning from Mega-City Regions in Europe. London: Earthscan.

Hamnett, C., 2003. Unequal city: London in the global arena. London: Routledge.

Hanson, J. and Hillier, B.,1987. The Architecture of Community: Some New Proposals on the Social Consequences of Architectural and Planning Decisions. *Arch and Comport./Arch. Behave*., 3, 251-273.

He, G. J., 1985. The Research on Urban Planning in Kao Gong Ji. Chinese architecture industry publishes. (in Chinese)

Healey, P., 1999. A Model for Urban Regeneration. In Latham, I, Swenarton, M. (ed.),*Brindleypalce: A Model for Urban Regeneration.* Right Angle Publishing Ltd., London.

Hebbert, M., 1992. One 'planning disaster' after another: London Docklands 1970–1992. *London Journal*, 17(2), 115–134.

Hebbert, M., 1998. London : more by fortune than design. John Wiley and Sons.

Hebbert, M., 2002. Urbanism. London: Academy Editions.

Hillier, B. and Hanson, J., 1984. The Social Logic of Space. Cambridge University Press.

Hillier, B. and Iida, S., 2005. Network and Psychological Effects in Urban Movement, In: A.G. Cohn and D.M. Mark (Eds.): COSIT 2005, LNCS 3693, pp. 475–490.

Hillier, B., 1988. Against Enclosure. In: Teymur, N., T.A. Markus and T. Woolley, eds. *Rehumanising Humanising*. Butterworths, pp. 63-88.

Hillier, B., 1989. The Architecture of the Urban Object. Ekistics, 334, 5-20.

Hillier, B., 1996a. Space is the Machine. Cambridge University Press.

Hillier, B., 1996b. Cities as Movement Economies. *Urban Design International*, 1(1), 41-60.

Hillier, B., 1999. Centrality as a Process: Accounting for Attraction Inequalities in Deformed Grids. *Urban Design International*, 3-4, p. 107-127.

Hillier, B., 1999. The Hidden Geometry of Deformed Grids: or, why space syntax works, when it looks as though it shouldn't. *Environment and Planning B: Planning and Design*, 26 169 - 191.

Hillier, B., 1973. In Defence of Space. Royal Institute of British Architects Journal, November, 1973. 539 - 544.

Hillier, B., 2001. A Theory of the City as Object; or, How the Social Construction of Space is Mediated by Spatial Laws. In: Proceedings of the Third Space Syntax Symposium. Atlanta, 02.1-02.28.

Hillier, B., 2009. Spatial Sustainability in Cities: Organic Patterns and Sustainable Forms. In: Koch, D. and Marcus, L. and Steen, J., (eds.) Proceedings of the 7th International Space Syntax Symposium. k01.1-20. Royal Institute of Technology (KTH): Stockholm, Sweden.

Hillier, B., and Penn, A., 1991. Visible Colleges: Structure and Randomness in the Place of Discovery from Science in Context. 4, 1 pp. 23-49.

Hillier, B., Burdett, R., Peponis, J., and Penn, A., 1987a. Creating Life: Or, Does Architecture Determine Anything? *Architecture and Comportment/ Architecture and Behaviour*, 3 (3). pp. 233-250.

Hillier, B., Greene, M., and Desyllas, J., 1999. Self-generated neighbourhoods: the role of urban form in the consolidation of informal settlements. In: Proceedings of the 2nd International Space Syntax Symposium, 01.1-01.24.Brasillia, Brazil.

Hillier, B., Hanson,J., Peponis, J., 1987b. The Syntactical Analysis of Settlement. *Architecture and Behavior*, 3(3), 217-231.

Hillier, B., Leaman, A., Stansall, P., and Bedford, M., 1976. Space Syntax. *Environment and Planning B: Planning and Design*, 3 (2) 147 - 185.

Hillier, B., Penn, A., Grajewski, T., and Xu., J., 1991. Brindleyplace, Birmingham: The UCL Study of the Potential of the Site and the Farrell Masterplan. Unit for Architectural Studies.

Hillier, B., Penn, A., Hanson, J., Grajewski, T., and Xu, J., 1993. Natural Movement: or. Configuration and Attraction in Urban Pedestrian Movement. *Environment Planning B*, 20(1) 29-66.

Hillier, B., Turner, A., Yang, T., Park, H.-T., 2007. Metric and topo-geometric properties of urban street networks: some convergences, divergences, and new results. In: 6th International Space Syntax Symposium, pp.001-1-22.Istanbul, Turkey.

Hillier, B., Turner, A., Yang, T., Park, H-T., 2010. Metric and topo-geometric properties of urban street networks: some convergencies, divergencies and new results. The Journal of Space Syntax, V(1) 2, 258-279.

Hillier, B., 1983. Space Syntax: A Different Urban Perspective. *Architects' Journal*, vol. 178, no. 48, Nov. 30, pp. 47-63.

Hillier, B., Yang, T., Turner, A., 2012. Advancing DepthMap to advance our understanding of cities: comparing streets and cities, and streets to cities. In: Green, M and Reyes, J and Castro, A, (eds.) Eighth International Space Syntax Symposium. Pontifica Universidad Catolica: Santiago, Chile.

Holyoak, J., 1999. City Edge- before Brindleyplace. In Latham, I, Swenarton, M. (ed.),*Brindleypalce: A Model for Urban Regeneratio.*Right Angle Publishing Ltd., London.

Hou R. Z., 1988. A Collection of the Historic Beijing Maps. Beijing Publisher. (in Chinese)

Howard, E., 1898/1965. Garden Cities of To-Morrow. The MIT Press.

HRH The Prince of Wales, 1989. A Vision of Britain: A Personal View of Architecture. London: Doubleday.

Jacob, J., 1961. The Death and Life of Great American Cities: The Failure of Town Planning. Random House, New York.

Johnson, S. D., 2002. Origin of the Neighbourhood Unit. *Planning Perspectives*, 17 (2002) 227–245.

Karimi, K., 1997. The Spatial Logic of Organic Cities in Iran and the Unitied Kingdom. In: Proceedings of 1st Space Syntax International Symposium, 1: 06.

Kasemsmook, A., 2003. Spatial and Functional Differentiation: A Symbiotic and Systematic Relationship.In: Proceedings of the 4th International Space Syntax Symposium, 11.1-11.18.

Katz, P., 1994. The New Urbanism: Toward an architecture of community. New York.

Kier, L., 1977. The City Within the City. *A + U*, Tokyo, Special Issue, November, 69-152.

Kier, L., 1998. Architecture Choice or Fate, Papadakis Publisher.

Kostof, S., 1992. The City Assembled: Elements of Urban Form through History. Little Brown, Boston.

Kostof, S., 1999. The City Shaped: Urban Patterns and Meanings Through History. Thames and Hudson, New York.

Krier, R., 2003, Town Spaces-Contemporary Interpretations in Traditional Urbanism, Publishers for Architecture, Berlin.

Larsen, K., 2005. Cities to Come: Clarence Stein's Postwar Regionalism. *Journal of Planning History,*2005; 4; 33-51.

Law, S. 2017. Defining Street-based Local Area and measuring its effect on house price using a hedonic price approach: The case study of Metropolitan London. Cities, vol. 60, 2017, 166-179.

Lawhon, L. L., 2009. The Neighborhood Unit: Physical Design or Physical Determinism?. *Journal of Planning History.*2009; 8, 111-32.

LCC, 1951. Administrative County of London Development Plan 1951. London County Council.

LDDC, 1998. Docklands Development Strategy. London Docklands Development Corporation: London.

Le Corbusier, 1947. Concerning Town Planning. London: the Architectural Press.

Le Corbusier, 1973. The Athens Charter, trans. A. Eardley, New York, Grossman.

Leccese M., and McCormick K., ed. 1999. Charter of the New Urbanism. McGraw-Hill.

Liang, S. C., 1952. The Construction of Beijing City. Beijing: Kepu Press. (in Chinese)

Liang, S. C., 2005. Chinese Architecture History, Baihua Publisher. (in Chinese)

Liu D. Z., 1980. Chinese Architecture History, China Architecture and Building Press. (in Chinese)

Long, K., 2000. EDAW's docklands master plan unveiled. *Building Design*, 28 April, 1438, 2.

LPAC, 1995. State of the Environment Report for London. London Planning Advisory Committee.

Lynch, K., 1981. A Theory of Good City Form. MIT Press.

Lynch, K.,1961. The Image of the City. MIT Press.

Madelin, R., 1999. Turning Ideas into Reality: Lessons from Brindleyplace., In Latham, I, Swenarton, M. (ed.), Brindleypalce: A Model for Urban Regeneration.Right Angle Publishing Ltd., London.

Major, M. D. 2018. The Syntax of City Space. London, Routledge.

Mayor of London, 2008. The London Plan: Spatial Development Strategy for Greater London Consolidated with Alterations Since 2004. London: Greater London Authority.

Mehaffy, M.W., Porta, S. and Romice, O. 2015. The "neighborhood unit" on trial: a case study in the impacts of urban morphology. Journal of Urbanism. Vol. 8, 199-217.

Meijers, E., 2009. Stein's 'Regional City' Concept Revisited Critical Mass and Complementarity in Contemporary Urban Networks. *Town Planning Review*, 485-506.

Mills, A. D., 2001. A Dictionary of London Place Names. Oxford University Press.

Morris, A. E. J., 1994. History of Urban Form. Longman Scientific Technical.

MoT, 1963. Traffic in Towns. London: HMSO.

Mumford, E., 2000. The CIAM Discourse on Urbanism, 1928–1960. Cambridge, Massachusetts: MIT Press.

Mumford, L., 1945. The Garden City Idea and Modern Planning. In: Osborn, F. J. (ed) 1965. *Garden Cities of To-morrow*. the MIT Press. pp.29-40.

Mumford, L., 1946.Garden Cities and the Metropolis: A Reply. *The Journal of Land and Public Utility Economics*, Vol. 22, No. 1,pp. 66-69.

Mumford, L., 1954. The Neighborhood and the Neighborhood Unit. *The Town Planning Review*, Vol. 24, No. 4, pp. 256-270.

Neal, P., ed. 2003. Urban villages and the making of communities. Spon Press.

Nylan, M., 2001. The Five 'Confucian' Classics. Yale University Press.

Olds, K., 2001. Globaliztion and Urban Change: Capital, Culture, and Pacific Rim Mega-projects. Oxford University Press Inc. New York.

Oliveira, V. 2016. The Study of Urban Form: Different Approaches. Urban Morphology pp 87-149.

Omer, I & Goldblatt, R. 2012. Urban spatial configuration and socio-economic residential differentiation: The case of Tel Aviv. Computers, Environment and Urban Systems. Vol. 36, Issue 2, .2012, 177-185.

Osborn, F.J., 1950. Sir Ebenezer Howard: The evolution of his ideas. Town Planning Review, 21, pp. 221–235.

Osborn, F.J., 1965. Preface to Garden Cities of To-morrow. Boston, The MIT Press.

Park, H.-T., 2005. Before Integration: A Critical Reivew of Integration Measure in Space Syntax. In: Proceedings of 5th Space Syntax Symposium, 555-572.

Park, H.-T., 2007. The Structural Similarity of Neighbourhoods in Urban Street Networks: A Case of London. In: Kubat, A.S. and Ertekin, O. and Guney, Y.I. and Eyuboglu, E., (eds.) 6th International Space Syntax Symposium, 093-1-18, pp.093-10.

Park, R., 1952. Human Communities. Free Press, New York.

Penn, A., 2001. Space Syntax and Spatial Cognition. Or, why the axial line? In: the Proceedings of the 3rd International Symposium on Space Syntax. Atlanta, GA, USA: Georgia Institute of Technology, pp. 11.1 - 11.16.

Peponis, J., 1989. Space, Culture and Urban Design in Late Modernism and After. *Ekistics*, 334, 93-108.

Perry, C., 1929. The Neighbourhood Unit: A scheme of arrangement for the Family Life Community. *The Regional Plan of New York and Its Environs*. Vol. 7. New York: Regional Plan Association.

Porta, S., Crucitti,P., Latora, V. 2006. The network analysis of urban streets: a primal approach. Environment and Planning B: planning and design, Vol 33 (5): 705-725.

Porta, S. and Romice, O. 2014. Plot-based urbanism: towards time-consciousness in place-making. In: Dortmunder Vorträge zur Stadtbaukunst [Dortmunder Lectures on Civic Art]. Niggli, Sulgen, DE, pp. 82-111.

Raford, N., 2004. Movement Economies in Fractured Urban Systems: The Case of Boston, Massachusetts. M.Sc. Thesis, UCL.

Raford, N., Hillier, B., (2005) Correlation Landscapes: A New Approach to Sub-area Definition in Low Intelligibility Spatial Systems. In: the Proceedings of the 5th Space Syntax Symposium.

Read, S., 1999. Space Syntax and the Dutch City. *Environment and Planning B: Planning and Design*, vol. 26, 251-264.

Read, S., 2001. 'Thick' Urban Space: Shape, Scale and The Articulation of 'the Urban' in An Inner-city Neighbourhood of Amsterdam. In: Proceedings of the 3rd Space Syntax Symposium, 18.1-18.12.

Read, S., 2005. Flat City: A Space Syntax Derived Urban Movement Network Model. In: Proceedings of the 5th Space Syntax Symposium, 341-357.

Ross, C. and Clark, J., 2008. London: The Illustrated History. Allen Lane.

Rossi, A., 1984. The Architecture of the City. Boston, MIT Press.

Serres, M, Latour B., 1995, Conversations on Science, Culture and Time, University of Michigan Press, Ann Arbor.

Sheppard, F., 1998. London: A History. OUP Oxford.

SOM, 1987a. Canary Wharf master plan. Chicago, IL: SOM.

SOM, 1987b. Canary Wharf design guidelines. Chicago, IL:SOM.

Stein, C., 1942. City Patterns Past and Future. Pencil Points, 23, 52-56.

Stein, C., 1951. Toward New Towns for America. MIT Press.

Steinhardt, N. S., 1999. Chinese Imperial City Planning, University of Hawaii Press.

Talen E., 2005. New Urbanism and American Planning. London, Routledge Taylor and Francis Group.

Thomas, M. J.,2004. Neighborhood Planning: Uses of Oral History. Journal of Planning History 2004; 3; pp50-70.

Thompson-Fawcett, M.,1998. Leon Krier and the Organic Revival within Urban Policy and Practice. Planning Perspectives 13:167–194.

Thornley, A., 1990. Thatcherism and the Erosion of the Planning System. In Montgomery, J., and Thornley, A., eds. *Radical Planning Initiatives,* pp.34–48. Aldershot: Gower.

Thornley, A., 1991. Urban Planning under Thatcherism: The Challenge of the Market. Routledge, London.

Tower Hamlets Borough, 1992. Unitary Development Plan, Tower Hamlets Strategic Development.

Tower Hamlets Borough, 1997. Planning Implications of LDDC Exit (Isle of Dogs) Report to Planning and Environment Committee.

Tripp, H., 1942. Town planning and road traffic. London: Edward Arnold.

Tripp, H., A., 1942. Town Planning and Road Traffic. Edward Arnold, London.

Turner, A. Penn, A. Hillier, B., 2005. An Algorithmic Definition Of The Axial Map. Environment and Planning B: Planning and Design 32(3) 425-444.

Turner, A., 2001. Angular Analysis. In Proceedings of the 3rd International Symposium of Space Syntax, 1-13.

Turner, A., 2004. DepthMap4: A Researcher's Handbook, UCL.

Turner, A., 2008. Getting Serious with DepthMap: Segment Analysis and Scripting. UCL.

Turner, A., 2009. The Role of Angularity in Route Choice: an analysis of motorcycle courier GPS traces. In: Stewart Hornsby, K. and Claramunt, C. and Denis, M. and Ligozat, G., (eds.) Spatial Information Theory. (pp. pp. 489-504). Springer Verlag: Berlin/ Heidelberg, Germany.

UTF, 1999. Towards an Urban Renaissance: Mission Statement. Routledge.

Vaughan, L., 1997, The Urban 'Ghetto': the Spatial Distribution of Ethnic Minorities. In: the Proceedings of 1st International Space Syntax Symposium, 2: 24.

Vaughan, L., and Penn, A., 2001. The Jewish 'Ghetto': Formation and Spatial Structure. In: the Proceedings of the Third International Space Syntax Symposium, pp. 55.1 - 55.16. Atlanta, Georgia, USA.

Vaughan, L. 2018. Mapping Society: The Spatial Dimensions of Social Cartography. London, UCL Press.

Whitehand, JWR. 2014. Conzenian research and urban landscape management. In: Paper presented at the 21st international seminar on urban form, Universidade do Porto, Porto (3–6 June 2014).

Willey, R., 2007. London Gazetteer. Chambers Harrap.

Wu, L.Y., 1994. The Old Beijing City and Juer Hu Tong. Beijing: China Construction Industry Publishing House. (in Chinese)

Yang, T. and Hillier, B., 2007. The fuzzy boundary: the spatial definition of urban areas, In: the Proceedings of 6th International Space Syntax Symposium, 091-16.

Yang, T. and Hillier, B., 2012. The Impact of Spatial Parameters on Spatial Structuring. In: Green, M and Reyes, J and Castro, A, (eds.) Eighth International Space Syntax Symposium. Pontifica Universidad Catolica: Santiago, Chile.

Yang, T., 2004. Morphological transformation of the old city of Beijing after 1949. Presented at: 3rd Great Asian Streets Symposium: a public forum of urban design. 2004 Street Urban Space and Representation, Singapore.

Yang, T., 2005. Impacts of Large-scale Development: Does Space Make A Difference? In: the Proceedings of the Fifth Space Syntax Symposium, Vol. 1, Technological University of Delft.

Yang, T., 2006. The role of space in the emergence of conceived urban areas. In Spatial Cognition ‘06. Space Syntax and Spatial Cognition Workshop Proceedings. University Bremen Germany.

Zhu, W. Y., 1993. Space - Symbol - City: A Theory of Urban Design. Beijing: China Construction Industry Publishing House. (in Chinese)